Green Chemistry

Cutting-edge research for a greener sustainable future

www.rsc.org/greenchem
Volume 8 | Number 10 | October 2006 | Pages 841–928

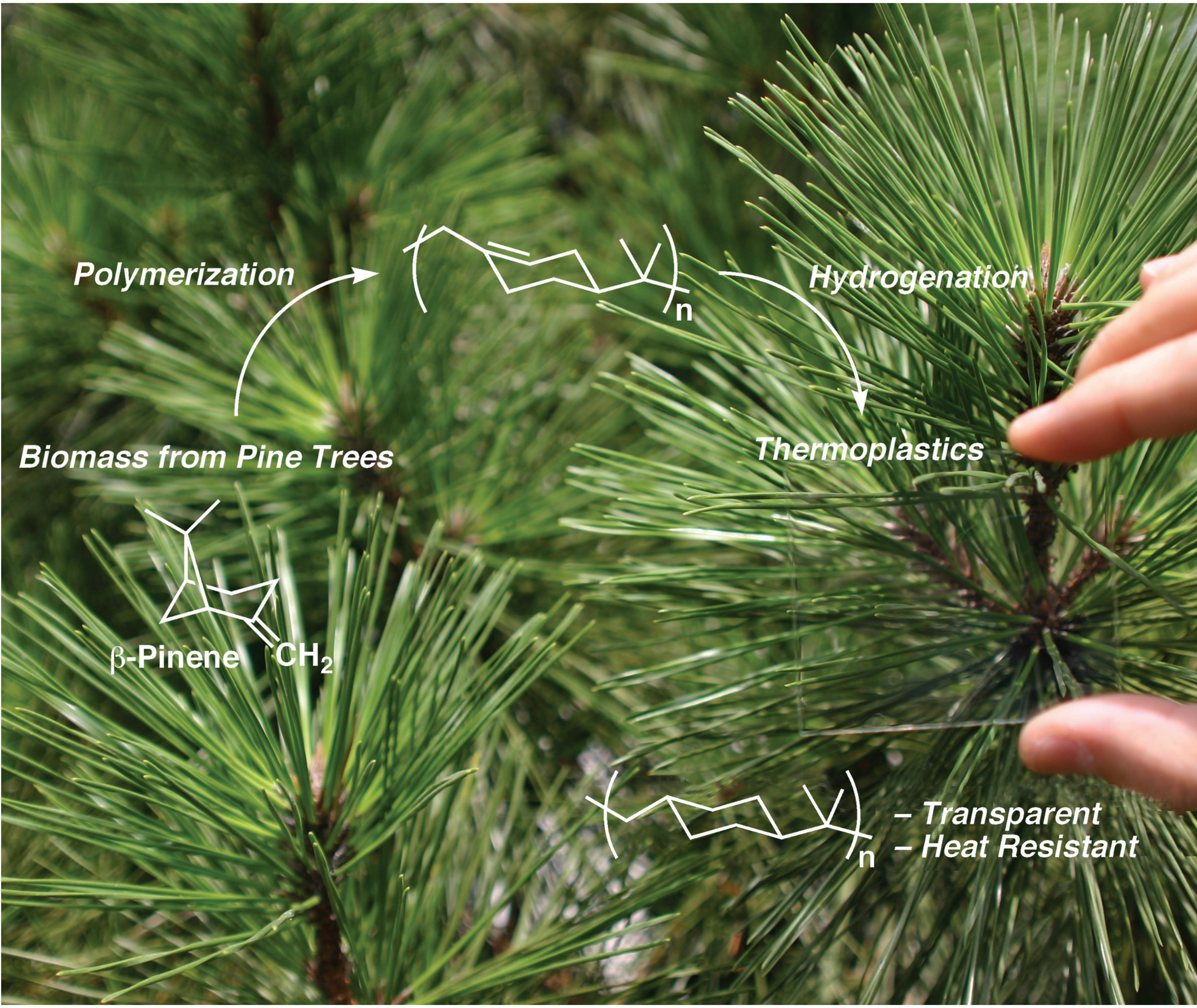

ISSN 1463-9262

Clark *et al.*
Green chemistry and the biorefinery

Satoh *et al.*
Biomass-derived heat-resistant alicyclic hydrocarbon polymers

Petrus and Noordermeer
Biomass to biofuels, a chemical perspective

Tundo *et al.*
Green chemistry: a tool for socio-economic development and environmental protection

RSC Publishing

1463-9262(2006)8:10;1-Z

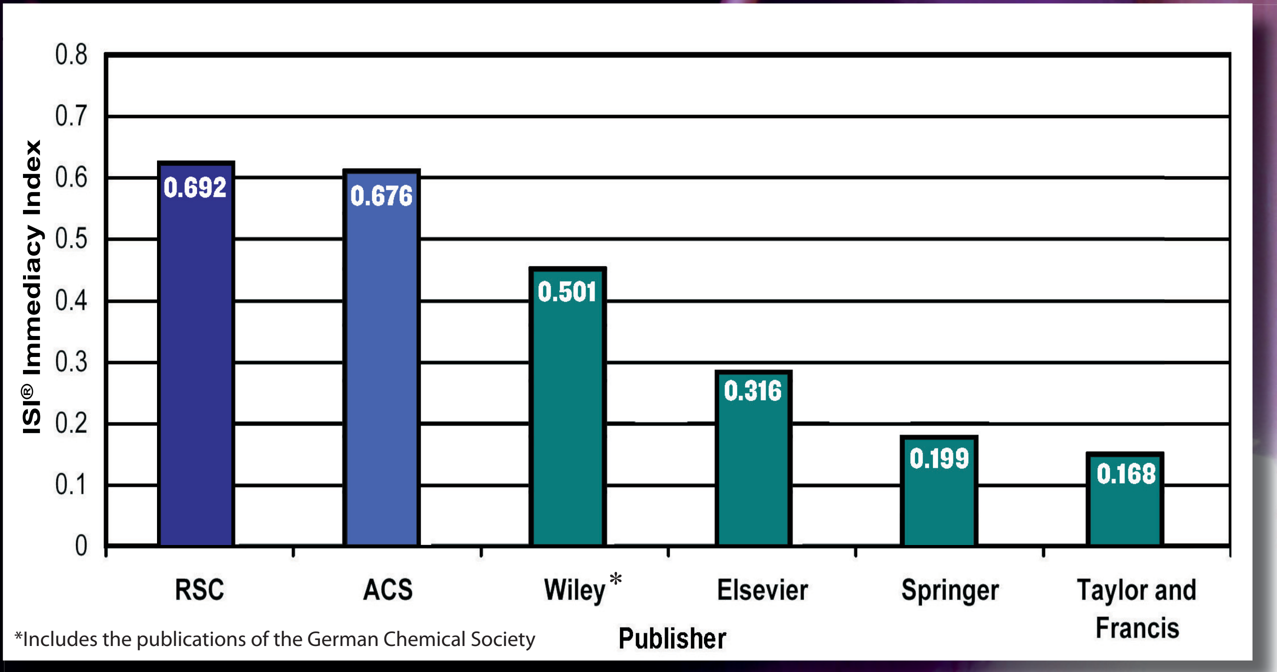
0.8
0.7
0.6
0.5
0.4
0.3
0.2
0.1
0
ISI® Immediacy Index
0.692
0.676
0.501
0.316
0.199
0.168
RSC
ACS
Wiley*
Elsevier
Springer
Taylor and Francis
Publisher

Green Chemistry

Cutting-edge research for a greener sustainable future
www.rsc.org/greenchem

RSC Publishing is a not-for-profit publisher and a division of the Royal Society of Chemistry. Any surplus made is used to support charitable activities aimed at advancing the chemical sciences. Full details are available from www.rsc.org

IN THIS ISSUE

ISSN 1463-9262 CODEN GRCHFJ 8(10) 841–928 (2006)

Cover
β-Pinene, obtained from pine trees, was polymerized by cationic polymerization and subsequently hydrogenated to give heat-resistant alicyclic hydrocarbon polymers, which can be used as biomass-derived optoelectronic materials with good transparency and nonhygroscopicity.
Image reproduced by permission of Masami Kamigaito, from *Green Chem.*, 2006, **8**(10), 878.

CHEMICAL TECHNOLOGY

NEWS

Green Chemistry

Cutting-edge research for a greener sustainable future

www.rsc.org/greenchem

Green Chemistry focuses on cutting-edge research that attempts to reduce the environmental impact of the chemical enterprise by developing a technology base that is inherently non-toxic to living things and the environment.

EDITORIAL STAFF

Editor
Sarah Ruthven

News writer
Markus Hölscher

Publishing assistant
Emma Hacking

Team leader, serials production
Stephen Wilkes

Technical editor
Edward Morgan

Administration coordinator
Sonya Spring

Editorial secretaries
Lynne Braybrook, Jill Segev, Julie Thompson

Publisher
Emma Wilson

Green Chemistry (print: ISSN 1463-9262; electronic: ISSN 1463-9270) is published 12 times a year by the Royal Society of Chemistry, Thomas Graham House, Science Park, Milton Road, Cambridge, UK CB4 0WF.

All orders, with cheques made payable to the Royal Society of Chemistry, should be sent to RSC Distribution Services, c/o Portland Customer Services, Commerce Way, Colchester, Essex, UK CO2 8HP. Tel +44 (0) 1206 226050; E-mail sales@rscdistribution.org

2006 Annual (print + electronic) subscription price: £859; US$1571. 2006 Annual (electronic) subscription price: £773; US$1414. Customers in Canada will be subject to a surcharge to cover GST. Customers in the EU subscribing to the electronic version only will be charged VAT.

If you take an institutional subscription to any RSC journal you are entitled to free, site-wide web access to that journal. You can arrange access via Internet Protocol (IP) address at www.rsc.org/ip. Customers should make payments by cheque in sterling payable on a UK clearing bank or in US dollars payable on a US clearing bank. Periodicals postage paid at Rahway, NJ, USA and at additional mailing offices. Airfreight and mailing in the USA by Mercury Airfreight International Ltd., 365 Blair Road, Avenel, NJ 07001, USA.

US Postmaster: send address changes to Green Chemistry, c/o Mercury Airfreight International Ltd., 365 Blair Road, Avenel, NJ 07001. All despatches outside the UK by Consolidated Airfreight.

PRINTED IN THE UK

EDITORIAL BOARD

INTERNATIONAL ADVISORY EDITORIAL BOARD

INFORMATION FOR AUTHORS

Full details of how to submit material for publication in Green Chemistry are given in the Instructions for Authors (available from http://www.rsc.org/authors). Submissions should be sent *via* ReSourCe: http://www.rsc.org/resource.

Authors may reproduce/republish portions of their published contribution without seeking permission from the RSC, provided that any such republication is accompanied by an acknowledgement in the form: (Original citation) – Reproduced by permission of the Royal Society of Chemistry.

Royal Society of Chemistry: Registered Charity No. 207890

HIGHLIGHT

851

Highlights

Markus Hölscher reviews some of the recent literature in green chemistry.

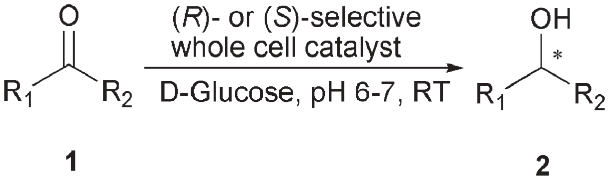

PERSPECTIVE

853

Green chemistry and the biorefinery: a partnership for a sustainable future

James H. Clark,* Vitaly Budarin, Fabien E. I. Deswarte, Jeffrey J. E. Hardy, Fran M. Kerton, Andrew J. Hunt, Rafael Luque, Duncan J. Macquarrie, Krzysztof Milkowski, Aitana Rodriguez, Owain Samuel, Stewart J. Tavener, Robin J. White and Ashley J. Wilson

By applying green chemical technologies to the transformation of biomass feedstock in biorefineries, we can build up new environmentally sustainable chemicals and materials industries.

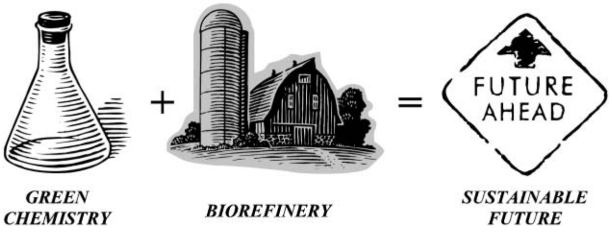

CRITICAL REVIEW

861

Biomass to biofuels, a chemical perspective

Leo Petrus and Minke A. Noordermeer*

Biofuels are an interesting sustainable option for the transport sector. The preferred use of biofuels in the current car fleet, as a blend with fossil fuels, has a large impact on the required biofuel product characteristics.

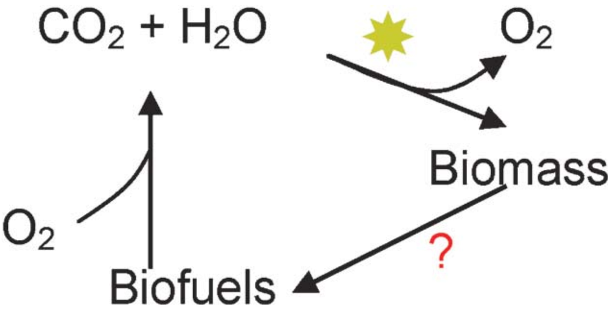

COMMUNICATIONS

868

Simple and eco-friendly reduction of nitroarenes to the corresponding aromatic amines using polymer-supported hydrazine hydrate over iron oxide hydroxide catalyst

Qixun Shi, Rongwen Lu,* Kun Jin, Zhuxia Zhang and Defeng Zhao

Polymer-supported hydrazine hydrate as a hydrogen donor has been used in the reduction of nitroarenes, which efficiently solves the problem of environmental pollution resulting from the release of excess hydrazine hydrate.

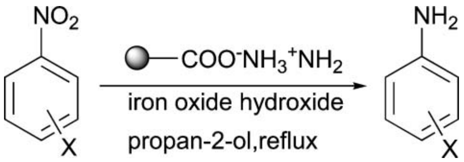

COMMUNICATIONS

871

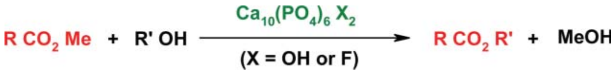

$$RCO_2Me + R'OH \xrightarrow[(X = OH\ or\ F)]{Ca_{10}(PO_4)_6X_2} RCO_2R' + MeOH$$

Transesterifications catalysed by solid, reusable apatite–zinc chloride catalysts

Abderrahim Solhy,* James H. Clark,* Rachid Tahir, Said Sebti and Mohamed Larzek

Hydroxyapatite and fluoroapatite materials are used for the first time as effective catalysts in transesterification reactions.

875

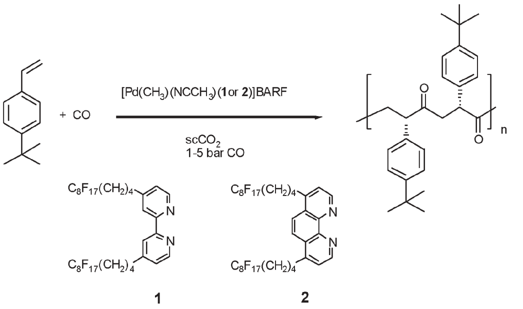

Alternating CO/*tert*-butylstyrene copolymerisation using soluble cationic palladium complexes in supercritical carbon dioxide

Marta Giménez-Pedrós, Clara Tortosa-Estorach, Amaia Bastero, Anna M. Masdeu-Bultó,* Maurizio Solinas and Walter Leitner*

Polyketones (M_w up to 87 000 g mol^{-1}) with low polydispersities have been obtained by CO/*tert*-butylstyrene copolymerisation in supercritical carbon dioxide using Pd complexes with perfluorinated bipyridine and phenanthroline ligands.

PAPERS

878

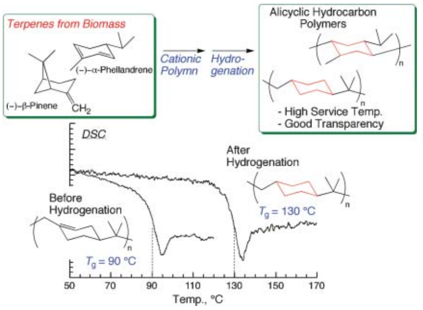

Biomass-derived heat-resistant alicyclic hydrocarbon polymers: poly(terpenes) and their hydrogenated derivatives

Kotaro Satoh, Hiroko Sugiyama and Masami Kamigaito*

Naturally-occurring terpenes, such as (−)-β-pinene and (−)-α-phellandrene, were cationically polymerized and subsequently hydrogenated into stable alicyclic hydrocarbon polymers with high glass transition and degradation temperatures.

883

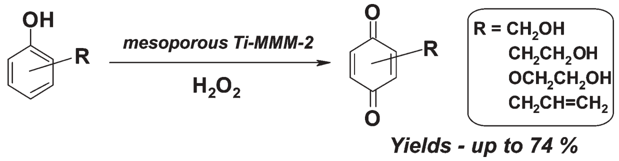

H_2O_2-Based oxidation of functionalized phenols containing several oxidizable sites to *p*-quinones using a mesoporous titanium-silicate catalyst

Olga V. Zalomaeva, Oxana A. Kholdeeva and Alexander B. Sorokin*

The oxidation of different phenols bearing oxidizable functional groups with aqueous H_2O_2 produces valuable synthetic building blocks with good to moderate yields keeping the other oxidizable sites intact.

887

Transesterification of methylsulfate and ethylsulfate ionic liquids—an environmentally benign way to synthesize long-chain and functionalized alkylsulfate ionic liquids

Simone Himmler, Stefanie Hörmann, Roy van Hal, Peter S. Schulz and Peter Wasserscheid*

A new environmentally friendly method to synthesize long-chain and functionalized alkylsulfate ionic liquids is reported. The reaction is halide-free, liberates methanol or ethanol as the only by-products, is solvent-free and scale-up is straight forward.

Synthesis protocol for the transesterification reaction

$$[NR_3R'][R'OSO_3] + R''OH \xrightarrow{H^+} [NR_3R'][R''OSO_3] + R'OH$$

R'=Me, Et

895

Microwave-assisted cationic ring-opening polymerization of a soy-based 2-oxazoline monomer

Richard Hoogenboom and Ulrich S. Schubert*

Microwave-assisted cationic ring-opening polymerization of a soy-based 2-oxazoline monomer led to the formation of well-defined polymers. The unsaturated fatty acid side chains of these polymers were applied to cross link the material.

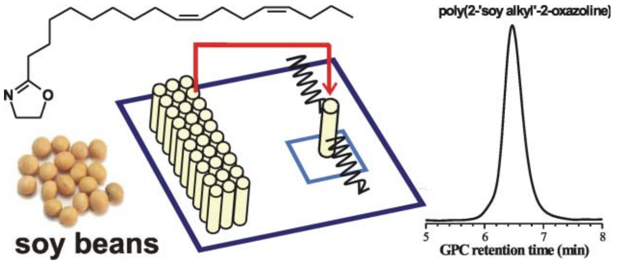

900

An environmentally benign catalytic system for alkene epoxidation with hydrogen peroxide electrogenerated *in situ*

Kam-Piu Ho, Tak Hang Chan and Kwok-Yin Wong*

Hydrogen peroxide was electrogenerated *in situ* in bicarbonate solutions for the epoxidation of various alkenes using Mn^{2+} as the catalyst.

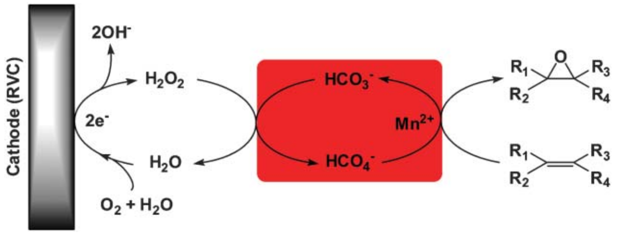

906

Comparative analysis of solvation and selectivity in room temperature ionic liquids using the Abraham linear free energy relationship

Michael H. Abraham and William E. Acree, Jr.*

The RTILs have solvation properties quite close to those for polar aprotic organic solvents.

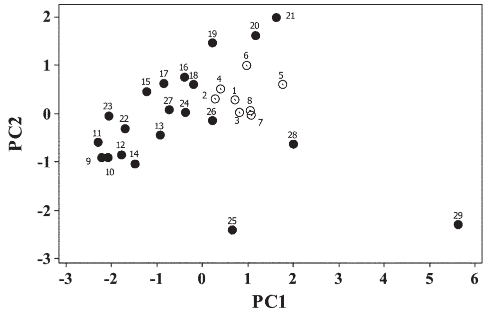

PAPERS

916

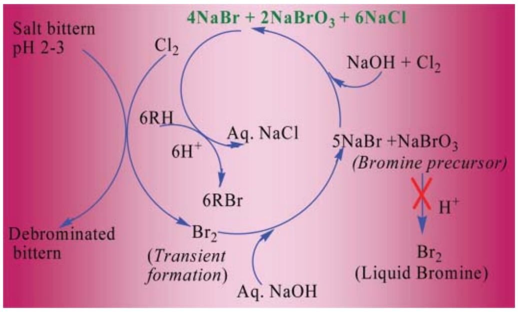

Eco-friendly and versatile brominating reagent prepared from a liquid bromine precursor

Subbarayappa Adimurthy, Gadde Ramachandraiah,* Ashutosh V. Bedekar, Sudip Ghosh, Brindaban C. Ranu* and Pushpito K. Ghosh*

Facile bromination of various organic substrates with high atom efficiency has been demonstrated with a 2 : 1 bromide : bromate reagent prepared cost-effectively from the intermediate stream of bromine recovery by cold process, thereby eliminating the formation and use of liquid bromine.

923

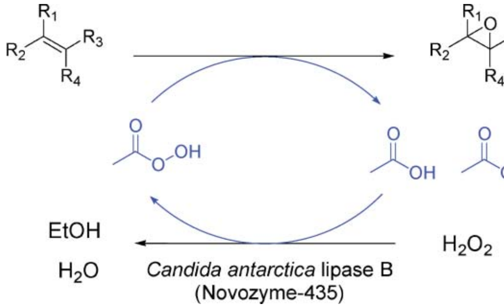

Lipase-mediated epoxidation utilizing urea–hydrogen peroxide in ethyl acetate

Emanuel G. Ankudey, Horacio F. Olivo* and Tonya L. Peeples

A practical and simple procedure for the epoxidation of electron rich alkenes utilizes a catalytic amount of Novozyme-435 and a stoichiometric amount of urea–hydrogen peroxide in ethyl acetate.

AUTHOR INDEX

FREE E-MAIL ALERTS AND RSS FEEDS

Contents lists in advance of publication are available on the web *via* www.rsc.org/greenchem - or take advantage of our free e-mail alerting service (www.rsc.org/ej_alert) to receive notification each time a new list becomes available.

RSS Try our RSS feeds for up-to-the-minute news of the latest research. By setting up RSS feeds, preferably using feed reader software, you can be alerted to the latest Advance Articles published on the RSC web site. Visit www.rsc.org/publishing/technology/rss.asp for details.

ADVANCE ARTICLES AND ELECTRONIC JOURNAL

Free site-wide access to Advance Articles and the electronic form of this journal is provided with a full-rate institutional subscription. See www.rsc.org/ejs for more information.

* Indicates the author for correspondence: see article for details.

Electronic supplementary information (ESI) is available *via* the online article (see http://www.rsc.org/esi for general information about ESI).

European Science Open Forum—ESOF2006 München, 15–18 July, 2006. Report on the session. *Green chemistry: a tool for socio-economic development and environmental protection*

DOI: 10.1039/b611593b

Green chemistry claims success at the 2006 European Science Open Forum. The session "Green chemistry: a tool for socio-economic development and environmental protection" was a popular one as is described by Pietro Tundo, Alvise Perosa and Alberto Procopio.

ESOF2006 was the second pan-European General Science Meeting held in Munich at the Forum am Deutschen Museum and the Deutsches Museum from July 15th to 19th, 2006, whose purpose was to promote interaction and dialogue between science and the general public.

Seven scientific themes were chosen to reflect the sessions: Combining Cultures, Dealing with Disasters, Earth and Environment, Particles and Planets, Science and Society, Fabric of Science, Workings of Life.

Finally success for green chemistry! It claimed its place on the same level as other more popular scientific disciplines and topical issues such as natural disaster prevention, biodiversity, genomics, evolution, medical science, and astronomy.

Within the Earth and Environment theme, green chemistry was indicated as one of the main options for environmental safeguarding, and this was highlighted on the posters placed at the entrance of the meeting. Plus, the session on green chemistry that took place in Munich represented the only session on chemistry.

"*Is green chemistry a real option?*" This question shows clearly what the press and society ask of chemistry. And a positive answer to this question was given by the panellists: Tundo, Poliakoff, Seddon, Mours, and Sydnes during the 2.5 h long session held on Sunday afternoon entitled: "*Green chemistry: a tool for socio-economic development and environmental protection*".

The crowded event was moderated by Barbara Schwerdtfeger, a science journalist. Among the participants were Francesco Fedi president of COST (European Cooperation in the field of Science and Technical Research), and Howard Moore senior advisor of ICSU (International Council for Science), and of the press (Berliner Zeitung), all wanted to know why green chemistry is an option, and why they should care.

The definition of green chemistry was illustrated by Martyn Poliakoff from Nottingham, who also showed how green chemistry is starting to move from academic research to industrial applications.

The international context, expectations, and philosophy were described in depth by Pietro Tundo from Venice, who placed emphasis on the need of green chemistry to foster development in developing nations, and on the newest international networking initiatives (see Box 1 and Box 2). Kenneth Seddon from Belfast illustrated one of the most recent and important networks, the International Green Network, founded by the G8 ministers of research, which is now starting thanks to national government funding of its activities.

Marian Mours of CEFIC (European Chemical Industry Council) offered the

IGN The mission of the International Green Network (IGN) includes research, coordination and sponsorship for scientific collaborations, targeted training for a new generation of scientists, and the support of sustainable development. IGN consists of eight research centres, one in each of the G8 countries, and it will accelerate movement towards a sustainable energy and materials economy by bringing together scientists, engineers, research institutions, firms, analysts and government regulators.

MEGREC The Mediterranean Green Chemistry Network constitutes a platform for the development of research and training in green chemistry in the countries of the Mediterranean basin, with focus on water management, exploitation of local natural resources, production and use of fertilizers, and monitoring and reducing the presence of toxic compounds in the food chain. With a clear focus on local priorities, but with the extended know-how of all the partners.

industrial perspective on green chemistry, and Leiv Sydnes, past president of IUPAC, from Bergen demonstrated how green chemistry is needed in order to address some of the major concerns affecting humanity, such as poverty, lack of resources in the developing nations, and widespread pollution.

The presentations were followed by an hour long discussion based on questions from the audience. Both science policy and research issues were addressed, as well as possible actions on how to improve the public understanding of chemistry.

Later on the same day, an informal and entertaining "round-up" of the day's sessions was presented by Quentin Cooper, a BBC radio science journalist. During this informal, and widely attended event two of the five speakers represented the green chemistry session: Ken Seddon and Martyn Poliakoff. They were targeted with numerous questions by the audience and proved that the green chemistry session was a large success and that awareness for chemistry is certainly rising.

The idea of this session was initiated, proposed and supported by the Interuniversity Consortium, INCA (www.unive.it/inca). It is the latest of a series of initiatives that are placing Europe in the lead in green chemistry.

Pietro Tundo, **Alvise Perosa and Alberto Procopio**
Consorzio Interuniversitario Nazionale "la Chimica per l'Ambiente" INCA, Italy

Highlights

DOI: 10.1039/b612784n

Markus Hölscher reviews some of the recent literature in green chemistry.

CO_2 and argon dependant surfactant switch

The stabilization of emulsions at certain stages of a variety of applications (*i.e.* manufacturing, oil recovery, chemical syntheses) is mandatory for the corresponding process to work. However at earlier or later stages it would be helpful to simply demulsify the corresponding emulsion, as these stages do not work or are hindered in the presence of an emulsion. If cleavable surfactants are used the emulsion can be broken, however the single components of the surfactant remain in solution, which again is undesirable in terms of efficient separation, work-up *etc*. Switchable surfactants, therefore, could help enormously as they can be turned "on" at a certain stage of the desired process and switched "off" at other stages, helping in this way to create more efficient and also more sustainable processes. Jessop *et al.* from Queen's University very recently investigated the switchability of amidine based surfactants which are tuned by using environmentally benign gases (CO_2, air).[1] Water–amidine or alcohol–amidine mixtures in the presence of CO_2 react to form the corresponding bicarbonate or alkylcarbonate salts.

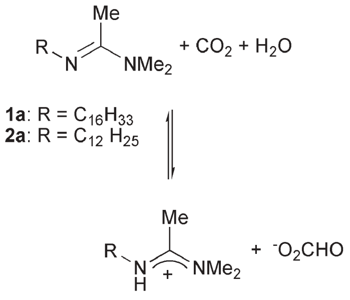

2a, **2b**

When N_2 or argon is bubbled through the resulting solution the process is reversed, re-generating the amidines. The authors performed a variety of checks of the applicability of the switch-concept. Mixtures of hexadecane and water in the presence of surfactant **1a** and after treatment with CO_2 remained stable for up to 3 hours, while the emulsion began to separate immediately when no CO_2 was used prior to mixing. When argon was bubbled through the stabilized solution the phases separated into two clear layers. The approach also was applied for emulsion polymerisations. Styrene was polymerized in a styrene–water emulsion, which was stabilized by **2b** under CO_2. When argon or nitrogen were bubbled through the mixture at elevated temperatures the surfactant was switched off and the polymer separated and settled.

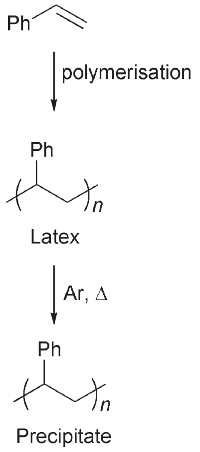

Without the Ar/N_2 treatment the polymer did not separate within a period of 3 days. Nanoparticle synthesis, polymerisations and also applications in the oil industry might benefit from this new technique significantly.

Crystalline walls in a mesoporous aluminosilicate

Microporous aluminosilicates are interesting materials as *e.g.* heterogeneous solid acid catalysts or adsorbents, and as such can contribute significantly to environmentally friendly catalytic processes. However, in contrast to their small pore counterparts the zeolites, they have amorphous walls, which are relatively unstable with regard to thermal or hydrothermal treatment, which severely limits their application. If the walls of the mesoporous materials could be altered from the amorphous to the crystalline state the material would retain its shape selective properties while thermal and chemical stability should increase. Accordingly the synthesis of such materials has been investigated, however one major step forward has only recently been made by the group of Hu from Dalian University of Technology.[2] The approach was to synthesize the mesoporous material with the mesopores filled by a carbon-based template in the first step. In the second step the amorphous walls are allowed to recrystallize in the presence of a template commonly used for zeolite synthesis, while the chemically inert carbon-based template remains in the mesopores. Under hydrothermal conditions, the presence of the zeolite template should then induce the formation/reordering of the amorphous walls into crystalline, zeolitic material. The authors used SBA-15/CMK-5 nanocomposite material, which was impregnated with tetrapropylammonium hydroxide solution in the presence of methanol. After evaporation of the organic solvent the mixture was sealed in an autoclave containing water to produce steam during the heating period. After cooling and work-up the carbon material was removed by heating in N_2 and O_2, and the template free material, named OMZ-1, was subjected to the typical set of analyses. XRD diffraction in the low angle area showed the typical reflections of hexagonally ordered materials with wide diameters. Additionally the wide-angle reflection data suggested the ZSM-5 zeolite structure to be present in the walls. The surface area was determined to be *ca.* 400 g m^{-2}, clearly showing the accessibility of the inner surface. Severe treatments to check the thermal and hydrothermal stability were applied to the OMZ-1 material showing high stability of both the mesopore and micropore structure. Catalytic performance of zirconium containing

Zr–OMZ-1 was tested in methylation of 2-methylnaphthalene, yielding either 2,6- or 2,7-dimethylnaphthalene (DMN). Conversion was determined to be 44%, with a ratio of 2,6-DMN to 2,7-DMN ranging between 2.6 and 2.7.

Ketone reduction with "designer cells" at high substrate concentrations

The synthesis of optically active alcohols can be accomplished by asymmetric ketone reduction using alcohol dehydrogenases. To make this environmentally friendly technology competitive in comparison to the highly efficient metal catalysed hydrogenation, it is mandatory to achieve a high substrate concentration in industrial applications and to be able to work without an "external" cofactor. Gröger and May from Degussa AG reported on such a novel technology, in which "designer cells", with high expression of the enzymes required, are used with no "external" cofactor.[3] Substrate concentrations were higher than 100 g L^{-1} and the desired *R*- and *S*-alcohols were obtained with conversions of higher than 90% and *ee*-values of >99%.

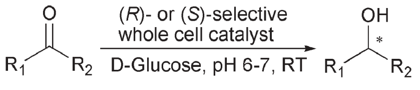

1 2

The concept relies on the use of cells which express the alcohol dehydrogenase. The host organism was *E. coli* DSM14459, while the genes coding for *S*-selective alcohol dehydrogenase from *Rhodococcus erythropolis* and glucose dehydrogenase from *Bacillus subtilis* were ligated into one plasmid (pNO14c). The reaction can be performed in water or aqueous buffer solution. A variety of ketones could be enantioselectively reduced, and very interesting for further chemical modifications is the fact that substrates can be used which carry another functional group, such as acetophenones carrying halogen atoms in the α-position.

Implementation Action Plan of the European Technology Platform for Sustainable Chemistry

The European Technology Platform for Sustainable Chemistry was founded in 2004 mainly by Cefic and EuropaBio, but the partnership was quickly extended to a number of partners, such as Dechema, ESAB, the GDCh and the RSC. The platform is devoted to creating and maintaining highly competitive chemical research for sustainable industrial chemistry production in Europe. After publication of a vision document in early 2005, the organisation developed a Stategic Research Agenda (SRA) in November 2005, which outlined the future priorities for European research efforts. In August 2006 an Implementation Action Plan (IAP) followed, that describes how the research priorities can be implemented in practice. The focus of this action plan is to describe the steps that need to be taken on the most important/urgent issues defined in the SRA. Among others, the platform defined the bio-based economy, energy, nanotechnology and sustainable product and process design to be the most urgent topics that need to be addressed. The IAP defines in high detail the different topics that need investigation/realisation within an issue, and shows how progress should be generated. It is an ambitious plan, but the efforts are worth it, as one of the central ideas behind the platform is no less than keeping Europe's academic and industrial chemistry competitive and sustainable, to help prevent the danger of Europe becoming a net importer of chemical products by 2015. The whole IAP can be downloaded from www.suschem.org.

Carbon dioxide storage testing in Ketzin

Since 1750 the burning of coal by mankind has released *ca.* 150 gigatonnes of carbon into the planet's atmosphere. Carbon dioxide levels in the atmosphere should not get higher than 550 ppm, the current level being *ca.* 380 ppm, while it was about 280 ppm in the 18th century. If the desired level is to be met, about a third of the emissions expected in the next 50 years must be avoided. How could that be done? Among other ways, one currently emerging technology is the carbon capture and storage (CCS) approach, by which carbon dioxide is pumped back into the earth by injecting the gas into water reservoirs far under the surface of the earth.[4] Ketzin, a small village not very far away from Berlin, is one of the testing areas for this new technology in Germany. During the next two years, it is planned to inject *ca.* 60 000 tons of CO_2 into a water layer 700 m beneath the village, and it is, with other spots on the earth, considered a model case to evaluate the storage with regard to leaking and other issues. If one would like to lock away *ca.* 250 million tonnes of carbon per year, which equals about 4% of the yearly emissions, one would need to inject 25 to 35 million barrels per day. This is certainly a technological challenge, however it only accounts for approximately one third of the flow of oil coming from reservoirs. As a result it should be possible to put this technology into practice. A good start would be to build the 1400 gigawatts worth of new coal plants needed to satisfy the estimated increase in energy demand (1.7% up to 2030) near appropriate reservoirs and directly inject the combustion gas. Governments worldwide have, by and large, been reluctant, which makes scientists believe that the new technology only will have a chance if the price of carbon dioxide emission rises substantially.

References

1 Y. Liu, P. G. Jessop, M. Cunningham, C. A. Eckert and C. L. Liotta, *Science*, 2006, **313**, 958–960.
2 Y. Fang and H. Hu, *J. Am. Chem. Soc.*, 2006, **128**, 10636–10637.
3 H. Gröger, F. Chamouleau, N. Orologas, C. Rollmann, K. Drauz, W. Hummel, A. Weckbecker and O. May, *Angew. Chem.*, 2006, **118**, 5806–5809.
4 Q. Schiermeier, *Nature*, 2006, **442**, 620–623.

Green chemistry and the biorefinery: a partnership for a sustainable future

James H. Clark,* Vitaly Budarin, Fabien E. I. Deswarte, Jeffrey J. E. Hardy,† Fran M. Kerton,‡ Andrew J. Hunt, Rafael Luque, Duncan J. Macquarrie, Krzysztof Milkowski, Aitana Rodriguez, Owain Samuel, Stewart J. Tavener, Robin J. White and Ashley J. Wilson

Received 27th March 2006, Accepted 24th July 2006
First published as an Advance Article on the web 14th August 2006
DOI: 10.1039/b604483m

Research into renewable bioresources at York and elsewhere is demonstrating that by applying green chemical technologies to the transformation of typically low value and widely available biomass feedstocks, including wastes, we can build up new environmentally compatible and sustainable chemicals and materials industries for the 21st century. Current research includes the benign extraction of valuable secondary metabolites from agricultural co-products and other low value biomass, the conversion of nature's primary metabolites into speciality materials and into bioplatform molecules, as well as the green chemical transformations of those platform molecules. Key drivers for the adoption of biorefinery technologies will come from all stages in the chemical product lifecycle (reducing the use of non-renewable fossil resources, cleaner and safer chemical manufacturing, and legislative and consumer requirements for products), but also from the renewable energy industries (adding value to biofuels through the utilisation of the chemical value of by-products) and the food industries (realising the potential chemical value of wastes at all stages in the food product lifecycle).

Introduction

While the 20th century saw the emergence and establishment of an organic chemicals manufacturing industry based on petroleum refining, the 21st century will see the development of a new organics industry based on biomass refining.[1–3] In both scenarios the driver is energy. The enormous demand for petroleum as a cheap, single-use fuel gave chemical manufacturing a large volume, low cost and continuous supply of hydrocarbons from which the petrochemical industry was built; chemical and engineering technology for cracking, separating, rearranging, polymerising and functionalising allowed us to take complex mixtures of simple chemicals and transform them into a multitude of higher value molecules with a seemingly never-ending range of applications from high volume, low cost plastics to small volume but highly expensive drugs. We are now at the beginning of an era where new, renewable sources of energy are sought with increasing vigour; biomass, renewable carbon, is guaranteed a place in the new energy portfolio for the foreseeable future. The growth in the bioenergy (*e.g.* biomass gasification) and biofuels (*e.g.* biodiesel) industries will add to the food industries in the consumption of renewable carbon.[2] Food production is wasteful—from the crop residues (*e.g.* wheat straw) through the processing (where substantial losses occur) to sale and consumption, we throw away an obscenely high proportion of food. However, what is *waste* to food manufacturing can be *feed* to the chemicals, energy and other industries. Wheat straw contains significant quantities of valuable wax compounds (fatty alcohols, alkanes, *etc*) and the lignocellulosic fraction can be used to make paper or ethanol;[4] rice husks from rice farming can be burned to yield the energy needed to drive the farm machinery, and the residues are rich in silica[5] that has diverse application value. Used food oils can be recovered and, through chemical transformation, turned into biodiesel.[6] The same biodiesel manufacturing process, encouraged by tax incentives and government targets for biofuel utilisation, produces glycerol as a co-product, which, through the right chemistry, can be turned into numerous higher value products. Food wastes can no longer be landfilled due to health concerns, so they ultimately need to be burned; alternatively they could be gasified and used to drive a gas turbine to produce electricity—combined heat and power units is an exciting possibility for the destination of low value residues and wastes. It may also be possible to gain chemical value from the destruction of food (and other biological) wastes; controlled pyrolysis can be used to produce small organic molecules that may have value in their own right, or in making polymeric materials, or as platform molecules for building up larger and more valuable chemical products.[7]

The refining of nature's daily bounty will provide a treasure trove of chemical potential from pre-treatment to incineration, as well as by devoting some of the raw material to bioprocessing.

A biorefinery can be considered as an integral unit that can accept different biological feedstocks and convert them to a range of useful products including chemicals, energy and materials (Fig. 1).[8,9]

Renewable resources research at York is directed at chemical aspects of biomaterials and bioenergy as well as

---

Green Chemistry Centre of Excellence, Department of Chemistry, University of York, York, UK YO10 5DD
† Current address: Royal Society of Chemistry, Burlington House, Piccadilly, London W1J 0BG
‡ Current address: Department of Chemistry, Memorial University of Newfoundland, St Johns, NLA1B 3X7, Canada.

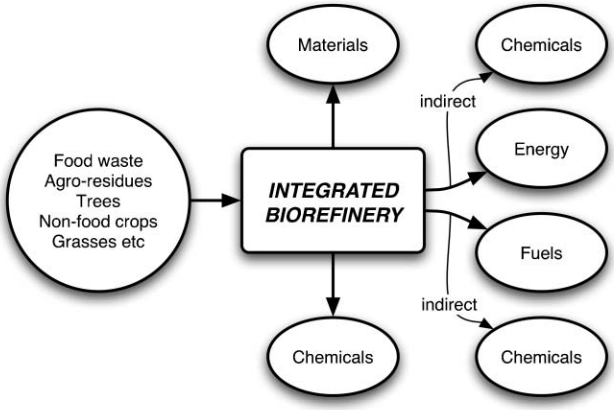

Fig. 1 The integrated biorefinery as a mixed feedstock source of chemicals, energy, fuels and materials.

bio-chemicals (Fig. 2).[10] Based on a wide range of renewable feedstocks (including low value plants such as trees, grasses and heathers; energy crops and food crops by-products; marine resource wastes and food wastes) we research the application of green chemical technologies (including supercritical fluid extraction; microwave processing; catalytic and other clean synthesis methods) with the aim of developing new, genuinely sustainable, low environmental impact routes to important chemical products, materials and bioenergy. In this article, we will outline with some new examples some of the key project areas in which we are currently engaged.

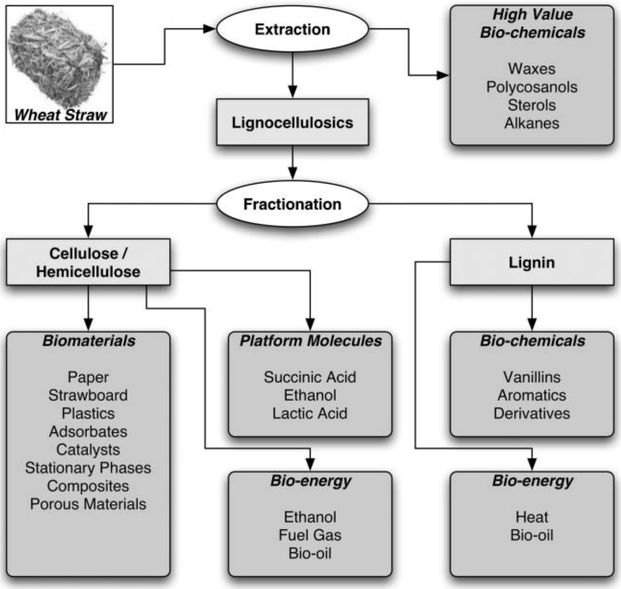

Fig. 3 The wheat straw biorefinery concept.

Supercritical fluid extraction of secondary metabolites from plant surfaces

Wheat straw is a good example of a low value, high volume agricultural by-product that can be the basis for a biorefinery. Materials, chemicals and bioenergy/fuels are all accessible from this chemically interesting feedstock (Fig. 3).[11]

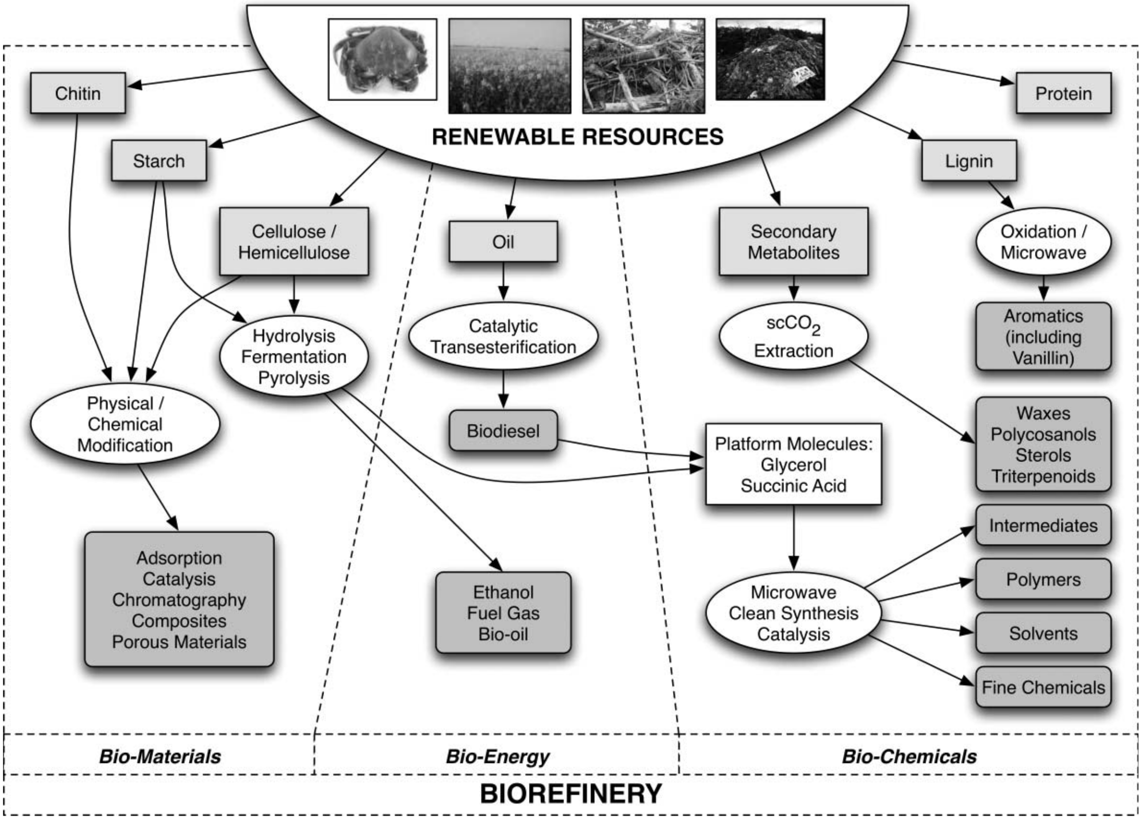

Fig. 2 Renewable Resources research at York: applying green chemistry to the biorefineries.

We recently reported the first successful use of supercritical fluid (SF) extraction and fractionation of waxes from wheat straw.[4] This can be considered as the first step in a biorefinery, with no effect on the bulk structure of the straw. Plant waxes are a complex mixture of linear compounds notably long chain alkanes, fatty alcohols and acids, and cyclic compounds, especially sterols, and while there is value in the mixture, more refined fractions can have much greater value in areas including cosmetics, insect semiochemicals and nutraceuticals.[4,12] Use of variable temperature and pressure (*T*/*P*) $scCO_2$ allowed us to fractionate the waxes on the surface of wheat straw, and to totally avoid contamination from more polar unwanted compounds that are always present in solvent extraction. The area has added appeal in countries such as the UK where we import our plant waxes and where demand is outstripping supply. An important additional factor is a growing reluctance to use animal derived products (even extending to lanolin from sheep's wool).

The use of an environmentally low impact extraction and fractionation method combined with a low or zero value feedstock is clearly attractive on both environmental and economic grounds. The potential for providing new business opportunities to rural areas, where farming income, for example, has been at a record low, completes the 'triple bottom line benefit' through social advantage.[13] We have extended the methodology to another UK-abundant low value plant material, heather (*Calluna vulgaris*). The new value in heather has a potentially important added benefit in that the poor economics of upland farming has been driving businesses away from these regions. There is a danger that these important regions will become unmanaged, with potentially devastating effects on water management—in the UK for example, some 70% of our fresh water supply comes from the uplands.[14] The surface waxes on the above ground components of heather are typically complex.[15] We demonstrated that they were rich in valuable products such as triterpenoids. The selectivity advantage of $scCO_2$ is immediately evident when comparing a typical extract with a solvent extract (Fig. 4). The chromatograms for these two mixtures are significantly different and of particular importance, the triterpenoids are almost absent from the former, both helping the purity of the $scCO_2$-derived extracts and also providing a route to triterpenoid fractionation.

It is clear that applying a benign extraction/fractionation technique to abundant and low value plants to generate valuable products has multiple benefits, especially in regions where land resource management needs better control and where the wax products are largely imported. There is even the added benefit of surface wax extraction adding to the value of the materials for use in the bioenergy and paper industries. We have taken this method up to large scale in collaboration with industry, and new product formulations based on these

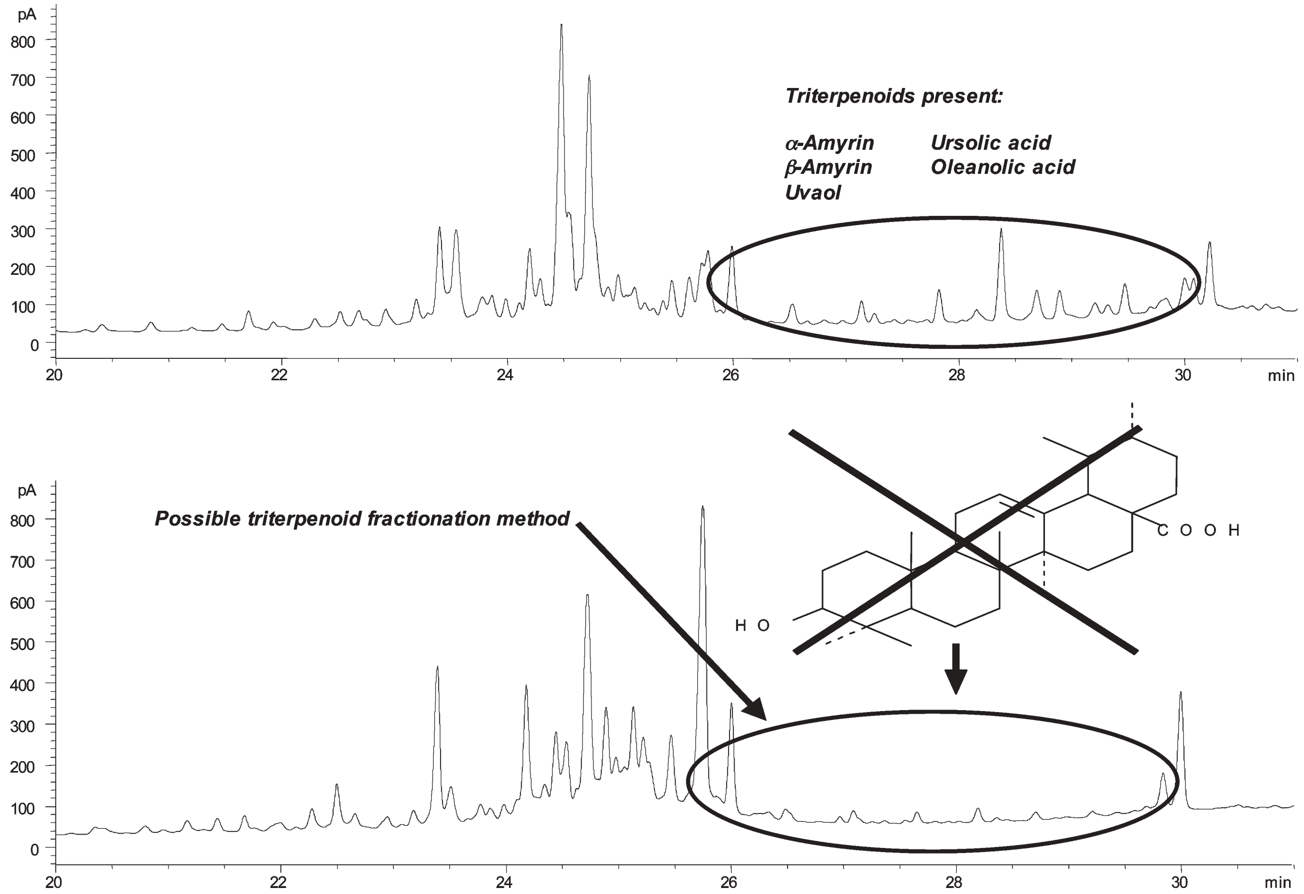

Fig. 4 Gas chromatograms of a solvent extracted sample from *Calluna vulgaris* (with triterpenoids present) and a supercritical carbon dioxide extracted sample (with no triterpenoids present).

sustainable "green" chemicals are currently being developed and tested.[4,12]

Trees as chemical factories

Trees represent an enormous renewable carbon resource in many countries worldwide.[2,16] In the UK for example, there are 2.7 million hectares of woodland. The total volume (standing biomass) of wood produced in the UK has been increasing over the past decade and future predictions suggest a continuing increase over the next twenty years. Trees planted during the boom of the 1970s and 1980s will come to maturity in the next decade, but prices for timber have slumped and the decline is continuing. Increasing supply at a time of low prices is likely to exacerbate current problems, and many plantations are unlikely to be worth extracting for timber or pulp. Finding ways of adding value to such wood resources will help stimulate rural enterprises and maintain the rural economy. This could include the utilisation of residues from the pulp and board industries such as bark. Other sources of wood currently not utilised include branches, although these can be widely scattered and their collection and transportation will consume resources. Alternatively, new wood-utilising industries could compete with the existing timber-based industries. Some examples of new applications include cellulose fibres for textiles and sawdust resins as adhesives.

Overall, only about a quarter of felled wood in Europe is converted to timber. The remainder is a rich composite of primary and secondary metabolites that are a largely unexploited resource for novel renewable products. Some of the green chemical technologies that we are applying to this challenge are shown in Fig. 5. In particular, we have been studying the major UK tree species, Sitka spruce.

We have already discussed the use of SF extraction for wheatstraw and heather. Trees are also rich in extractable secondary metabolites including terpenes, flavonoids, sterols and resin acids, as well as waxes. Some of these have been shown to be valuable including polyphenolic flavonoids as antioxidants.[17]

Among the major compounds in trees we have focused our attention on lignin and cellulose, each of which we will now discuss in more detail.

Vanillin from lignin

Lignin represents nature's greatest store of aromatic molecules and one of the greatest challenges chemists and biologists face is to find efficient and low environmental impact ways of unlocking that store.[18] Petroleum has provided us with a cheap abundance of aromatic compounds from benzene upwards, and aromatic products in pharmaceuticals, agrochemicals, polymers and many other sectors have become well established. We need to develop sustainable sources of aromatic compounds that we can build up to help compensate for a future shortfall and increasing costs of petro-derived aromatic platform molecules such as phenol.

Vanillin is one useful aromatic compound that can be obtained directly from lignin.[2,7] We have carried out preliminary studies comparing the yields of vanillin obtained by different methods of activation—conventional heating with base, microwave heating with base, and in the presence of redox metal salts (Table 1). In addition to vanillin, up to 1.3% vanillic acid was detected.

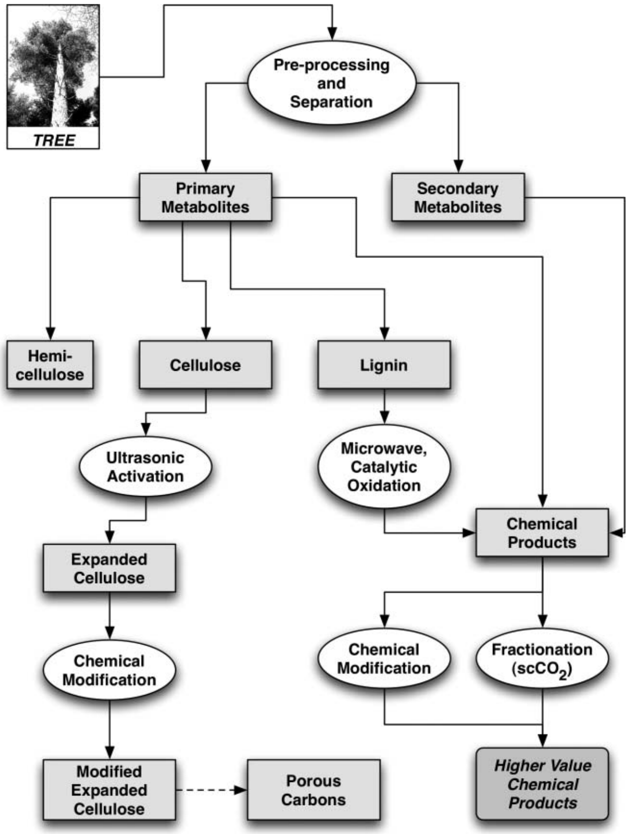

Fig. 5 Possible green chemical routes to exploit and add value to tree metabolites.

Table 1 Lignin oxidation routes to vanillin

Method	Conditions	% Vanillin (by standardised HPLC)
Conventional heating	2N NaOH/160 °C/24 h	3.5
Microwave	2N NaOH/160 °C/15 min	5.1
Conventional heating	$FeCl_3$ (0.5 wt%)/160 °C/24 h	5.8
Conventional heating	$CuSO_4$ (0.5 wt%)/160 °C/24 h	4.8

Clearly the use of microwave activation can have a dramatic effect on the reaction kinetics, which is especially important given how slow the reaction is under conventional heating. Even the presence of redox metal catalysts only causes a modest increase in the rate of reaction. We are currently investigating sequential reactions with different clean technologies, *e.g.* use of microwave activation to partly break down the lignin structure followed by catalytic oxidation using air or H_2O_2 as the two more environmentally friendly consumable sources of oxygen.

Expanded biomaterials: high value applications for cellulose and starch

We recently reported the first use of expanded starch as a stationary phase for liquid chromatography.[19] The physical expansion of starch is achieved by a gelatinisation–retrogradation–dehydration process, whereby natural starch (potato, corn, pea, *etc*) with a surface area of *ca.* 1 $m^2 g^{-1}$ is converted into a material with a surface area of 100–200 $m^2 g^{-1}$. As significantly, the starch is rendered mesoporous and with a particularly high mesopore volume/micropore volume compared to more traditional stationary phases, which is advantageous for chromatographic applications.

The initial gelatinisation step is achieved by heating in water, a process that causes swelling and then collapse of the starch granules giving a gel. Rapid gelatinisation can be achieved using microwave heating. There is even a rough correlation between the intensity of microwave radiation (fixed irradiation time but variable power) and the surface area of the final expanded material, with 300 W for 2 min giving a surface area of >190 $m^2 g^{-1}$. The subsequent retrogradation occurs on maintaining the gel at low temperatures (above the glass transition temperature) that converts the amorphous state into a more ordered state. The rate of retrogradation is dependent on the amylose content of the starch, with high amylose content materials retrograding in a few hours, while those with higher proportions of the more structurally complex amylopectin require longer periods. The final dehydration process relies on controlled removal of the bulk of the water using solvent exchange and/or exchange using supercritical CO_2.

The complete process for preparing expanded starch using ethanol in the solvent exchange is illustrated in Fig. 6. This includes scanning electron micrographs, which reveal dramatic differences between smooth, well-defined particles of normal starch and the irregular porous continuum of expanded starch. The expanded starches decompose at *ca.* 265 °C, but at temperatures somewhat below that there is evidence (by variable temperature diffuse reflectance IR spectroscopy) for some chemical changes, with the appearance of a carbonyl band probably indicative of some cleavage between glucose units and the formation of aldehyde functions. Remarkably, in the presence of a small quantity of acid, expanded starch starts to decompose and form carbonaceous materials at temperatures as low as 100 °C. We have nicknamed these materials "Starbons" since they have a combination of properties reminiscent of starch (high surface energy oxygen-rich surfaces) and carbon (developing aromatic character, insolubility), while maintaining largely mesoporous structures even up to 700 °C.[20]

The expanded starch was originally prepared as a separation medium for plant extracts—both to develop a more efficient stationary phase for complex mixtures of natural products and to keep a low environmental footprint for the whole process of extraction and separation. Better separation compared to silica has been achieved, for example in the separation of sterol esters and waxes, which can both be extracted from the surface of plants such as heather. The separation of the lipids extracted from *Calluna vulgaris* was quicker and cleaner over expanded starch compared to silica. The purification of these lipids, to remove polar lipids, pigments and sugars could be achieved using 100% hexane over expanded starch, while the equivalent separations over silica required almost twice the volume of a hexane–ether mixture (90 : 10 v/v). These observations are

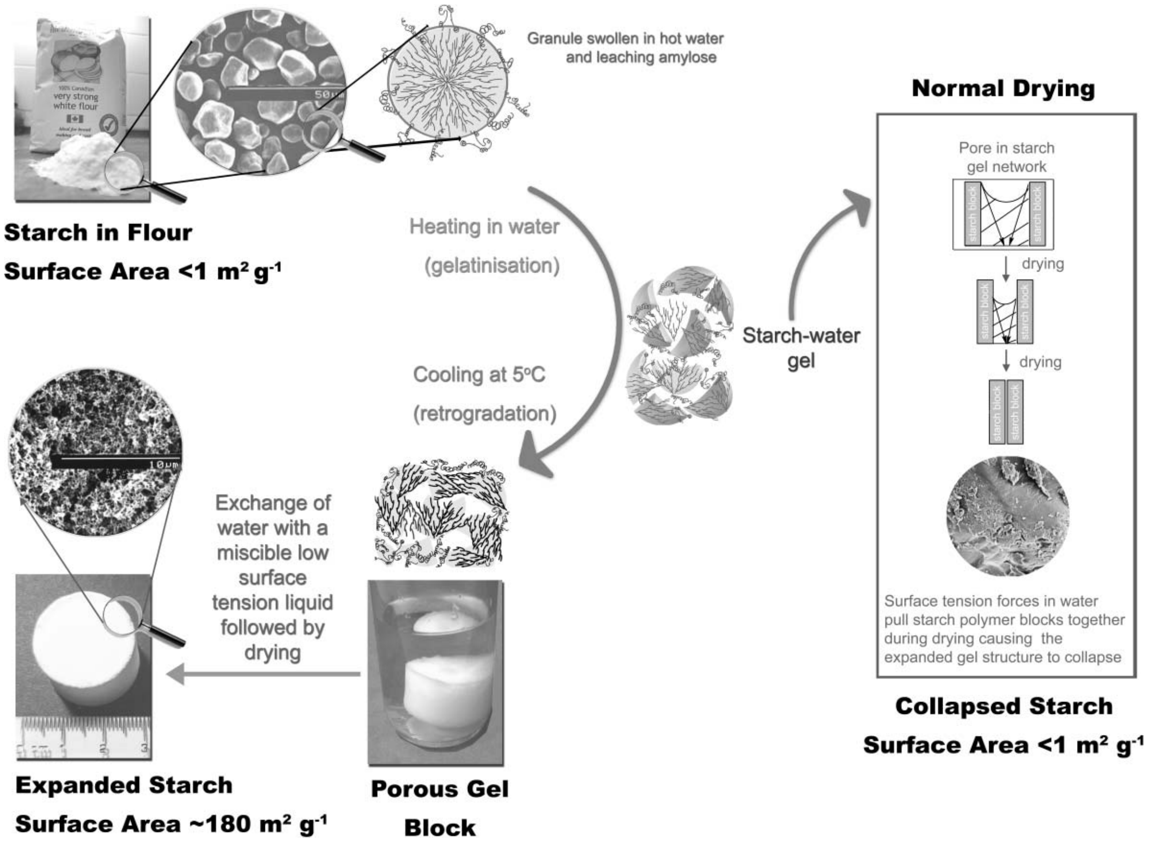

Fig. 6 Diagrammatic representation of the preparation of expanded starch.

consistent with the measured relative polarities of the two stationary phases (silica > starch). Other, and less solvent-demanding, separations over expanded starch have been consistently observed for a number of complex plant extracts in our laboratory.

Other proven applications for expanded starches include as a catalyst support,[21,22] and in composites.[23] We are currently studying other applications.

Increasing the surface area of cellulose

Cellulose, the most abundant polysaccharide on earth, consists of long linear chains of glucose. Unlike starch, it does not easily gel in water but we have found it possible to increase its surface area by first heating in water and then removing the water with ethanol. Cellulose can, however, be expanded into a higher surface area form by ultrasonic activation. Surface areas increase with time of extraction and with increasing temperature up to *ca.* 50 °C, although the maximum value we have been able to obtain is *ca.* 70 $m^2\ g^{-1}$ (Fig. 7). Ultrasonic probe activation can give these values in a matter of minutes, whereas activation in a bath is much slower.

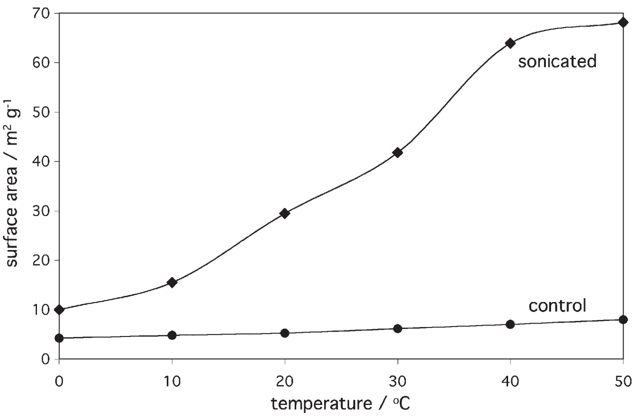

Fig. 7 Effect of temperature upon surface area of cellulose (sonicated in EtOH for 30 min).

These expanded, high surface area forms of cellulose are less stable than expanded starch with respect to water, and require storage in a dry environment. We are currently studying methods of stabilising the materials (*e.g.* in composites) and investigating applications for these low cost, easy to prepare and biodegradable porous solids. Initial results show separation abilities as a stationary chromatographic phase similar to those achieved using expanded starches, as well as the ability to trap organic molecules from solution. A detailed account of the preparation and applications of expanded cellulose will be published separately.

Chitosan

Chitosan is deacetylated chitin from the shells of crustaceans, cell walls of fungi and exoskeletons and gut linings of insects, and one of nature's largest volume materials. It is therefore truly sustainable, as well as being significantly different to nature's other large volume, renewable materials cellulose and starch in that it offers a mixture of amino and hydroxyl functions rather than hydroxyl groups alone.

The amino function opens up a number of interesting possibilities including metal binding for the remediation of toxic waste streams, applications as a solid base, and the ability to bind metal complexes for catalytic applications.[24–26]

We have shown that chitosan forms stable (leaching-resistant) complexes with palladium and nickel by borrowing surface complexation developed for silica.[27] The resulting chitosan–metal complexes show comparable activity to the original silica materials in Heck and Suzuki coupling reactions (Pd catalysts) and in Baeyer–Villiger oxidations (Ni catalysts) (Fig. 8).

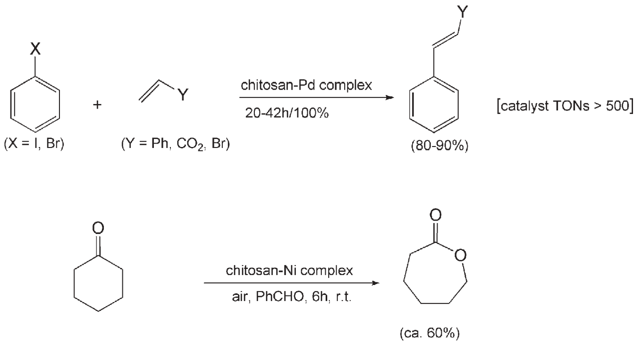

Fig. 8 Reactions catalysed by chitosan–Pd complex catalysts.

The ability to cast thin films of catalytically active materials can be very useful, for example in microreactors and in intensive processing devices, such as spinning disc reactors. We have had some success in casting chitosan films on aluminium substrates, and were then able to modify this to achieve promising catalytic activity, for example in Pd-catalysed oxidations. We have also found it is possible to cast fibres of chitosan mixed with expanded starch, further opening the way for novel applications for these renewable raw materials.

Biomass platform molecules

We have already described our research with lignin, and specifically with attempts to increase the selectivity of the cracking of this complex natural material to vanillin. This is one of a number of organic compounds that can be made in large quantities from a renewable feedstock.[7] These should steadily replace the traditional platform molecules derived from petroleum such as ethene, propene and benzene.

In green chemistry we need to apply our clean synthesis methods, including heterogeneous catalysis, to building up these new platform molecules into marketable products. Only by following renewable feedstocks with green chemical processing can we hope to build up a library of truly sustainable and environmentally friendly chemicals.

Two other interesting and very promising biomass platform molecules that we are currently studying are glycerol and succinic acid. Both are readily and sustainably obtainable from large volume raw materials, although the availability of one (glycerol) has been rapidly accelerated by political drivers (demand for biodiesel).[6] Indeed, the availability and cost of these and other biomass platform molecules are likely to be influenced as much by the complex politico-economic issues associated with the inter-related food and bioenergy aspects of the biorefinery as chemical markets.

Glycerol is the co-product in the production of biodiesel (alcohol + triglyceride to ester + glycerol). Given the political pressure and financial incentives to substantially increase the production of biodiesel, the volume of glycerol coming on to markets such as northern Europe will far exceed demand. At the time of writing, in the UK alone, over 300 companies are in the early stages of biodiesel manufacture. Reminiscent of the start of ultra-large volume petroleum production in the 1930s, the energy industry will again result in large volumes of low cost chemicals becoming available, and with reasonable expectancy of continued supply into the foreseeable future. Glycerol has been traditionally manufactured in a multi-step process starting from propene—clearly this will change as the relative price of petroleum and biomass derived molecules changes, although we must not underestimate the costs and relative complexity of working with impure, biologically derived compounds.

As a platform molecule, glycerol has good multiple functionality and a number of immediately valuable or promising products can be envisaged based on the exploitation of green chemistry and green chemical technologies. Some of these are shown in Fig. 9. This could include the use of fast and atom-efficient chlorination using HCl under microwave activation that we have recently described to products including 2,3-dichloropropanol that can easily be converted to the valuable industrial chemical, epichlorohydrin, (ironically an intermediate in one traditional route to glycerol starting from propene).[28] Glycerol reacts with environmentally benign dimethylcarbonate (prepared from the reaction of CO_2 with methanol) to form glycerol carbonate, that has been shown to be a valuable intermediate *en route* to aliphatic polyethers.[29] Amino acid-based cationic surfactants derived from glycerol have recently been reported.[30] More established chemistries for glycerol are selective reduction to 1,3-propanediol and selective oxidation to products including glyceric acid. It is vital that we develop the most environmentally benign technologies for doing this, and we are currently studying the use of highly efficient, recoverable heterogeneous catalysts, including supported metals and supported enzymes to achieve this.

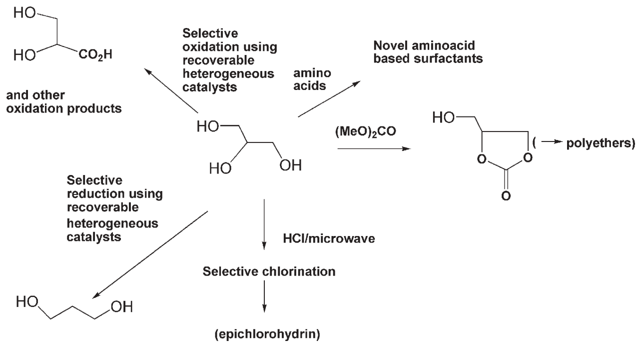

Fig. 9 Green chemical transformations of glycerol to valuable products.

Succinic acid is currently produced largely from petroleum in a multistep process (butane → maleic anhydride → maleic acid → succinic acid), amounting to *ca.* 15 × 10^3 tpa. It has a number of established markets but these are mostly speciality, as its price excludes its use as a larger volume molecule (up to €8 per kg).[31] The potential for larger volume use to make new biodegradable plastics, as well as solvents and large volume intermediates is considerable. It has been shown that bio-based succinic acid produced from glucose could be considerably cheaper than the petro-based substance, with an estimated operating cost as low as €0.5 per kg,[31,32] easily placing it in the commodity chemical price range as well as having assured sustainability of supply (*e.g.* from bioprocessing of agro and food by-products). This would open up large new markets, including polymers and solvents.

Examples of the green chemical technologies we are currently studying in relation to succinic acid, in collaboration with biochemical engineers (as well as other bio-platform molecule acids), are shown in Fig. 10. Methodologies that are tolerant of impure and dilute feeds are of particular interest to us given the high energy costs that would be associated with concentrating and purifying fermentation broths.

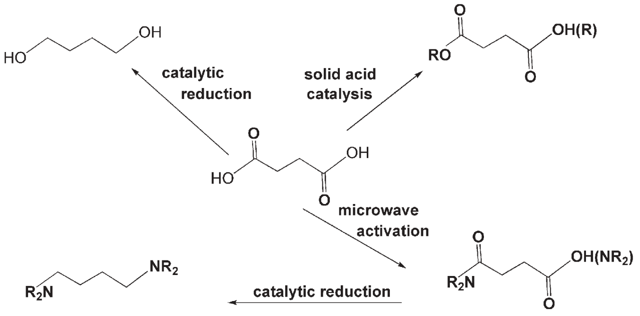

Fig. 10 Green chemical transformations for succinic acid.

Conclusion

The rapidly escalating costs of petroleum and petrochemicals are likely to accelerate the shift towards chemical products derived from renewable, biological feedstocks. While the majority of proven examples are low volume speciality chemicals, the new Solvay process for manufacturing a commodity chemical (epichlorohydrin) from bio-glycerine shows the way to larger volume chemical production.[28] We can expect more and more biorefinery-type facilities where some combination of chemical, energy and food processing are used to add value to biomass feeds. The more use we can make of food and bioenergy by-products to make chemicals, the lower the cost of those chemicals and the quicker we can expect their successful market entry. It is vital to the future of sustainable chemical production that we employ only low environmental impact chemistry to convert these by-products into valuable chemicals and materials.[33] This is likely to include benign extraction technology (*e.g.* supercritical CO_2), physical and green chemical enhancement of cellulose, chitin and starch (*e.g.* physical expansion), the use of highly efficient heating methods (*e.g.* microwave activation), and the right combination of biochemical and low environmental impact chemical methods to build up biomass platform molecules.

Green Chemistry and the biorefinery is a partnership for a sustainable future.

Acknowledgements

We are indebted to our many sponsors including EPSRC, DEFRA, the EU, Yorkshire Forward, the University of York and CSL, as well as our many collaborators, notably at the Universities of Newcastle (Chemical Engineering), Manchester (Satake Centre for Grain Processing Engineering) and CSL, and Mr Paul Elliott, Chief Technician at the York Green Chemistry Centre.

References

1 Feedstocks for the Future, ed. J. Bozell and M. K. Patel, ACS, New York, 2006.
2 Renewable Resources, ed. C. V. Stevens and R. V. Verhe, Wiley, Chichester, 2004.
3 A. J. Ragauskas, *et al.*, *Science*, 2006, **311**, 484.
4 F. E. I. Deswarte, J. H. Clark, J. J. E. Hardy and P. M. Rose, *Green Chem.*, 2006, **8**, 39.
5 V. Kalapathy, A. Proctor and J. Schultz, *Bioresour. Technol.*, 2002, **85**, 285.
6 http://www.biodiesel.org/.
7 *Top Value Chemicals from biomass*, ed. T. Werpy and G. Petoser, http://www1.eere.energy.gov/biomass/pdfs/35523.pdf.
8 http://www.nrel.gov/biomass/biorefinery.html.
9 E. Audsley and J. E. Annetts, *Agric. Syst.*, 2003, **76**, 39.
10 http://www.greenchemistry.net.
11 R. Sun, J. M. Lawther and W. B. Banks, *Ind. Crops Prod.*, 1996, **5**, 291.
12 J. H. Clark, F. E. I. Deswarte and J. J. E. Hardy, *PCT Pat. Appl.*, PCT/GB0502337.9, 2005.
13 *State of the Countryside Report*, The Countryside Agency, 2001.
14 http://www.moorlandassociation.org.
15 R. D. Pancost, M. Baas, B. V. Geel and J. S. S. Damste, *Org. Geochem.*, 2002, **33**, 675.
16 D. B. Turley, Q. Chaudhry, R. W. Watkins, J. H. Clark and F. E. I. Deswarte, *Ind. Crops Prod.*, 2006, in press.
17 H. L. Hergert, *Lignans – natural products of woody plants*, ed. J. W. Rowe, Springer Verlag, Berlin, 1989.
18 D. Fengel and G. Wegener, in *Wood Chemistry; Ultrastructure, Reactions*, ed. W. De Gruyter, Berlin, New York, 1984.
19 V. Budarin, J. H. Clark, F. E. I. Deswarte, J. J. E. Hardy, A. J. Hunt and F. M. Kerton, *Chem. Commun.*, 2005, 2869.
20 V. Budarin, J. H. Clark, J. J. E. Hardy, R. Luque, K. Milkowski, S. J. Tavener and A. J. Wilson, *Angew. Chem., Int. Ed.*, 2006, **45**, 3782.
21 J. H. Clark, S. Doi, K. Milkowski and D. J. Macquarrie, *Chem. Commun.*, 2002, 2632.
22 M. J. Gronnow, R. Luque, D. J. Macquarrie and J. H. Clark, *Green Chem.*, 2005, **7**, 552.
23 K. Milkowski, J. H. Clark and S. Doi, *Green Chem.*, 2004, **6**, 189.
24 D. J. Macquarrie, J. J. E. Hardy, S. Hubert, A. J. Deveaux, M. Bandini, R. Luque and M. Chabriel, in *Feedstocks for the Future*, ed. J. Bozell ACS, New York, 2006.
25 J. J. E. Hardy, S. Hubert, D. J. Macquarrie and A. J. Wilson, *Green Chem.*, 2004, **6**, 53.
26 D. J. Macquarrie and J. J. E. Hardy, *Ind. Eng. Chem. Res.*, 2005, **44**, 8499.
27 E. B. Mubofu, J. H. Clark and D. J. Macquarrie, *Green Chem.*, 2000, **2**, 53; E. B. Mubofu, J. H. Clark and D. J. Macquarrie, *Green Chem.*, 2001, **3**, 23.
28 J. H. Clark, D. J. Macquarrie and M. C. Reid, *Green Chem.*, 2006, **8**, 437, http://www.solvaypress.com/pressreleases/O,38695-2-0,00.htm.
29 G. Rokicki, P. Rakoczy, P. Parzuckowski and M. Sobiecki, *Green Chem.*, 2005, **7**, 529.
30 N. Perez, L. Perez, M. R. Infante and M. T. Garcia, *Green Chem.*, 2005, **7**, 540.
31 J. G. Zeikus, M. K. Jain and P. Elankovan, *Appl. Microbiol. Biotechnol.*, 1999, **51**, 545.
32 M. Paster, *Industrial bioproducts: today and tomorrow*, report for the US DoE, 2003.
33 J. H. Clark, *Green Chem.*, 2006, **8**, 17.

Biomass to biofuels, a chemical perspective

Leo Petrus† **and Minke A. Noordermeer***

Received 6th April 2006, Accepted 27th July 2006
First published as an Advance Article on the web 15th August 2006
DOI: 10.1039/b605036k

Biomass is an interesting starting material for transportation fuels because of its renewable nature. The main constituents of biomass are the carbohydrate polymers cellulose and hemi-cellulose, and lignin. Current transportation fuels are mixtures of mainly hydrocarbons derived from crude oil. Biomass derived biofuels are preferably used as blends with fossil fuels to avoid the need for adaptations in the existing car fleet. The total blend then needs to meet the set fuel specifications for fossil fuels. The conversion of biomass to biofuels therefore centres on the removal of oxygen from carbohydrates to obtain hydrocarbons. Oxygen is preferably eliminated in the form of CO_2 or H_2O, because the heat of combustion of these molecules is zero and all energy is concentrated in the remaining products. Based on gross chemical formulae, the conversion options from biomass to biofuels have been investigated, and interesting intermediates have been identified. Conversion routes from carbohydrates to hydrocarbons tend to proceed *via* C_1-intermediates (CO, CH_4 and carbon). Gasification and subsequent Fischer Tropsch synthesis seems the logical processing route to obtain hydrocarbons from biomass *via* these intermediates. If oxygen containing products are allowed, conversion can proceed *via* larger intermediates. For blending with gasoline, ethanol emerges as an interesting component. Longer carbon chain molecules are required for diesel. These can only be obtained by at least two process steps, involving the combination of carbon chains (*e.g.* by etherification or esterification), and reduction of polarity (by hydrogenation or oligomerisation). The lignin present in biomass has a complex, highly cross-linked structure, and can probably best be converted to syngas *via* gasification or applied directly as solid fuel.

Introduction

Fuels for transportation purposes are currently mainly crude oil based. Gasoline and diesel fuels are used for vehicles travelling over land, kerosene for aircraft and heavy fuel oils for ships. Crude oil supply is finite, but there is still plenty of

Leo Petrus

Leo Petrus, born in Den Helder (The Netherlands) in 1953, studied chemical engineering at the University of Groningen. In 1982 he received his PhD at the same university with a thesis on 'Hydration of lower alkenes catalysed by strong acid ion exchangers'. From 1982 till 2000 he worked for Shell Chemicals in different functions, from exploratory researcher to process technologist at a production plant. In 2001 he became teamleader of the biofuels research at Shell Global Solutions in Amsterdam, and in 2005 he was appointed Chief Scientist Bioscience at Shell. Leo was an inspiring scientist with plenty ideas to realise a world in which sustainable biofuels would play an important role. He was a member of the Royal Society of Chemistry and former member of the Green Chemistry editorial board. Leo would have become a part-time professor at the University of Twente but unexpectedly passed away in March 2006.

Minke Noordermeer

Minke Noordermeer, born in Vlaardingen (The Netherlands) in 1972, studied chemistry at Utrecht University. In 2001 she received her PhD at the Bijvoet Center for Biomolecular Research, Utrecht University, with a thesis on 'Cloning and characterisation of alfalfa hydroperoxide lyase'. From 2001 till 2002 she worked as a postdoctoral fellow in the same group on the application of hydroperoxide lyase in a biocatalytic process. In 2002 she joined Shell Global Solutions as exploratory researcher in biofuels. She works as a project leader on fermentative routes towards biofuels, and is involved in B-Basic (Bio-Based Sustainable Industrial Chemistry), a joint research effort of industry, universities and research institutes, subsidised by the Dutch government.

Shell Global Solutions International B.V., Department of Innovation and Research, P.O. Box 38000, 1030 BN Amsterdam, The Netherlands. E-mail: minke.noordermeer@shell.com

† Deceased.

coal available, which can also be converted to transport fuels. There is however an increasing demand for sustainable fuels, especially in the land transport market. The main arguments are the building-up of greenhouse gases, the Kyoto protocol, the increasing dependency of the USA and the EU on imported crude oil and the demand for cleaner fuels. In the global energy market the main sustainable options are: solar, wind, hydro, biomass and geothermal energy. None of these is very well suited to be used directly for transport purposes, and these primary energy sources need to be converted to energy carriers such as electricity, hydrogen or biofuels. Electrical vehicles are emerging, but efficient storage of large amounts of electrical energy is still a challenge. Hydrogen is the ideal fuel for an energy efficient fuel cell and generates only water as the waste product. However, the conversion routes from primary energy source to hydrogen are generally not very energy efficient, although the efficiency of catalytic conversion of biomass (and biomass-derived compounds) to hydrogen was substantially improved recently.[1,2] Furthermore, the storage of hydrogen still requires further development, before being able to come close to the energy densities ($J\ L^{-1}$) reached with fuels like gasoline and diesel. Once these limitations for hydrogen have been overcome, there is still the issue of building an infrastructure for the distribution of hydrogen. All these aspects leave an interesting window for the use of biomass based liquid biofuels. Biofuels may even facilitate a hydrogen economy as these can be used to make hydrogen on board by catalytic partial oxidation.[3] Biofuels are already on the market in the form of ethanol for gasoline engines and fatty acid methyl esters (FAMEs) for diesel engines. Usually these components are used for blending in crude oil derived gasoline and diesel. Blending small amounts of biofuels, typically 2–10%, has the advantage that existing engines and fuel systems can use such blends without the need for modification. Furthermore, only minor changes are needed in the distribution chain (fuel transport and storage, filling stations *etc.*). On the other hand, the total mixture then needs to meet the set specifications for fossil fuels, which demands rather stringent biofuel product properties (*e.g.* vapour pressure, viscosity, density, octane/cetane number). Higher percentages of biofuels require adjustments, for example of fuel/air ratios, because of the lower energy content of such components. The development of dual-fuel and multi-fuel cars shows that arbitrary mixtures of such fuels can be accepted by adjusting the control systems of vehicles.

This paper focuses on possible routes from biomass to biofuels as seen from a chemical perspective. Only the main components and main conversion routes are considered, and not much attention is paid to the actual processes and conditions required. This simplified view might also be given the title Carbohydrate to Hydrocarbon. A broader view on the use of biomass for biofuels and biomaterials was recently published by A. Ragauskas *et al.*[4]

Biomass

An overview of the components typically present in biomass is given in Fig. 1. The main components are formed from CO_2 and H_2O using sunlight as energy source. Lignin and (hemi)cellulose together form a sort of fibre reinforced composite structure, in which cellulose is the fibre part and lignin forms a cross-linked three-dimensional resinous structure. Such ligno-cellulose gives strength to trees and plants. Cellulose is a polymer of glucose, hemi-cellulose is an oligomer of both C_6- and C_5-sugars (mainly glucose and xylose). Lignin is a highly cross-linked polymer built up of syringyl and sinapyl units, both substituted phenols containing C_3- and/or methoxy substituents. Typically, dry ligno-cellulosic biomass contains 40–50 wt% cellulose, 25 wt% hemicellulose and 25 wt% lignin. Especially in seeds and certain algae species, energy storage compounds and building materials can be found, such as lipids, sugars and starch. The energy content per mass unit increases with decreasing oxygen content of the building blocks. In the following series of materials the energy content per component decreases: terpenes, vegetable oils, lignin, sugars (including oligomers and polymers like hemicellulose, cellulose and starch). In principle, materials high in energy content and preferably liquid are the most interesting starting compounds for the production of biofuels. However, biomass usually contains only limited amounts of such components like terpenes and triglycerides. The bulk of the material is ligno-cellulose to build stems and leaves, required for harvesting sunlight. Therefore, ligno-cellulose is the most interesting source for large-scale production of biofuels. Minerals are minor components in biomass, but an important factor to consider. Current legislation does not always allow the recycling of such components as fertilisers in the form of ash, because ash is sometimes defined as chemical waste.

Biomass

$$CO_2 + H_2O + \text{sunlight} \Rightarrow \text{biomass} + O_2$$

Main components	
Cellulose/Starch	$[C_6(H_2O)_5]_n$
Hemi-cellulose	$[C_5(H_2O)_4]_n$
Lignin	$[C_{10}H_{12}O_3]_n$

Other components	
Terpenes	$C_{10}H_{16}$
Triacylglycerols	$[C_xH_yO_6]$, x ~ 50-60
Other organicsProteins	[C,O,N,S]; Nucleotides; Phospholipids [C,O,P] *etc.*
Inorganics	K, Se, Si, Mg, Ca, Fe *etc.*

Fig. 1 Biomass components.

Transportation fuels

Current transportation fuels range from very low boiling to high boiling mixtures of hydrocarbons, mainly produced from crude oil. Table 1 gives an overview of conventional and alternative/sustainable transport fuels, ranked according to their boiling range.

Low boiling fuels are compressed natural gas (CNG) and liquefied petroleum gas (LPG), both used in spark ignited Otto engines. Alternative components, having a similar volatility, are hydrogen and dimethyl ether (DME). The latter component has a vapour pressure in the same range as LPG, but can best be applied as fuel for diesel engines, because of its high cetane number.[5] DME can be produced from methanol *via* dehydration or directly from synthesis gas. The debate on the

Table 1 Overview of conventional and alternative transportation fuels. (CNG = compressed natural gas, LPG = liquefied petroleum gas, DME = dimethyl ether, ETBE = ethyl tertiary butyl ether, GTL = gas to liquids, FAME = fatty acid methyl esters, FAEE = fatty acid ethyl esters, HTU = hydrothermal upgrading)

Conventional	Alternative components
CNG	H_2
LPG	DME (in diesel)
Gasoline	Ethanol, ethers (ETBE) *others*
Kerosene	GTL-kerosene
Diesel	FAME, FAEE GTL-diesel *others*
Heavy fuel oils	Pyrolysis oil HTU oil

possible additional risk related to fuels stored under pressure is still on-going. Obviously CNG is, among the fossil fuels, the most benign fuel with respect to CO_2 emission.

Gasoline, kerosene and diesel (gasoil) are the most popular transportation fuels. They are all stored at ambient conditions as liquids having a high energy density, around 40 MJ kg^{-1}. Gasoline is mostly used in passenger cars with an Otto engine, kerosene in aircraft having jet engines, and gasoil in trucks having diesel engines. Gasoline is a mixture of paraffins, olefins, naphtenes and aromates in the C_5–C_{10} range (boiling point up to ~220 °C). The overall composition of gasoline varies between $[\text{–CH–}]_n$ and $[\text{–CH}_2\text{–}]_n$, and the overall octane number should be around 95. Components having a high octane rating are (highly) branched and aromatic components: 2,2,4-trimethylpentane or "*iso*-octane" has an octane number of 100, *n*-heptane has an octane number of zero, by definition. The ignition of gasoline in an engine is started by a spark, and early ignition, the harmful "knocking" of an engine, should be avoided. High octane components such as branched alkanes and aromatic structures are more resistant to auto-ignition, forming more stable tertiary and aromatic radicals as intermediates. Alternative fuels in the gasoline range are ethanol and ethers such as ethyl tertiary butyl ether (ETBE). Ethanol and the ethanol part of ETBE are usually derived from crops rich in sugar or starch, *via* fermentation. Both ethanol and ETBE are octane boosters, which can replace the environmentally unfriendly anti-knocking agents methyl tertiary butyl ether (MTBE) and lead complexes.[6] The amount of ethanol that can be used in blends is limited by the flash point specification. The tendency to form vapour bubbles in the fuel suction lines from the tank to the fuel pump ('vapour lock'), especially on hot summer days, sets an upper limit to the vapour pressure of the total mixture. ETBE has a lower vapour pressure and can be used up to higher percentages than ethanol.

Diesel fuels are usually characterised by their cetane number (around 45) and a boiling range of ~250–360 °C (C_{12}–C_{20} hydrocarbons). The cetane number is a measure of ignition quality. A diesel engine does not have spark ignition but compression ignition and, in contrast to gasoline, easily igniting compounds such as straight chain hydrocarbons are preferred in diesel. Cetane is the old name for a straight C_{16} alkane (hexadecane), which has a cetane number of 100 by convention. The compound 1-methylnaphthalene has been given a cetane number of zero. The overall composition of diesel is thus much closer to $[\text{–CH}_2]_n$ than in the case of gasoline. Alternative fuels in the diesel range are fatty acid methyl esters (FAMEs) and GTL products. Vegetable oils are too viscous and usually have a too high free fatty acid content (causing corrosion) to be used directly. FAMEs can be obtained *via* trans-esterification of (vegetable) oils or fats with methanol. The trans-esterification lowers the molecular weight and viscosity by converting triglyceryl esters of fatty acids to their methyl esters and glycerol. The overall molecular formula of a typical component in FAMEs, the methyl ester of oleic acid, is $C_{19}H_{36}O_2$. Due to the oxygen content of FAMEs, their density is higher than that of corresponding alkanes. In view of the often tight density specifications for diesel fuels, to limit the amount of aromatic components, the higher density of FAMEs can only be accommodated by selecting the proper (low) density base fuel or by adjusting the density using for instance kerosene. Instead of methyl esters, the fully bio-derived fatty acid ethyl esters (FAEEs) can also be used.[7] The viscosity of these FAEEs is slightly higher than the viscosity of the corresponding FAMEs. FAMEs (and FAEEs) can replace the environmentally unfriendly sulfur containing compounds in fuel as lubricating agents for the fuel pump and engine. GTL (gas to liquids) products are produced from syngas in the so called Fischer Tropsch process.[8] Current GTL-plants use natural gas or coal as feed to gasification reactors. The catalysts used in the Fischer Tropsch process are very sensitive to impurities in the syngas. When using biomass as a feedstock, removal of impurities is still an important issue, and therefore this is not applied on industrial scale yet.[9,10] The syngas produced requires extensive cleaning and/or difficult gasification conditions (*e.g.* high temperatures to reduce tar formation). The crude GTL product is a mixture of high molecular weight paraffins, which need to be cracked to the desired carbon number range to obtain hydrocarbons in the kerosene or diesel range.[11]

Low volatility heavy fuel oils are often used in diesel engines of ships. The viscosity of these oils may require heating of the fuel before use, to make it pumpable. Alternatives based on biomass might be pyrolysis oil or HTU (Hydro Thermal Upgrading) oil. Pyrolysis oil is obtained as the liquid fraction after condensation of the pyrolysis products of relatively dry ligno-cellulosic biomass. Typical pyrolysis conditions are: residence time in the order of seconds, pressures around atmospheric pressure and temperatures around 500 °C. The HTU process, invented by Shell in Amsterdam in the 1980's, converts biomass in liquid water at high temperature and pressure to a two phase mixture.[12] The oil-like top layer is HTU oil, the lower layer is rich in water. Typical HTU conditions are: residence times of several minutes, temperatures around 300 °C and pressures enabling liquid full operation (100–200 bar). Neither pyrolysis oil nor HTU oil can be used directly as substitute for heavy fuel oils or other transport fuels. Research on methods to upgrade these biomass derived crude oils is still on-going.

In this paper, we focus on the bulk transport fuels gasoline and diesel in which the introduction of bio-derived components such as ethanol and FAMEs is already taking place. Introduction of oxygenates in kerosene is less desirable,

Table 2 Main differences between the composition of a carbohydrate-rich biomass and gasoline or diesel

	Carbohydrate	Gasoline	Gasoil/ diesel
Carbon chain length	$[5–6]_n$	5–10	12–20
O/C molar ratio	1	0	0
H/C molar ratio	2	1–2	~2
Phase behaviour [at ambient *T*]	solid	liquid	liquid
Polarity	polar	non polar	non polar
Preferred structure	linear/cyclic	branched/aromatic/ cyclic/unsaturated	linear/ saturated

due to the fact that the presence of oxygen lowers the energy density of a fuel. It does not make sense to carry oxygen, in the form of an oxygenated fuel, to a height where oxygen for combustion is still abundantly available.

From cellulosic biomass to transportation fuels: from carbohydrate to hydrocarbon

The main differences between cellulosic biomass and gasoline or diesel are shown in Table 2. The underlying cause of a large number of differences between fossil fuels and biofuels is the oxygen present in the latter. In view of this, emphasis will be put on techniques to eliminate oxygen from biomass. Another difficulty is the chain lengthening required for components in the diesel range.

Removal of all oxygen from carbohydrate-rich biomass and upgrading to higher alkanes

Elimination of molecular oxygen from cellulosic biomass to form hydrocarbons would be very unfavourable as it is the opposite of partial combustion of hydrocarbons, and thus highly endothermic. To retain almost all energy in the remaining products, removal of oxygen in the form of CO_2 or H_2O is preferred. Both compounds are final products of full combustion processes and have a combustion enthalpy equal to zero. The formation of carbon dioxide as the oxygen carrying molecule from a C_6– hydrocarbon would result in $[C_3H_{12}]$, a hypothetical molecule too rich in hydrogen (Fig. 2). The $[C_3H_{12}]$ species would most likely split into three methane (CH_4) units. Alternatively, they might split into *e.g.* propane and two hydrogen molecules: $C_3H_8 + 2H_2$. In the case of H_2O as the oxygen carrier, carbon (*e.g.* charcoal) would be the final product. Another option for complete removal of oxygen is in the form of carbon monoxide, which would result in the co-formation of hydrogen. Starting from a carbohydrate, the synthesis gas would have a 1 : 1 H_2/CO molar ratio, and the overall reaction would be mildly endothermic.

Methane, charcoal or synthesis gas cannot be blended with liquid transport fuels, so conversion to higher alkanes is necessary. In the case of methane (biogas) as product, after eliminating all oxygen from biomass as CO_2, the option exists to form higher alkanes *via* the methane coupling reaction. In practice this reaction is never used, because no suitable catalysts have been discovered yet. Oxidative complexing of methane to C_2H_4/C_2H_6 is still a challenge.[13]

Elimination of all oxygen [O] as: CO_2, H_2O, CO

$C_6H_{12}O_6$	=>	$3\ CO_2 + [C_3H_{12}]$	Splits : $3CH_4$ (Biogas)
$C_6H_{12}O_6$	=>	$6\ H_2O + 6\ [C]$	"Charcoal"
$C_6H_{12}O_6$	=>	$6\ CO + 6\ H_2$	Synthesis gas

Fig. 2 Elimination of oxygen species from carbohydrates.

$$nCH_4 + ½nO_2 \Rightarrow [–CH_2–]_n + nH_2O$$

Charcoal, the main product after eliminating all oxygen in the form of H_2O, can theoretically be hydrogenated to higher alkanes. However, also for this reaction there are no suitable catalysts available yet.

$$n[C] + nH_2 \Rightarrow [–CH_2–]_n$$

Usually methane and charcoal are converted to higher alkanes *via* syngas as an intermediate, which can be formed by partial oxidation and/or steam reforming:[14]

$$nCH_4 + ½nO_2 \Rightarrow nCO + 2nH_2 \text{ (main route)}$$

$$nCH_4 + nH_2O \Rightarrow nCO + 3nH_2$$
(endothermic, used to adjust the CO/H_2 ratio)

$$n[C] + nH_2O \Rightarrow nCO + nH_2$$

From synthesis gas, hydrocarbons are usually formed by the Fischer Tropsch reaction, which requires an approximately 2 : 1 H_2 to CO ratio to form alkanes [–CH_2–] and water according to the equation:

$$nCO + 2nH_2 \Rightarrow [–CH_2–]_n + nH_2O$$

However, as shown in Fig. 2, syngas from carbohydrates has a 1 : 1 molar ratio of hydrogen and CO. This mismatch in the hydrogen to CO ratio can be adjusted *by* the water gas shift reaction:

$$CO + H_2O \Leftrightarrow CO_2 + H_2$$

The energy balance of the overall reaction can be adjusted, and even be made exothermic, by oxidizing part of the feed or products using oxygen, either in pure form or diluted as air.

Elimination of all oxygen from carbohydrates in biomass thus automatically leads to a conversion route with synthesis gas as intermediate from which higher alkanes for diesel can be derived by the Fischer Tropsch reaction.

Partial elimination of oxygen from carbohydrates as CO_2 or H_2O

Another option for upgrading biomass to biofuel components is the elimination of less than the maximum amount of CO_2 and H_2O. Starting from the carbohydrate $C_6H_{12}O_6$ a maximum of three CO_2 molecules can be obtained when eliminating all oxygen (Fig. 2). If just two CO_2 molecules are released, the hypothetical product $[C_4H_{12}O_2]$ results. $[C_4H_{12}O_2]$ is too rich in hydrogen, but if split into two equal parts, two C_2H_6O molecules are obtained. In anaerobic fermentation of sugars, executed at a large scale, ethanol (C_2H_6O) is usually the main product together with CO_2.

Another product having the same gross formula is dimethyl ether. An asymmetric split of $[C_4H_{12}O_2]$ might lead to combinations of products like methanol + (1- or 2-) propanol, or ethane + ethanediol.

$$C_6H_{12}O_6 \Rightarrow 2CO_2 + [C_4H_{12}O_2] \Rightarrow 2C_2H_6O$$

Elimination of two CO_2 molecules and one H_2O molecule from $C_6H_{12}O_6$ gives $C_4H_{10}O$. The gross formula $C_4H_{10}O$ corresponds for instance with 1-butanol, the main product of anaerobic fermentation of sugars by *Clostridia* bacteria. Acetone and ethanol are co-products in this fermentation. Diethyl ether, which is usually formed by dehydration of two ethanol molecules, is another compound having the same overall composition. Other possible products are 2-butanol, 2-methyl-1-propanol, methyl-propyl ether, methyl isopropyl ether. Splitting of $C_4H_{10}O$ should also be considered, resulting in methanol + propene, methane + acetone *etc*.

$$C_6H_{12}O_6 \Rightarrow 2CO_2 + H_2O + C_4H_{10}O$$

C_4H_8 is obtained if two CO_2 and two H_2O molecules are released from $C_6H_{12}O_6$. The gross formula corresponds to that of "butenes", such as 1- or 2-butene and 2-methylpropene (isobutene). Using the splitting analogy, it can also represent two molecules of ethene, for instance obtained by the dehydration of ethanol.

$$C_6H_{12}O_6 \Rightarrow 2CO_2 + 2H_2O + C_4H_8$$

Elimination of only one molecule of CO_2 together with increasingly larger amounts of water is illustrated below. Overall reaction equations are given with examples of possible products formed with and without splitting of the carbon chain.

$$C_6H_{12}O_6 \Rightarrow CO_2 + C_5H_{12}O_4$$
Tetrahydroxypentanes. With split: lactic acid + ethanol,
acetic acid + propanediol.

$$C_6H_{12}O_6 \Rightarrow CO_2 + H_2O + C_5H_{10}O_3$$
Hydroxypentanoic acid, ethyl lactate. With split:
succinic dialdehyde + methanol, acetic acid + acetone.

$$C_6H_{12}O_6 \Rightarrow CO_2 + 2H_2O + C_5H_8O_2$$
Ethyl lactate, γ-valerolactone. With split: ethyl acrylate.

$$C_6H_{12}O_6 \Rightarrow CO_2 + 3H_2O + C_5H_6O$$
Methylfuran

$$C_6H_{12}O_6 \Rightarrow CO_2 + 4H_2O + C_5H_4$$
Pentadiyne

If no CO_2 is removed, the starting compound $C_6H_{12}O_6$ can give the following products by splitting of the carbon chain: succinic acid + ethanediol, two lactic acid, three acetic acid or three glycolaldehyde molecules. Production of lactic acid by microbial conversion of glucose or sucrose is executed on a fairly large scale. Microbial formation of succinic acid is feasible as well, *e.g.* from wood hydrolysates.[15] Glycolaldehyde was found as the main product after hydrothermal treatment of glucose (340 °C, 27.5 MPa, 120 s), and a recent patent claims yields of over 50% of glycolaldehyde upon thermolysis of glucose at 520–560 °C with short residence times.[16,17]

If no CO_2, but increasing amounts of H_2O, are eliminated the following products can be formed:

$$C_6H_{12}O_6 \Rightarrow H_2O + C_6H_{10}O_5$$
2,3 Dimethyl malate. With split: levulinic acid + formic acid,
succinic acid + acetaldehyde.

$$C_6H_{12}O_6 \Rightarrow 2H_2O + C_6H_8O_4$$
Lactide, 3-hexene-1,6-dioic acid. With split:
furanone + acetic acid.

$$C_6H_{12}O_6 \Rightarrow 3H_2O + C_6H_6O_3$$
Trihydroxy benzene (1,2,4-isomer), hydroxymethylfurfural
(HMF)

$$C_6H_{12}O_6 \Rightarrow 4H_2O + C_6H_4O_2$$
Benzoquinone

Further elimination of water leads to the production of charcoal with loss of all oxygen.

Generally speaking, the elimination of water from carbohydrates is much easier than the elimination of CO_2. An interesting situation occurs upon the elimination of three water molecules from the C_6-carbohydrate, which seems to be a fairly easy process.[18] The main products formed are 1,2,4-trihydroxybenzene (THB) or hydroxymethylfurfural (HMF).[16,18,19] Both components have the same overall formula: $C_6H_6O_3$. When looking at the carbon chain it is clear that the terminal carbon atoms (number 1 and 6) have formed a bond in THB, whereas the carbon chain in HMF remained relatively straight. This has consequences for further reaction paths. In view of the stability of the aromatic ring in THB, this product is unlikely to release CO_2. It can either remain unchanged or it can lose additional water, going into the direction of quinones, polycyclic aromatics and charcoal. The stability of HMF is lower than that of THB, and HMF can still release CO_2. During conversion steps involving the dehydration of a C_6-carbohydrate, hydroxymethylfurfural (HMF) seems to be the kinetically preferred product and trihydroxybenzene (THB) the thermodynamically preferred compound. The formation of charcoal from biomass rich in carbohydrates, such as wood, is therefore preferably carried out at modest temperatures and may take about one week.

An overview of the main products obtained by partial elimination of oxygen from C_6-sugars is shown in Fig. 3. In this scheme, the loss of CO_2 is plotted on the horizontal axis and the loss of H_2O on the vertical axis. Fig. 4 illustrates the elimination of CO_2 and/or H_2O from C_5-carbohydrates. The effects observed are similar to those in Fig. 3 for C_6-carbohydrates. Differences are caused by the fact that these C_5-carbohydrates have an odd number of carbon atoms. Upon elimination of two CO_2 molecules from $C_5H_{10}O_5$ the resulting species is $[C_3H_{10}O]$, which cannot split into two or three equal parts. This species may split into CH_4 and C_2H_6O (ethanol or dimethyl ether) or into CH_4O (methanol) and C_2H_6 (ethane). These products do also appear in the top right corner of Fig. 3 for the C_6-carbohydrates. Elimination of three molecules of water from $C_5H_{10}O_5$ leads to $C_5H_4O_2$, best known as furfural, the main product often observed in

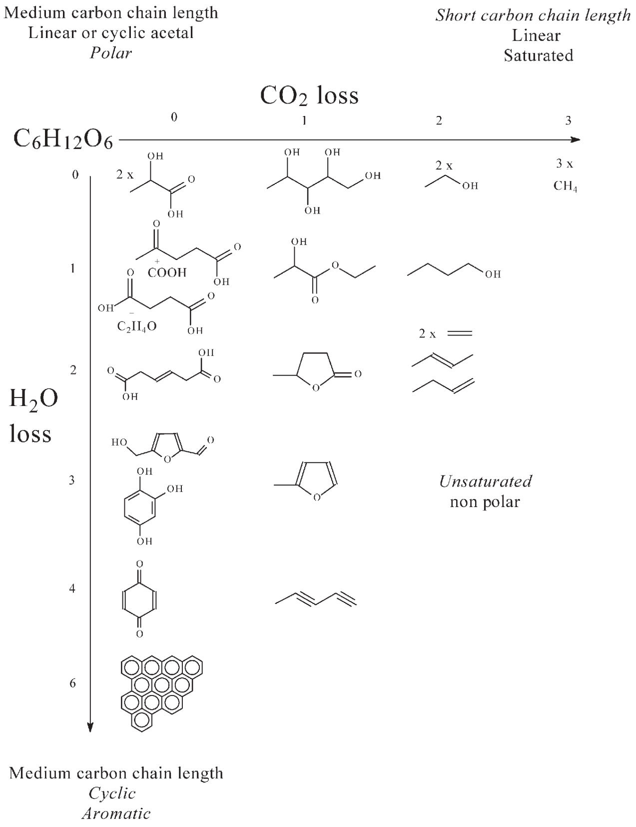

Fig. 3 Decarboxylation and dehydration of C_6-carbohydrates, overview scheme.

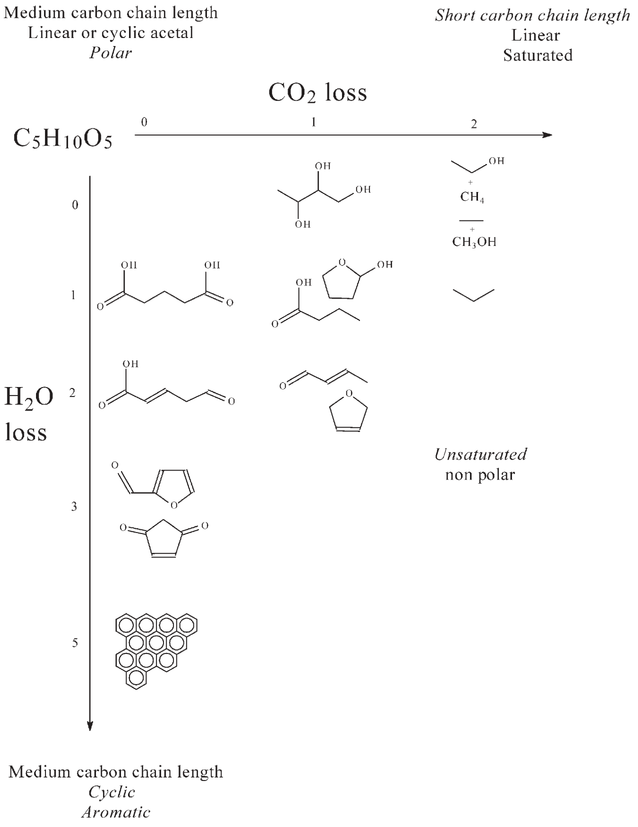

Fig. 4 Decarboxylation and dehydration of C_5-carbohydrates, overview scheme.

the (acid catalysed) conversion of C_5-sugars.[20] Starting from a C_5-carbohydrate, an aromatic C_6-species cannot be formed easily. The structure of furfural, containing only 5 carbon atoms and three conjugated double bonds, is thermodynamically the next best option ("pseudo aromatic").

Applicability of partially deoxygenised biomass products in transport fuels

Starting at the carbohydrate, it is clear that this component has a medium chain length (5 or 6 carbon atoms) and a cyclic structure in equilibrium with a small amount (<1%) of linear structural isomers. Upon elimination of CO_2, the structure of components formed remains linear and saturated. Some of the products near the top right corner of Fig. 3 and 4 may be suitable as components for gasoline. Examples are alcohols, lactones and furans. However, the reduction in chain length is a major disadvantage, especially for the use in diesel fuel. Introduction of too small components in diesel leads to a considerable increase in vapour pressure. As a consequence, the vapour pressure of the total mixture (*i.e.* the diesel fuel) can be raised to a value above the lower explosion limit, in the middle of the explosive regime. For safety reasons—cars sometimes collide—this effect is not acceptable. In gasoline cars an increase in vapour pressure can be accepted from a safety point of view, because the vapour pressure of gasoline in the ullage of the tank is above its higher explosion limit and therefore in a safe area, but is limited to prevent formation of a vapour lock.

If H_2O is released, the carbon chain length remains intact. Progressively more unsaturated, aromatic and cyclic structures are obtained. Such structures are not attractive for diesel, and the amount of aromatic components in gasoline is strictly regulated and has been recently reduced (for example through EN228 in Europe). The elimination of both CO_2 and H_2O leads away from the carbohydrate starting point towards the components near the bottom right diagonal in Fig. 3 and 4. These products are usually rather non-polar, a desired property. However, the substantial loss of oxygen has also resulted in "unsaturation": double and triple carbon-carbon bonds and aromatic structures. None of the positions in the scheme gives components directly suited as blending components in diesel, because the products are either too polar, too short, too unsaturated or too aromatic. Another important boundary condition for the application of a new bio-component is the miscibility with the fossil fuel. Measures to further reduce polarity and increase carbon chain length are required. Interesting processes to achieve both effects are:

- etherification
- esterification
- aldolisation
- formation of acetals and ketals
- formation of anhydrides and ortho esters
- dehydration

The first three of these processes, etherification, esterification, and aldolisation lead to fairly stable products.

The unsaturation introduced by dehydration can be reduced by:

- hydrogenation
- oligomerisation and cyclisation

Hydrogenation is a universally applicable technique to reduce unsaturation, but requires the availability of hydrogen. Hydrogen can be produced from biomass, for instance *via* gasification and fermentation routes. Other sustainable energy sources, such as solar, wind and tidal energy, can also be used to generate hydrogen, for example by electrolysis of water. Recently, formation of liquid alkanes in the range of C_7–C_{15} from carbohydrates was described.[21] This was achieved by successive acid-catalysed dehydration, aldol condensation over solid base catalysts and dehydration/hydrogenation over bifunctional catalysts. Oligomerisation is mainly interesting for ethene, since straight chain hydrocarbons (the most interesting ones for diesel) can only be obtained from this alkene. Oligomerisation of other alkenes leads to branched structures, which may be interesting for gasoline (*e.g.* the dimer of iso-butene). Cyclisation gives naphtenes, which as cyclic structures are less interesting for diesel. In the case of olefins having three or more carbon atoms, these cyclic alkenes will also be branched.

From lignin to fuels

When plants are considered as "fibre reinforced structures", cellulose is the fibrous material and lignin the resin that "glues" everything together. Lignin is a three dimensional cross-linked network, having a chemical structure resembling that of "Bakelite", a phenol-formaldehyde resin. The repeating unit of lignin contains a phenol group, optionally substituted with one or two methoxy groups at the *ortho*-position and a C_3-group at the *para*-position. The C_3-group may carry oxygen atoms as hydroxy-, aldehyde- or carboxylic acid groups. Carbon–carbon double bonds may be formed by the loss of a hydroxy group. An approximate molecular formula of the basic unit in lignin is $C_{10}H_{12}O_3$. Trans coniferyl alcohol gives the approximate chemical structure of the basic unit of lignin. Lignin is a very stable solid material, due to its chemical structure and highly cross-linked nature. As a result lignin is a difficult building block for chemical conversion steps. In view of its relatively low oxygen content and therefore large energy content, it is usually applied as fuel. It can either be burnt directly or converted to synthesis gas. Other applications include oxidation to vanillin and production of dimethyl sulfoxide.

Conclusions

The easiest way to convert ligno-cellulosic biomass into hydrocarbons in the transport fuel range is *via* routes involving C_1-building blocks (syngas).

Routes not involving C_1- or C_2-building blocks usually give polar, unsaturated or aromatic components, which often need further conversion steps to become suitable as (blending) components for transport fuels.

The production of (blending) components for transport fuels requires careful selection of process routes and process conditions.

Acknowledgements

The authors would like to thank Herman van Bekkum (TU Delft, The Netherlands) for advice and critically reading the manuscript.

References

1 S. Freni, S. Cavallaro, N. Mondello, L. Spadaro and F. Frusteri, Production of hydrogen for MC fuel cell by steam reforming of ethanol over MgO supported Ni and Co catalysts, *Catal. Commun.*, 2003, **4**(6), 259–268; F. Frusteri, S. Freni, L. Spadaro, V. Chiodo, G. Bonura, S. Donato and S. Cavallaro, H_2 production for MC fuel cell by steam reforming of ethanol over MgO supported Pd, Rh, Ni and Co catalysts, *Catal. Commun.*, 2004, **5**(10), 611–615.

2 G. W. Huber, J. W. Shabaker and J. A. Dumesic, Raney Ni–Sn catalyst for H_2 production from biomass-derived hydrocarbons, *Science*, 2003, **300**(5628), 2075–2077.

3 L. F. Brown, A comparative study of fuels for on-board hydrogen production for fuel-cell-powered automobiles, *Int. J. Hydrogen Energy*, 2001, **26**, 381–397.

4 A. J. Ragauskas, C. K. Williams, B. H. Davison, G. Britovsek, J. Cairney, C. A. Eckert, W. J. Frederick, Jr., J. P. Hallett, D. J. Leak, C. L. Liotta, J. R. Mielenz, R. Murphy, R. Templer and T. Tschaplinski, The path forward for biofuels and biomaterials, *Science*, 2006, **311**, 484–489.

5 S. C. Sorenson, Dimethyl ether in diesel engines: Progress and perspectives, *J. Eng. Gas Turbines Power*, 2001, **123**(3), 652–658.

6 M. Iborra, J. F. Izquierdo, J. Tejero and F. Cunill, Getting the lead out with ethyl t-butyl ether, *CHEMTECH*, 1988, **18**(2), 120–122.

7 W. Zhou, S. K. Konar and D. G. B. Boocock, Ethyl esters from the single-phase base-catalyzed ethanolysis of vegetable oils, *J. Am. Oil Chem. Soc.*, 2003, **80**(4), 367.

8 M. E. Dry, Practical and theoretical aspects of the catalytic Fischer-Tropsch process, *Appl. Catal.*, 1996, **138**, 319–344.

9 A. V. Bridgwater, Renewable fuels and chemicals by thermal processing of biomass, *Chem. Eng. J.*, 2003, **91**, 87–102.

10 A. V. Bridgwater, *Progress in Thermochemical Biomass Conversion*, Blackwell Scientific Publications, Oxford, UK, 2001.

11 S. T. Sie and R. Krishna, Process development and scale up, *Rev. Chem. Eng.*, 1998, **14**, 159–202.

12 F. Goudriaan and D. G. R. Peferoen, Liquid fuels from biomass via a hydrothermal process, *Chem. Eng. Sci.*, 1990, **45**(8), 2729–2734.

13 S. Liu, X. Tan, K. Li and R. Hughes, Methane coupling using catalytic membrane reactors, *Catal. Rev. Sci. Eng.*, 2001, **43**(1&2), 147–198.

14 Y. H. Hu and E. Ruckenstein, Binary MgO-based solid solution catalysts for methane conversion to syngas, *Catal. Rev. Sci. Eng.*, 2002, **44**(3), 423–453.

15 P. C. Lee, S. Y. Lee, S. H. Hong, H. N. Chang and S. C. Park, Biological conversion of wood hydrolysate to succinic acid by *Anaerobiospirillium succiniproducens*, *Biotechnol. Lett.*, 2003, **25**, 111–114.

16 Z. Srokol, A.-G. Bouche, A. van Estrik, R. C. J. Strik, T. Maschmeyer and J. A. Peters, Hydrothermal upgrading of biomass to biofuel; studies on some monosaccharide model compounds, *Carbohydr. Res.*, 2004, **339**, 1717–1726.

17 P. A. Majerski, J. K. Piskorz and D. Radlien, Production of glycolaldehyde by hydrous thermolysis of sugars, *US Pat.* 2 004 022 912, 2004.

18 G. C. A. Luijkx, F. van Rantwijk and H. van Bekkum, Hydrothermal formation of 1,2,4-benzenetriol from 5-hydroxymethyl-2-furaldehyde and D-fructose, *Carbohydr. Res.*, 1993, **242**, 131–139.

19 C. Moreau, M. N. Belgacem and A. Gandini, Recent catalytic advances in the chemistry of substituted furans from carbohydrates and in the ensuing polymers, *Top. Catal.*, 2004, **27**(1–4), 11–30.

20 O. Theander and D. A. Nelson, Aqueous, high-temperature transformation of carbohydrates relative to utilization of biomass, *Adv. Carbohydr. Chem. Biochem.*, 1988, **46**, 273.

21 G. W. Huber, J. N. Chheda, C. J. Barrett and J. A. Dumesic, Production of liquid alkanes by aqueous-phase processing of biomass-derived carbohydrates, *Science*, 2005, **308**(5727), 1446–1450.

Simple and eco-friendly reduction of nitroarenes to the corresponding aromatic amines using polymer-supported hydrazine hydrate over iron oxide hydroxide catalyst†

Qixun Shi, Rongwen Lu,* Kun Jin, Zhuxia Zhang and Defeng Zhao

Received 11th May 2006, Accepted 19th July 2006
First published as an Advance Article on the web 3rd August 2006
DOI: 10.1039/b606705k

Aromatic amines were conveniently, rapidly and, importantly, environmentally benignly prepared in excellent yields through chemoselective reduction of the corresponding aromatic nitro compounds with polymer-supported hydrazine hydrate in the presence of iron oxide hydroxide catalyst.

Introduction

In recent years, with the increasing interest in human health and environmental protection, the need for clean and easily recycled reagents in organic synthesis has meant that solid-supported reagents and scavengers have received more and more attention from organic chemists.[1] Compared to the traditional solution-phase reactions, the use of solid-supported reagents and scavengers simplifies the work-up operations by allowing simple filtration, and avoids release of excess reactants or by-products into the environment.[2] Furthermore, the reclaimed solid-supported reagents and scavengers can be reused through simple regeneration in most cases.

Aromatic amines are an important class of compounds frequently used as key intermediates in the synthesis of pharmaceutical products, dyestuffs and polymers. Various methods have been reported for the preparation of aromatic amines from the corresponding aromatic nitro compounds. The methods employed generally are metal–acid reduction[3] and catalytic hydrogenation.[4] However, these two approaches need either strong acid medium which erodes the reaction equipment seriously or hazardous molecular hydrogen and high-pressure reactors. In order to overcome these shortcomings, catalytic transfer hydrogenation, as a safer and greener way, has been developed.[5] Hydrazine hydrate is usually used as hydrogen donor in catalytic transfer hydrogenation because the hydrazine reduction produces harmless by-products such as nitrogen gas and water.[6] Nevertheless, the excess hydrazine hydrate used for the sake of shortening reaction time and driving reactions to completion is normally dissolved in water during the disposal and drained into environment. In view of the well-known toxicity of hydrazine hydrate, the release of excess hydrazine hydrate may create many serious problems.

With the development of solid-supported chemistry, a solid-supported strategy has also been adopted in the reduction of aromatic nitro compounds.[7] However, most of the research is focused on solid-supported nitroarenes. Herein, we report the use of polymer-supported hydrazine hydrate employed as a solid-supported hydrogen donor for preparing aromatic amines from the corresponding nitroarenes. To our knowledge, this is the first report about the use of polymer-supported (macroporous weak acidic resin) hydrazine hydrate in the reduction of nitroarenes. In consideration of the broad application of hydrazine hydrate in many reactions as a known excellent reductant, the strategy described here may be a good alternative to reduce the pollution resulting from the release of excess hydrazine hydrate.

Experimental

Preparation of polymer-supported hydrazine hydrate

The D113 (macroporous weak acidic ion-exchange resin, exchange capacity: 10 mmol g^{-1}, Dandong Dongfang Resin Factory, Dandong, China) was washed with a 50% solution of hydrazine hydrate in methanol. Then the resulting polymer was washed thoroughly with methanol and dried under vacuum. The resin obtained[8] was ready for further application for catalytic transfer hydrogenation.

General procedure for the preparation of aromatic amines

A mixture of aromatic nitro compound (1 mmol), polymer-supported hydrazine hydrate (2.0 g), propan-2-ol (10 mL) and iron oxide hydroxide catalyst (0.2 g), prepared according to the literature,[9] was stirred under reflux for several minutes. After completion of the reduction (monitored by TLC), the reaction mixture was filtered and the solid was washed thoroughly with methanol. Then the filtrate was evaporated *in vacuo*. The crude product was purified by column chromatography on silica gel using *n*-hexane and ethyl acetate as eluent. For recycling purposes, at the end of the reaction the resin was separated from iron oxide hydroxide and washed completely with methanol, a 50% solution of hydrazine hydrate in methanol and finally methanol again. Then the activated resin was dried under reduced pressure and reused for the subsequent cycles.

Results and discussion

Reduction of aromatic nitro compounds was carried out by using polymer-supported hydrazine hydrate and iron oxide hydroxide

---

State Key Laboratory of Fine Chemicals, Dalian University of Technology, Dalian, 116012, P. R. China. E-mail: lurw@dlut.edu.cn; Fax: +86 411 88993800; Tel: +86 411 88993829

† Electronic supplementary information (ESI) available: Experimental details and powder X-ray diffraction pattern of iron oxide hydroxide catalyst, as well as analytical data for products. See DOI: 10.1039/b606705k

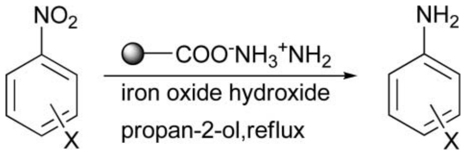

Scheme 1

catalyst in refluxing propan-2-ol (Scheme 1). The results of reduction of various nitroarenes were shown in Table 1. From Table 1 we could see that the reaction proceeded very smoothly and the yields were almost quantitative. The azoxy, azo and hydrazo compounds as the usual side products of reduction of nitroarenes under basic condition were not observed in the final reaction system. At the same time, it was also noteworthy that the present method was highly chemoselective and some sensitive functional groups such as –Cl and –$COOC_2H_5$ did not undergo any change under the reaction conditions. Moreover, many other substituted groups, such as –CH_3, –OH, –NH_2 and –OCH_3, were intact during the reaction.

Control experiments were performed according to general procedure; but by replacing polymer-supported hydrazine hydrate with D113 or without the use of iron oxide hydroxide the reactions did not produce any desired product. This clearly indicated that the hydrazine hydrate and iron oxide hydroxide were indispensable for the reduction of nitroarenes in our reaction system. For the purpose of checking the regeneration and reuse of polymer-supported hydrazine hydrate, consecutive reaction/regeneration cycles were executed and the results, summarized in Table 2, showed that the yield was unaffected for up to eight recycle runs.

The role of iron oxide hydroxide in this type of reaction has been investigated in detail by R. Prins *et al.*[10] and P. Rys *et al.*[9] Mössbauer spectroscopy showed that Fe(III) in iron oxide hydroxide was first reduced to Fe(II) by hydrazine hydrate during the reaction, then the Fe(II) was immediately reoxidized to Fe(III) by nitroarenes. Thus, R. Prins *et al.* suggested that this type of reaction proceeded by a Mars–van Krevelen mechanism, and the iron oxide hydroxide played the role of hydrogen transfer catalyst in the reaction. Owing to the similarity of the reaction system, we assumed that iron oxide hydroxide in our reaction played a similar role with that suggested by R. Prins *et al.* and P. Rys *et al.*

Table 1 Reduction of nitroarenes with polymer-supported hydrazine hydrate/iron oxide hydroxide[a]

Entry	Substrate	Time/min	Product[b]	Yield[c] (%)
1	$C_6H_5NO_2$	44	$C_6H_5NH_2$	98
2	o-$CH_3C_6H_4NO_2$	48	o-$CH_3C_6H_4NH_2$	97
3	m-$CH_3C_6H_4NO_2$	44	m-$CH_3C_6H_4NH_2$	98
4	p-$CH_3C_6H_4NO_2$	43	p-$CH_3C_6H_4NH_2$	97
5	o-$ClC_6H_4NO_2$	42	o-$ClC_6H_4NH_2$	93
6	m-$ClC_6H_4NO_2$	30	m-$ClC_6H_4NH_2$	98
7	p-$ClC_6H_4NO_2$	46	p-$ClC_6H_4NH_2$	99
8	3,4-$(Cl)_2C_6H_3NO_2$	39	3,4-$(Cl)_2C_6H_3NH_2$	98
9	o-$OHC_6H_4NO_2$	50	o-$OHC_6H_4NH_2$	96
10	o-$NH_2C_6H_4NO_2$	44	o-$NH_2C_6H_4NH_2$	95
11	m-$NH_2C_6H_4NO_2$	46	m-$NH_2C_6H_4NH_2$	97
12	p-$NH_2C_6H_4NO_2$	45	p-$NH_2C_6H_4NH_2$	96
13	p-$CH_3OC_6H_4NO_2$	39	p-$CH_3OC_6H_4NH_2$	99
14	p-$C_2H_5CO_2C_6H_4NO_2$	47	p-$C_2H_5CO_2C_6H_4NH_2$	95

[a] Reaction conditions: 1 mmol of aromatic nitro compound, 2.0 g of polymer-supported hydrazine hydrate, 0.2 g of iron oxide hydroxide, 10 mL propan-2-ol, reflux. [b] All the products were characterized by comparison of their ^1H NMR spectra and MS with those of authentic samples. [c] Isolated yields were based on a single experiment and were not optimized.

Table 2 Recycling of polymer-supported hydrazine hydrate for the reduction of 1,2-dichloro-4-nitrobenzene

Cycle	Time/min	Yield(%)
1	40	98
2	40	98
3	40	98
4	40	97
5	43	98
6	43	98
7	48	97
8	48	97

Conclusions

In conclusion, we report here a novel approach for the preparation of aromatic amines from the corresponding aromatic nitro compounds using polymer-supported hydrazine hydrate over iron oxide hydroxide catalyst. This method is mild, exceedingly efficient and highly chemoselective. In comparison to the traditional hydrazine hydrate reduction, where an excess of hydrazine hydrate is used for driving the reaction to completion, the most important novelties are that (1) the present approach avoids the release of toxic hydrazine by being bound to the D113 ion-exchange resin and (2) it simplifies the handling procedures, and the separation of the products from the reaction system can be achieved by simple filtration followed by solvent removal. In addition, it is also worth noting that, once the polymer-supported hydrazine hydrate has been prepared, the exposure of operating personnel to hydrazine hydrate, which is a universal problem with the use of the liquid hydrazine hydrate, can be minimized. Therefore this method is 'green' to both the environment as well as workers.

Notes and references

1 B. Desai and T. N. Danks, *Tetrahedron Lett.*, 2001, **42**, 5963; T. N. Danks and B. Desai, *Green Chem.*, 2002, **4**, 179; B. Desai, T. N. Danks and G. Wagner, *Tetrahedron Lett.*, 2005, **46**, 955; B. Basu, M. M. H. Bhuiyan, P. Das and I. Hossain, *Tetrahedron Lett.*, 2003, **44**, 8931; G. Yang, Z. Chen and H. Zhang, *Green Chem.*, 2003, **5**, 441; K. I. Okuyama, J. I. Sugiyama, R. Nagahata, M. Asai, M. Ueda and K. Takeuchi, *Green Chem.*, 2003, **5**, 563; Z. Y. Wang, H. F. Jiang, C. R. Qi, Y. G. Wang, Y. S. Dong and H. L. Liu, *Green Chem.*, 2005, **7**, 582; R. Skouta, R. S. Varma and C. J. Li, *Green Chem.*, 2005, **7**, 571; K. I. Fujita, S. Hashimoto, M. Kanakubo, A. Oishi and Y. Taguchi, *Green Chem.*, 2003, **5**, 549.

2 S. V. Ley, I. R. Baxendale, R. N. Bream, P. S. Jackson, A. G. Leach, D. A. Longbottom, M. Nesi, J. S. Scott, R. I. Storer and S. J. Taylor, *J. Chem. Soc., Perkin Trans. 1*, 2000, 3815; A. Chesney, *Green Chem.*, 1999, **1**, 209.

3 K. M. Doxsee, M. Feigel, K. D. Stewart, J. W. Canary, C. B. Knobler and D. J. Cram, *J. Am. Chem. Soc.*, 1987, **109**, 3098; C. A. Merlic, S. Motamed and B. Quinn, *J. Org. Chem.*, 1995, **60**, 3365.

4 A. M. Tafesh and J. Weiguny, *Chem. Rev.*, 1996, **96**, 2035.

5 S. K. Mohapatra, S. U. Sonavane, R. V. Jayaram and P. Selvam, *Org. Lett.*, 2002, **4**, 4297; S. K. Mohapatra, S. U. Sonavane, R. V. Jayaram and P. Selvam, *Tetrahedron Lett.*, 2002, **43**, 8527.

6 M. Kumarraja and K. Pitchumani, *Appl. Catal., A*, 2004, **265**, 135; P. S. Kumbhar, J. S. Valente and F. Figueras, *Tetrahedron Lett.*, 1998, **39**, 2573; N. R. Ayyangar, A. G. Lugade, P. V. Nikrad and V. K. Sharma, *Synthesis*, 1981, 640.

7 A. Kamal, K. L. Reddy, V. Devaiah and G. S. K. Reddy, *Tetrahedron Lett.*, 2003, **44**, 4741; A. Kamal, G. S. K. Reddy and K. L. Reddy, *Tetrahedron Lett.*, 2001, **42**, 6969; A. Hari and B. L. Miller, *Tetrahedron Lett.*, 1999, **40**, 245; A. Hari and B. L. Miller, *Angew. Chem., Int. Ed.*, 1999, **38**, 2777; K. Abiraj, G. R. Srinivasa and D. C. Gowda, *Aust. J. Chem.*, 2005, **58**, 149; A. Vass, J. Dudás, J. Tóth and R. S. Varma, *Tetrahedron Lett.*, 2001, **42**, 5347; C. R. Zhang, Y. L. Wang and J. Y. Wang, *J. Chin. Chem. Soc.*, 2004, **51**, 569.

8 IR spectra indicated that the adsorption of COOH (1716 cm^{-1}) in the D113 almost entirely disappeared and the absorption of COO^- (1558 cm^{-1}) appeared. Hydrazine hydrate loading, which was determined by iodometric titration, was approximately 5.95 mmol g^{-1}.

9 M. Lauwiner, P. Rys and J. Wissmann, *Appl. Catal., A*, 1998, **172**, 141; M. Lauwiner, R. Roth and P. Rys, *Appl. Catal., A*, 1999, **177**, 9.

10 M. Benz, A. M. van der Kraan and R. Prins, *Appl. Catal., A*, 1998, **172**, 149; M. Benz and R. Prins, *Appl. Catal., A*, 1999, **183**, 325.

Transesterifications catalysed by solid, reusable apatite–zinc chloride catalysts

Abderrahim Solhy,[*ac] **James H. Clark,**[*b] **Rachid Tahir,**[c] **Said Sebti**[c] **and Mohamed Larzek**[d]

Received 24th April 2006, Accepted 27th July 2006
First published as an Advance Article on the web 3rd August 2006
DOI: 10.1039/b605835n

We report for the first time the use of low cost and safe to handle fluoroapatite and hydroxyapatite supported zinc chloride reagents as solid and reusable catalysts for a wide range of transesterification reactions

Introduction

Transesterification is an important organic reaction that can be used to synthesize various intermediates in the synthesis of complex natural products, pheromones and paint additives.[1] Its value has been considerably enhanced by its use as a key step in the manufacture of biodiesel, one of the more environmentally friendly and sustainable fuels we have available today. The enormous and growing volume of this "green" fuel in regions such as Northern Europe should make us especially conscious of all aspects of its production (along with all other stages in its lifecycle) and, in the context of this article, we need to strive towards the greenest catalytic system for the key transesterification stage.

Transesterification can be catalysed by strong acids[2] and by soluble bases such as caustic soda,[3,4] neither of which is ideal from a green chemistry perspective. Rather, we should seek safe-to-handle and store, environmentally benign and reusable, typically solid, catalysts. This has led to reports of a number of active synthetic basic solids as transesterification catalysts, including mixed metal hydrotalcites[5] and zeolites.[6] Drawbacks with such catalysts include the use of hazardous reagents in the preparation of the catalyst (*e.g.* KO^{t}Bu) and pore blockage with larger substrates (for zeolite materials). Hydroxyapatite (HAP; $Ca_{10}(PO_4)_6(OH)_2$) is a highly abundant, natural material, being the major component of teeth and bones. It is also considered to have durable acid–base properties and high adsorption capacity, making it a promising support material. This has been demonstrated in the use of HAP-supported Lewis acids in Friedel–Crafts alkylations[7], and more recently in Michael addition of indoles to electron-deficient olefins.[8] Here we report for the first time the use of $ZnCl_2$–HAP, along with its fluorinated equivalent, as a highly effective, reusable and cheap solid catalyst for transesterifications.

Experimental

Hydroxyapatite

Hydroxyapatite was synthesised by the co-preciptation method (Scheme 1). 250 ml of a solution containing 7.92 g of diammonium hydrogen phosphate, maintained at a pH greater than 12, by addition of ammonium hydroxide (BDH) (60–70 ml), was dropped into 150 ml of a solution containing 23.6 g of calcium nitrate [$Ca(NO_3)_2·4H_2O$], with constant stirring. The suspension was refluxed for 4 h. Doubly distilled water (DDW) was used to prepare the solutions. The HAP crystallites were filtered, washed with DDW, dried overnight at 80 °C and calcined in air at 700 °C for 30 min. before use.

The structure of obtained apatite was confirmed by X-ray diffraction (Fig. 1), infrared spectra and chemical analysis.

The hydroxyapatite crystallizes in the hexagonal system with the space group $P6_{3/m}$. The lattice parameters of the prepared HAP are in excellent agreement with standard data: a = 6.883 Å and

$$6(NH_4)_2HPO_4 + 10Ca(NO_3)_2 + 8NH_4OH$$
$$\longrightarrow Ca_{10}(PO_4)_6(OH)_2 + 20NH_4(NO_3) + 6H_2O$$

Scheme 1

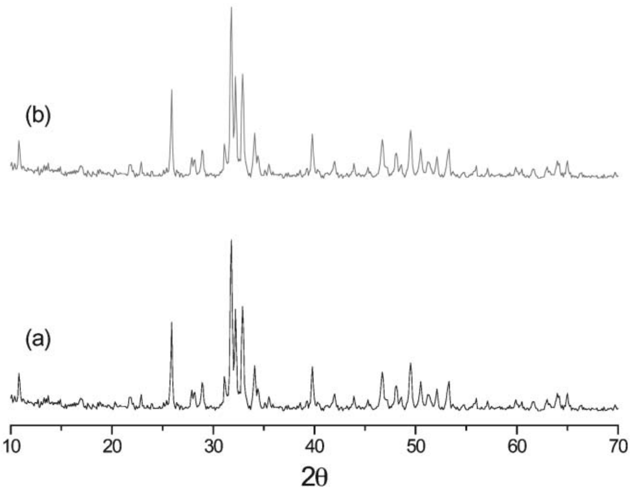

Fig. 1 XRD patterns of (a) HAP, (b) $ZnCl_2$–HAP.

---

[a] *Dto. Quimica Aplicada. Edificio los acebos. Campus Arrosadia. Universidad Publica de Navarra, Pamplona, 31006, Spain. E-mail: solhyabderrahim@unavarra.es; Fax: +34 948 169606; Tel: +34 658198369*
[b] *Clean Technology Centre, Department of Chemistry, University of York, York, UK YO10 5DD. E-mail: jhc1@york.ac.uk; Fax: +44-1904-432705; Tel: +44-1904-432559*
[c] *Laboratoire de Chimie Organique Catalyse et Environnement. Université Hassan II, Faculté des Sciences Ben M'Sik B.P. 7955, Casablanca, 20702, Morocco. E-mail: saidsebti@yahoo.fr; tahirrachid@yahoo.fr; Fax: +212 22 24 96 72; Tel: +212 61 46 48 19*
[d] *La Société MAFER, 36 Boulevard Grande Ceinture, Hay Mohammadi, Casablanca, Morocco. Tel: +212 22 60 25 20/21*

$$10Ca(NO_3)_2 + 6(NH_4)_2HPO_4 + 2NH_4F \longrightarrow Ca_{10}(PO_4)_6F_2 + 20NH_4OH + 6H_2O$$

Scheme 2

c = 9.422 Å. The surface area of calcined HAP was determined by the BET method from the adsorption–desorption isotherm of nitrogen at 77 K, and was found to be $S = 38.26\ m^2\ g^{-1}$. The total pore volume was calculated by the BJH method at $P/P_0 = 0.98$ ($VT = 0.157\ cm^3\ g^{-1}$).

Fluoroapatite was synthesised by the co-precipitation method (Scheme 2). 250 ml of a solution containing 7.92 g of diammonium hydrogen phosphate and 1 g of ammonium fluoride, maintained at a pH greater than 12 by addition of ammonium hydroxide (15 ml), was dropped into 150 ml of a solution containing 23.6 g of calcium nitrate, with constant stirring. The suspension was refluxed for 4 h. DDW was used to prepare the solutions. The FAD crystallites were filtered, washed with DDW, dried overnight at 80 °C and calcined in air at 700 °C for 30 min before use

$ZnCl_2$–HAP

The preparation of 1 mmol g^{-1} $ZnCl_2$–HAP was as follows: 10 mmol of $ZnCl_2$ and 10 g of HAP were mixed in 100 ml of water and then evaporated to dryness and dried for 2 h at 150 °C before use.

General procedure for transesterification

Ester **1** (2 mmol), alcohols **2** (11 mmol) and catalyst (HAP 100 mg, and $ZnCl_2$–HAP 50 mg) were refluxed with thorough mixing in toluene. Work-up by simple filtration followed by evaporation under reduced pressure and purification by column chromatography (hexane–ethylacetate 95 : 5) gave the desired product, which was analysed by ^{1}H NMR and IR.

Results and discussion

The XRD patterns of $ZnCl_2$–HAP are similar to that of HAP as shown in Fig. 1. The modification of the HAP by $ZnCl_2$ impregnation does not change the crystalline structure of the solid material. The intensity of typical diffraction peaks did not significantly change, indicating no disorganisation of the crystalline structure of HAP. It should be noted that no $ZnCl_2$ phases were detected on the doped material in all cases, indicating that $ZnCl_2$ was highly dispersed in the solid HAP.

The $ZnCl_2$–HAP and HAP alone were used as heterogeneous catalysts in the transesterification reaction between methyl benzoate and 1-butanol used as a model reaction (Scheme 3).

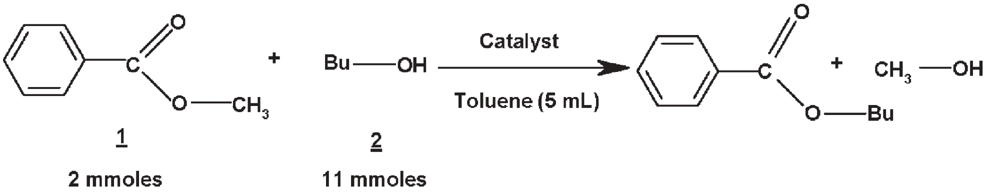

Scheme 3

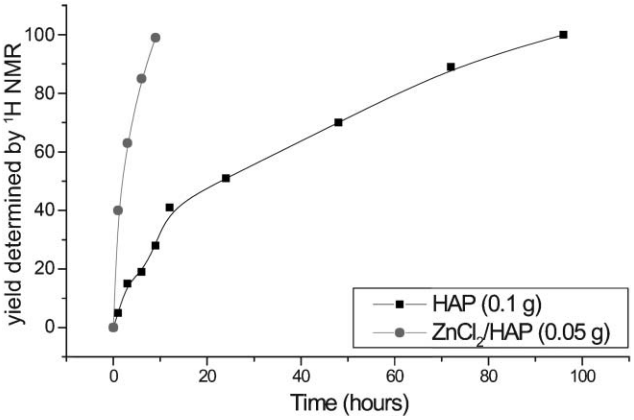

Fig. 2 Transesterification reaction between methyl benzoate and butanol using HAP and $ZnCl_2$–HAP.

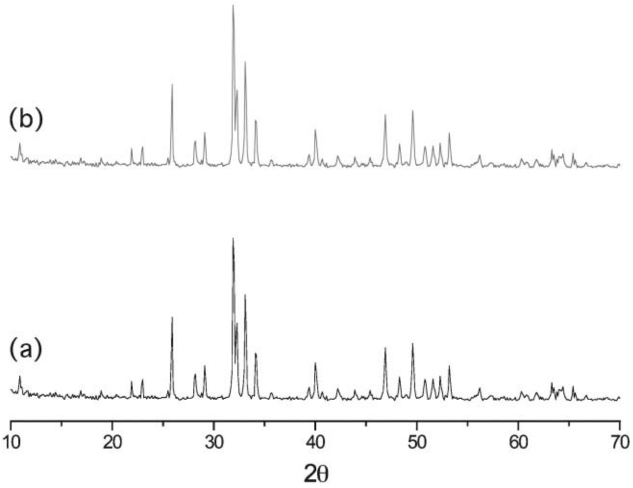

Fig. 3 XRD patterns of (a) FAP, (b) $ZnCl_2$–FAP.

The supported Lewis acid is a much more active catalyst in this reaction even when used in smaller quantities (Fig. 2).

The $ZnCl_2$–HAP catalyst is reusable in the reaction with comparable activity simply by filtration followed by drying at 150 °C; only a 3% reduction in yield is observed by the third run.

We were able to successfully extend the use of the catalyst to a series of transesterifications (Table 1). In all cases the supported Lewis acid is considerably more active than the support itself although the latter does show some activity.

The efficiency of the catalyst in transesterifications seems largely insensitive to changing from aromatic to aliphatic esters, from short chain to long chain alcohols, or to cyclic and aromatic

Table 1 Transesterification reactions catalysed by HAP and $ZnCl_2$–HAP

				Yield(%) (Time/h)	
Entry	Substrate **1**	Substrate **2**	Product	With HAP[a]	With $ZnCl_2$–HAP[b]
1	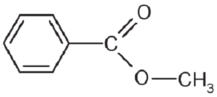	Et–OH	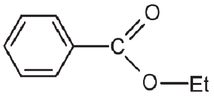	33 (24)	76 (6) 89 (9)
2	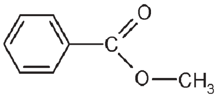	Bu–OH	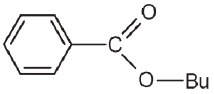	51 (24)	85 (6) 99 (9)
3	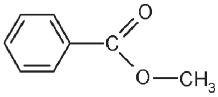	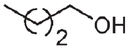	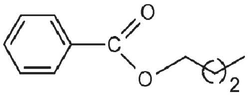	55 (24)	95 (6)
4	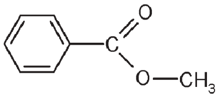	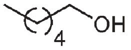	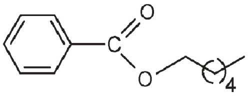	60 (24)	92 (6)
5	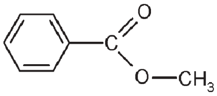	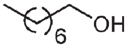	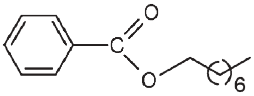	58 (24)	97 (6)
6	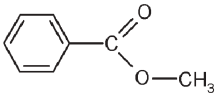	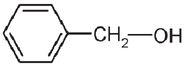	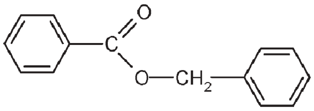	49 (24)	93 (6)
7	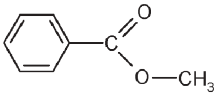	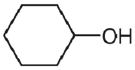	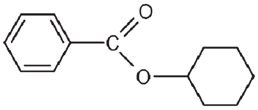	60 (24)	75 (3) 94 (6)
8	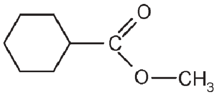	Bu–OH	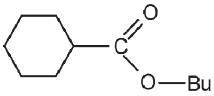	50 (24)	94 (6)
9	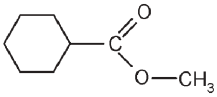	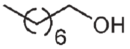	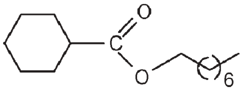	57 (24)	93 (6)
10	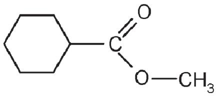	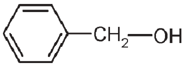	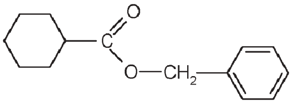	50 (24)	90 (6)
11	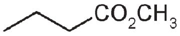	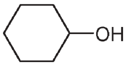	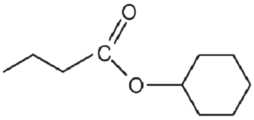	23 (24)	52 (6) 93 (12)
12		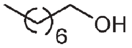	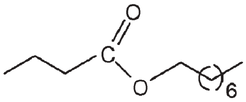	29 (24)	58 (6) 90 (12)
13	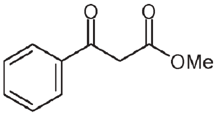	Bu–OH	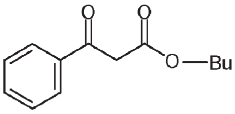	53 (24)	89 (6)
14	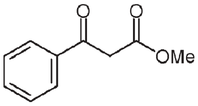	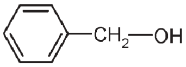	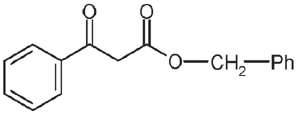	59 (24)	92 (6)

[a] Determined by ^1H NMR [b] Yields of pure isolated products

View Online

systems, demonstrating the considerable versatility of $ZnCl_2$–HAP as an active and simple and safe to use transesterification catalyst, as well as one that can be easily recovered and reused. In a parallel investigation we also studied the use of fluoroapatite, $Ca_{10}(PO_4)_6F_2$ and $ZnCl_2$ supported on the material as catalysts in the same reactions. The XRD pattern of FAP and $ZnCl_2$–FAP are shown in Fig. 3. As with the HAP analogues, no significant differences are seen between the patterns for the support and supported reagent, consistent with a non-disorganised FAP crystalline structure, and a well dispersed $ZnCl_2$. No significant difference in the activity of these catalysts compared to the hydroxyl analogues was detected. This suggests that the primary origin of the activity of $ZnCl_2$–HAP is the well dispersed Lewis acid. We were able to further confirm this by analysing the reaction mixtures for the presence of Zn^{2+} ions and obtained no detectable metal ions in solution by atomic absorption spectroscopy.

Acknowledgements

Financial assistance of the company MAFER is gratefully acknowledged.

Notes and references

1 J. Otera, *Chem. Rev.*, 1993, 1449.
2 C. E. Rethberg and C. H. Fisher, *J. Am. Chem. Soc.*, 1944, **66**, 1203.
3 O. Meth-Cohn, *J. Chem. Soc., Chem. Commun.*, 1986, 695.
4 J. H. Billman, W. T. Smith, Jnr and J. L. Rendall, *J. Am. Chem. Soc.*, 1947, **69**, 2056.
5 B. M. Choudary, M. L. Kantam, C. V. Reddy, S. Aranganathan, P. L. Santhi and F. Figueras, *J. Mol. Catal. A: Chem.*, 2000, **159**, 411.
6 B. S. Balaji and B. M. Choudary, *Tetrahedron*, 1998, **54**, 13237.
7 S. Sebti, R. Tahir, R. Nazih and S. Boulaajaj, *Appl. Catal., A*, 2003, **218**, 21.
8 R. Tahir, K. Banert, A. Solhy and S. Sebti, *J. Mol. Catal. A: Chem.*, 2005, **246**, 39.

COMMUNICATION www.rsc.org/greenchem | Green Chemistry

Alternating CO/*tert*-butylstyrene copolymerisation using soluble cationic palladium complexes in supercritical carbon dioxide†

Marta Giménez-Pedrós,[a] Clara Tortosa-Estorach,[a] Amaia Bastero,[a] Anna M. Masdeu-Bultó,*[a] Maurizio Solinas[b] and Walter Leitner*[b]

Received 30th May 2006, Accepted 27th July 2006
First published as an Advance Article on the web 7th August 2006
DOI: 10.1039/b607610f

Polyketones (M_w = 56 000–87 000 g mol^{-1}) with very narrow molecular weight distributions have been obtained by CO/*tert*-butylstyrene copolymerisation in supercritical carbon dioxide using palladium complexes with perfluorinated bipyridine and phenanthroline ligands.

Introduction

In the past few years there has been a growing interest in the synthesis of alternating polyketones of general formula $[C(O)CH(R)CH_2]_n$ from carbon monoxide and olefins (Scheme 1).[1–4] These polyketones represent a class of low-cost thermoplastics whose synthesis, properties and applications are still the object of intense fundamental and applied research. The copolymerisation of styrene and its derivatives with CO requires the use of cationic palladium catalyst associated with N,N-chelating ligands and weakly coordinating anions to be effectively accomplished. Enantioselective copolymerisation can also be achieved by the use of P,N-chelating ligands, and only relatively few examples using P,P-ligands have been reported.[3,5] Among the Pd–N,N-donor ligand catalyst precursors, the systems reported by Brookhart *et al.* based on Pd(II) complexes with bipyridine or phenanthroline are one of the most active.[6–9] The copolymerisation reactions are carried out using conventional organic solvents, such as methanol, 2,2,2-trifluoroethanol (TFE) or chlorobenzene.

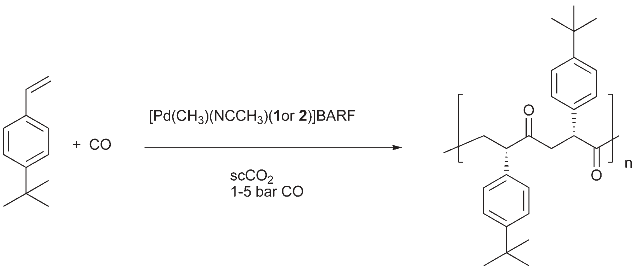

Scheme 1 CO/*tert*-butylstyrene copolymerisation.

During the past years, supercritical carbon dioxide ($scCO_2$) has received growing attention as an alternative reaction media for homogeneous catalysis. Supercritical carbon dioxide is an environmentally friendly and cheap solvent combining liquid-like solubility properties with gas-like mass transport properties.[10–12] $ScCO_2$ is highly miscible with gases such as carbon monoxide, allowing for the adjustment of single phase reaction mixtures with liquid substrates. Furthermore, the medium is highly compressible, has low viscosity and thus high diffusivity. Polymers of sufficient molecular weight are generally insoluble in $scCO_2$, allowing catalytic precipitation polymerisation without the use of organic solvents.[13] Despite these possible advantages, only a limited number of studies have been reported using $scCO_2$ as a reaction media for transition metal complex catalysed polymerisation reactions.[14] This is at least partly due to the low solubilising power of $scCO_2$, which makes ligand modification necessary to increase the solubility of organometallic catalytic systems. The presently most successful option to overcome this hurdle is the introduction of perfluorinated chains in the ligand.[11]

Herein we describe the alternating CO/*tert*-butylstyrene copolymerisation in supercritical carbon dioxide as a reaction media using new palladium cationic complexes of general formula $[Pd(CH_3)(NCCH_3)(N,N\text{-donor})]X$ containing monochelated bipyridine and phenanthroline ligands with perfluorinated chains, **1** and **2** (Fig. 1).

Results and discussion

The synthesis of perfluorinated ligand **1** was described by Pozzi *et al.*[15] and **2** was prepared following a similar procedure.[16] The palladium neutral complexes $[PdCl(CH_3)(L)]$ (**3**: L = **1** and **4**: L = **2**) were prepared by stoichiometric reaction of $[PdCl(CH_3)(cod)]$ (cod = 1,5-cyclooctadiene) with the corresponding ligand in anhydrous dichloromethane (Scheme 2). Cationic palladium complexes $[Pd(CH_3)(NCCH_3)(L)]BARF$ (**5**: L = **1** and **6**: L = **2**,

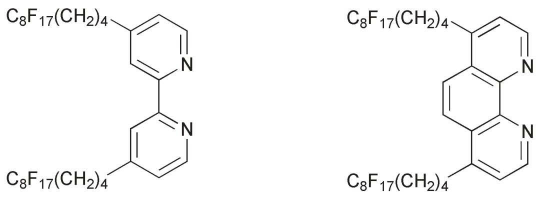

1

2

Fig. 1 Ligands **1** and **2**.

---

[a] *Departament de Química Física i Inorgànica, Universitat Rovira i Virgili, c/Marcel·lí Domingo, s/n, Tarragona, 43007, Spain. E-mail: annamaria.masdeu@urv.net; Fax: +34 977559563; Tel: +34 977558779*
[b] *Institut für Technische und Makromolekulare Chemie, Worringerweg 1, Aachen, D-52074, Germany. E-mail: leitner@itmc.rwth-aachen.de; Fax: +49-(0)241-80 221 77; Tel: + 49-(0)241-80 264 80*

† Electronic supplementary information (ESI) available: Detailed experimental procedures for the preparation of **2–6**. See DOI: 10.1039/b607610f

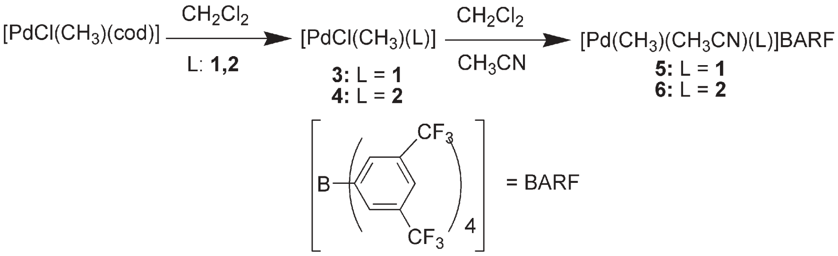

Scheme 2 Syntheses of complexes **3–6**.

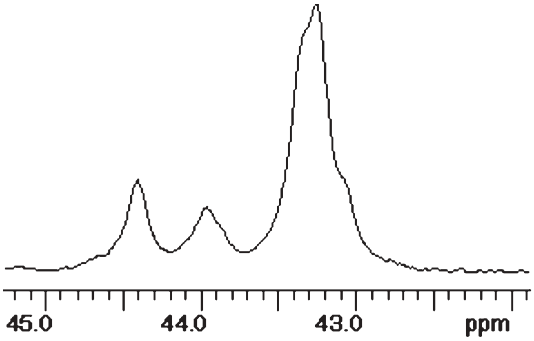

Fig. 2 $^{13}C\{^1H\}$ NMR spectrum in the region of methylene carbon atom corresponding to the copolymer obtained in entry 7 (Table 1).

BARF = $B(3,5-(CF_3)_2C_6H_3)_4^-$) were prepared by reaction of NaBARF in presence of CH_3CN and CH_2Cl_2.[17]

Catalytic runs in $scCO_2$ were performed using the preformed complexes in a 10 ml stainless steel autoclave equipped with thick-wall borosilicate windows. The solubility behaviour of the palladium complexes in supercritical carbon dioxide was examined by visual inspection. Both catalyst precursors and *tert*-butylstyrene were soluble in supercritical carbon dioxide at the catalytic conditions studied. As expected, the polyketone is not soluble in $scCO_2$, and precipitated during the reaction. The polymers obtained were characterised by ^1H and $^{13}C\{^1H\}$ NMR, and are consistent with a high syndiotactic copolymer structure (Fig. 2).[6]

Table 1 gives an overview of the polymerisation experiments in $scCO_2$ under various conditions. Experiments using dichloromethane or TFE as solvent are included for comparison. Productivities and molecular weight measurements were found to be reproducible within ±4% for selected experiments. Using carbon monoxide at 1 bar partial pressure (entries 1 and 2), low productivities were obtained using either dichloromethane or supercritical carbon dioxide as a solvent, although higher molecular weights were obtained in $scCO_2$. Increasing the partial pressure of carbon monoxide lead to an enhancement of both productivity and molecular weight (entries 2, 3 and 5). Most significantly, a strong increase in the molecular weight (M_W) was observed upon increasing the total pressure of $scCO_2$ from 170 to 250 bar, retaining at the same time a very narrow distribution (entries 7 and 5). Carrying out the polymerisation without stirring gave similar productivities and PDIs, but the molecular weight decreased to half the value (entry 8 *vs.* 7). Presumably, this reflects a less efficient mass transfer between the precipitated polymer and the $scCO_2$ phase in the non-agitated system. Catalyst precursor **6** gave similar productivities in $scCO_2$ although the molecular weight of the polyketone was lower than with **5** under identical conditions (entry 9 *vs.* 7).

Comparing the results with catalyst **5** in CH_2Cl_2 and $scCO_2$ under comparable conditions shows that similar activities are obtained in both solvents. Significantly higher productivites are achieved in the fluorinated alcohol TFE (entry 10). In contrast to both organic solvents, however, the supercritical reaction medium allows control of the molecular weight at significantly lower polydispersities. For example, the polydispersity decreased from 5.3 in dichloromethane to 1.2 in $scCO_2$ with a concomitant increase of M_w by a factor of two (entry 7 *vs.* 4). When TFE was used as solvent, M_w was higher than that obtained in $scCO_2$ but the polydispersity increased to 2.8.

Conclusion

In conclusion, we showed that palladium catalysed copolymerisation of CO and *tert*-butylstyrene could be accomplished using supercritical carbon dioxide avoiding the use of classical organic or fluorinated solvents. The cationic palladium catalysts were

Table 1 Copolymerisation of CO/TBS in supercritical carbon dioxide using **5** or **6** as catalyst precursor[a]

Entry	Precursor	Solvent	Productivity[b] [g CP/g Pd)]	P(CO)/bar	P(CO_2)/bar	M_W (M_W/M_n)
1[c]	**5**	CH_2Cl_2	43	1	—	6300 (1.3)
2	**5**	$scCO_2$	53	1	150	8800 (1.0)
3	**5**	$scCO_2$	139	3.5	170	11 100 (1.8)
4[c]	**5**	CH_2Cl_2	290	5	—	43 700 (5.3)
5	**5**	$scCO_2$	269	5	170	56 100 (1.5)
6[d]	**5**	$scCO_2$	243	5	200	63 000 (1.8)
7	**5**	$scCO_2$	235	5	250	87 800 (1.2)
8[e]	**5**	$scCO_2$	257	5	250	39 700 (1.3)
9	**6**	$scCO_2$	206	5	250	28 000 (1.5)
10	**5**	TFE	1066	1	—	115 000 (2.8)

[a] Reaction conditions: 0.0125 mmol catalyst, substrate/cat. = 620, 24 h, V = 10 ml, T = 37 °C. [b] Productivity: g of isolated copolymer (CP)/g Pd. [c] T = 25 °C; 0.00625 mmol catalyst, substrate/cat. = 620, 24 h, V = 5 ml. [d] 16 h. [e] No stirring.

rendered sufficiently CO_2-philic by introduction of perfluoroalkyl side chains in the chelating N,N-ligand. The polyketones obtained in $scCO_2$ are highly syndiotactic and have high and controllable molecular weights with improved polydispersities. Further studies are in progress to increase the productivity of the catalytic systems.

Experimental

Standard copolymerisation experiment

In a standard catalytic experiment, a solution of the catalyst precursor **5** or **6** (0.0125 mmol) in 2 ml of CH_2Cl_2 was placed under argon in a stainless steel high pressure reactor (V = 10 mL) equipped with thick-wall glass windows, the solvent was removed under vacuum and then the *tert*-butylstyrene (1.24 g, 7.75 mmol) was introduced into the reactor under argon. The reactor was charged with CO and with CO_2 to the desired pressure. The reactor was heated up to 37 °C and stirred during the reaction time. After reaction, the autoclave was cooled down to room temperature and was carefully vented. The copolymer obtained was dissolved in CH_2Cl_2 and precipitated by pouring the solution into 800 ml of rapidly stirred methanol. The product was filtered off, washed with MeOH and vacuum dried.

Safety warning

Experiments involving pressurised gases can be hazardous and must only be conducted with suitable equipment and following appropriate safety conditions.

Acknowledgements

We thank the Ministerio de Ciencia y Tecnologia (PPQ01-0452), the European Community (HPRN-CT-2002-00127) and Generalitat de Catalunya (DURSI ACI 2002-32) for financial support.

Notes and references

1 A. Sen, *Acc. Chem. Res.*, 1993, **26**, 303.
2 E. Drent and P. H. M. Budzelaar, *Chem. Rev.*, 1996, **96**, 663.
3 C. Bianchini and A. Meli, *Coord. Chem. Rev.*, 2002, **225**, 35.
4 J. Durand and B. Milani, *Coord. Chem. Rev.*, 2006, **250**, 542.
5 K. Nozaki, H. Komaki, Y. Kawashima, T. Hiyama and T. Matsubara, *J. Am. Chem. Soc.*, 2001, **123**, 534; J.-C. Yuan and S.-J. Lu, *Organometallics*, 2001, **20**, 2697.
6 M. Brookhart, F. C. Rix and J. M. DeSimone, *J. Am. Chem. Soc.*, 1992, **114**, 5894.
7 A. Sen and Z. Jiang, *Macromolecules*, 1993, **26**, 911.
8 A. Macchioni, G. Bellachioma, G. Cardaci, M. Travaglia, C. Zuccaccia, B. Milani, G. Corso, E. Zangrando, G. Mestroni, C. Carfagna and M. Formica, *Organometallics*, 1999, **18**, 3061; B. Milani, A. Scarel, G. Mestroni, S. Gladiali, R. Taras, C. Carfagna and L. Mosca, *Organometallics*, 2002, **21**, 1323; A. Scarel, B. Milani, E. Zangrado, M. Stener, S. Furlan, G. Fronzoni, G. Mestroni, S. Gladiali, C. Carfagna and L. Mosca, *Organometallics*, 2004, **23**, 5593.
9 A. Scarel, J. Durand, D. Franchi, E. Zangrando, G. Mestroni, B. Milani, S. Gladiali, C. Carfagna, B. Binotti, S. Bronco and T. Gragnoli, *J. Organomet. Chem.*, 2005, **690**, 2106.
10 P. G. Jessop, T. Ikariya and R. Noyori, *Chem. Rev.*, 1999, **99**, 475.
11 W. Leitner, *Acc. Chem. Res.*, 2002, **35**, 746.
12 D. J. Cole-Hamilton, *Science*, 2003, **299**, 1702.
13 For leading references, see:J. M. DeSimone, Z. Guan and C. S. Elsbernd, *Science*, 1992, **257**, 945; A. I. Cooper, *J. Mater. Chem.*, 2000, **10**, 207.
14 Typical examples: C. D. Mistele, H. H. Thorp and J. M. DeSimone, *Pure Appl. Chem.*, 1996, **A33**, 953; A. Fürstner, D. Koch, K. Langemann, W. Leitner and C. Six, *Angew. Chem., Int. Ed. Engl.*, 1997, **36**, 2466; H. Hori, C. Six and W. Leitner, *Macromolecules*, 1999, **32**, 3178; T. J. de Vries, R. Duchateau, M. A. G. Vortsman and J. F. Keurentjes, *Chem. Commun.*, 2000, 263; W. Kläui, J. Bongards and G. J. Reiβ, *Angew. Chem., Int. Ed.*, 2000, **39**, 3894; A. Wegner, *PhD Thesis*, Universitat Jena/MPI für Kohlenforschung, 2000; M. Kemmere, T. J. de Vries, M. Vorstman and J. Keurentjes, *Chem. Eng. Sci.*, 2001, **56**, 4197; K. Nozaki, F. Shibahara, S. Elzner and T. Hiyama, *Can. J. Chem.*, 2001, **79**, 593; A. Bastero, G. Franciò, W. Leitner and S. Mecking, *Chem.–Eur. J.*, 2006, **12**, 6110.
15 S. Quici, M. Cavazzini, S. Ceragioli, F. Montanari and G. Pozzi, *Tetrahedron Lett.*, 1999, **40**, 3647.
16 Spectroscopic data for **2**: ^{1}H NMR (300 MHz, $CDCl_3$): δ ^{1}H NMR (300 MHz, $CDCl_3$): 1.78 (m, 8H, $(CH_2)_{3'-4'}$), 2.08 (m, 4H, $(CH_2)_{2'}$), 3.13 (t, 4H, $(CH_2)_{1'}$, ^{2}J = 7.6 Hz), 7.38 (d, 2H, $H_{3,8}$, $^{3}J_{ortho}$ = 4.5 Hz), 7.98 (s, 2H, $H_{5,6}$), 9.02 (d, $^{3}J_{ortho}$ = 4.8 Hz, 2H, $H_{2,9}$).
17 Spectroscopic data: **5**: ^{1}H NMR (400 MHz, $CDCl_3$): δ ^{1}H NMR (400 MHz, $CDCl_3$): 0.97(s, 3H, CH_3), 1.72 (2 m, 8H, $(CH_2)_{3''-4''}$), 2.10 (m, 4H, $(CH_2)_{2''}$), 2.32 (s, 3H, CH_3CN), 2.74 (dt, 4H, $(CH_2)_{1''}$, ^{2}J = 7.6 Hz); 7.23 (d, 1H, J = 5.2 Hz), 7.34 (d, 1H, J = 5.2 Hz), 7.50 (s, 4H, BAr′), 7.68 (s, 8H, BAr′), 7.85 (s, 1H), 7.87 (s, 1H), 8.23 (d, J = 5.2 Hz, 1H), 8.36 (d, J = 5.6 Hz, 1H); **6**: δ ^{1}H NMR (300 MHz, $CDCl_3$): 1.05 (s, 3H, CH_3), 1.74 (2 m, 8H, $(CH_2)_{3'-4'}$), 2.05 (m, 4H, $(CH_2)_{2'}$), 2.29 (s, 3H, CH_3CN), 3.12 (t, 2H, $(CH_2)1'$, ^{2}J = 7.8 Hz), 3.17 (t, 2H, $(CH_2)1'$, ^{2}J = 7.2 Hz), 7.04 (s, 4H, BAr′), 7.48 (d, 1H, J = 5,1 Hz), 7.57 (d overlapped, 1H), 7.61 (s, 8H, BAr′), 8.08 (d, 2H, J = 2,4 Hz), 8.51 (d, 1H, J = 5,1 Hz), 8.64 (d, J = 5.7 Hz, 1H).

Biomass-derived heat-resistant alicyclic hydrocarbon polymers: poly(terpenes) and their hydrogenated derivatives

Kotaro Satoh, Hiroko Sugiyama and Masami Kamigaito*

Received 1st June 2006, Accepted 9th August 2006
First published as an Advance Article on the web 29th August 2006
DOI: 10.1039/b607789g

Naturally-occurring terpenes, such as (−)-β-pinene and (−)-α-phellandrene, were cationically polymerized and subsequently hydrogenated into stable alicyclic hydrocarbon polymers with a rigid backbone. In contrast to the already known poly(terpenes), the hydrogenated poly(β-pinene) with a high molecular weight ($M_w > 50\,000$) showed a high glass transition temperature (T_g = 130 °C) and degradation temperature (10% loss at > 400 °C), suggesting new promising biomass-derived materials for practical use.

Introduction

From the viewpoint of environmentally benign and sustainable chemistry, biomass resources have been attracting much attention as alternatives for traditional petrochemical raw materials.[1,2] A wide range of alicyclic polymerizable olefins can occur in various biomass species, among which terpenes, such as limonene, terpinen, phellandrene, and pinene, are popular and abundant in nature.[3,4] Since the 1950's, the polymerization of terpenes has been intensively investigated using the carbocationic mechanism.[5] However, this resulted in low molecular weight polymers with a low service temperature ($T_g < 100$ °C), which has limited the commercial utilization of these polymers or of their hydrogenated forms as additives, such as tackifiers in adhesives, or modifiers in molding compounds.

On the other hand, alicyclic hydrocarbon polymers originating from petroleum resources are now extensively utilized especially in the optoelectronic fields, not only because of the rigid backbone having a high service temperature and high mechanical strength, but also because of a low dielectric constant, nonhygroscopicity, and good transparency.[6] Vinyl ionic addition polymerization of cyclic olefins is one of the most promising methods that can readily produce amorphous polymers that retain the cyclic structures, whereas another approach has recently been developed and applied on an industrial scale by ring-opening metathesis polymerization of polycyclic olefins or coordination polymerization of cyclic olefins in the petroleum fraction.[7–9]

Cationic addition polymerization, which can be easily conducted with commercially available simple Brønsted or Lewis acid catalysts for various vinyl monomers with electron-donating substituents, has been also widely employed for a large number of monocyclic and polycyclic olefins since the 1920's.[5,6] In particular, the cyclic monomers with conjugated double bonds, such as indene and cyclopentadiene, were readily polymerized into high molecular weight polymers due to their stable carbocationic propagating species while the other unconjugated vinyl monomers, including terpenes, only gave oligomers due to the unstable cationic chain ends that undergo chain transfer reactions. Quite recently, we have reported that a novel petroleum-derived bicyclic conjugated diene, bicyclo[4.3.0]-2,9-nonadiene, was cationically polymerized by Lewis acid catalysts to give alicyclic hydrocarbon polymers with high thermal properties.[10]

In this paper, we focus our attention on the cationic polymerizations of naturally-occurring terpenes and the subsequent hydrogenations for developing terpene-based alicyclic polymers having good properties for practical use, especially their thermal properties with a high service temperature and durability. β-Pinene proved one of the most promising sustainable resources for this purpose in terms of not only availability and abundance, but also the polymerizability and the polymer properties.

Results and discussion

We first investigated the cationic polymerizations of (−)-β-pinene and (−)-α-phellandrene (Scheme 1). Whereas the polymerization of the latter has not been reported, there are many studies on the cationic polymerization of the former, which generally resulted in low molecular weight polymers with poor thermal properties.[11–15] A series of Lewis acid catalysts were thus employed for the cationic polymerization of these monomers at −78 °C in various solvents, in which a small amount of adventitious water may act as an initiator (protogen or cationogen). For both monomers, the polymerizations proceeded smoothly. Table 1 summarizes the number-average molecular weight (M_n) and the polydispersity

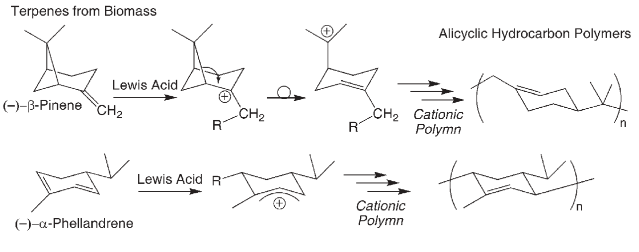

Scheme 1 Cationic polymerization of (−)-β-pinene and (−)-α-phellandrene.

Department of Applied Chemistry, Graduate School of Engineering, Nagoya University, Furo-cho, Chikusa-ku, Nagoya, 464-8603, Japan. E-mail: kamigait@apchem.nagoya-u.ac.jp; Fax: +81-52-789-5112; Tel: +81-52-789-5400

Table 1 Cationic polymerization of (−)-β-pinene and (−)-α-phellandrene with various Lewis acids at −78 °C[a]

Entry	Monomer	Lewis acid	Solvent	Time	Conversion (%)[b]	M_n[c]	M_w[c]	M_w/M_n[c]	T_g/°C[d]
1	(−)-β-pinene	$EtAlCl_2$	CH_2Cl_2	30 min	97	7400	14 400	1.95	—
2	(−)-β-pinene	$EtAlCl_2$	CH_2Cl_2–MCHx[e]	6 min	98	25 100	54 700	2.18	90
3	(−)-β-pinene	$EtAlCl_2$	MCHx	40 h	95	3800	5600	1.48	65
4	(−)-β-pinene	$Et_3Al_2Cl_3$	CH_2Cl_2–MCHx[e]	60 min	99	21 000	40 740	1.94	—
5	(−)-β-pinene	Et_2AlCl	CH_2Cl_2–MCHx[e]	5 h	25	7600	13 700	1.80	—
6	(−)-β-pinene	$AlCl_3$	CH_2Cl_2–MCHx[e]	0.5 min	>99	13 700	27 500	2.01	86
7	(−)-β-pinene	$TiCl_4$	CH_2Cl_2–MCHx[e]	8 h	66	3800	5900	1.55	65
8	(−)-β-pinene	$SnCl_4$	CH_2Cl_2–MCHx[e]	1 h	32	4900	8800	1.79	—
9	(−)-β-pinene	BF_3OEt_2	CH_2Cl_2–MCHx[e]	12 h	16	3800	5900	1.54	—
10	(−)-α-phellandrene	$EtAlCl_2$	CH_2Cl_2	3 h	82	6000	11 800	1.97	132
11	(−)-α-phellandrene	$EtAlCl_2$	CH_2Cl_2–MCHx[e]	2.5 h	83	3800	7000	1.85	—
12	(−)-α-phellandrene	$EtAlCl_2$	MCHx	20 h	65	5700	10 300	1.81	131
13	(−)-α-phellandrene	$SnCl_4$	CH_2Cl_2	4 h	79	4000	7100	1.77	—
14	(−)-α-phellandrene	BF_3OEt_2	CH_2Cl_2	150 h	80	3700	6500	1.77	130

[a] Polymerization conditions: $[\text{monomer}]_0 = 0.13$ (for entries 1–9 and 11) or 0.5 M (for entries 10 and 12–14); $[\text{Lewis acid}]_0 = 40.0$ mM. [b] Monomer conversion determined by gas chromatography. [c] The number-average (M_n) and weight-average (M_w) molecular weight and polydispersity index (M_w/M_n) determined by size-exclusion chromatography against polystyrene standards. [d] The glass transition temperature (T_g) determined by differential scanning calorimeter. [e] CH_2Cl_2–methylcyclohexane(MCHx) = 1 : 1 v/v.

index (M_w/M_n; M_w: weight-average molecular weight) calculated by size-exclusion chromatography (SEC) on the basis of a polystyrene (PSt) calibration. Whereas (−)-α-phellandrene was polymerized by Lewis acids into low molecular weight polymers ($M_w \sim 1 \times 10^4$), relatively high molecular weight polymers were obtained from β-pinene with some Lewis acids. Among them, the aluminium-based Lewis acids gave the highest molecular weight ($M_w > 5 \times 10^4$), as also reported by Kennedy *et al.*[13] More specifically, $EtAlCl_2$ and $Et_3Al_2Cl_3$, which have moderate Lewis acidity, gave the best results in a 1 : 1 mixture solvent of CH_2Cl_2 and methylcyclohexane (MCHx) in terms of molecular weights as well as yields of polymers or conversion of monomer (entries 2 and 4 in Table 1). However, a stronger Lewis acid, $AlCl_3$, induced an extremely fast polymerization (99% monomer conversion in 0.5 min) to result in a lower molecular weight ($M_w = 27\,500$) (entry 6), while a weaker acid, Et_2AlCl, resulted in a very slow reaction (only 25% conversion in 5 h) and a lower molecular weight ($M_w = 13\,700$) (entry 5). In general, a stronger Lewis acid generates a less nucleophilic counteranion, which cannot stabilize the growing carbocation, and causes chain-transfer reactions due to β-proton elimination, resulting in a lowering of the molecular weights.[5] In contrast, a weak Lewis acid does not have enough acidity to induce cationic polymerization efficiently. The choice of solvents is also crucial for determining the molecular weights. Generally, a polar solvent generates dissociated carbocationic species to result in concurrently occurring side reactions such as chain transfer, while a nonpolar solvent cannot lead to an efficient polymerization. It is also the case for the cationic polymerization of β-pinene, in which the simple use of a polar (CH_2Cl_2) or nonpolar solvent (MCHx) gave unsatisfactory results (entries 1 and 3). The key to the high molecular weight poly(β-pinene) is thus considered to be the judicious choice of the Lewis acids as well as the solvents.

The differential scanning calorimetry (DSC) analysis showed that the glass transition temperature (T_g) of poly(β-pinene) increased with the molecular weights and reached around 90 °C with the highest M_w, which is much higher than the T_g previously reported (65 °C).[13]

Fig. 1 shows the T_g dependence on the molecular weight of the obtained poly(β-pinene) and poly(α-phellandrene). The T_g increased with the molecular weights of the polymers. The T_g at the infinite molecular weight (T_g^∞) can be determined by the linear plot of T_g versus $1/M_n$ according to the following Flory and Fox equation:[16,17]

$$T_g = T_g^\infty - K/M_n \quad (1)$$

where K is the characteristic material constant. A linear relationship was observed for both polymers, where the T_g^∞ values were thus estimated to be 93.9 and 134.9 °C, and the K values were 11.0×10^4 and 1.90×10^4 for β-pinene and α-phellandrene, respectively. The relatively high T_g^∞ values indicate their possible practical use as a neat material even for poly(β-pinene).[17]

The optical activity of poly(β-pinene) was also examined. The poly(β-pinene) obtained with $EtAlCl_2$ showed specific rotations: $[\alpha]_{589} = -57.8°$ and $[\alpha]_{365} = -200°$ in THF at 20 °C. To the best of our knowledge, there have been no reports on the optical activity of the homopolymer of (−)-β-pinene,

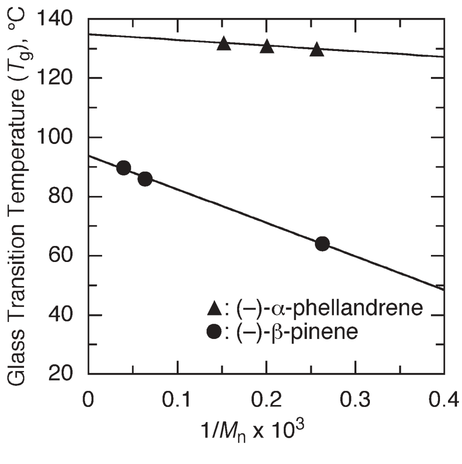

Fig. 1 Glass transition temperature (T_g) of poly(terpenes) obtained by cationic polymerization at −78 °C as a function of $1/M_n$. Terpene: ●, (−)-β-pinene; ▲, (−)-α-phellandrene.

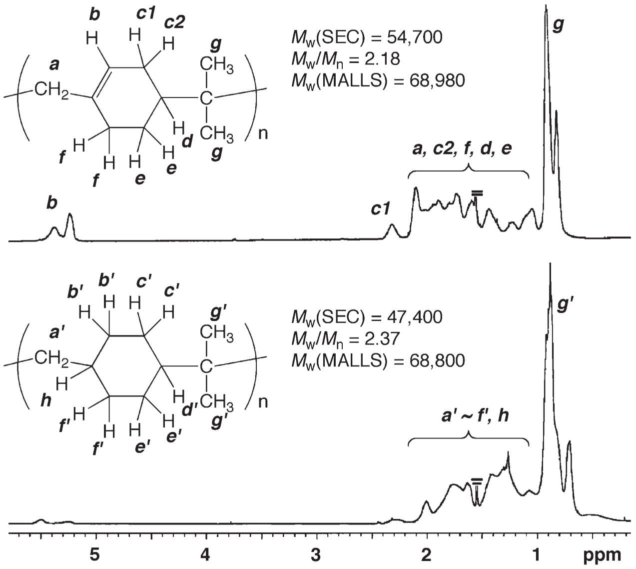

Fig. 2 ^{1}H NMR spectra ($CDCl_3$, 25 °C) of poly(β-pinene) (upper) and its hydrogenated derivative (hydrogenation degree = 91%) (bottom) obtained with $EtAlCl_2$ in CH_2Cl_2–methylcyclohexane (1 : 1 v/v) at −78 °C.

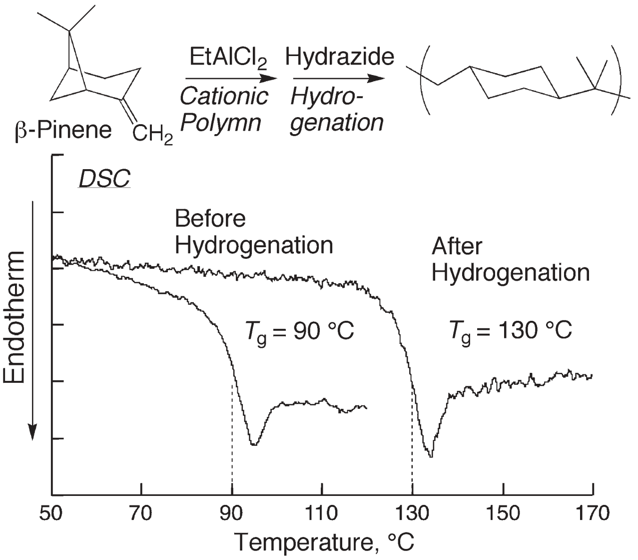

Fig. 3 Differential scanning calorimetry analysis of poly(β-pinene) and its hydrogenated derivative obtained in the same experiments as for Fig. 2.

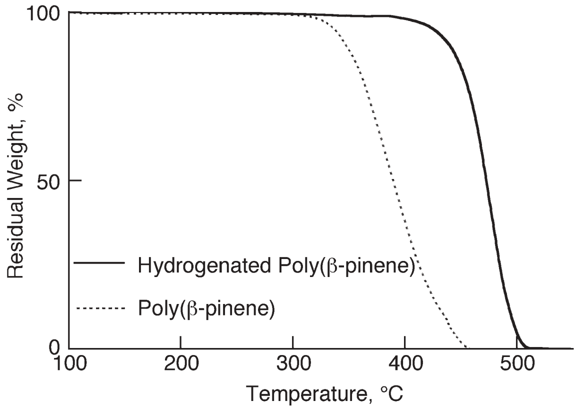

Fig. 4 Thermogravimetric analysis under N_2 gas flow of poly(β-pinene) (dotted line) and its hydrogenated derivative (solid line) obtained in the same experiments as for Fig. 2.

though some optically active copolymers of (−)-β-pinene were synthesized during the radical copolymerizations.[18,19]

The hydrogenation of poly(β-pinene) was then carried out using *p*-toluenesulfonyl hydrazide in *o*-xylene at 135 °C for 12 h.[20,21] Fig. 2 shows the ^{1}H NMR spectra of the poly(β-pinene) before and after the hydrogenation. After the hydrogenation, the spectrum only showed the signals of saturated hydrocarbons, while the unsaturated protons (*b*) almost completely disappeared (conversion $\geqslant$ 91% based on the residual olefin peaks). The molecular weights of the polymers were characterized by an SEC equipped with multiangle laser light-scattering (MALLS) and refractive index as a dual detector. There was almost no difference in their absolute molecular weights measured by MALLS before and after the hydrogenation [M_w(MALLS) = 68 980 and 68 800 (g mol^{-1}), respectively], while the M_n calculated on the basis of a PSt calibration slightly decreased. These results indicate that the successful reduction of the carbon–carbon double bonds proceeded by the hydrazide without a significant chain scission and that the hydrodynamic volume of the polymers changed during the hydrogenation.

In general, the hydrogenation of unsaturated polymers provides a higher thermal resistance and durability to the polymers. The thermal properties of the hydrogenated poly(β-pinene) were then evaluated by DSC and thermogravimetric analyses (TGA). Fig. 3 shows the DSC profiles of the polymers. The T_g value was improved by hydrogenation from 90 °C up to 130 °C. In addition, the TGA showed that the hydrogenated polymer has a relatively high pyrolysis temperature as shown in Fig. 4. Whereas the thermal degradation of the unsaturated poly(β-pinene) proceeded around 300 °C, that of the hydrogenated form occurred above 400 °C (10% weight loss at 440 °C). Thus, the hydrogenated poly(β-pinene) has both a better thermal durability and higher service temperature than the unsaturated precursor.

Conclusions

In conclusion, (−)-β-pinene and (−)-α-phellandrene were polymerized using a carbocationic mechanism to afford polymers with an alicyclic hydrocarbon structure. The poly(β-pinene) with a relatively high molecular weight was hydrogenated to obtain a polymer with a high glass transition temperature and degradation temperature. These thermal properties rival or even exceed those of oil-based commercially available amorphous thermoplastics, such as polystyrene and poly(methyl methacrylate) (T_g = 100–110 °C). Furthermore, the hydrocarbon polymers, lacking heteroatoms and even phenyl rings, should have good properties for optoelectronic materials, such as a low dielectric constant, nonhygroscopicity, and good transparency. Thus, alicyclic hydrocarbon polymers obtained from a naturally-occurring biomass would meet certain requirements in current markets.

Experimental

Materials

(−)-β-pinene (Aldrich; 99%) and (−)-α-phellandrene (Aldrich; >95%) were distilled from calcium hydride under reduced pressure before use. $SnCl_4$ (Aldrich, 99.995%), boron trifluoridediethyl etherate (BF_3OEt_2) (Aldrich, redistilled), $TiCl_4$ (Aldrich, >99.995%), $ZnCl_2$ (Aldrich, 1.0 M solution in *n*-diethyl ether), $AlCl_3$ (Aldrich, 99.99%), Et_2AlCl (Kanto, 1.0 M solution in *n*-hexane), Et_2AlCl (Kanto, 1.0 M solution in *n*-hexane) and $EtAlCl_2$ (Kanto, 1.0 M solution in *n*-hexane) were used as received. *p*-Toluenesulfonyl hydrazide (Wako, >95%) was used as received. Dichloromethane (Kanto, >99.5%) as a solvent was distilled from calcium hydride before use. Methylcyclohexane (Tokyo Kasei, >99%) and *o*-xylene (Wako, >98%) as solvents, and 1,2,3,4-tetrahydronaphthalene (Kishida, >99.5%) as an internal standard for gas chromatography were dried overnight over calcium chloride and distilled from sodium benzophenone ketyl before use.

Polymerization

Polymerization was carried out under dry nitrogen in baked glass tubes equipped with a three-way stopcock. A typical example for the polymerization procedure is given below. The reaction was initiated by addition of prechilled solutions (0.6 mL) of $SnCl_4$ (0.03 mmol) *via* dry syringes into a monomer solution [in CH_2Cl_2–methylcyclohexane(MCHx) (1 : 1 v/v); 2.4 mL] containing a monomer (0.39 mmol) and 1,2,3,4-tetrahydronaphthalene (0.1 mL). The total volume of the reaction mixture was 3.0 mL. After stirring at −78 °C, the polymerization was terminated with prechilled methanol (1.0 mL) containing a small amount of ammonia. Monomer conversion was determined from the concentration of residual monomer measured by gas chromatography with 1,2,3,4-tetrahydronaphthalene as an internal standard. The polymer yield by gravimetry was in good agreement with the gas chromatographic conversion of the monomer. The quenched reaction mixture was washed with dilute hydrochloric acid, aqueous sodium hydroxide solution, and then water to remove initiator residues, evaporated to dryness under reduced pressure, and vacuum-dried to give the product polymers.

Hydrogenation of polymers

Hydrogenation was performed following a modified literature protocol.[20,21] The reaction was carried out under dry nitrogen in a baked glass flask equipped with a three-way stopcock. The copolymer was dissolved in *o*-xylene under nitrogen at room temperature to give a 1–3 wt% solution. *p*-Toluenesulfonyl hydrazide (5 molar equivalent with respect to the unsaturated bonds) was added to the flask in the presence of 2,6-di-*tert*-butyl-4-methyl phenol (0.1 molar equivalent) as a stabilizer, and the mixture was refluxed at 135 °C under nitrogen for 5 h under stirring. The solution was allowed to cool, and the polymer was precipitated in methanol, filtered off, and dried *in vacuo*.

Measurements

Monomer conversion was determined from the concentration of residual monomer measured by gas chromatography [Shimadzu GC-8A equipped with a thermal conductivity detector and a 3.0 mm i.d. × 2 m stainless steel column packed with SBS-200 (Shinwa Chemical Industries Ltd.) supported on Shimalite W; injection and detector temperature = 200 °C, column temperature = 160 °C] with 1,2,3,4-tetrahydronaphthalene as an internal standard under He gas flow. ^{1}H NMR spectra were recorded in $CDCl_3$ at 25 °C on a Varian Gemini 2000 spectrometer, operating at 400 MHz. The number-average molecular weight (M_n) and polydispersity index (M_w/M_n) of the product (co)polymers were determined by size-exclusion chromatography (SEC) in THF at 40 °C on two polystyrene gel columns [Shodex K-805L (pore size: 20–1000 Å; 8.0 mm i.d. × 30 cm) × 2; flow rate 1.0 mL min^{-1}] connected to a Jasco PU-980 precision pump and a Jasco 930-RI detector. The columns were calibrated against 8 standard polystyrene samples (Shodex; M_p = 520–900 000; M_w/M_n = 1.01–1.14). The MALLS analysis was performed in THF on a Dawn DSP instrument (Wyatt Technology; Ga–As laser, λ = 690 nm). The refractive index increments (d*n*/d*c*) were measured in THF at 40 °C on an Optilab rEX (Wyatt Technology) (λ = 690 nm). Glass transition temperature (T_g) of the polymer was recorded on an SSC-5200 differential scanning calorimeter (Seiko Instruments Inc.). Samples were first heated to 200 °C at 15°C min^{-1}, equilibrated at this temperature for 5 min, and cooled to 40 °C at 5°C min^{-1}. After being held at this temperature for 5 min, the samples were then reheated to 250 °C at 10 °C min^{-1}. All T_g values were obtained from the second scan, after removing the thermal history. Thermogravimetric analyses (TGA) were also performed on SSC-5200 system at 10 °C min^{-1} under N_2 gas flow.

Acknowledgements

This work was supported in part by the 21st Century COE Program "Nature-Guided Materials Processing", Sekisui Chemical Grant Program for Research Projects Based on Learning from Nature, and the Sumitomo Foundation.

References

1 P. T. Anastas and J. C. Warner, *Green Chemistry Theory and Practice*, Oxford University Press, Oxford, 1998.
2 C. Okkerse and H. van Bekkum, *Green Chem.*, 1999, **1**, 107–114.
3 D. L. Klass, *Biomass for Renewable Energy, Fuels, and Chemicals*, Academic Press, San Diego, 1998.
4 C. M. Byrne, S. D. Allen, E. B. Lobkovsky and G. W. Coates, *J. Am. Chem. Soc.*, 2004, **126**, 11404–11405.
5 J. P. Kennedy, *Cationic Polymerization of Olefins: A Critical Inventory*, Wiley-Interscience, New York, 1975.
6 V. Dragutan and R. Streck, *Catalytic Polymerization of Cycloolefins*, Studies in Surface Science and Catalysis, vol. 131, Elsevier Science, Amsterdam, 2000.
7 T. M. Trnka and R. H. Grubbs, *Acc. Chem. Res.*, 2001, **34**, 18–29.
8 G. W. Coates, *Chem. Rev.*, 2000, **100**, 1223–1252.
9 I. Tritto, L. Boggioni and D. R. Ferro, *Coord. Chem. Rev.*, 2006, **250**, 212–241.
10 N. Mizuno, K. Satoh, M. Kamigaito and Y. Okamoto, *J. Polym. Sci., Part A: Polym. Chem.*, DOI: 10.1002/pola.21714.

11 W. J. Roberts and A. R. Day, *J. Am. Chem. Soc.*, 1950, **72**, 1226–1230.
12 F. Martinez, *J. Polym. Sci., Polym. Chem. Ed.*, 1984, **22**, 673–677.
13 B. Keszler and J. P. Kennedy, *Adv. Polym. Sci.*, 1992, **100**, 1–9.
14 J. Lu, M. Kamigaito, M. Sawamoto, T. Higashimura and Y.-X. Deng, *Macromolecules*, 1997, **30**, 22–26.
15 R. P. F. Guiné and J. A. A. M. Castro, *J. Appl. Polym. Sci.*, 2001, **82**, 2558–2565.
16 T. G. Fox and P. J. Flory, *J. Appl. Phys.*, 1950, **21**, 581–591.
17 R. F. Boyer, *Macromolecules*, 1974, **7**, 142–143.
18 J. Ma'sli'nsk'-Solich and I. Rudnicka, *Eur. Polym. J.*, 1988, **24**, 453–456.
19 M. Paz-Pazos and C. Pugh, *J. Polym. Sci., Part A: Polym. Chem.*, 2006, **44**, 3114–3124.
20 H. J. Harwood, D. B. Russell, J. J. A. Verthe and J. Zymonas, *Makromol. Chem.*, 1973, **163**, 1–12.
21 L. A. Mango and R. W. Lenz, *Makromol. Chem.*, 1973, **163**, 13–36.

H_2O_2-Based oxidation of functionalized phenols containing several oxidizable sites to *p*-quinones using a mesoporous titanium-silicate catalyst

Olga V. Zalomaeva,[ab] **Oxana A. Kholdeeva**[a] **and Alexander B. Sorokin***[b]

Received 2nd May 2006, Accepted 28th June 2006
First published as an Advance Article on the web 17th July 2006
DOI: 10.1039/b606120f

The oxidation of 2-allylphenol and different phenols bearing alcohol functional groups with aqueous H_2O_2 as oxidant and heterogeneous titanium-silicate Ti-MMM-2 as catalyst exhibits an unusual selectivity affording the corresponding *p*-quinones with good to moderate yield and keeping the other oxidizable sites intact. The use of hydrogen peroxide and heterogeneous titanium-silicate catalyst is a green alternative to the stoichiometric oxidation with hypervalent iodine compounds that provides better yields of structurally complex quinones in one step.

Introduction

Quinones often exhibit biological activity and occur within the molecular frameworks of the natural products.[1] Therefore, quinones are attractive synthetic targets. They can be prepared using different synthetic strategies,[2] but stoichiometric oxidation of aromatic compounds is still frequently used resulting in large amounts of waste. A typical example is the production of synthetic vitamin K_3 (2-methyl-1,4-naphthoquinone, MNQ) *via* stoichiometric oxidation of 2-methylnaphtalene (2-MN) by CrO_3 in sulfuric acid.[3–5] Along with the oxidants based on heavy metals, hypervalent iodine compounds are also widely used for preparation of quinones *via* oxidation of phenols and its less accessible methoxy derivatives.[6,7] Although these stoichiometric oxidations (however, an excess of oxidant is usually used) give quinones with reasonable yields, a very low active oxygen content in these oxidants leads to significant amounts of waste thus causing a lot of problems with their disposal. *E*-factor introduced by Sheldon as waste/useful product weight ratio[8] for these oxidations is typically in the range of 10–20.

Evidently, current demand for environmentally friendly processes requires the development of green oxidation methods that employ clean oxidants such as peroxides or dioxygen and a catalyst. The catalytic procedures based on the oxidation of 2-MN with hydrogen peroxide or *tert*-butyl hydroperoxide (^{t}BuOOH) have been reported.[9–16] The main drawback of these methods is a moderate yield of the target product (typically 40–60%). The low selectivity of 2-MN oxidation to MNQ can be explained by the presence of several oxidizable sites at 2-MN leading to several oxidation pathways. First, two isomeric quinones, MNQ and 6-methyl-1,4-naphthoquinone, can be formed usually in about 3 : 1 ratio. Along with aromatic oxidation, oxidation of methyl group occurs. Products of the oxidative coupling of intermediate radicals and over-oxidation products can be also formed. Selective oxidation of the substrate having several oxidizable sites involving only one oxidation pathway while keeping other oxidizable sites intact is therefore a key issue.

In the past decade, a considerable amount of research has been dedicated to the preparation of various mesoporous materials, containing transition metal ions highly dispersed in inorganic, mostly silicate matrixes, and their use as catalysts in selective oxidation of bulky organic substrates with hydroperoxides.[17–27] Previously, we found that mesoporous titanium-silicates, both well-ordered and amorphous ones, catalyze effectively the oxidation of 2,3,6-trimethylphenol (TMP) to 2,3,5-trimethyl-1,4-benzoquinone (TMBQ, vitamin E precursor).[25,26] However, most of these catalytic materials suffered from hydrolytic instability, which restricted their practical use. Recently, we have reported the preparation and characterization of the novel highly active and hydrothermally stable titanium-silicate Ti-MMM-2 and demonstrated a true heterogeneous nature of catalysis and its reusability in selective oxidations with aqueous H_2O_2.[27,28]

Ti-MMM-2 catalyst was successfully used in the oxidation of 2-methyl-1-naphtol (MNL).[29] This recyclable catalyst allowed one to obtain MNQ with selectivity as high as 75% at complete substrate conversion. The promising selectivity in aromatic oxidation prompted us to check the scope of this catalyst in even a more challenging oxidation of various phenols having easily oxidizable sites, *e.g.* alcoholic function, double bond and benzylic/allylic positions.

In the case of the oxidation of phenols bearing an alcohol group, especially in the benzylic position, the oxidation to aldehyde group often prevails over aromatic oxidation. For example, 2-hydroxybenzyl alcohol (2-HBA) is usually oxidized to salicylaldehyde (SA) over noble metal catalysts.[30] A stoichiometric oxidation of 2-HBA to 2-hydroxymethyl-1,4-benzoquinone (2-HQ) by polymer-supported hypervalent iodine reagents represents the only example of aromatic oxidation with the yield of 2-HQ about 30%.[31] The stoichiometric oxidation of a less available and easily oxidizable methoxy-derivative of phenol with hypervalent iodine oxidants to 2-HQ has been published.[32] 2-HQ can be obtained electrochemically from 2,5-dimethoxyphenyl-methanol; however, the yield does not exceed 30%.[33] Noteworthy, a low selectivity is typical for such oxidations.

---

[a] *Boreskov Institute of Catalysis, Pr. Ac. Lavrentieva 5, Novosibirsk, 630090, Russia*
[b] *Institut de Recherches sur la Catalyse, CNRS, 2, avenue A. Einstein, 69626, Villeurbanne Cedex, France. E-mail: sorokin@catalyse.cnrs.fr; Fax: +33 472445399; Tel: +33 472445337*

Here we report the oxidation of the functionalized phenols to the corresponding quinones over titanium-silicate Ti-MMM-2 using aqueous H_2O_2 as oxidant.

Results and discussion

Titanium-silicate catalyst Ti-MMM-2 was prepared as described previously[27] using $Na_2Si_2O_5$ and $TiOSO_4 \cdot H_2SO_4$ as silica and titanium source, respectively, and cetyltrimethyl ammonium bromide as template. This material was characterized by synchrotron XRD, nitrogen adsorption techniques and DR UV-vis spectroscopy. The textural, structural and spectroscopic characteristics were similar to those reported in ref. 27–29. In particular, the Ti-MMM-2 samples have uniform mesopores with a diameter of 3 nm and a silicate wall thickness of about 1.0 nm.

From the group of phenols with alcohol function we first studied the oxidation of 2-HBA. The oxidation products were identified and quantified by GC-MS and ^{1}H NMR methods. The 2-HBA (0.02 M solution, 7 H_2O_2 equiv.) was oxidized over Ti-MMM-2 (6 mol%) in CD_2Cl_2 at 30 °C to 2-HQ with selectivity 26% and conversion 14%. The use of acetonitrile as solvent and increasing the reaction temperature up to 80 °C allowed to increase the selectivity to quinone to 54% at 87% conversion. Along with SA, 2-hydroxymethyl-1,4-hydrobenzoquinone, catechol and 2,5-dihydroxybenzaldehyde were identified by GC-MS as minor reaction products. No overoxidation products issued from the cleavage of aromatic cycle were found.

To find optimized reaction conditions, we evaluated the influence of the oxidant/substrate ratio, 2-HBA concentration and catalyst loading. Progressive increasing H_2O_2/2-HBA ratio from 5 to 11 resulted in increasing 2-HQ yield from 45 to 71% (Fig. 1). A further increasing of H_2O_2 amount did not result in the increase of 2-HQ yield. When the oxidation of 2-HBA was performed in the presence of 5 equiv. of H_2O_2 and 4 equiv. of H_2O with respect to the substrate a 55% yield of 2-HQ was obtained suggesting a positive effect of H_2O_2 on the selectivity of aromatic oxidation. A further optimisation of the catalytic system was performed using H_2O_2/2-HBA = 9 ratio.

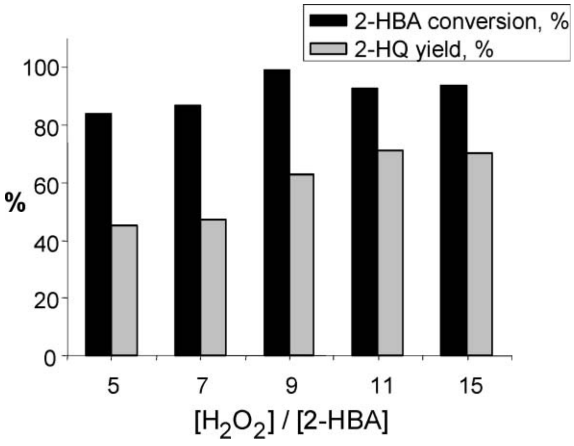

Fig. 1 Influence of H_2O_2/2-HBA ratio on the oxidation of 2-HBA. Reaction conditions: 1 mL of 0.02 M 2-HBA solution in CD_3CN, 6 mol% of Ti-MMM-2, 80 °C, 2 h.

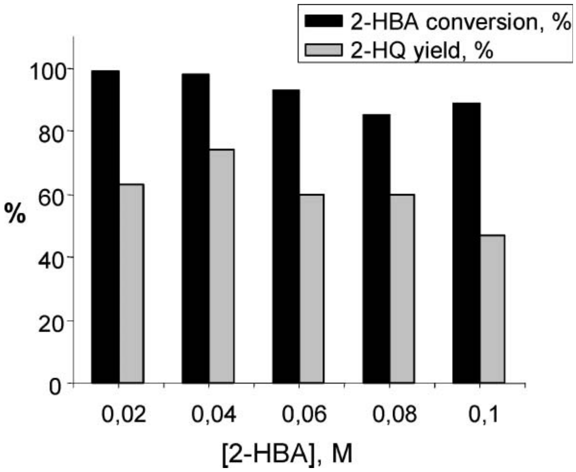

Fig. 2 Influence of the initial concentration of 2-HBA on the oxidation. Reaction conditions: 1 mL of 2-HBA solution in CD_3CN, $[H_2O_2]/[2\text{-HBA}] = 9/1$, 6 mol% of Ti-MMM-2, 80 °C, 2 h.

The yield of 2-HQ was also sensitive to the initial concentration of 2-HBA solution (Fig. 2). The optimal 2-HBA concentration was 0.04 M to give a 74% yield of 2-HQ. The optimal loading of catalyst was found to be 6 mol%. Further increasing of the catalyst loading did not provide better 2-HQ yield. According to the results obtained, the optimal reaction conditions for oxidation of 2-HBA are as follows: [2-HBA] = 0.04 M, H_2O_2/2-HBA = 9/1, 6 mol% of catalyst, 80 °C, acetonitrile, 2 h reaction time. Ti-MMM-2 was used for three cycles in the oxidation of 2-HBA which showed consistent selectivity and a small decrease in activity.

The scope of the method has been extended to the oxidation of functionalized phenols. The oxidation of different substrates, including 3,5-dihydroxybenzyl alcohol containing two hydroxyl groups, also produced quinones with 38–71% selectivity (Table 1, entries 2–5). No oxidation occurred without catalyst. The products of oxidation of alcohol function accounted only for 3–5% indicating that the main oxidation pathway was again the aromatic oxidation.

Another type of phenol, exemplified by 2-allylphenol with easily oxidizable double bond and benzylic/allylic position, also afforded quinone although selectivity was moderate in this case (Table 1, entry 6). However, it should be emphasized that no selective oxidation of alkenylphenols to quinones keeping double bond intact has been reported in the literature. Typically, allylphenols react with oxidants to give epoxides or products of cyclization.[34] To prepare allylquinones the allylation of quinones with allyltin[35] and allylindium[36] reagents have been used.

Experimental

General

Solvents and chemicals were obtained from Sigma-Aldrich and used without purification unless indicated. Deuterated acetonitrile-d_3 (99.8%) was available from Euriso-top.

Liquid-state nuclear magnetic resonance spectra were recorded using the AM 250 Bruker spectrometer.

Table 1 Oxidation of phenols by hydrogen peroxide catalyzed by Ti-MMM-2 catalyst[a]

Substrate	Product	Time/ h	Conversion (%)	Selectivity (%)
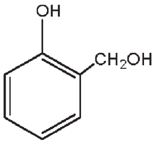	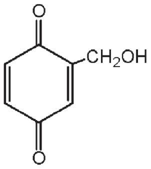	2	96	76
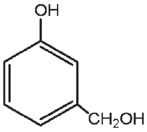	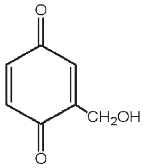	3	87	53
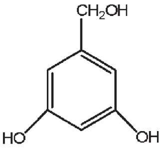	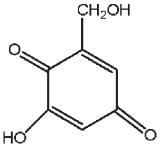	0.5	100	41
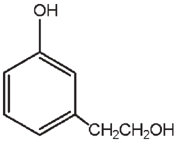	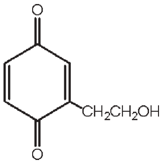	3	82	71
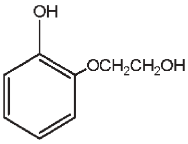	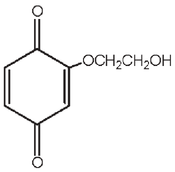	0.5	98	38
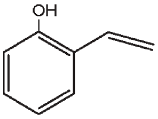	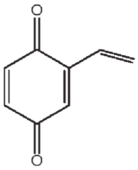	6	84	36
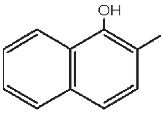	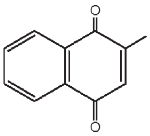	0.5	100	75[b]

[a] Percent conversion and product yield were determined by ^{1}H NMR spectroscopy using biphenyl as internal standard. [b] From ref. 29.

The products of oxidation were identified by NMR and GC-MS methods. The quantitative GC analyses were not reproducible because of instability of the substrates and/or reaction products under GC conditions. Therefore, conversions and product yields were determined by NMR using biphenyl as internal standard.

The reaction products were identified by GC-MS (Hewlett Packard 5973/6890 system ; electron impact ionization at 70 eV, He carrier gas, 30 m × 0.25 mm crosslinked 5% PHME siloxane (0.25 μm coating) capillary column, HP-5MS).

The products of the degradation of aromatic rings were analyzed by GC-MS (capillary column VF5-MS, 100% dimethylpolysiloxane, 30 m × 0.25 mm, 0.25 μm coating) using trimethylsulfonium hydroxide as a derivatization agent.[37]

Preparation of Ti-MMM-2 catalyst

Ti-MMM-2 was prepared and characterized as described previously[27] using $Na_2Si_2O_5$ and $TiOSO_4{\cdot}H_2SO_4$ as silica and titanium source, respectively, and cetyltrimethyl ammonium bromide (CTAB) as a template. At the first step, the aqueous mixture of CTAB, $Na_2Si_2O_5$ and $TiOSO_4{\cdot}H_2SO_4$ was prepared at pH 0.5–1.5. To this mixture, a solution of sodium silicate was added keeping the pH of the reaction mixture between 2.0 and 3.5. The resulting mixture was kept at 50 °C for 15–20 min. Final molar ratio was $SiO_2 : TiO_2$: CTAB : HCl : $H_2O = (1 - x) : (x) : (0.16–0.2) : (1) :(165)$, $x = 0.01–0.1$. CTAB was removed from the materials by calcination at 550–600 °C for 6 h in the presence of air. Ti-MMM-2 sample contained 2.0 wt% of Ti.

Typical procedure for the oxidation of phenols

To a 0.04 M solution of substrate and 0.0096 M of biphenyl (internal standard) in 1 mL of deuterated solvent was added 6 mg of catalyst ($2.4{\cdot}10^{-6}$ mol Ti). The reaction was started by the addition of a 35% aqueous H_2O_2 and was carried out at 80 °C. After the reaction the catalyst was separated by filtration and the reaction mixture was analyzed by ^{1}H NMR. Product yields and conversion were determined by integration of the corresponding proton signals relatively to internal standard signals.

2-Hydroxybenzyl alcohol. MS (EI) *m/z* (relative int.): 124 (45, $[M]^+$), 106 (64, $[M - H_2O]^+$), 78 (100, $[M - H_2O - CO]^+$).

^{1}H NMR (CD_3COCD_3, 250 MHz): δ 4.70 (s, 2H, CH_2), 6.74–6.80 (m, 2H, CH aromatic), 7.05–7.25 (m, 2H, CH aromatic).

2-Hydroxymethyl-1,4-benzoquinone. MS (EI) *m/z* (relative int.): 138 (20, $[M]^+$), 122 (16, $[M - O]^+$), 110 (100, $[M - CO]^+$), 94 (10, $[M - 2O]^+$), 82 (28, $[M - 2CO]^+$).

^{1}H NMR (CD_3COCD_3, 250 MHz): δ 4.44 (s, 2H, CH_2), 6.74–6.78 (m, 3H, CH aromatic).

3-Hydroxybenzyl alcohol. MS (EI) *m/z* (relative int.): 124 (100, $[M]^+$), 123 (29, $[M - H]^+$) , 107 (18, $[M - OH]^+$), 106 (16, $[M - H_2O]^+$), 105 (23, $[M - H_2O - H]^+$), 95 (60, $[M - COH]^+$), 77 (60, $[M - H_2O - COH]^+$).

^{1}H NMR (CD_3COCD_3, 250 MHz): δ 4.13 (t, 1H, OH, J = 5.7 Hz), 4.54 (d, 2H, CH_2, J = 5.7 Hz), 6.55 (d, 1H, CH aromatic, J = 3.38 Hz), 6.77–6.85 (m, 2H, CH aromatic), 7.11 (t, 1H, CH aromatic, J = 7.8 Hz).

3,5-Dihydroxybenzyl alcohol. MS (EI) *m/z* (relative int.): 140 (100, $[M]^+$), 139 (12, $[M - H]^+$) , 123 (14, $[M - OH]^+$), 122 (15, $[M - H_2O]^+$), 121 (18, $[M - H_2O - H]^+$), 111 (54, $[M - COH]^+$), 93 (22, $[M - H_2O - COH]^+$).

^{1}H NMR (CD_3COCD_3, 250 MHz): δ 4.38 (s, 2H, CH_2), 6.14 (t, 1H, CH aromatic, J = 2.3 Hz), 6.25–6.28 (m, 2H, CH aromatic).

2-Hydroxy-6-hydroxymethyl-1,4-benzoquinone. MS (EI): unstable under analysis conditions.

^{1}H NMR (CD_3COCD_3, 250 MHz): δ 4.34 (s, 2H, CH_2), 5.8 (d, 1H, CH aromatic, J = 2.5 Hz), 6.51 (d, 1H, CH aromatic, J = 2.5 Hz).

3-Hydroxyphenetyl alcohol. MS (EI) *m/z* (relative int.): 138 (61, $[\mathrm{M}]^+$), 120 (6, $[\mathrm{M} - \mathrm{CO}]^+$), 108 (70, $[\mathrm{M} - \mathrm{CH_2O}]^+$), 107 (100, $[\mathrm{M} - \mathrm{CH_2OH}]^+$), 90 (12, $[\mathrm{M} - \mathrm{CH_2O} - \mathrm{H_2O}]^+$), 77 (35, $[\mathrm{M} - \mathrm{CHCH_2O} - \mathrm{H_2O}]^+$).

^{1}H NMR ($\mathrm{CD_3COCD_3}$, 250 MHz): δ 2.71 (t, 2H, $\mathrm{CH_2CH_2OH}$, J = 7.0 Hz), 3.70 (t, 2H, $\mathrm{CH_2CH_2OH}$, J = 7.0 Hz), 6.63–6.70 (m, 3H, CH aromatic), 7.07 (t, 1H, CH aromatic, J = 7.7 Hz).

2-(2-Hydroxyethyl)-1,4-benzoquinone. MS (EI): unstable under analysis conditions.

^{1}H NMR ($\mathrm{CD_3COCD_3}$, 250 MHz): δ 2.54 (t, 2H, $\mathrm{CH_2OH}$, J = 6.3 Hz), 3.65 (t, 2H, $\mathrm{CH_2CH_2OH}$, J = 6.3 Hz), 6.57–6.72 (m, 3H, CH aromatic).

2-Allylphenol. MS (EI) *m/z* (relative int.): 134 (100, $[\mathrm{M}]^+$), 133 (38, $[\mathrm{M} - \mathrm{H}]^+$), 119 (33, $[\mathrm{M} - \mathrm{CH_3}]^+$), 115 (34, $[\mathrm{M} - \mathrm{H_2O} - \mathrm{H}]^+$), 107 (19, $[\mathrm{M} - \mathrm{CH_2CH}]^+$), 105 (21, $[\mathrm{M} - \mathrm{COH}]^+$), 91 (41, $[\mathrm{M} - \mathrm{CH_2} - \mathrm{COH}]^+$), 77 (30, $[\mathrm{M} - \mathrm{CH_2CH_2} - \mathrm{COH}]^+$).

^{1}H NMR ($\mathrm{CD_3CN}$, 250 MHz): δ 3.34 (d, 2H, $\mathrm{CH_2CH{=}CH_2}$, J=6.5 Hz), 5.00–5.08 (m, 2H, $\mathrm{CH_2CH{=}CH_2}$), 5.92–6.08 (m, 1H, $\mathrm{CH_2CH{=}CH_2}$), 6.78–6.81 (m, 2H, CH aromatic), 6.84 (s, 1H, OH), 7.03–7.10 (m, 2H, CH aromatic).

2-Allyl-1,4-benzoquinone. MS (EI) *m/z* (relative int.): 148 (33, $[\mathrm{M}]^+$), 147 (42, $[\mathrm{M} - \mathrm{H}]^+$), 131 (6, $[\mathrm{M} - \mathrm{OH}]^+$), 120 (54, $[\mathrm{M} - \mathrm{CO}]^+$), 105 (13, $[\mathrm{M} - \mathrm{CH_2} - \mathrm{COH}]^+$), 92 (13, $[\mathrm{M} - 2\mathrm{CO}]^+$), 91 (100, $[\mathrm{M} - 2\mathrm{CO} - \mathrm{H}]^+$).

^{1}H NMR ($\mathrm{CD_3CN}$, 250 MHz): δ 3.15 (dd, 2H, $\mathrm{CH_2CH{=}CH_2}$, J_1 = 6.8 Hz, J_2 = 1.4), 4.98–5.12 (m, 2H, $\mathrm{CH_2CH{=}CH_2}$), 5.80–6.10 (m, 1H, $\mathrm{CH_2{-}CH{=}C}$), 6.54–6.77 (m, 3H aromatic).

Conclusions

Titanium-silicate Ti-MMM-2 catalyst exhibits an unusual selectivity in the oxidation of phenols bearing alcohol functions or double bond favoring aromatic oxidation to corresponding quinones rather than oxidation of these easily oxidizable groups. This considerable extension of the catalytic activity of titanium based catalysts provide a basis for new promising green route to aromatic compounds having carbonyl functions, double bonds and alcohol group in adjacent position on an aromatic cycle. These valuable synthetic intermediates have been previously prepared by stoichiometric oxidation with hypervalent iodine oxidants. The proposed catalytic method is a green alternative since it involves hydrogen peroxide oxidant and recyclable solid catalyst. Selective oxidation of such functionalized substrates gives the possibility to access directly to structurally complex targets thus avoiding multistep synthesis.

Acknowledgements

This work was supported by the Associated European Laboratory (Institut de Recherches sur la Catalyse, Villeurbanne and Boreskov Institute of Catalysis, Novosibirsk) and Russian Foundation for Basic Research (grant RFBR-CNRS 05-03-05-03-34760). O. V. Z. acknowledges the financial support from the Embassy of France in Moscow for a doctoral fellowship. Dr M. S. Melgunov is kindly acknowledged for his help with the preparation of the Ti-MMM-2 material.

References

1 *The Chemistry of Quinonoid Compounds*, ed. S. Patai and Z. Rappoport, Wiley-Interscience, New York, 1988.
2 (*a*) W. M. Owton, *J. Chem. Soc., Perkin Trans. 1*, 1999, 2409; (*b*) Y. Naruta and K. Maruyama, in *The Chemistry of Quinonoid Compounds*, ed. S. Patai and Z. Rappoport, Wiley-Interscience, New York, 1988, ch. 8, pp. 241–401.
3 S. Araki, N. Katsumura and Y. Butsugan, *J. Organomet. Chem.*, 1991, **415**, 7.
4 L. F. Fieser, *J. Biol. Chem.*, 1940, **133**, 391.
5 R. A. Sheldon, *Top. Curr. Chem.*, 1993, **164**, 21.
6 V. V. Zhdankin and P. J. Stang, *Chem. Rev.*, 2002, **102**, 2523.
7 (*a*) T. Wirth, *Top. Curr. Chem.*, 2003, **224**, 185; (*b*) K. C. Nicolaou, K. Sugita, P. S. Baran and Y.-L. Zhong, *J. Am. Chem. Soc.*, 2002, **124**, 2221.
8 R. A. Sheldon, *Chem. Ind.*, 1992, 903.
9 J. Kowalski, J. Ploszynska and A. Sobkowiak, *Catal. Commun.*, 2003, **4**, 603.
10 W. Adam, W. A. Herrmann, W. Lin, C. R. Saha-Moller, R. W. Fischer and J. D. G. Correia, *Angew. Chem., Int. Ed. Engl.*, 1994, **33**, 2475.
11 W. A. Herrmann, J. J. Haider and R. W. Fischer, *J. Mol. Catal. A: Chem.*, 1999, **138**, 115.
12 S. Yamaguchu, M. Inoue and S. Enomoto, *Chem. Lett.*, 1985, 827.
13 O. S. Anunziata, L. B. Pierella and A. R. Beltramone, *J. Mol. Catal. A: Chem.*, 1999, **149**, 255.
14 O. S. Anunziata, A. R. Beltramone and J. Cussa, *Appl. Catal., A*, 2004, **270**, 77.
15 A. B. Sorokin and A. Tuel, *Catal. Today*, 2000, **57**, 45.
16 A. B. Sorokin, S. Mangematin and C. Pergrale, *J. Mol. Catal. A: Chem.*, 2002, **182–183**, 267.
17 B. Notari, *Adv. Catal.*, 1996, **41**, 253.
18 A. Corma, M. T. Navarro and J. Perez Pariente, *J. Chem. Soc., Chem. Commun.*, 1994, 147.
19 A. Corma, *Chem. Rev.*, 1997, **97**, 2373.
20 M. Schneider and A. Baiker, *Catal. Today*, 1997, **35**, 339.
21 W. Zhang, M. Froba, J. Wang, P. T. Tanev, J. Wong and T. J. Pinnavaia, *J. Am. Chem. Soc.*, 1996, **118**, 9164.
22 P. T. Tanev, M. Chibwe and T. J. Pinnavaia, *Nature*, 1994, **368**, 321.
23 A. Sayari, *Chem. Mater.*, 1996, **8**, 1840.
24 X. Gao and I. E. Wachs, *Catal. Today*, 1999, **51**, 233.
25 N. N. Trukhan, V. N. Romannikov, E. A. Paukshtis, A. N. Shmakov and O. A. Kholdeeva, *J. Catal.*, 2001, **202**, 110.
26 O. A. Kholdeeva, N. N. Trukhan, M. P. Vanina, V. N. Romannikov, V. N. Parmon, J. Mrowiec-Bialon and A. B. Jarzebski, *Catal. Today*, 2002, **75**, 203.
27 O. A. Kholdeeva, M. S. Melgunov, A. N. Shmakov, N. N. Trukhan, V. V. Kriventsov, V. I. Zaikovskii and V. N. Romannikov, *Catal. Today*, 2004, **91–92**, 205.
28 O. A. Kholdeeva, M. S. Melgunov, A. N. Shmakov, N. N. Trukhan, M. E. Malyshev, V. B. Fenelonov, V. N Parmon and V. N. Romannikov, *Russian Patent*, 2 229 930, 2004.
29 O. A. Kholdeeva, O. V. Zalomaeva, A. N. Shmakov, M. S. Melgunov and A. B. Sorokin, *J. Catal.*, 2005, **236**, 62.
30 C. Milone, R. Ingoglia, G. Neri, A. Pistone and S. Galvagno, *Appl. Catal., A*, 2001, **211**, 251and references therein.
31 S. Ficht, M. Mülbaier and A. Giannis, *Tetrahedron*, 2001, **57**, 4863.
32 (*a*) Y. Tamura, T. Yakura, H. Tohma, K. Kikuchi and Y. Kita, *Synthesis*, 1989, 126; (*b*) S. V. Ley, A. W. Thomas and H. Finch, *J. Chem. Soc., Perkin Trans. 1*, 1999, 669.
33 C. C. Zeng and J. Y. Becker, *J. Org. Chem.*, 2004, **69**, 1053.
34 A. Lattanzi and A. Scettri, *Synlett*, 2002, 942.
35 Y. Naruta, *J. Am. Chem. Soc.*, 1980, **102**, 3774.
36 S. Araki, N. Katsumura and Y. Butsugan, *J. Organomet. Chem.*, 1991, **415**, 7.
37 W. Butte, J. Eilis and M. Kirsh, *Anal. Lett.*, 1982, **15**, 841.

Transesterification of methylsulfate and ethylsulfate ionic liquids—an environmentally benign way to synthesize long-chain and functionalized alkylsulfate ionic liquids

Simone Himmler,[a] Stefanie Hörmann,[a] Roy van Hal,[b] Peter S. Schulz[a] and Peter Wasserscheid*[a]

Received 2nd February 2006, Accepted 28th June 2006
First published as an Advance Article on the web 24th July 2006
DOI: 10.1039/b601583b

A new environmentally friendly method to synthesize long-chain and functionalized alkylsulfate ionic liquids is reported. The two-step synthesis comprises the synthesis of a methylsulfate or ethylsulfate ionic liquid by direct alkylation in the first step. In the second step, this intermediate is transformed in a transesterification reaction, using different functionalized and non-functionalized alcohols, to the corresponding new alkylsulfate melts. The entire reaction sequence is halide-free and liberates methanol or ethanol as the only by-products. Moreover, it is carried out in a solvent-free manner and scale-up is straight forward.

Introduction

Ionic liquids have received a great increase in attention during the last decade. More and more, ionic liquids are used as innovative solvent substitutes in academic and industrial research laboratories. Today, the applications under investigation range from synthesis,[1,2] transition metal catalysis[3,4] and biocatalysis[5] to electrochemistry,[6,7] from active materials in sensors[8,9] and analytical devices[10] to performance additives for paints,[11] and from process fluids for separation technologies[12,13] to heat transfer agents[14,15] and innovative lubrication.[7] In particular, their extremely low vapour pressure at ambient conditions makes ionic liquids extremely interesting for many technical purposes.

For a long time the "work horses" in the field of ionic liquid research used to be 1-butyl-3-methylimidazolium hexafluorophosphate ([BMIM][PF_6]) and 1-butyl-3-methylimidazolium tetrafluoroborate ([BMIM][BF_4]). One reason for this was certainly the fact that these ionic liquids are relatively easy to prepare and to purify as they are non-miscible with water ([BMIM][PF_6]) or at least hydrophobic enough to be extractable from water ([BMIM][BF_4]). However, the hydrolytical instability of hexafluorophosphate and tetrafluoroborate anions has become quite obvious[16] and, as the decomposition of $[PF_6]^-$ and $[BF_4]^-$ leads to the formation of highly toxic and corrosive HF, the use of these ionic liquids will be limited to either applications under anhydrous conditions or to those cases where a certain extent of degradation may be acceptable. Apart from hexafluorophosphates and tetrafluoroborates, a group of hydrophobic and hydrolysis-stable ionic liquids have been published, and the most prominent representative, carrying the bis(trifluoromethylsulfonyl)imide ion, has been used in many publications.[7,17] Other examples of hydrophobic and hydrolysis-stable anions include nonafluorobutanesulfonate[18] and tris(pentafluoroethyl)trifluorophosphate.[19]

However, these systems suffer from the intrinsically high price of the anion, making them unsuitable for larger scale applications. Moreover, the fluorinated anions restrict the disposal options for these ionic liquids to some extent, *e.g.* incineration requires special HF treatment.

In the light of all these considerations, the synthesis and application of ionic liquids with halogen-free anions has become an important area of research. Several of these systems have been described, *e.g.* alkyl and aryl sulfonates,[20] alkylsulfates,[21] and organoborate[22] anions. Methylsulfate and ethylsulfate ionic liquids have found particularly wide application as they are easily accessible by direct alkylation using cheap alkylation agents. In the reaction of methylimidazole with the very strong alkylation agents dimethylsulfate or diethylsulfate, the corresponding alkylsulfate ionic liquid is obtained in a solvent-free synthesis with high reaction rates[23] and excellent purity. Moreover, 1-methyl-3-ethylimidazolium ethylsulfate ([EMIM][$EtOSO_3$]) has become one of the first commercial ionic liquid available on ton-scale,[24] with a set of toxicological data generated in an official registration process indicating that this ionic liquid is a safe and non-toxic chemical, meaning that no labelling is required. Furthermore, methylsulfate and ethylsulfate ionic liquids also show attractive physico-chemical properties with low viscosities and melting points well below room temperature for many compounds.[25] But, unfortunately, methyl- and ethylsulfate anions are also prone to hydrolysis, especially under acidic conditions and elevated temperatures. In this case the formation of $[HSO_4]^-$ and methanol or ethanol is observed.

In contrast, long-chain alkylsulfate ions show a much higher hydrolytic stability, and hence much better hydrolytic stability has been found for ionic liquids incorporating these ions, *e.g.* [BMIM][octylsulfate].[26] Our group has presented a procedure that involves, as the key step, the metathesis of 1,3-dialkylimidazolium chloride intermediates with sodium alkylsulfate salts. This method requires extensive drying of the sodium alkylsulfate salt, large amounts of dry solvents (such as

---

[a] *Lehrstuhl für Chemische Reaktionstechnik der Friedrich-Alexander-Universität Erlangen-Nürnberg, Egerlandstrasse 3, Erlangen, D-91058, Germany. E-mail: wasserscheid@crt.cbi.uni-erlangen.de; Fax: +499131-8527421; Tel: +499131-8527420*
[b] *Solvent Innovation GmbH, Köln, Nattermannallee 1, Köln, D-50829, Germany*

dichloromethane or acetone) and a cumbersome filtration procedure under inert atmosphere to obtain an ionic liquid with at least acceptable contents of chloride impurities. Later, we published a more general approach that also gives access to long-chain alkylsulfate and functionalized alkylsulfate ionic liquids in which the anion is not a commercial chemical as sodium or ammonium salt.[27] This method involves sulfatation of alcohols with sulfamic acid (giving the corresponding ammonium alkylsulfate salt) followed by metathesis with *e.g.* [BMIM]Cl. Again, the metathesis step requires large amounts of an organic solvent and absolutely water-free conditions to realize the complete removal of chloride ions through filtration of NH_4Cl.

In this paper we report for the first time in detail a simple, two-step synthesis to obtain long-chain and functionalized alkylsulfate ionic liquids in a much more efficient way. As displayed in Scheme 1 this is realized by a transesterification reaction of methyl- or ethylsulfate intermediates.

This synthetic route can easily be scaled up using standard laboratory equipment, as will be demonstrated in this paper. The use of organic solvents in the synthesis is not required. By variation of the starting materials a plethora of new, halogen- and halide-free ionic liquids is readily available in high quality. Many of the new ionic liquids easily accessible by this method show interesting physico-chemical properties, and may also be of technical interest.

Results and discussion

Synthesis

Quaternization step. For the first step, the quaternization with dimethyl- or diethylsulfate, many nucleophiles such as alkylimidazoles, substituted pyridines, tertiary phosphines or tertiary amines can be used. Many of these compounds, especially the tertiary amines, are commercially available at low cost. Some of the quaternization products are liquid at room temperature or slightly above. The ionic liquids described in this paper are all derived from 1-*N*-methylimidazole or 1-*N*-butylimidazole. Results using other starting materials will be published in the future.

The quaternization of 1-*N*-methylimidazole with diethylsulfate is carried out without a solvent under efficient cooling of the reaction mixture with a cold water- or icebath. In this way a nearly colourless product is obtained. Effective heat removal is very important, as this influences the colour of the the final product, and thereby the purity.

1.step: quaternisation

$$NR_3 + R'_2SO_4 \longrightarrow [NR_3R'][R'OSO_3]$$

2. step: transesterification

$$[NR_3R'][R'OSO_3] + R''OH \overset{H^+}{\rightleftharpoons} [NR_3R'][R''OSO_3] + R'OH$$

R'=Me, Et

Scheme 1 Two-step synthesis of alkylsulfate ionic liquids by quaternization and transesterification exemplified for a tetraalkylammonium system.

Transesterification step. In the transesterification step, a long-chain alcohol and an acidic catalyst are added to the compound obtained after the initial quaternization reaction. In this study we report on our work using primary alcohols (*n*-butanol, *n*-hexanol and *n*-octanol) and some ethyleneglycol-based alcohols (2-methoxyethanol, 2-ethoxyethanol, 2-butoxyethanol, diethyleneglycolmonoethylether and diethyleneglycolmonomethylether).

Pre-drying of the alcohol is advised as water leads to hydrolysis of the short-chain alkylsulfate and forms hydrogensulfate impurities. 0.4 mol% of a Brønsted acidic catalyst (methanesulfonic acid) has been used for the synthesis of the alkylsulfate ionic liquids characterized and described in this paper. This amount conduces the neutralization of the remaining free methylimidazole from the quaternization step and assures a slightly acidic reaction mixture for the transesterification reaction. Too much acid is not beneficial, as the amount of acidic by-products during the transesterification step may increase.

In order to shift the equilibrium of the transesterification reaction towards the desired products, ethanol (or methanol) liberated in the transformation must be efficiently removed, a well-known procedure in transesterification reactions. One main problem we encountered during the investigation of this specific aspect was the fact that components such as alcohols show different vapour pressure when dissolved in ionic liquids (a fact that is technically used in extractive distillation with ionic liquids being used as entrainer fluids[28]). The strong interactions between the ionic liquids and the highly polar methanol or ethanol decrease the vapour pressure of these short chain alcohols significantly. Therefore, mild vacuum has to be applied—even at elevated temperatures—to remove methanol and ethanol from the reaction mixture. In all cases an excess of at least 1.5 equivalents of the long-chain alcohols (R″OH in Scheme 1) is necessary, as some of it is removed in the vapour mixture together with the lower alcohol (R′OH in Scheme 1) during the vacuum procedure. This excess has the additional advantage of shifting the equilibrium further towards the product side. When using alcohols with a relatively low boiling point (*e.g.* butanol, bp 118 °C) the molar ratio of alcohol to starting material was between 2 and 3, alcohols with higher boiling points (*e.g.* octanol, bp 198 °C) show good results with 1.5 equivalents. However, it has to be noted that the excess of the remaining higher alcohol used in the transesterification step has to be removed at the end of the transesterification reaction to obtain the pure product. This can be achieved by applying high vacuum at elevated temperatures. In most cases, 80–100 °C at about 0.2 mbar was enough to remove even diethyleneglycolmonomethylether or 1-octanol. The removed alcohol can be recycled for another reaction making the overall procedure an efficient process. Another way of removing excess alcohol is the extraction with diethylether. This was usually carried out in cases where the purity of the products was crucial, in particular for the determination of physico-chemical properties.

Kinetic aspects of the transesterification step

As the transesterification reaction is the key-step of our new synthetic procedure to long-chain and functionalized alkylsulfate ionic liquids, we were interested in the kinetics of this reaction. Here we present fundamental kinetic data concerning the transesterification of [EMIM][EtOSO$_3$] to [EMIM][BuOSO$_3$].

First, we carried out several kinetic experiments in order to get information on the initial rate of the reaction and the time needed until the equilibrium is reached under atmospheric pressure and equimolar conditions. All experiments were observed by ^{1}H-NMR spectroscopy of both reaction mixture and condensate. The samples of the reaction mixture were quenched by immediate cooling. It has been verified that under these cold conditions no further reaction takes place in the NMR tube that could affect the result. Fig. 1 shows the concentration–time profiles of the reactants and products for the synthesis of 1-ethyl-3-methylimidazolium butylsulfate ([EMIM][BuOSO$_3$]).

For an equimolar mixture of [EMIM][EtOSO$_3$] and 1-butanol (1.4 mol% methansulfonic acid as catalyst), the following results were obtained: (1) The transesterification is a second order reaction (first order with respect to each of the starting materials), with an activation energy of 73.01 kJ mol^{-1} and a collision factor of 1.6 × 10^{12} min^{-1}. (2) The reaction is much faster than expected. Equilibrium was fully reached, at temperatures $\geqslant$60 °C, within less than 90 min (Fig. 1), and in only 15 min at 90 °C (Fig. 2).

The molar ratios of the starting materials were varied from [EMIM][EtOSO$_3$]/1-butanol 1 : 10 to 10 : 1 in order to investigate the effects on the conversion according to the law of mass action. When an excess of butanol of 10 equivalents was used, a conversion higher than 90% was obtained (Fig. 3).

However, the use of large quantities of butanol is rather impractical for technical production, as the remaining amount has to be removed from the product. Alternatively, ethanol can be removed under reduced pressure during the reaction. Consequently, the best results (all yields >99%) were obtained in this manner (*T* = 90 °C; [EMIM][EtOSO$_3$]/1-butanol = 1 : 3; apparatus with distillative EtOH removal). The colour of the products obtained in this procedure remained almost colourless with a light yellowish shade.

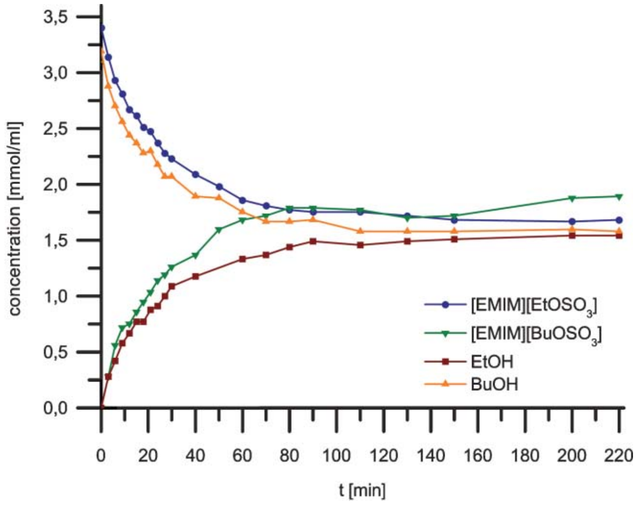

Fig. 1 Concentration–time profile for an equimolar ratio of [EMIM][EtOSO$_3$] and 1-butanol at 60 °C (atmospheric pressure) and a catalyst concentration (methanesulfonic acid) of 1.4 mol%.

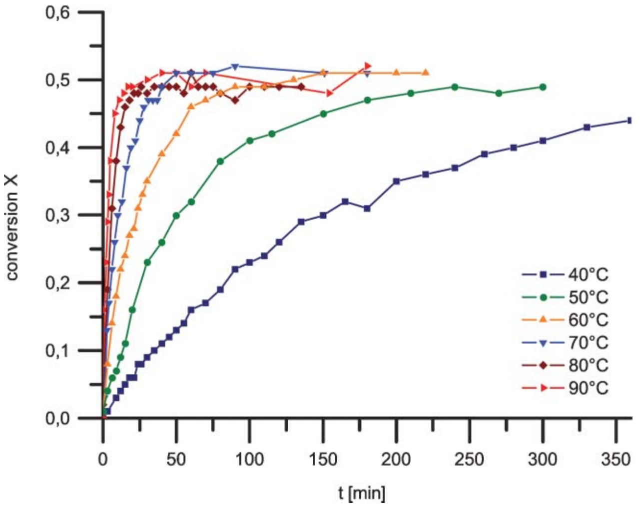

Fig. 2 Effect of reaction temperature on conversion of [EMIM][EtOSO$_3$] and 1-butanol to [EMIM][BuOSO$_3$] for an equimolar ratio of [EMIM][EtSO$_3$] and 1-butanol and a catalyst concentration (methanesulfonic acid) of 1.4 mol%.

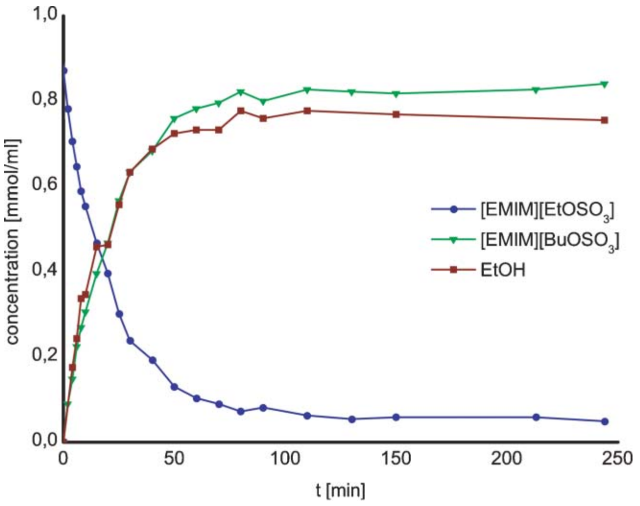

Fig. 3 Concentration–time profile for a molar ratio of [EMIM][EtOSO$_3$]/1-butanol = 1/10 at 60 °C and a catalyst concentration (methanesulfonic acid) of 4.7 mol%.

It is noteworthy, however, that reaction temperatures should not exceed 100 °C. At higher temperatures yields start to decrease due to the formation of [HSO$_4$]$^-$ anions and also the product's colour becomes more intense.

Catalyst identification and optimization. In the early days of this study it was realized that the transesterification requires a certain amount of a Brønsted-acidic catalyst. As a small excess of methylimidazole is present in the starting material [EMIM][EtOSO$_3$] (typically 0.2%) the acid serves two purposes. It neutralizes the small amount of free base (1-methylimidazole) and it acts as the catalyst for the transesterification.

In our quest for the best catalyst for our specific purpose we first focused on solid acids, since these heterogeneous catalysts are frequently used in industrial transesterification reactions.[29] Moreover, such systems would be easy to remove after the reaction from the reaction mixture. Consequently, Dowex® MSC-1 from Dow Chemicals and Amberlyst® 15 from Rohm and Haas Co. were tested, both materials containing free sulfonic acid groups. Unfortunately, it was found that with these catalysts large amounts of acid groups were formed after full conversion of the short-chain alkylsulfate (up to 9 mol% as determined by titration with 0.1 M NaOH). Presumably, $[HSO_4]^-$ is formed during the reaction from water present in the acidic catalyst by degradation of the short-chain alkylsulfates. The acid formed in this way can be neutralised by addition of base (in our case NaOH was applied) to give a product with neutral pH-value. However, in this case the purity of the product suffers from large amounts of Na_2SO_4 impurities. Calculations show that acid contents up to 3 mol% still result in 1 mass% of Na_2SO_4 in the final product after neutralization. This amount could be considered as the limit for an acceptable technical product quality.

Acid contents below 3 mol% could be obtained by using homogeneous, liquid acids as the catalyst. Methanesulfonic acid was found to be eminently useful for the transesterification as it is cheap, commercially available in water-free form and easy to handle. An obvious drawback is the fact that liquid acids in a homogeneous mixture cannot be removed after the reaction. Neutralization with a base leads to mixtures of mesylate salts and (alkyl)sulfates, both of them relatively inert anions. However, due to the fact that very small amounts of liquid catalyst (usually 0.4 mol% have been used) have already proved very efficient in catalyzing the transesterification reaction, this method is much superior to the application of solid acids.

Quality analysis

During synthesis of both steps, the alkylation and the transesterification, acid–base-titration was found to be a simple, cheap and fast method to analyse the product's quality.

In the alkylation reaction the small excess of 1-methylimidazole could be analysed by titration of an aqueous solution with 0.1 M methanesulfonic acid, using bromothymol blue as the pH indicator. The 1-methylimidazole content was also checked by HPLC measurements. Both methods agreed within an error margin of 0.1 mol%.

For the determination of the acid content in the final product the same indicator was used with 0.1 M sodium hydroxide solution as the titrant.

Physico-chemical properties

Concerning the physico-chemical properties of the new ionic liquids prepared in this study, the following 1-ethyl-3-methylimidazolium based melts were analyzed: [EMIM][X], with $[X]^-$ being *n*-butylsulfate, *n*-hexylsulfate, *n*-octylsulfate, 2-methoxyethylsulfate, 2-ethoxyethylsulfate, 2-butoxyethylsulfate, 2-(2-ethoxyethoxy)-ethylsulfate and 2-(2-methoxyethoxy)ethylsulfate. To check for cation effects, the following 1-butyl-3-methylimidazolium based ionic liquids were also investigated: [BMIM][Y], with $[Y]^-$ being *n*-butylsulfate, *n*-hexylsulfate and *n*-octylsulfate. All ionic liquids under investigation, except $[EMIM][BuOSO_3]$ (mp 12 °C) and $[EMIM][HexOSO_3]$ (mp 7 °C), were still liquids at 0 °C. However, due to the fact that these ionic liquids are supercooled melts below zero, the melting points could not be detected by DSC.

Viscosity. To produce reliable viscosity data we routinely checked the water content for all substances under investigation before the viscosity measurements. The determination of the water content was carried out by Karl–Fischer titration. All data displayed in Fig. 4 and Table 1 originate from samples with a water content of 600 ± 100 ppm (0.06 ± 0.01 mass% water). All ionic liquids under investigation showed Newtonian behaviour in the applied temperature range (their viscosity does not change with changing shear rates).

The comparison of [EMIM] *vs.* [BMIM] ionic liquids carrying the same anion reveals a pronounced effect, with [EMIM] melts always showing significantly lower viscosity. For example, a viscosity of 386 mPa s was determined for $[BMIM][BuOSO_3]$ at 30 °C, whereas the value for $[EMIM][BuOSO_3]$ (123 mPa s) was found to be more than three times lower at the same temperature.

For the less viscous [EMIM] based alkylsulfate ILs the viscosity data were recorded in a temperature range from 20 °C to 100 °C (Fig. 4). Interestingly, the melts that contain ethylene glycol-functionalized anions like $[EMIM][Et(EG)OSO_3]$ (EG = ethylenglycol unit) show very low viscosities compared to the alkylsulfate with similar length of side chain but no oxygen functionalization. For example, $[EMIM][Et(EG)_2OSO_3]$ shows only 169 mPa s at 20 °C compared to 649 mPa s for $[EMIM][OcOSO_3]$, which can be viewed as the same melt with just the two O-atoms substituted by CH_2-groups.

Density. The densities of the new ionic liquids were also measured with samples of defined water content (600 ± 100 ppm). Densities and viscosities for different alkylsulfate melts are displayed in Table 1. As expected, the densities of melts containing anions with functionalized side chains are much higher than the values for non-functionalized anions,

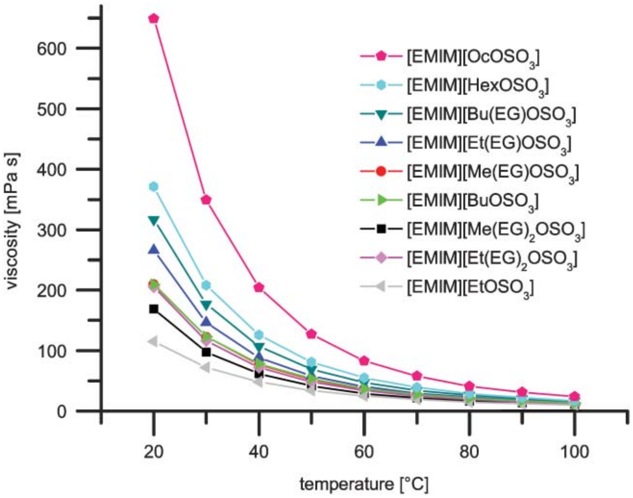

Fig. 4 Viscosities of [EMIM] based ionic liquid at different temperatures.

Table 1 Alkylsulfate ionic liquids and their properties

ILs	Formula	Yield	Density/g mL^{-1}	Viscosity/mPa s	T_{dec}^{a}/°C	mp^{b}/°C
[EMIM][EtOSO$_3$]	$C_8H_{16}N_2O_4S$	>99%	1.22	115^{c}	357	<0
[EMIM][BuOSO$_3$]	$C_{10}H_{20}N_2O_4S$	>99%	1.18	209^{c}	328	12
[EMIM][HexOSO$_3$]	$C_{12}H_{24}N_2O_4S$	99%	1.13	371^{c}	314	7
[EMIM][OcOSO$_3$]	$C_{14}H_{28}N_2O_4S$	99%	1.10	649^{c}	325	<0
[EMIM][Me(EG)OSO$_3$]	$C_9H_{18}N_2O_5S$	99%	1.32	210^{c}	332	<0
[EMIM][Et(EG)OSO$_3$]	$C_{10}H_{20}N_2O_5S$	99%	1.30	266^{c}	331	<0
[EMIM][Bu(EG)OSO$_3$]	$C_{12}H_{24}N_2O_5S$	99%	1.21	317^{c}	337	<0
[EMIM][Me(EG)$_2$OSO$_3$]	$C_{11}H_{22}N_2O_6S$	99%	1.23	205^{c}	336	<0
[EMIM][Et(EG)$_2$OSO$_3$]	$C_{12}H_{24}N_2O_6S$	99%	1.23	169^{c}	336	<0
[BMIM][BuOSO$_3$]	$C_{12}H_{24}N_2O_4S$	99%	nm	532^{d}	327	<0
[BMIM][HexOSO$_3$]	$C_{14}H_{28}N_2O_4S$	99%	nm	542^{d}	313	<0
[BMIM][OcOSO$_3$]	$C_{16}H_{32}N_2O_4S$	99%	1.05	940^{d}	324	<0

[a] T_{dec}: temperature of thermal decomposition. [b] mp: melting point. [c] Viscosities measured at 20 °C. [d] Viscosities measured at 25 °C.

due to the formation of intra- and inter-molecular O···H-bonds. This results in a more dense arrangement of the ions per volume unit. For example, [EMIM][Me(EG)$_2$OSO$_3$] has a density of 1.32 g cm^{-3}, whereas [EMIM][OcOSO$_3$] shows only a density of only 1.10 g cm^{-3} at room temperature.

Thermal and hydrolytical stability. The thermal stability of several new ionic liquids was also investigated. Thereby we found out that all melts that were analyzed showed a decomposition temperature higher than 300 °C (displayed in Table 1). However, as no clear trend concerning chain length in relation to thermal stability could be seen, we also studied the hydrolytical stability of two representative ionic liquids: [EMIM][EtOSO$_3$] and [EMIM][OcOSO$_3$]. Hydrolysis of alkylsulfate ionic liquids leads to the formation of [HSO$_4$]$^-$ and therefore to decreasing pH values. Hence, we recorded the alteration of pH values *versus* time for mixtures of [EMIM][EtOSO$_3$] and [EMIM][OcOSO$_3$] with water, with a molar ratio of ionic liquid/water = 1 : 100 at 95 °C. As expected the long-chain ionic liquid [EMIM][OcOSO$_3$] proved to be more stable towards hydrolysis than the short-chain melt [EMIM][EtOSO$_3$]. As shown in Fig. 5 an amount of [EMIM][EtOSO$_3$] is hydrolysed immediately after mixing with an excess of water. The same was recorded for [EMIM][OcOSO$_3$] but the decrease of the pH value is by far not as pronounced as it is for the short-chain melt.

Experimental

Chemicals

All reagents used were purchased from Aldrich, Dow Chemicals, Fluka, Riedel-de Haën, Rohm and Haas Co. and Solvent Innovation GmbH, with commercial grades >99%. The alcohols were dried under high vacuum before application in the transesterification.

Quaternization: synthesis of [EMIM][EtOSO$_3$]

21 mol of diethylsulfate (>99%) were slowly added (200 ml at a time) to 21.04 mol of 1-methylimidazole (>99%) that was pre-cooled to 4 °C in a 10 l glass reactor by an external cooling bath. After two hours of stirring under argon atmosphere the mixture was heated up to 60 °C and was stirred under argon for another 6 hours. The product (yield >99%) was obtained in the form of a slightly yellowish liquid, analysed by ^{1}H-NMR.

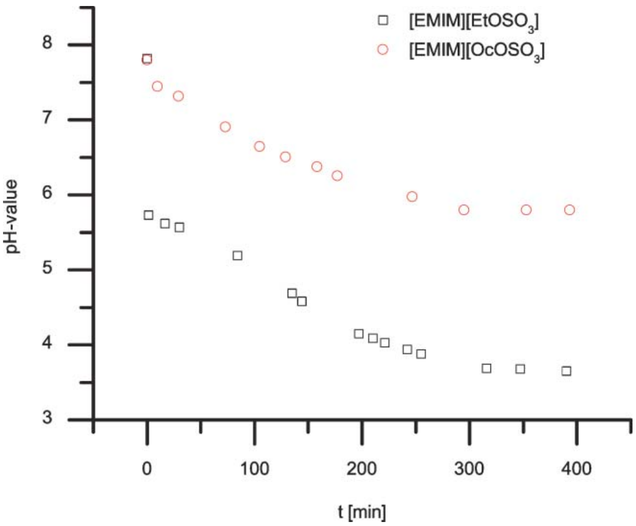

Fig. 5 pH value–time profile at 95 °C for a molar ratio of [EMIM][EtOSO$_3$]/water and [EMIM][OcOSO$_3$]/water = 1/100.

Transesterification: synthesis of alkylsulfate based ionic liquids

For the transesterification reaction we used a commercial rotary evaporator. 100 mmol of an alcohol were mixed with 50 mmol of 1-ethyl-3-methylimidazolium ethylsulfate ([EMIM][EtOSO$_3$]). 5 mmol of the catalyst, methanesulfonic acid, were added to the mixture. The reaction mixture was heated to 70 °C with constant stirring . Ethanol formed during the reaction was removed under vacuum by applying a pressure ramp (100–2 mbar). After five hours, 50 mmol of the alcohol were added, and after stirring for half an hour the remaining ethanol was removed under vacuum (1 mbar). After neutralizing the obtained ionic liquid with sodium hydroxide, a twofold (volumetric) excess of diethylether was added to extract the remaining alcohol from the product. This process was repeated five times. The rest of diethylether was removed under high vacuum. Yields: [EMIM][Me(EG)OSO$_3$] 99%, [EMIM][Et(EG)OSO$_3$] 99%, [EMIM][Bu(EG)OSO$_3$] 99%, [EMIM][Et(EG)$_2$OSO$_3$] 99%, [EMIM][Me(EG)$_2$OSO$_3$] 99%, [EMIM] [BuOSO$_3$] >99%, [EMIM][HexOSO$_3$] 99%,

[EMIM][OcOSO$_3$] 99%. For upscaling we used a 25 litre rotary evaporator (Büchi). The procedure was the same as described above. For the synthesis of [EMIM][BuOSO$_3$] the following amounts of reactants were used: 44.6 mol [EMIM][EtOSO$_3$], 134 mol BuOH and 0.45 mol methanesulfonic acid. Yield: [EMIM][BuOSO$_3$] 98%.

Kinetic experiments

For the kinetic investigations the reactions were carried out batch-wise at standard pressure in an isothermal round bottom flask using 1-butanol and [EMIM][EtOSO$_3$] as reactants. Temperatures were varied from 40 °C to 90 °C in steps of 10 °C. The amount of catalyst, methanesulfonic acid, was kept at 1.4 mol% for equimolar ratios of the reagents. The molar ratios of the starting materials 1-butanol and [EMIM][EtOSO$_3$] were varied from 10 : 1 to 1 : 10, and 4.7 mol% of methanesulfonic acid was used for these experiments. The rates of depletion for 1-butanol, and [EMIM][EtOSO$_3$], as well as the rate of formation of ethanol and [EMIM][BuOSO$_3$], were analyzed by ^{1}H-NMR spectroscopy.

All NMR spectra were recorded on a JEOL ECX spectrometer in d_6-DMSO.

1-Ethyl-3-methylimidazolium ethylsulfate [EMIM][EtOSO$_3$]. ^{1}H-NMR (400 MHz, d_6-DMSO, [ppm])

δ = 1.09 (t, 3H, $\mathrm{OCH_2C}H_3$, J = 7.13 Hz), 1.40 (t, 3H, $\mathrm{NCH_2C}H_3$, J = 7.31 Hz), 3.75 (q, 2H, $\mathrm{OC}H_2\mathrm{CH_3}$, J = 7.14 Hz), 3.84 (s, 3H, $\mathrm{NC}H_3$), 4.19 (q, 2H, $\mathrm{NC}H_2\mathrm{CH_3}$, J = 7.30 Hz), 7.70 (s, 1H, $\mathrm{NC}H\mathrm{CHN}$), 7.80 (s, 1H, $\mathrm{NCHC}H\mathrm{N}$), 9.10 (s, 1H, $\mathrm{NC}H\mathrm{N}$). ^{13}C-NMR (100 MHz, d_6-DMSO, [ppm]) δ = 15.0 ($C\mathrm{H_3CH_2O}$, $C\mathrm{H_3CH_2N}$), 35.6 ($C\mathrm{H_3N}$), 44.1 ($\mathrm{CH_3}C\mathrm{H_2N}$), 61.7 ($\mathrm{CH_3}C\mathrm{H_2O}$), 121.9 ($\mathrm{N}C\mathrm{HCHN}$), 123.5 ($\mathrm{NCH}C\mathrm{HN}$), 136.5 ($\mathrm{N}C\mathrm{HN}$)

1-Ethyl-3-methylimidazolium 2-methoxyethylsulfate [EMIM][Me(EG)OSO$_3$]. ^{1}H-NMR (400 MHz, d_6-DMSO, [ppm]) δ = 1.41 (t, 3H, $\mathrm{NCH_2C}H_3$, J = 7.35 Hz), 3.235 (s, 2H, $\mathrm{OCH_2CH_2OC}H_3$), 3.48 (m, 2H, $\mathrm{OCH_2C}H_2\mathrm{OCH_3}$), 3.81 (m, 2H, $\mathrm{OC}H_2\mathrm{CH_2OCH_3}$), 3.85 (s, 3H, $\mathrm{NCH_3}$), 4.13 (q, 2H, $\mathrm{NC}H_2\mathrm{CH_3}$, J = 7.31 Hz), 7.70 (s, 1H, $\mathrm{NC}H\mathrm{CHN}$), 7.8 (s, 1H, $\mathrm{NCHC}H\mathrm{N}$), 9.13 (s, 1H, $\mathrm{NC}H\mathrm{N}$). ^{13}C-NMR (100 MHz, d_6-DMSO, [ppm]) δ = 15.6 ($C\mathrm{H_3CH_2N}$), 36.20 ($C\mathrm{H_3N}$), 44.7 ($\mathrm{CH_3}C\mathrm{H_2N}$), 58.5 ($C\mathrm{H_3OCH_2CH_2O}$), 65.4 ($\mathrm{CH_3O}C\mathrm{H_2CH_2O}$), 71.3 ($\mathrm{CH_3OCH_2}C\mathrm{H_2O}$), 122.5 ($\mathrm{N}C\mathrm{HCHN}$), 124.1 ($\mathrm{NCH}C\mathrm{HN}$), 137.0 ($\mathrm{N}C\mathrm{HN}$)

1-Ethyl-3-methylimidazolium 2-ethoxyethylsulfate [EMIM][Et(EG)OSO$_3$]. ^{1}H-NMR (400 MHz, d_6-DMSO, [ppm]) δ = 1.09 (m, 3H, $\mathrm{OCH_2CH_2OCH_2C}H_3$), 1.40 (t, 3H, $\mathrm{NCH_2C}H_3$, J = 7.30 Hz), 3.42 (m, 4H, $\mathrm{OCH_2C}H_2\mathrm{OC}H_2\mathrm{CH_3}$), 3.80 (m, 2H, $\mathrm{OC}H_2\mathrm{CH_2OCH_2CH_3}$), 3.85 (s, 3H, $\mathrm{NC}H_3$), 4.13 (q, 2H, $\mathrm{NC}H_2\mathrm{CH_3}$, J = 7.31 Hz), 7.70 (s, 1H, $\mathrm{NC}H\mathrm{CHN}$), 7.8 (s, 1H, $\mathrm{NCHC}H\mathrm{N}$), 9.13 (s, 1H, $\mathrm{NC}H\mathrm{N}$). ^{13}C-NMR (100 MHz, d_6-DMSO, [ppm]) δ = 15.6 ($C\mathrm{H_3CH_2OCH_2CH_2O}$, $C\mathrm{H_3CH_2N}$), 36.2 ($C\mathrm{H_3N}$), 44.7 ($\mathrm{CH_3}C\mathrm{H_2N}$), 65.7 ($\mathrm{CH_3}C\mathrm{H_2OCH_2CH_2O}$), 66.0 ($\mathrm{CH_3CH_2O}C\mathrm{H_2CH_2O}$), 69.3 ($\mathrm{CH_3CH_2OCH_2}C\mathrm{H_2O}$), 122.5 ($\mathrm{N}C\mathrm{HCHN}$), 124.1 ($\mathrm{NCH}C\mathrm{HN}$), 136.9 ($\mathrm{N}C\mathrm{HN}$)

1-Ethyl-3-methylimidazolium 2-butoxyethylsulfate [EMIM][Bu(EG)OSO$_3$]. ^{1}H-NMR (400 MHz, d_6-DMSO, [ppm]) δ = 0.87 (t, 3 H, $\mathrm{OCH_2CH_2OCH_2CH_2CH_2C}H_3$, J = 7.34 Hz), 1.37 (m, 7H, $\mathrm{OCH_2CH_2OCH_2C}H_2\mathrm{C}H_2\mathrm{CH_3}$, $\mathrm{NCH_2C}H_3$), 3.42 (m, 4H, $\mathrm{OCH_2C}H_2\mathrm{OC}H_2\mathrm{CH_2CH_2CH_3}$, 2 × $\mathrm{CH_2}$), 3.80 (m, 2H, $\mathrm{OC}H_2\mathrm{CH_2OCH_2CH_2CH_2CH_3}$), 3.85 (s, 3H, $\mathrm{NC}H_3$), 4.2 (q, 2H, $\mathrm{NC}H_2\mathrm{CH_3}$, J = 7.31 Hz), 7.70 (s, 1H, $\mathrm{NCHC}H\mathrm{N}$), 7.8 (s, 1H, $\mathrm{NC}H\mathrm{CHN}$), 9.13 (s, 1H, NCHN). ^{13}C-NMR (100 MHz, d_6-DMSO, [ppm]) δ = 14.3 ($C\mathrm{H_3CH_2CH_2CH_2OCH_2CH_2O}$), 15.6 ($C\mathrm{H_3CH_2N}$), 19.4 ($\mathrm{CH_3}C\mathrm{H_2CH_2CH_2OCH_2CH_2O}$), 31.9 ($\mathrm{CH_3CH_2}C\mathrm{H_2CH_2OCH_2CH_2O}$), 36.2 ($C\mathrm{H_3N}$), 44.7 ($\mathrm{CH_3}C\mathrm{H_2N}$), 65.7 ($\mathrm{CH_3CH_2CH_2CH_2O}C\mathrm{H_2CH_2O}$), 69.5 ($\mathrm{CH_3CH_2CH_2}C\mathrm{H_2OCH_2CH_2O}$), 70.5 ($\mathrm{CH_3CH_2CH_2CH_2OCH_2}C\mathrm{H_2O}$), 122.5 ($\mathrm{N}C\mathrm{HCHN}$), 124.1 ($\mathrm{NCH}C\mathrm{HN}$), 137.0 ($\mathrm{N}C\mathrm{HN}$)

1-Ethyl-3-methylimidazolium 2-(2-ethoxyethoxy)ethylsulfate [EMIM][Et(EG)$_2$OSO$_3$]. ^{1}H-NMR (400 MHz, d_6-DMSO, [ppm]) δ = 1.09 (t, 3H, $C\mathrm{H_3CH_2OCH_2CH_2OCH_2CH_2O}$, J = 7.0 Hz), 1.41 (t, 3H, $\mathrm{NCH_2C}H_3$, J = 7.32 Hz), 3.46 (m, 6H, $\mathrm{CH_3C}H_2\mathrm{OC}H_2\mathrm{C}H_2\mathrm{OC}H_2\mathrm{CH_2O}$), 3.80 (m, 2H, $\mathrm{CH_3CH_2OCH_2CH_2OCH_2C}H_2\mathrm{O}$), 3.85 (s, 3H, $\mathrm{NC}H_3$), 4.19 (q, 2H, $\mathrm{NC}H_2\mathrm{CH_3}$, J = 7.30 Hz), 7.70 (s, 1H, $\mathrm{NC}H\mathrm{CHN}$), 7.8 (s, 1H, $\mathrm{NCHC}H\mathrm{N}$), 9.1 (s, 1H, $\mathrm{NC}H\mathrm{N}$). ^{13}C-NMR (100 MHz, d_6-DMSO, [ppm]) δ = 15.6 ($C\mathrm{H_3CH_2N}$), 15.7 ($C\mathrm{H_3CH_2OCH_2CH_2OCH_2CH_2O}$), 36.2 ($C\mathrm{H_3N}$), 44.7 ($\mathrm{CH_3}C\mathrm{H_2N}$), 65.6 ($\mathrm{CH_3}C\mathrm{H_2OCH_2CH_2OCH_2CH_2O}$), 66.1 ($\mathrm{CH_3CH_2OCH_2CH_2O}C\mathrm{H_2CH_2O}$), 69.8 ($\mathrm{CH_3CH_2O}C\mathrm{H_2CH_2OCH_2CH_2O}$), 69.9 ($\mathrm{CH_3CH_2OCH_2}C\mathrm{H_2OCH_2CH_2O}$), 70.3 ($\mathrm{CH_3CH_2OCH_2CH_2OCH_2}C\mathrm{H_2O}$), 122.5 ($\mathrm{N}C\mathrm{HCHN}$), 124.1 ($\mathrm{NCH}C\mathrm{HN}$), 137.0 ($\mathrm{N}C\mathrm{HN}$)

1-Ethyl-3-methylimidazolium 2-(2-methoxyethoxy)ethylsulfate [EMIM][Me(EG)$_2$OSO$_3$]. ^{1}H-NMR (400 MHz, d_6-DMSO, [ppm]) δ = 1.41 (t, 3H, $\mathrm{NCH_2C}H_3$, J = 7.32 Hz), 3.23 (s, 3H, $\mathrm{C}H_3\mathrm{OCH_2CH_2OCH_2CH_2O}$), 3.45 (m, 6H, $\mathrm{CH_3OC}H_2\mathrm{CH_2OC}H_2\mathrm{CH_2O}$), 3.81 (m, 2H, $\mathrm{CH_3OCH_2CH_2O{–}CH_2C}H_2\mathrm{O}$), 3.85 (s, 2H, $\mathrm{NCH_3}$), 4.13 (q, 2H, $\mathrm{NC}H_2\mathrm{CH_3}$, J = 7.31 Hz), 7.70 (s, 1H, $\mathrm{NC}H\mathrm{CHN}$), 7.8 (s, 1H, $\mathrm{NCHC}H\mathrm{N}$), 9.13 (s, 1H, $\mathrm{NC}H\mathrm{N}$). ^{13}C-NMR (100 MHz, d_6-DMSO, [ppm]) δ = 14.8 ($C\mathrm{H_3CH_2N}$), 35.6 ($\mathrm{N}C\mathrm{H_3}$), 43.8 ($\mathrm{CH_3}C\mathrm{H_2N}$), 58.0 ($C\mathrm{H_3OCH_2CH_2OCH_2CH_2O}$), 65.0 ($\mathrm{CH_3OCH_2CH_2O}C\mathrm{H_2CH_2O}$), 69.2 ($\mathrm{CH_3OCH_2CH_2OCH_2}C\mathrm{H_2O}$), 69.4 ($\mathrm{CH_3OCH_2}C\mathrm{H_2OCH_2CH_2O}$), 71.2 ($\mathrm{CH_3O}C\mathrm{H_2CH_2OCH_2CH_2O}$), 122.2 ($\mathrm{N}C\mathrm{HCHN}$), 123.5 ($\mathrm{NCH}C\mathrm{HN}$), 136.5 ($\mathrm{N}C\mathrm{HN}$)

1-Ethyl-3-methylimidazolium *n*-butylsulfate [EMIM][BuOSO$_3$]. ^{1}H-NMR (400 MHz, d_6-DMSO, [ppm]) δ = 0.84 (t, 3H, $\mathrm{C}H_3\mathrm{CH_2CH_2CH_2O}$, J = 7.35 Hz), 1.35 (m, 7H, $\mathrm{CH_3C}H_2\mathrm{C}H_2\mathrm{CH_2O}$, $\mathrm{C}H_3\mathrm{CH_2N}$), 3.70 (t, 2H, $\mathrm{CH_3CH_2CH_2C}H_2\mathrm{O}$, J = 6.64 Hz), 3.85 (s, 3H, $\mathrm{NC}H_3$), 4.19 (q, 2H, $\mathrm{NC}H_2\mathrm{CH_3}$, J = 7.30 Hz), 7.70 (s, 1H, $\mathrm{NC}H\mathrm{CHN}$), 7.8 (s, 1H, $\mathrm{NCHC}H\mathrm{N}$), 9.13 (s, 1H, $\mathrm{NC}H\mathrm{N}$). ^{13}C NMR (100 MHz, d_6-DMSO, [ppm]) δ = 13.4 ($C\mathrm{H_3CH_2CH_2CH_2O}$), 14.8 ($C\mathrm{H_3CH_2N}$), 18.4 ($\mathrm{CH_3}C\mathrm{H_2CH_2CH_2O}$), 30.8 ($\mathrm{CH_3CH_2}C\mathrm{H_2CH_2O}$), 35.4 ($C\mathrm{H_3N}$), 43.8 ($\mathrm{CH_3}C\mathrm{H_2N}$), 64.9 ($\mathrm{CH_3CH_2CH_2}C\mathrm{H_2O}$), 121.7 ($\mathrm{N}C\mathrm{HCHN}$), 123.3 ($\mathrm{NCH}C\mathrm{HN}$), 136.0 ($\mathrm{N}C\mathrm{HN}$)

1-Ethyl-3-methylimidazolium *n*-hexylsulfate [EMIM][HexOSO$_3$]. ^{1}H-NMR (400 MHz, d_6-DMSO, [ppm]) δ = 0.85

(t, 3H, $CH_3CH_2CH_2CH_2CH_2CH_2O$, J = 6.63 Hz), 1.25 (m, 6H, $CH_3CH_2CH_2CH_2CH_2CH_2O$), 1.42 (t, 3H, NCH_2CH_3, J = 7.31 Hz), 1.47 (m, 2H, $CH_3CH_2CH_2CH_2CH_2CH_2O$), 3.70 (t, 2H, $CH_3CH_2CH_2CH_2CH_2CH_2O$, J = 6.63 Hz), 3.85 (s, 3H, NCH_3), 4.13 (q, 2H, NCH_2CH_3, J = 7.31 Hz), 7.70 (s, 1H, NCHCHN), 7.8 (s, 1H, NCHCHN), 9.13 (s, 1H, NCHN). ^{13}C-NMR (100 MHz, d_6-DMSO, [ppm]) δ = 13.8 ($CH_3CH_2CH_2CH_2CH_2CH_2O$), 14.8 ($CH_3CH_2N$), 22.0 ($CH_3CH_2CH_2CH_2CH_2CH_2O$), 25.2 ($CH_3CH_2CH_2CH_2CH_2CH_2O$), 29.0 ($CH_3CH_2CH_2CH_2CH_2CH_2O$), 31.0 ($CH_3CH_2CH_2CH_2CH_2CH_2O$), 35.4 ($NCH_3$), 43.8 ($CH_3CH_2N$), 65.5 ($CH_3CH_2CH_2CH_2CH_2CH_2O$), 121.9 (NCHCHN), 123.3 (NCHCHN), 136.0 (NCHN)

1-Ethyl-3-methylimidazolium *n*-octylsulfate [EMIM][OcOSO$_3$]. ^{1}H-NMR (400 MHz, d_6-DMSO, [ppm]) δ = 0.86 (t, 3H, $CH_3CH_2CH_2CH_2CH_2CH_2CH_2CH_2O$, J = 6.81 Hz), 1.24 (m, 10H, $CH_3CH_2CH_2CH_2CH_2CH_2CH_2CH_2O$), 1.48 (t, 3H, NCH_2CH_3, J = 7.35 Hz), 1.47 (m, 2H, $CH_3CH_2CH_2CH_2CH_2$–$CH_2CH_2CH_2O$), 3.69 (t, 2H, $CH_3CH_2CH_2CH_2CH_2CH_2CH_2CH_2O$, J = 6.20 Hz), 3.85 (s, 3H, NCH_3), 4.13 (q, 2H, NCH_2CH_3, J = 7.31 Hz), 7.70 (s, 1H, NCHCHN), 7.8 (s, 1H, NCHCHN), 9.13 (s, 1H, NCHN). ^{13}C-NMR (100 MHz, d_6-DMSO, [ppm]) δ = 15.0 (CH_3CH_2N), 22.6 ($CH_3CH_2CH_2CH_2CH_2CH_2CH_2CH_2O$), 26.1 ($CH_3CH_2CH_2CH_2CH_2CH_2CH_2CH_2O$), 29.2 ($CH_3CH_2CH_2CH_2CH_2CH_2$–$CH_2CH_2O$), 29.3 ($CH_3CH_2CH_2CH_2CH_2CH_2CH_2CH_2O$), 29.6 ($CH_3CH_2CH_2CH_2CH_2CH_2CH_2CH_2O$), 31.8 ($CH_3CH_2CH_2CH_2CH_2CH_2CH_2CH_2O$), 36.2 ($CH_3N$), 44.6 ($CH_3CH_2N$), 66.1 ($CH_3CH_2CH_2CH_2CH_2CH_2CH_2CH_2O$), 122.5 (NCHCHN), 124.1 (NCHCHN), 136.9 (NCHN)

1-Butyl-3-methylimidazolium *n*-butylsulfate [BMIM][BuOSO$_3$]. ^{1}H-NMR (400 MHz, d_6-DMSO, [ppm]) δ = 0.85 (t, 3H, $CH_3CH_2CH_2CH_2O$, J = 7.34 Hz), 0.89 (t, 3H, $CH_3CH_2CH_2CH_2N$, J = 7.34 Hz), 1.27 (m, 4H, $CH_3CH_2CH_2CH_2N$, $CH_3CH_2CH_2CH_2O$), 1.47 (m, 2H, $CH_3CH_2CH_2CH_2O$), 1.768 (q, 2H, $CH_3CH_2CH_2CH_2N$, J = 7.37 Hz), 3.70 (t, 2H, $CH_3CH_2CH_2CH_2O$, J = 6.63 Hz), 3.86 (s, 3H, NCH_3), 4.18 (t, 2H, $CH_3CH_2CH_2CH_2N$, J = 7.16 Hz), 7.72 (s, 1H, NCHCHN), 7.79 (s, 1H, NCHCHN), 9.15 (s, 1H, NCHN). ^{13}C-NMR (100 MHz, d_6-DMSO, [ppm]) δ = 13.2 ($CH_3CH_2CH_2CH_2N$), 13.6 ($CH_3CH_2CH_2CH_2O$), 18.6 ($CH_3CH_2CH_2CH_2O$), 18.7 ($CH_3CH_2CH_2CH_2N$), 31.1 ($CH_3CH_2CH_2CH_2O$), 31.4 ($CH_3CH_2CH_2CH_2N$), 35.7 (NCH_3), 48.5 ($CH_3CH_2CH_2CH_2N$), 65.2 ($CH_3CH_2CH_2CH_2O$), 122.3 (NCHCHN), 123.6 (NCHCHN), 139.2 (NCHN)

1-Butyl-3-methylimidazolium *n*-hexylsulfate [BMIM][HexOSO$_3$]. ^{1}H-NMR (400 MHz, d_6-DMSO, [ppm]) δ = 0.86 (t, 3H, $CH_3CH_2CH_2CH_2CH_2CH_2O$, J = 6.13 Hz), 0.90 (t, 3H, $CH_3CH_2CH_2CH_2N$, J = 7.33 Hz), 1.25 (m, 8 H, $CH_3CH_2CH_2CH_2N$, $CH_3CH_2CH_2CH_2CH_2CH_2O$), 1.48 (m, 2H, $CH_3CH_2CH_2CH_2CH_2CH_2O$, 1.77 (q, 2H, $CH_3CH_2CH_2CH_2N$, J = 7.37 Hz), 3.70 (t, 2H, $CH_3CH_2CH_2CH_2CH_2CH_2O$, J = 6.63 Hz), 3.86 (s, 3H, NCH_3), 4.18 (t, 2H, $CH_3CH_2CH_2CH_2N$, J = 7.16 Hz), 7.72 (s, 1H, NCHCHN), 7.79 (s, 1H, NCHCHN), 9.15 (s, 1H, NCHN). ^{13}C-NMR (75MHz, d_6-DMSO, [ppm]) δ = 13.2 ($CH_3CH_2CH_2CH_2N$), 13.8 ($CH_3CH_2CH_2CH_2CH_2CH_2O$), 18.7 ($CH_3CH_2CH_2CH_2N$), 22.0 ($CH_3CH_2CH_2CH_2CH_2CH_2O$), 25.2 ($CH_3CH_2CH_2CH_2CH_2CH_2O$), 29.0 ($CH_3CH_2CH_2CH_2CH_2CH_2O$), 31.0 ($CH_3CH_2CH_2CH_2CH_2CH_2O$), 31.4 ($CH_3CH_2CH_2CH_2N$), 35.66 ($NCH_3$), 48.5 ($CH_3CH_2CH_2CH_2N$), 65.5 ($CH_3CH_2CH_2CH_2CH_2CH_2O$), 122.3 (NCHCHN), 123.6 (NCHCHN), 139.3 (NCHN)

1-Butyl-3-methylimidazolium *n*-octylsulfate [BMIM][OcOSO$_3$]. ^{1}H-NMR (400 MHz, d_6-DMSO, [ppm]) δ = 0.86 (t, 3H, $CH_3CH_2CH_2CH_2CH_2CH_2CH_2CH_2O$, J = 6.20 Hz), 0.90 (t, 3H $CH_3CH_2CH_2CH_2N$, J = 7.32 Hz), 1.25 (m, 12H, $CH_3CH_2CH_2CH_2N$, $CH_3CH_2CH_2CH_2CH_2CH_2CH_2CH_2O$), 1.48 (m, 2H, $CH_3CH_2CH_2CH_2CH_2CH_2CH_2CH_2O$), 1.77 (q, 2H, $CH_3CH_2CH_2CH_2N$, J = 7.35 Hz), 3.69 (t, 2H, $CH_3CH_2CH_2CH_2CH_2CH_2CH_2CH_2O$, J = 6.02 Hz), 3.86 (s, 3H, NCH_3), 4.18 (t, 2H, $CH_3CH_2CH_2CH_2N$, J = 7.16 Hz), 7.72 (s, 1H, NCHCHN), 7.79 (s, 1H, NCHCHN), 9.15 (s, 1H, NCHN). ^{13}C-NMR (75MHz, d_6-DMSO, [ppm]) δ = 13.2 ($CH_3CH_2CH_2CH_2N$), 13.9 ($CH_3CH_2CH_2CH_2CH_2CH_2CH_2CH_2O$), 18.7 ($CH_3CH_2CH_2CH_2N$), 22.0–31.2 ($CH_3CH_2CH_2CH_2CH_2CH_2CH_2CH_2O$), 31.4 ($CH_3CH_2CH_2CH_2N$), 35.7 ($NCH_3$), 48.5 ($CH_3CH_2CH_2CH_2N$), 65.5 ($CH_3CH_2CH_2CH_2CH_2CH_2$– CH_2CH_2O), 122.3 (NCHCHN), 123.57 (NCHCHN), 139.3 (NCHN)

Determination of acid content

The acid content was determined by titration with 0.1 M NaOH solution. Bromothymol blue was used as pH indicator.

Determination of water content

After synthesis, the ionic liquids were dried over night under vacuum (<1 mbar) at 70 °C. The water content was determined by coulometric Karl–Fischer titration using a Metrohm 756 KF Coulometer with a Hydranal® Coulomat AG reagent.

Determination of melting points

Differential scanning calorimetry (DSC) was carried out using a Netzsch DSC 205 Phoenix, under an argon atmosphere, with samples hermetically sealed in Al pans and cooled to −140 °C and then reheated, at a cooling and heating rate of 10 K min^{-1}. The melting points (mp) were determined from the DSC thermograms during the programmed reheating steps.

Viscosity

The viscosities of the [EMIM] based alkylsulfates were measured under argon atmosphere using a MCR 100 rheometer from Anton Paar, Graz. Temperature control was maintained by a peltier element. The viscosities of the [BMIM] based melts were recorded on a RS 100 viscosimeter from Haake, with an external thermostat for temperature control. Viscosity measurements were always carried out with samples of defined water content (600 ± 100 ppm) that was determined directly prior to the measurement by coulometric Karl–Fischer titration.

Density

Density was measured at room temperature in a BLAUBRAND pyknometer with a defined volume of 5.330 ml according to DIN ISO 3507.

Thermal stability

Thermogravimetric measurements were conducted on a Netzsch TG 209 with the samples placed in an open Al_2O_3 pan and heated from room temperature up to 500 °C at a heating rate of 10 K min^{-1} under a protective gas atmosphere. The temperature of decomposition (T_{dec}) was determined by using the TG-onset temperature, which is the intersection of the baseline below their decomposition temperature with the tangent to the mass loss *versus* temperature plots in the TGA experiment.

Hydrolytical stability

For the determination of the hydrolytical stability, samples of ionic liquids with molecularly defined water content were stirred at 95 °C while the pH-values were recorded using a Schott CG 842 pH meter.

Conclusions

In this paper we have demonstrated a new, two-step synthesis to long-chain and functionalized alkylsulfate ionic liquids. The key-step of this method is the acid-catalysed transesterification of methyl- or ethylsulfates with an alcohol of choice. Due to the great number of commercially available functionalized and non-functionalized alcohols, the method can lead to a large number of different products. A first set of [EMIM] based substances has been described in this paper, and it has become clear that some of the new ionic liquids now accessible have a significant potential for technical application, especially when low viscous, hydrolysis stable, halogen-free and cheap ionic liquids are required. The fact that a large number of new ionic liquids is accessible through this route from one intermediate ionic liquid makes this route also ideal for future ionic liquid structure optimization in a combinatorial or parallel manner. Apart from this potential to create new ionic liquid structures, the method presented in this paper also offers significant advantages over traditional methods when it comes to the synthesis of ionic liquids that are already well-known and that have so far been prepared by metathesis from chloride salts. In contrast to those traditional procedures, the new two-step synthesis requires no solvents for the entire production process. Moreover, almost no waste is produced during the very atom-efficient synthesis, as methanol or ethanol are the only by-products in the process (and even those are recovered and could in general be recycled). Most important for many technical applications is the fact that the new methodology provides alkylsulfate ionic liquids which are essentially free of chloride and any other traces of halides, as the whole synthesis does not involve any halogen-containing reagents. This is of importance for all different kinds of applications for the resulting ionic liquids, whether transition metal catalysis (where halides are known as poisons) or mechanical applications (with related corrosion aspects) are considered. Finally we have also demonstrated in our laboratories that the method described here is easy to scale up. In our 25 litre rotary evaporator we managed to produce 10 litres of [EMIM][$BuOSO_3$] in a couple of hours from [EMIM][$EtOSO_3$] in >98% yield. Based on these results, we anticipate that our new methodology will be of great use to further explore the future technical potential of alkylsulfate ionic liquids.

Acknowledgements

The authors like to thank Dr. Marc Uerdingen (Solvent Innovation, GmbH, Cologne) for fruitful discussions.

References

1 M. Maase, K. Massonne, K. Halbritter, R. Noe, M. Bartsch, W. Siegel, V. Stegmann, M. Flores, O. Huttenloch and M. Becker, BASF AG, Germany, *World Pat. Application*, WO 2003-EP545 2003062171,2003.
2 *Ionic Liquids in Synthesis*, ed. P. Wasserscheid and T. Welton, Wiley-VCH, Weinheim, 2003.
3 P. Wasserscheid, *Transition Metals for Organic Synthesis*, ed. M. Beller and C. Bolm, Wiley-VCH, Weinheim, 2004, vol. 2, p. 559.
4 T. Welton and P. J. Smith, *Adv. Organomet. Chem.*, 2004, **51**, 251.
5 R. A. Sheldon, R. M. Lau, M. J. Sorgedrager, F. van Rantwijk and K. R. Seddon, *Green Chem.*, 2002, **4**, 147.
6 R. Kawano, H. Matsui, C. Matsuyama, A. Sato, M. A. B. H. Susan, N. Tanabe and M. Watanabe, *J. Photochem. Photobiol., A*, 2004, **164**, 87.
7 Q. Lu, H. Wang, C. Ye, W. Liu and Q. Xue, *Tribol. Int.*, 2004, **37**, 547.
8 T. Brinz and U. Simon, Robert Bosch G.m.b.H., Germany, *German Pat. Application*, DE 2002-10245337 10245337, 2004.
9 K. Fukumoto, M. Yoshizawa and H. Ohno, *J. Am. Chem. Soc.*, 2005, **127**, 2398.
10 A. Bosmann and T. J. S. Schubert, Germany, *Br. Pat. Application*, GB 2005-10772 2414553, 2005.
11 B. Weyershausen and K. Lehmann, *Green Chem.*, 2005, **7**, 15.
12 Y. A. Beste, H. Schoenmakers, W. Arlt, M. Seiler and C. Jork, BASF AG, Germany, *German Pat. Application*, DE 2003-10336555 10336555, 2005.
13 C. Jork, M. Seiler, Y.-A. Beste and W. Arlt, *J. Chem. Eng. Data*, 2004, **49**, 852.
14 G. Olbert, T. Mattke, M. Fiene, O. Huttenloch and U. Hammon, BASF AG, Germany, *German Pat. Application*, DE 2003-10316418 1031641, 2004.
15 M. E.Van Valkenburg, R. L. Vaughn, M. Williams and J. S. Wilkes, *Proc. Electrochem. Soc.*, 2002, **2002–19**, 112.
16 R. P. Swatloski, J. D. Holbrey and R. D. Rogers, *Green Chem.*, 2003, **5**, 361.
17 F. Endres, *Z. Phys. Chem. (Munich)*, 2004, **218**, 255.
18 P. Wasserscheid and C. Hilgers, Solvent Innovation Gmbh, Germany, *Eur. Pat. Application*, EP, 2000-118441 1182196, 2002.
19 M. Schmidt, U. Heider, W. Geissler, N. Ignatyev and V. Hilarius, Merck Patent G.m.b.H., Germany, *Eur. Pat. Application*, EP 2001-111953 1162204, 2001.
20 M. Maase, K. Massonne and L. Szarvas, BASF AG, Germany, *World Pat. Application*, WO 2005-EP752 2005070896, 2005.
21 P. Wasserscheid, R. van Hal and A. Boesmann, *Abstracts of Papers, 224th ACS National Meeting, Boston, MA, United States, August 18–22, 2002*, 2002, IEC.
22 Z.-B. Zhou, H. Matsumoto and K. Tatsumi, *Chem. Lett.*, 2004, **33**, 680.
23 A. G. Boewing, A. Jess and P. Wasserscheid, *Chem.-Ing.-Tech.*, 2005, **77**, 1430.
24 *e.g.* from Solvent Innovation GmbH, Cologne (www.solvent-innovation.de) or BASF AG (www.basionics.de).
25 J. D. Holbrey, W. M. Reichert, R. P. Swatloski, G. A. Broker, W. R. Pitner, K. R. Seddon and R. D. Rogers, *Green Chem.*, 2002, **4**, 407.
26 P. Wasserscheid, R. van Hal and A. Boesmann, *Green Chem.*, 2002, **4**, 400.
27 P. Wasserscheid, R. van Hal and A. Boesmann, *Proc. Electrochem. Soc.*, 2002, **2002–19**, 146.
28 M. Seiler, C. Jork and W. Arlt, *Chem.-Ing.-Tech.*, 2004, **76**, 735.
29 G. Gelbhard, *Ind. Eng. Chem. Res.*, 2005, **44**, 8468.

Microwave-assisted cationic ring-opening polymerization of a soy-based 2-oxazoline monomer

Richard Hoogenboom and Ulrich S. Schubert*

Received 16th January 2006, Accepted 19th July 2006
First published as an Advance Article on the web 8th August 2006
DOI: 10.1039/b600616g

The microwave-assisted cationic ring-opening polymerization of a soy-based 2-oxazoline monomer (SoyOx) was investigated. Kinetic investigations of the SoyOx polymerization in both acetonitrile and without additional solvent revealed the formation of well-defined poly(2-oxazoline)s with fatty acid side chains in a living manner. The living cationic ring-opening polymerization of bulk SoyOx reached full conversion within 8 minutes. The unsaturated bonds of the fatty acids are unaffected by the applied polymerization procedure. In addition, it was demonstrated that these double bonds can be used to cross-link the soy-based poly(2-oxazoline)s under UV-irradiation.

Introduction

Nowadays, the increasing oil-prices and the concerns about oil supplies stimulate the use of renewable feedstock in academic research and the chemical industry.[1] In polymer chemistry, the use of monomers based on renewable resources has obtained increasing attention as well.[2] The utilized renewable resources include, *e.g.*, starch,[3] saccharides[4] and fatty acids.[5] In particular, the use of fatty acids seems to be a promising approach in polymer science due to their versatility: the unsaturated bonds can be directly used for polymerization[6] and/or the acid-functionality can be converted into a polymerizable group. The polymerization of such monomers results in polymers with hydrophobic fatty-acid side chains.[7] These fatty acid based polymers can be applied in a wide variety of applications including, *e.g.*, coatings, adhesives and rubbers.[5] An additional advantage of polymers with fatty acid side chains is the possibility to cross-link the material using, *e.g.*, UV-irradiation.[8,9] The atom transfer radical polymerization of cardanyl acrylate is, to the best of our knowledge, the only example in which the preparation of well-defined polymers with unsaturated fatty acid side chains is reported up to now.[9]

In this contribution, we describe the microwave-assisted cationic ring-opening polymerization of a soy-based 2-oxazoline monomer (SoyOx), which was previously synthesized by Henkel.[10] Although microwave irradiation is a clean and efficient alternative heat source,[11] microwave-assisted polymerizations are still rather unexplored.[12] Nevertheless, we have recently demonstrated a 400-fold acceleration of the cationic ring-opening polymerization of 2-oxazolines under pressurized microwave irradiation (compared to conventional polymerizations at ambient pressure).[13] This acceleration was found to originate from the increased polymerization temperature and could be reproduced using conventionally heated pressure reactors.[14] The present study combines the use of a monomer based on a renewable resource and the use of microwave irradiation as alternative heat source. Kinetic studies of the polymerization of SoyOx were performed to study whether this microwave-assisted polymerization proceeds in a living manner. Subsequent cross-linking of the unsaturated bonds in the synthesized pSoyOx under UV-irradiation will be discussed as well.

Experimental section

Materials

Acetonitrile (Aldrich) was dried over molecular sieves (size 3 Å) before usage as the polymerization solvent. SoyOx (donated by Henkel and reported in ref. 10) was purified over aluminum oxide with hexane as eluent. After drying over BaO it was stored under argon. Methyl tosylate (Aldrich) was distilled and stored under argon.

Instrumentation

Polymerizations were carried out in an Emrys Liberator (Biotage, formerly PersonalChemistry) utilizing capped reaction vials. These vials were heated to 105 °C, allowed to cool to room temperature and filled with argon prior to use. All microwave polymerizations were performed with temperature control (IR sensor). ^{1}H NMR spectra were recorded in $CDCl_3$ on a Varian AM-400 spectrometer or a Varian Gemini 300 spectrometer. Chemical shifts are given in ppm relative to TMS or residual solvent signals. Gel Permeation Chromatography (GPC) was performed on a Shimadzu system with a SCL-10A system controller, a LC-10AD pump, a RID-6A refractive index detector, a SPD-10A UV detector and a PLgel 5 μm Mixed-D column with chloroform–triethylamine–2-propanol (94 : 4 : 2) as eluent and the column oven set to 50 °C (polystyrene calibration). GC measurements were performed on an Interscience Trace GC with a Trace Column RTX-5 connected to a PAL autosampler. For the injection of polymerization mixtures, a special Interscience liner with additional glass wool was used. GC-MS analysis was

---

Laboratory of Macromolecular Chemistry and Nanoscience, Eindhoven University of Technology and Dutch Polymer Institute (DPI), PO Box 513, 5600 MB Eindhoven, The Netherlands. E-mail: u.s.schubert@tue.nl

performed on a Shimadzu GC-MS-QP5000, the mass values are reported as mass/charge ratio (*m*/*z*). Cross-linking of the pSoyOx was performed in a UV-irradiation chamber with 5.8 J cm^{-2}.

Kinetic investigations on the microwave-assisted polymerization of 2-soy alkyl-2-oxazoline (SoyOx)

Solution. A stock solution of SoyOx (3.32 g; 11.1 mmol), methyl tosylate (initiator; 34.9 mg; 0.187 mmol) and acetonitrile (3.194 g; 4.1 mL) was prepared resulting in a 1.5 M SoyOx solution with a monomer to initiator ratio of 60. This stock solution was divided over 5 different microwave vials (600 μL each) that were heated for 1, 2.5, 5, 8.33, or 13.33 minutes to 140 °C. After heating, the polymerization mixture was cooled to 38 °C and quenched by the addition of water. GC and GPC samples were prepared from the polymerization mixtures to determine the monomer conversion and the molecular weight (distribution) of the resulting polymers. Due to partial insolubility of pSoyOx in CH_3CN, the polymerization mixtures were first homogenized by the addition of *o*-dichlorobenzene before sampling. The CH_3CN was used as internal standard for the GC-analysis.

Bulk. The bulk polymerizations were performed in a similar manner as the polymerizations in CH_3CN utilizing a stock solution of SoyOx (5.01 g; 16.7 mmol) and methyl tosylate (51.8 mg; 0.28 mmol). The polymerizations were performed for 1, 2, 3, 4, 5 and 6 minutes at 140 °C. The resulting polymerization mixtures were analyzed by ^{1}H-NMR spectroscopy and GPC.

^{1}H NMR of the poly(SoyOx) at full conversion ($CDCl_3$): δ = 7.71 (d, J = 8.1 Hz, 2H, C*H*CS tosylate), 7.16 (d, J = 8.1 Hz, 2H, C*H*CCH$_3$ tosylate), 5.45–5.20 (br, 82H, *H*C=C*H*), 3.6–3.3 (br, 230H, NC*H*$_2$C*H*$_2$N), 2.75 (br, 80H), 2.45–2.20 (br, 132H, C=OC*H*$_2$), 2.08–1.95 (br, 105H, C*H*$_2$), 1.65–1.50 (br, 153H, C*H*$_2$), 1.38–1.20 (br, 1270H, C*H*$_2$), 0.90–0.82 (br, 200H, C*H*$_3$). DP_{NMR} = 58.

Results and discussion

The microwave-assisted polymerization of a sustainable soy-based 2-‘soy alkyl’-2-oxazoline (SoyOx) monomer was investigated. Besides the green character of using a monomer based on soy-beans, the unsaturated nature of the fatty acids is transferred into the SoyOx monomer providing cross-linking possibilities for the resulting polymers. The SoyOx was synthesized by coupling soy bean fatty acids with ethanolamine followed by ring-closure in the presence of a titanium catalyst as depicted in Scheme 1.[10]

The resulting SoyOx is a mixture of 2-oxazolines with different fatty acid side chains. Fig. 1 depicts the gas chromatography (GC) spectrum of the purified monomer with the structures that could be assigned by the mass spectra from the GC-MS. The spectrum showed four signals, which could all be assigned to different 2-oxazoline species with 16 or 17 carbon atoms and 0 to 2 unsaturated bonds in the side chain. The average composition of the side chain is 17 carbon atoms and 1.5 double bonds, which corresponds reasonably to the previously reported composition of soybean fatty acids, namely 90% C18 with on average 1.76 double bonds.[15]

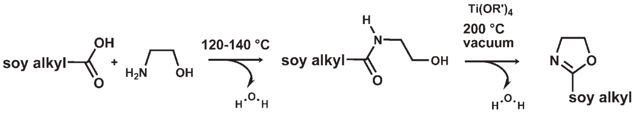

Scheme 1 Synthesis of the soy-based 2-oxazoline monomer (SoyOx).

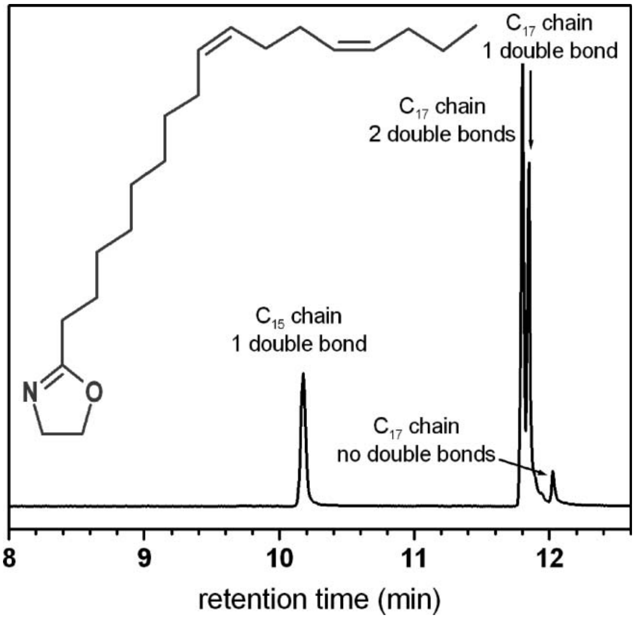

Fig. 1 Gas chromatography spectrum and schematic representation of the SoyOx monomer. The peaks were assigned using the mass spectrometry detector.

The microwave-assisted polymerization of the purified SoyOx was investigated in the common polymerization solvent acetonitrile (CH_3CN) and in bulk, which excludes the addition of organic solvent. The polymerizations were performed at 140 °C with methyl tosylate as initiator, and a monomer to initiator ratio of 60. The mechanism of the living cationic ring-opening polymerization of 2-oxazolines is schematically depicted in Scheme 2. Upon heating, the free electron pair of the nitrogen atom of the 2-oxazoline ring will attack the electrophilic initiator, resulting in a cationic oxazolinium species. The C–O bond in this oxazolinium species is weakened and propagation occurs through the nucleophilic attack of the next monomer onto this carbon atom resulting in the formation of the ring-opened poly(2-oxazoline). The addition of a nucleophile to the polymerization mixture will lead to termination of the polymerization process, as depicted in Scheme 2 for the addition of water. Since all polymer chains start growing at the same time and all oxazolinium species have the same reactivity, polymers with similar chain length and narrow molecular weight distributions are obtained.

The polymerization kinetics of the cationic ring-opening polymerization of SoyOx in both CH_3CN and bulk were investigated under microwave irradiation. A stock solution of the polymerization mixture was divided over different microwave vials and each vial was heated for a different reaction time. The polymerizations in acetonitrile resulted in

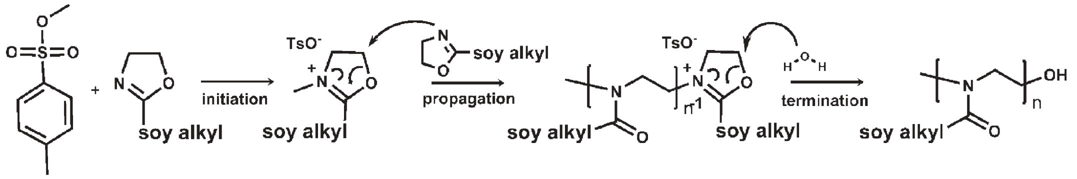

Scheme 2 Schematic representation of the living cationic ring-opening polymerization of SoyOx.

precipitated pSoyOx after microwave heating. Direct precipitation of the pSoyOx might be advantageous to simplify the work-up procedure into one single filtration step, which also allows simple recycling of the acetonitrile (after, *e.g.*, distillation for purification). However, for further analysis of the polymerization mixtures, *o*-dichlorobenzene was added to homogenize the polymerization mixtures. The resulting polymerization mixtures were analyzed by GC (CH_3CN polymerizations) and ^1H NMR spectroscopy (bulk polymerizations) to determine the monomer conversion, and by gel permeation chromatography (GPC) to obtain the molecular weight (distribution) of the resulting polymers. Fig. 2 depicts the ^1H-NMR spectra that were obtained after different polymerization times for the bulk polymerization of SoyOx. With increasing reaction time, the 2-oxazoline monomer signals at 3.8 and 4.2 ppm decrease and the polymer backbone signal at 3.4 ppm increases, indicating that monomer is converted into polymer. Moreover, the signals of the double bonds at 5.4 ppm remain constant demonstrating that they are unaffected by the cationic polymerization. This demonstrates that the resulting pSoyOx contains a large amount of double bonds in the side-chains.

The GPC traces obtained for the bulk polymerization of SoyOx in time are depicted in Fig. 3. In these traces, both the polymer and the large monomer are separated from the solvent signal. With increasing reaction time, the monomer signal decreased and the polymer signal increased and moved to lower retention times, indicating an increase in molecular weight. Moreover, the narrow single distributions of the molecular weight indicate that the polymers were made in a living fashion. From integration of both monomer and polymer signals in the GPC traces, the monomer conversion could be calculated; it was assumed that both the monomer and the monomer incorporated in the polymer have the same effect on the refractive index of the solution.

The monomer conversion over time for the microwave-assisted SoyOx polymerizations is shown in Fig. 4. The conversion is depicted as $\ln([M]_0/[M]_t)$ since the living cationic ring-opening polymerization of 2-oxazolines is known to be first order in monomer concentration. As a result, the observation of linear first order kinetics would demonstrate a constant concentration of active species during the polymerization, indicative of a living polymerization mechanism. The different methods to determine the monomer conversion gave similar results. Both the polymerizations in bulk and CH_3CN revealed linear first order kinetics suggesting a living polymerization mechanism. The faster polymerization in bulk is due to the higher monomer concentration (3.3 M) compared to the solution polymerizations (1.5 M, corresponding to 45 wt%), but both the microwave assisted SoyOx polymerizations in bulk (7.5 minutes) and acetonitrile (12.5 minutes) reached more than 95% conversion in very short reaction times.

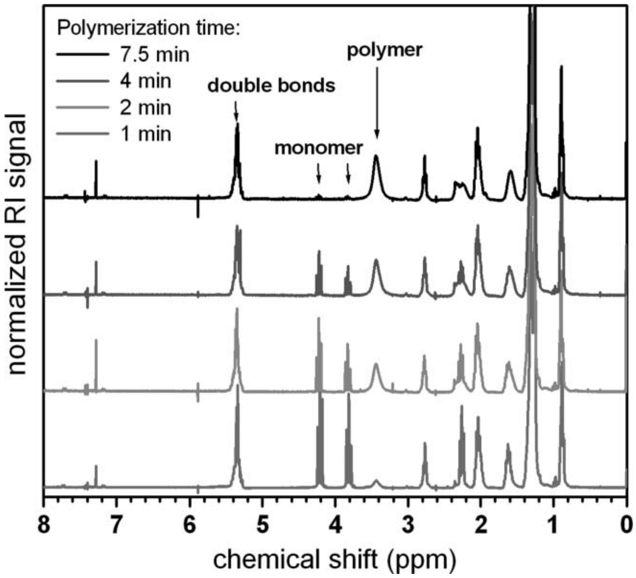

Fig. 2 ^1H NMR spectra that were obtained after different polymerization times for the microwave-assisted bulk polymerization of SoyOx at 140 °C. The spectra were recorded in $CDCl_3$.

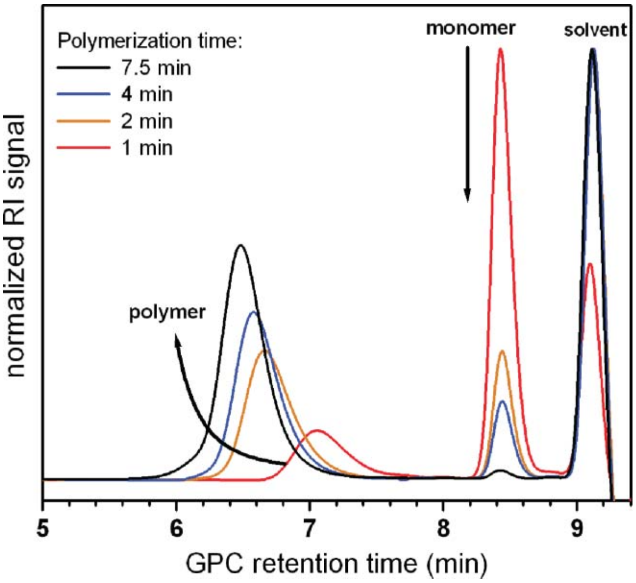

Fig. 3 GPC traces spectra that were obtained after different polymerization times for the microwave-assisted bulk polymerization of SoyOx at 140 °C. The GPC characterization was performed with chloroform–triethylamine–isopropanol (94 : 4 : 2) as eluent.

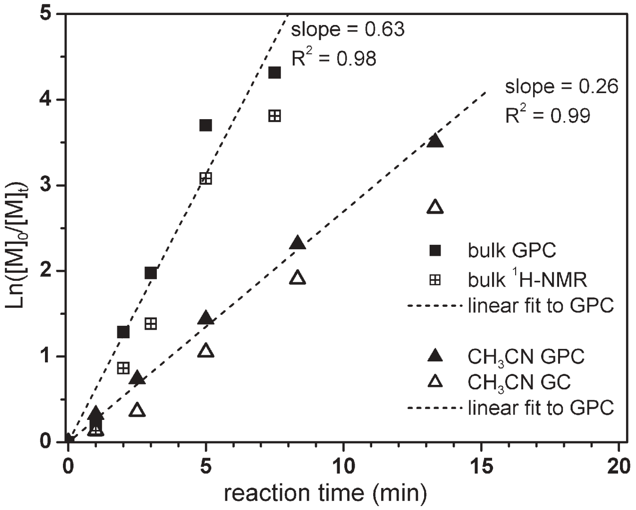

Fig. 4 First order kinetic plot for the microwave-assisted polymerization of SoyOx at 140 °C in bulk (squares) and CH_3CN (triangles).

In addition to the first order kinetics, the increase of number average molecular weight (M_n) with monomer conversion was investigated. In a living polymerization, all polymer chains keep on growing throughout the entire polymerization process and thus the M_n should increase linearly with conversion. This was indeed observed, as depicted in Fig. 5, proving the living character of the SoyOx polymerizations in both bulk and CH_3CN. However, the observed M_n's are significantly lower than the theoretical molecular weight, which is most likely due to the utilized polystyrene standards that were used to calibrate the GPC using an RI-detector. The pSoyOx will have a different folding behavior than polystyrene and thus the hydrodynamic volume will be very different, resulting in an uncertainty of the calculated M_n values. Nevertheless, the observed trend in the M_n values and the molecular weight distributions will not be significantly influenced by the applied calibration. The observed polydispersity indices (PDI's) are around 1.20, which also suggests that the polymers were synthesized in a living manner. Surprisingly, it was found that SoyOx can be polymerized in a living manner in bulk, although the living bulk polymerization of other 2-oxazoline monomers was previously found to be impossible.[13] The combination of linear first order kinetics, a linear increase of M_n with conversion as well as the observed low PDI's prove the livingness of the SoyOx polymerizations.

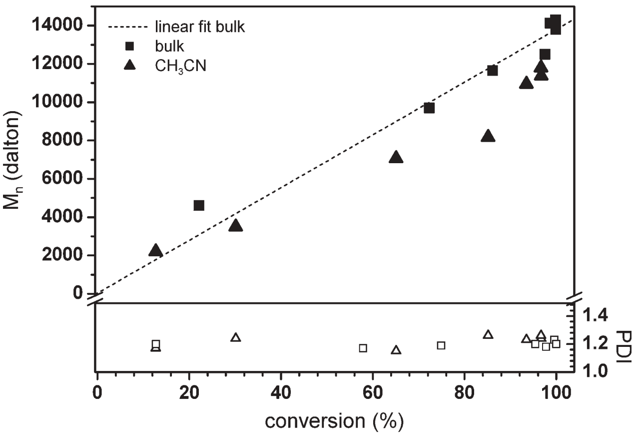

Fig. 5 Dependence of number average molecular weight (M_n) and molecular weight distribution (PDI) on conversion for the SoyOx polymerizations under microwave irradiation at 140 °C in both bulk (squares) and CH_3CN (triangles).

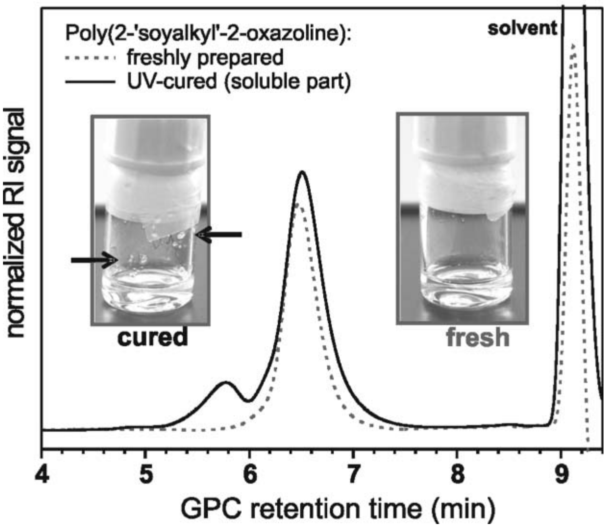

Fig. 6 GPC traces of pSoyOx before and after UV-irradiation (only soluble part). The inset pictures show the appearance of solutions of pSoyOx in CH_2Cl_2 before and after UV-irradiation, demonstrating the insolubility of the cross-linked pSoyOx.

In a next step, cross-linking of the double bonds in the pSoyOx side-chains was attempted by UV-irradiation. After 2 hours UV-irradiation, the pSoyOx did not dissolve in CH_2Cl_2 anymore indicating successful cross-linking. The photographs in Fig. 6 show the solutions of pSoyOx in CH_2Cl_2 before and after cross-linking, the swollen particles of pSOyOx are clearly visible (see arrows) after UV-irradiation. Next to this first visual proof, GPC was measured from the minor soluble part of the UV-cured pSoyOx (Fig. 6). The GPC-trace after UV-irradiation shows the presence of uncoupled polymer and a second small distribution of two polymers coupled together. Apparently, coupling of more chains together results in insoluble cross-linked pSoyOx, which cannot be detected by GPC. ^1H NMR spectroscopy on the swollen cross-linked pSoyOx revealed that 16% of all present double bonds had disappeared after UV-irradiation. The advantages of UV-cross-linking SoyOx containing poly(2-oxazoline)s has been recently exploited for the preparation of cross-linked micelles as well.[16]

Conclusions

We have demonstrated that the renewable SoyOx monomer can be polymerized in a living manner by cationic ring-opening polymerization under microwave-irradiation. To the best of our knowledge, this is only the second example (after the previously reported controlled radical polymerization of a cardanyl acrylate)[9] of the successful preparation of well-defined polymers with unsaturated fatty acid side chains, and it is the first example using cationic ring-opening polymerization. ^{1}H NMR spectroscopy revealed that the unsaturated bonds of the fatty acids were not affected by the cationic polymerization and, thus, they were incorporated in the polymer side-chains. Kinetic investigations demonstrated that the SoyOx polymerization was a living polymerization in both bulk and acetonitrile, thus the SoyOx polymerization in bulk is the first example of a living cationic polymerization in bulk monomer without additional solvent present. Noteworthy is the very short polymerization time, less than 8 minutes, that was required to reach full conversion under these microwave-assisted polymerization conditions. The resulting pSoyOx was successfully cross-linked by UV-irradiation, as was demonstrated by its insolubililty in dichloromethane. The success of cross-linking was further confirmed by GPC and ^{1}H NMR spectroscopy.

In conclusion, we have demonstrated that soy-based monomers are versatile building blocks in polymer science. Besides the advantage of making materials based on renewable resources, the unsaturated side-chains provide added-value by the possibility of cross-linking the resulting polymers.

Acknowledgements

The authors would like to thank the Dutch Scientific Organization (NWO), the Dutch Polymer Institute (DPI) and the Fonds der Chemischen Industrie for financial support. Henkel is acknowledged for providing the SoyOx.

References

1 U. Biermann, W. Friedt, S. Lang, W. Lühs, G. Machmüller, J. O. Metzger, M. R. Klaas, H. J. Schäfer and M. P. Schneiderüsch, *Angew. Chem., Int. Ed.*, 2000, **39**, 2206–2224.
2 M. S. Lindblad, Y. Liu, A.-C. Albertsson, E. Ranucci and S. Kalsson, *Adv. Polym. Sci.*, 2002, **157**, 139–161.
3 V. D. Athwale and V. Lele, *Starch*, 2001, **53**, 7–13; K. Milkowski, J. H. Clark and S. Doi, *Green Chem.*, 2004, **6**, 189–190.
4 U. Koch and E.-J. Yaacoub, *J. Polym. Sci., Part A: Polym. Chem.*, 2003, **41**, 788–803; A. Imaz, M. Ayerbe, J. Ramos and J. Forcada, *J. Polym. Sci., Part A: Polym. Chem.*, 2006, **44**, 443–457.
5 L. H. Sperling, J. A. Manson, S. Qureshi and A. M. Fernandez, *Ind. Eng. Chem. Prod. Res. Dev.*, 1981, **20**, 163–166; M. C. Lubi and A. T. Thachil, *Des. Monomers Polym.*, 2000, **3**, 123–153.
6 T. Tsujimoto, H. Uyama and S. Kobayashi, *Macromolecules*, 2004, **37**, 1777–1782; W. Liu, M. Misra, P. Askeland, L. T. Drzal and A. K. Mohanty, *Polymer*, 2005, **46**, 2710–2721.
7 H. P. Bhunia, G. B. Nando, T. K. Chaki, A. Basak, S. Lenka and P. L. Nayak, *Eur. Polym. J.*, 1999, **35**, 1381–1391; E. Dzunuzovic, S. Tasic, B. Bozic, D. Babic and B. Dunjic, *Prog. Polym. Sci.*, 2005, **52**, 136–143.
8 W. F. Lee, *J. Appl. Polym. Sci.*, 1993, **47**, 61–71.
9 K. I. Suresh and M. Jaikrishna, *J. Polym. Sci., Part A: Polym. Chem.*, 2005, **43**, 5953–5961.
10 M. Beck, P. Birnbrich, U. Eicken, H. Fischer, W. E. Fristad, B. Hase and H.-J. Krause, *Angew. Makromol. Chem.*, 1994, **223**, 217.
11 B. L. Hayes, *Microwave synthesis: Chemistry at the speed of light*, CEM Publishing, Matthews, NC, USA, 2002; C. O. Kappe and A. Stadler, in *Microwaves in organic and medicinal chemistry*, ed. R. Mannhold, H. Kubinyi and G. Folkers, Wiley VCH, Weinheim, Germany, 2005.
12 F. Wiesbrock, R. Hoogenboom and U. S. Schubert, *Macromol. Rapid Commun.*, 2004, **25**, 1739–1764.
13 F. Wiesbrock, R. Hoogenboom, C. H. Abeln and U. S. Schubert, *Macromol. Rapid Commun.*, 2004, **25**, 1895–1899; F. Wiesbrock, R. Hoogenboom, M. A. M. Leenen, M. A. R. Meier and U. S. Schubert, *Macromolecules*, 2005, **38**, 5025–5034.
14 R. Hoogenboom, M. A. M. Leenen, F. Wiesbrock and U. S. Schubert, *Macromol. Rapid Commun.*, 2005, **26**, 1773–1778; R. Hoogenboom, M. W. M. Fijten, R. M. Paulus, H. M. L. Thijs, S. Hoeppener, G. Kickelbick and U. S. Schubert, *Polymer*, 2006, **47**, 75–84.
15 F. O. Ayorinde, K. Garvin and K. Saeed, *Rapid Commun. Mass Spectrom.*, 2000, **14**, 608–615.
16 H. Huang, R. Hoogenboom, M. A. M. Leenen, P. Guillet, A. M. Jonas, U. S. Schubert and J.-F. Gohy, *J. Am. Chem. Soc.*, 2006, **128**, 3784–3788.

An environmentally benign catalytic system for alkene epoxidation with hydrogen peroxide electrogenerated *in situ*

Kam-Piu Ho, Tak Hang Chan and Kwok-Yin Wong*

Received 6th April 2006, Accepted 28th June 2006
First published as an Advance Article on the web 2nd August 2006
DOI: 10.1039/b605009c

Hydrogen peroxide was electrogenerated in-situ in aqueous bicarbonate solutions for the epoxidation of alkenes using Mn^{2+} as the catalyst. Water-soluble alkenes were epoxidized with excellent yields and high current efficiencies. The catalytic system could be adapted for the epoxidation of lipophilic alkenes in *tert*-butanol–water mixture. The electrochemical method allows the release of hydrogen peroxide to the reaction medium in a controlled manner and minimizes the problem of hydrogen peroxide wastage through catalytic decomposition by Mn^{2+}.

Introduction

Epoxides are important starting materials in organic synthesis, as they can be easily transformed into other functionalities.[1] Although there are many existing routes to prepare epoxides, most of these processes involve toxic chemicals and volatile organic solvents that cause pollution to the environment.[2] There is thus a pressing need to develop 'greener' routes for epoxide production. Hydrogen peroxide (H_2O_2) as the terminal oxidant for epoxidation is an attractive option both on environmental and economic grounds. It is relatively cheap and readily available, and gives water as the only co-product.[3] However, there is concern about the potential hazards associated with the storage and transportation of concentrated H_2O_2. Industrially, H_2O_2 is produced through the anthraquinone (AQ) process in which toxic organic solvents such as methylnaphthalene and trimethylbenzene[4] are used for recycling the catalysts, and thus the 'green' oxidant is 'non-green' in its production.[5]

Catalytic epoxidation with H_2O_2 electrogenerated *in situ* is of particular interest for a number of reasons. Firstly, H_2O_2 is produced at the cathode under mild conditions by the reduction of oxygen. Secondly, its usage as a dilute solution greatly reduces the hazards associated with the explosive nature of H_2O_2 and leaves no residues in the reaction. Murray and co-workers[6] were the first to describe this electrocatalytic approach for epoxidation with H_2O_2 electrogenerated in dichloromethane using a manganese *meso*-tetraphenylporphyrin catalyst, but undesirable elements such as the requirement for external proton sources, instability of catalyst and involvement of volatile organic solvents make this method impractical. Recently, similar approaches were reported by Shen *et al.*[7] and Zimmer *et al.*[8] using titanium silicate (TS-1) and bis(acetyl-acetonato)oxovanadium(IV) respectively as catalysts. However, the alkenes epoxidized were only limited to water-soluble alkenes as water was used as the solvent. Recently, we have reported the epoxidation of some α,β-unsaturated ketones with hydrogen peroxide electrogenerated in the ionic liquid 3-butyl-1-methylimidazolium tetrafluoroborate.[9] To broaden the scope of substrates and to increase the electrocatalytic efficiency, an improved catalytic system is definitely needed.

Water is the most environmentally benign medium and some organic reactions can be carried out in water effectively.[10] However, the major obstacle in replacing organic solvents in epoxidation reaction is the low solubility of lipophilic alkenes in water. The HCO_3^-/H_2O_2 system reported by Richardson[11] and Burgess,[12,13] which involves the generation of an active peroxymonocarbonate (HCO_4^-) species in *tert*-butanol (or acetonitrile)–water mixture, is considered a 'green' system applicable to a wide range of alkene substrates, as no toxic chemicals are used or formed in the whole process. Herein, we will describe our study on coupling this catalytic system with the H_2O_2 electrogenerated *in situ* in water or *tert*-butanol–water mixture (Scheme 1). *tert*-Butanol was chosen in this study because it is relatively non-toxic and it can dissolve most lipophilic alkenes.

Experimental

Instrumentation

Cyclic voltammetry (CV) and differential pulse voltammetry (DPV) were performed by a Bioanalytical Systems (BAS) model 100 W electrochemical analyzer in a conventional two-compartment cell. Constant potential electrolyses were conducted by an EG&G Princeton Applied Research model 273 A Potentiostat with a microflow cell purchased from

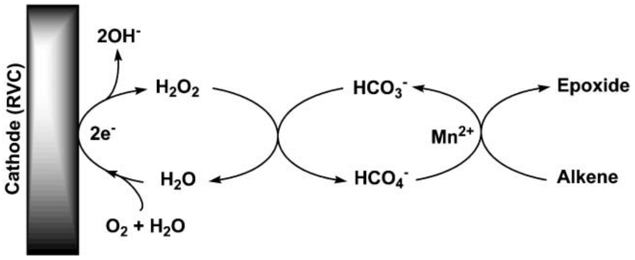

Scheme 1

Department of Applied Biology and Chemical Technology, The Hong Kong Polytechnic University, Hunghom, Kowloon, Hong Kong, P. R. China. E-mail: bckywong@polyu.edu.hk; Fax: (+852) 2364 9932; Tel: (+852) 3400 8686

ElectroCell AB, Sweden. The cathode was a 33 mm × 27 mm × 5 mm reticulated vitreous carbon (Electrosynthesis Co., 60 pores per inch (ppi)) mounted onto a graphite plate by conducting glue of epoxy resin (Araldite) and graphite powder (Merck). The anode was a platinum-coated titanium plate. The two compartments were separated by a Nafion 424 cation permeable membrane. The reference electrode was a saturated calomel electrode (SCE) and all potentials are quoted to this reference.

A Waters HPLC system with a LC-18 Column (Supelco) and a Hewlett-Packard model 8900 gas chromatograph–mass spectrometer equipped with an EC$^{\text{TM}}$-1 or EC$^{\text{TM}}$-WAX column (Alltech Associate, Inc.) were used for monitoring the product yields of reactions. ^{1}H and ^{13}C NMR spectra were recorded on a Bruker DPX-400 MHz NMR spectrometer.

Hydrogen peroxide electrogeneration

The two reservoirs were filled with the electrolyte solutions (50 ml each, Fig. 1). Electrolysis was carried out in the microflow cell with a flow rate of 500 ml min^{-1}. Oxygen was supplied to the catholyte either by continuous bubbling at a steady flow rate of 80 ml min^{-1} or through a rubber balloon filled with a fixed amount of oxygen gas (Fig. 1). H_2O_2 was electrogenerated by constant potential electrolysis. The concentration of H_2O_2 generated was monitored *in situ* by differential pulse voltammetry in the catholyte at regular time intervals. Oxidation of water to oxygen was the reaction occurring at the anode.

Epoxidation of alkene with hydrogen peroxide electrogenerated *in situ*

The experimental conditions were similar to the hydrogen peroxide electrogeneration alone except that the alkene substrate and the Mn^{2+} catalyst had been added to the electrolyte. For the water-soluble alkenes, 1 M $NaHCO_{3(aq)}$ and 2 M $H_2SO_{4(aq)}$ were used as the catholyte and anolyte respectively. A *tert*-butanol–water (2 : 3 v/v) mixture containing 0.24 M $NaHCO_3$ and 0.1 M NaCl was adapted for the lipophilic alkenes and the anolyte was a mixture of *tert*-butanol–water (2 : 3 v/v) with 2 M H_2SO_4. At regular intervals, 0.1 ml of the reaction mixture was withdrawn for product analysis. The product yield was determined by either HPLC or GC-MS with internal standard.

Results and discussion

Electrogeneration of H_2O_2 in bicarbonate solutions

$$O_2 + e^- \rightarrow O_2^{\cdot -} \qquad (1)$$

$$2O_2^{\cdot -} + 2H_2O \rightleftarrows O_2 + H_2O_2 + 2OH^- \qquad (2)$$

$$O_2 + 2H_2O + 2e^- \rightarrow H_2O_2 + 2OH^- \qquad (3)$$

$$O_2 + 2H_2O + 4e^- \rightarrow 4OH^- \qquad (4)$$

The cyclic voltammograms of dioxygen reduction at a glassy carbon electrode in bicarbonate solutions are shown in Fig. 2. In 1 M $NaHCO_{3(aq)}$ solution, two irreversible reduction peaks at −352 mV (I) and −613 mV (II) *vs.* SCE are observed. Sawyer *et al.*[14] and Yeager *et al.*[15] proposed that the first peak (I) is the 1-electron reduction of O_2 to $O_2^{\cdot -}$ (eqn (1)), which is followed by a dismutation reaction to generate H_2O_2 (eqn (2)). The second peak (II) was assigned as the overall 2-electron reduction to generate H_2O_2 directly from O_2 (eqn (3)).[16,17] Comparing the peak height and area, the latter is the dominant

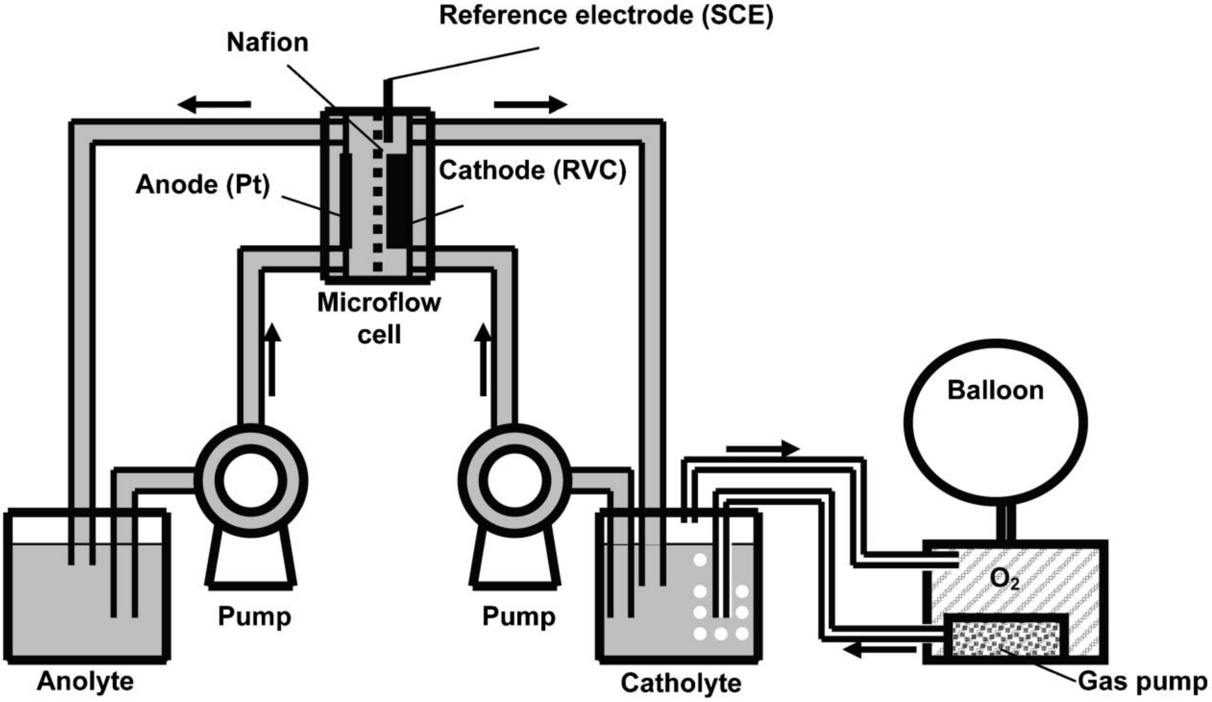

Fig. 1 Schematic diagram showing the flow of electrolyte and gas in the epoxidation of alkenes with H_2O_2 electrogenerated *in situ*.

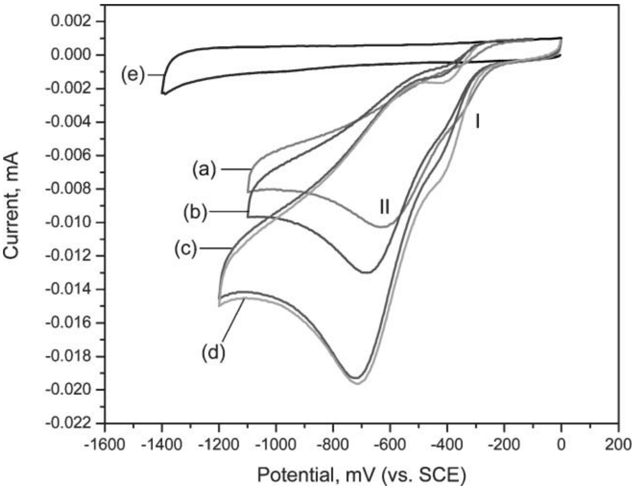

Fig. 2 Cyclic voltammograms of O_2 reduction in (a) 1 M $NaHCO_{3(aq)}$ solution, (b) a mixture of *tert*-butanol–water (1 : 4 v/v) + $NaHCO_3$ (0.24 M), (c) a mixture of *tert*-butanol–water (2 : 3 v/v) + $NaHCO_3$ (0.24 M) and (d) a mixture of *tert*-butanol–water (2 : 3 v/v) + $NaHCO_3$ (0.24 M) + NaCl (0.1 M). (e) 1 M $NaHCO_{3(aq)}$ under argon atmosphere. Working electrode: 0.2 cm^2 glassy carbon. Scan rate: 50 mV s^{-1}.

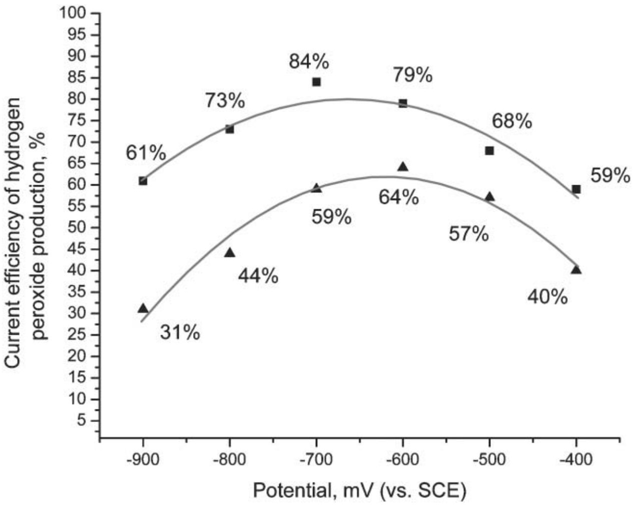

Fig. 3 The effect of applied potential on the current efficiency of H_2O_2 electrogenerated in 1 M aqueous $NaHCO_3$ (▲) and a mixture of *tert*-butanol–water (2 : 3 v/v) + $NaHCO_3$ (0.24 M) + NaCl (0.1 M) (■).

process, where the potential should be held in massive electrogeneration of H_2O_2.

When *tert*-butanol was added to the aqueous $NaHCO_3$ solution, the two irreversible reduction peaks are also observed (Fig. 2b–d), indicating the electrochemical processes are similar to those in aqueous bicarbonate solutions. It was noted that the size of the reduction waves increases with the amount of *tert*-butanol in the electrolyte. This can be attributed to the higher solubility of O_2 in *tert*-butanol than in water.[18,19]

The effect of applied potential on the electrogeneration of H_2O_2 in 1 M $NaHCO_{3(aq)}$ solution is shown in Fig. 3. A great improvement on the current efficiency of H_2O_2 production was observed when the potential was lowered from peak II in the cyclic voltammogram (Fig. 2a). When the potential was further lowered to below −600 mV, the current efficiency dropped as a result of side reactions such as the 4-electron reduction of dioxygen to hydroxide ion (eqn (4)).

tert-Butanol is a tertiary alcohol which is stable against oxidation. In combination with an appropriate catalytic system, it provides a suitable medium for epoxidation. The effect of *tert*-butanol on the H_2O_2 electrogenerated in $NaHCO_{3(aq)}$ solution is summarized in Table 1. While the presence of *tert*-butanol improves the solubility of O_2 and hence the current efficiency of H_2O_2 production, it also causes a drop in the conductivity of the electrolyte as $NaHCO_3$ is less soluble in *tert*-butanol than in water. The conductivity problem, however, can be partly remedied by the addition of 0.1 M NaCl (last entry, Table 1).

In the *tert*-butanol–$NaHCO_{3(aq)}$–NaCl mixture, the optimal applied potential for H_2O_2 electrogeneration is about 100 mV more cathodic than the optimal potential in 1 M $NaHCO_3$ aqueous solution due to the higher resistance of the electrolyte (Fig. 3). This is consistent with the cyclic voltammograms shown in Fig. 2, indicating the peak potential shifts cathodically upon the addition of *tert*-butanol.

Epoxidation of alkenes with hydrogen peroxide electrogenerated *in situ*

The effect of applied potential on the current efficiency of epoxide production using sodium 4-styrenesulfonate as the substrate is shown in Fig. 4. When the applied potential is in the range of −400 mV to −600 mV, the current efficiency of epoxidation can be as high as 97%, indicating that the H_2O_2 electrogenerated is effectively consumed for the subsequent epoxidation reaction. However, when the potential goes beyond −600 mV, the current efficiency declines sharply because of energy wastage on the direct reduction of dioxygen to hydroxide ion (eqn (4)).

Table 1 Electrogeneration of H_2O_2 in aqueous $NaHCO_3$ solutions containing different amounts of *tert*-butanol[a]

Concentration of *tert*-butanol (%, v/v)	Concentration of $NaHCO_3$/M	Conductivity/ mS cm^{-1}	Current density/mA cm^{-2}	Concentration of H_2O_2/mM	Current efficiency (%)
0	1	>20	1.03	26	64
10	0.72	>20	1.09	28	66
20	0.48	13.75	1.28	29	70
30	0.35	8.69	1.41	31	77
40	0.24	5.19	1.47	34	79
[b]40	0.24	7.79	1.60	37	84

[a] Anolyte: *tert*-butanol–water (2 : 3 v/v) + H_2SO_4 (2 M) mixture. Cathode: 33 mm × 27 mm × 5 mm RVC (60 ppi). Applied potential: −700 mV. Electrolysis time: 50 mins. [b] In the presence of 0.1 M NaCl.

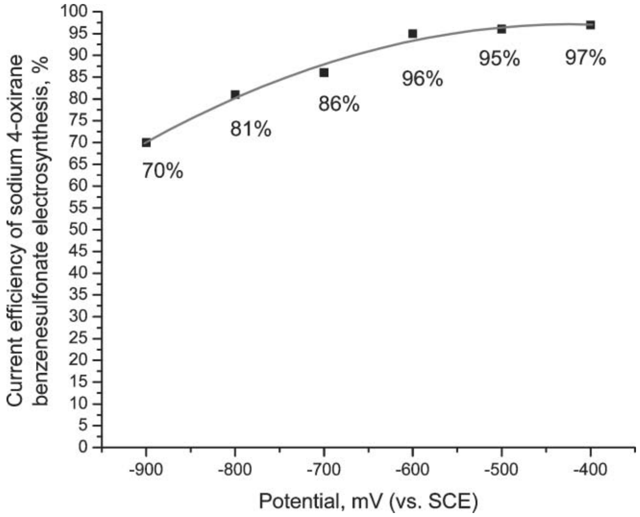

Fig. 4 The effect of applied potential on the current efficiency of sodium 4-oxiranebenzenesulfonate production in 1 M $NaHCO_{3(aq)}$ solution. Catholyte: 1 M $NaHCO_{3(aq)}$. Anolyte: 2 M $H_2SO_{4(aq)}$. Substrate: sodium 4-styrenesulfonate. $MnSO_4$: 0.06 mol% of the substrate.

When pure O_2 was replaced by air (O_2 content: 21%), the current efficiency for epoxide production was found to decrease. This is because of the exceedingly long time required for epoxidation due to the lower concentration of H_2O_2, which would cause hydrolysis of epoxides in the reaction medium.

During electrolysis, hydroxide ion is formed as a by-product in H_2O_2 generation (eqn (3)). The rise in pH is, of course, not favorable for the subsequent epoxidation, as the optimal pH value for the Mn^{2+}/HCO_3^- catalytic system is around 8.[12] This can be partly attributed to the deprotonation of HCO_3^- (pK_a = 10.3) to CO_3^{2-} in strongly alkaline medium, which would reduce the amount of HCO_4^- present in the catalytic mixture (Scheme 1). When concentrated $H_2SO_{4(aq)}$ (>2 M) is used as the anolyte, the acid provides a proton source, which can transport through the cation selective nafion membrane, to neutralize the excess hydroxide ions generated in the cathode compartment. Thus, an excessive increase in pH in the catholyte can be avoided. However, we cannot use 2 M $H_2SO_{4(aq)}$ directly as electrolyte in the cathode compartment because HCO_3^- is unstable in acidic medium and the low pH would promote acid-catalyzed hydrolysis of epoxides.

The effect of Mn^{2+} concentration on epoxide yield and current efficiency of epoxide production is shown in Fig. 5. The best yield of epoxide was obtained when the Mn^{2+} concentration is higher than 0.03 mM (0.06 mol%). The epoxide yield is lower when the concentration of $MnSO_4$ is below 0.002 mM. Presumably, at this catalyst level, the H_2O_2 generated at the cathode was not consumed fast enough by the epoxidation reaction. As a result, some of the H_2O_2 could have been wasted through catalytic decomposition by Mn^{2+}.

The optimal applied potential and $MnSO_{4(aq)}$ concentration used for the electrosynthesis of epoxides were chosen to be −600 mV and 0.03 mM (0.06 mol%) respectively. Under these conditions, H_2O_2 was electrogenerated effectively and the subsequent epoxidation also occurred at a reasonable rate. Table 2 (entries 1–5) summarizes the water-soluble alkenes that were tested for epoxidation in this study. The water-soluble styrenes (entries 1 and 2) were converted to the corresponding epoxides at high yields and current efficiencies. For the other water-soluble alkenes (entries 3–5), the yields are comparatively lower, which is in accordance with the lower reactivity of the carbon–carbon double bond in these alkenes.

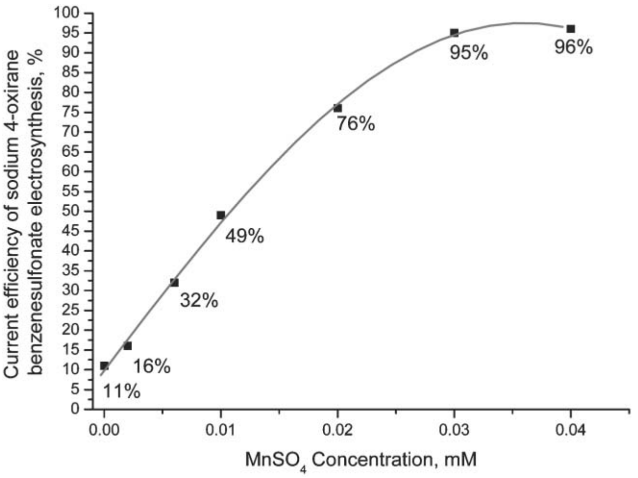

Fig. 5 The effect of $MnSO_{4(aq)}$ concentration on the current efficiency of sodium 4-oxiranebenzenesulfonate production in 1 M $NaHCO_{3(aq)}$. Catholyte: 1 M $NaHCO_{3(aq)}$. Anolyte: 2 M $H_2SO_{4(aq)}$. Substrate: sodium 4-styrenesulfonate. Potential: −600 mV (*vs.* SCE).

As mentioned above, the optimal potential for H_2O_2 electrogeneration in the *tert*-butanol–$NaHCO_3$–NaCl mixture has been shown to be about −700 mV *vs.* SCE (Fig. 3). However, only moderate current efficiency was obtained when this potential was applied for the epoxidation of lipophilic alkenes. This could be caused by the relatively slow rate of epoxidation (H_2O_2 consumption) as compared to the H_2O_2 generation rate due to the lower concentration of bicarbonate in *tert*-butanol. Raising the potential to −400 mV greatly improved the current yield for the lipophilic alkenes. At this potential, the H_2O_2 generation is slow enough to keep pace with the subsequent epoxidation reaction and its loss due to Mn^{2+}-catalyzed decomposition is minimized.

The lipophilic alkenes epoxidized by this system, summarized in Table 2 (entries 6–12), illustrate that the epoxidation of styryl alkenes proceeded efficiently with reasonable yields of 45–78%. The oxidation of cyclooctene (entry 11) gives only a fair yield (42%) probably because of angle strain in the cyclic alkene. α-Pinene oxide (entry 12) is less reactive in this catalytic system due to its sterically hindered carbon–carbon double bond.

Conclusions

Using dioxygen as the oxygen source, the electrogeneration of H_2O_2 for *in situ* epoxidation using the Mn^{2+}/HCO_3^- catalytic system has been achieved. *tert*-Butanol assists both the solubility of O_2 and the lipophilic alkenes in the reaction mixture. In this electrocatalytic system, H_2O_2 was generated continuously at relatively low concentration and hence the problem of wastage through Mn^{2+} decomposition was minimized. This appears to be a distinct advantage of the electrochemical method.

Table 2 Manganese-mediated epoxidation of alkenes in bicarbonate solutions with electrogenerated H_2O_2

Entry	Substrate	Electrolysis time/min	Epoxide yield[a] (%)	Current efficiency (%)
1[b]	Sodium 4-styrenesulfonate 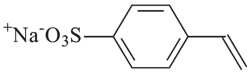	45	97	95
2[b]	Sodium 4-vinylbenzoate 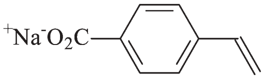	50	96	81
3[b]	Methylvinylketone 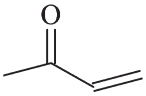	80	44	32
4[b]	Ethylacrylate 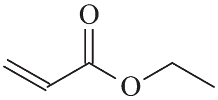	90	51	17
5[b]	Ethyl *trans*-crotonate 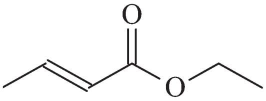	90	58	21
6[c]	Cinnamyl acetate 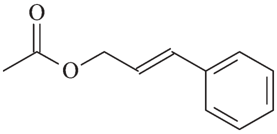	90	78	23
7[c]	1,2-Dihydronaphthalene 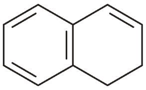	90	73	43
8[c]	α-Methylstyrene 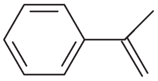	90	45	32
9[c,d]	β-Methylstyrene 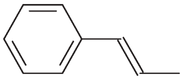	80	60	29
10[c]	Styrene 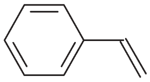	70	50	40
11[c]	Cyclooctene 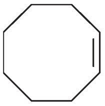	80	42	29
12[c]	α-Pinene 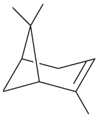	90	23	8

[a] Epoxide yields were calculated on the basis of converted alkenes and determined by GC-MS *versus* an internal standard. [b] Catholyte: 1 M $NaHCO_{3(aq)}$. Anolyte: 2 M $H_2SO_{4(aq)}$. Substrate: 2.5 mmol. $MnSO_4$: 0.06 mol% of substrate. Potential: −600 mV (*vs.* SCE). [c] Catholyte: *tert*-butanol–water (2 : 3 v/v) + 0.24 M $NaHCO_3$ + 0.1 M NaCl. Anolyte: *tert*-butanol–water (2 : 3 v/v) + 2 M H_2SO_4. Substrate: 2.5 mmol. $MnSO_4$: 0.06 mol% of substrate. Applied potential: −400 mV vs. SCE. [d] Only *trans*-epoxide was detected.

One limitation of coupling the Mn^{2+}/HCO_3^- epoxidation system with *in situ* electrogeneration of H_2O_2 is that the catalytic system works best at pH ∼8, and the H_2O_2 electrogenerated at this pH is in its neutral form (pK_a for $H_2O_2 = 11.6$ at 25 °C). A certain amount of H_2O_2 is wasted by diffusion across the nafion membrane to the anode compartment. One way to improve this is to couple the electrogeneration of H_2O_2 with an efficient epoxidation system which works at pH > 12. Under such circumstances, the electrogenerated hydrogen peroxide is in the form of HO_2^-, and the loss through diffusion across the nafion membrane can be minimized. Work in this direction is under progress in our laboratory.

Acknowledgements

We acknowledge support by the Hong Kong Polytechnic University and the Research Grants Council (PolyU 5014/03P).

References

1 F. E. Bailey, *Alkylene oxides and their polymers*, Dekker, New York, 1991.
2 R. V. Young and S. Sessine, *World of chemistry*, Gale Group, Detroit, 2000.
3 I. Arends and R. A. Sheldon, *Top. Catal.*, 2002, **19**, 133–141.
4 *The Dictionary of substances and their effects*, ed. S. Gangolli, Royal Society of Chemistry, Cambridge, 2005.
5 G. Strukul, *Catalytic oxidations with hydrogen peroxide as oxidant*, Kluwer Academic Publishers, London, 1992.
6 H. Nishihara, K. Pressprich, R. W. Murray and J. P. Collman, *Inorg. Chem.*, 1990, **29**, 1000–1006.
7 Y. Shen, M. Atobe, W. Li and T. Nonaka, *Electrochim. Acta*, 2003, **48**, 1041–1046.
8 A. Zimmer, D. Monter and W. Reschetilowski, *J. Appl. Electrochem.*, 2003, **33**, 933–937.
9 C. Y. Tang, K. Y. Wong and T. H. Chan, *Chem. Commun.*, 2005, **10**, 1345–1347.
10 T. H. Chan and C. J. Li, *Organic reactions in aqueous media*, Wiley, New York, 1997.
11 H. R. Yao and D. E. Richardson, *J. Am. Chem. Soc.*, 2000, **122**, 3220–3221.
12 B. S. Lane, M. Vogt, V. J. DeRose and K. Burgess, *J. Am. Chem. Soc.*, 2002, **124**, 11946–11954.
13 B. S. Lane and K. Burgess, *J. Am. Chem. Soc.*, 2001, **123**, 2933–2934.
14 D. T. Sawyer and E. T. Seo, *Inorg. Chem.*, 1977, **16**, 499–501.
15 E. Yeager, *Electrochim. Acta*, 1984, **29**, 1527–1537.
16 R. J. Taylor and A. A. Humffray, *J. Electroanal. Chem. Interfacial Electrochem.*, 1975, **64**, 63–84.
17 R. J. Taylor and A. A. Humffray, *J. Electroanal. Chem. Interfacial Electrochem.*, 1975, **64**, 85–94.
18 J. Pardo, A. M. Mainar, M. C. Lopez, F. Royo and J. S. Urieta, *Fluid Phase Equilib.*, 1999, **155**, 127–137.
19 I. Kutsche, G. Gildehaus, D. Schuller and A. Schumpe, *J. Chem. Eng. Data*, 1984, **29**, 286–287.

Comparative analysis of solvation and selectivity in room temperature ionic liquids using the Abraham linear free energy relationship

Michael H. Abraham[a] **and William E. Acree, Jr.***[b]

Received 4th May 2006, Accepted 10th July 2006
First published as an Advance Article on the web 28th July 2006
DOI: 10.1039/b606279b

Gas to RTIL (room temperature ionic liquid) partition coefficients have been compiled for a series of solutes for a number of RTILs. These partition coefficints can be converted into water to RTIL partition coefficients using corresponding gas to water partition coefficients. The gas to RTIL and water to RTIL partition coefficients have been correlated through the Abraham solvation equations to yield equations that can be used for the prediction of further partition coefficients. The coefficients in the Abraham solvation equations yield quantitative information on solute–solvent (RTIL) interactions. It is shown that the RTILs have solvation properties quite close to those for polar aprotic organic solvents. The equations for gas to RTIL and gas to solvent partition coefficients can be used to predict the selectivity of RTILs and organic solvents towards pairs of solutes. It is shown that the selectivity of RTILs is not extraordinary, but is about the same as the selectivity of polar aprotic solvents.

Introduction

Room temperature ionic liquids (RTILs) are ionic organic compounds that are liquid at ambient room temperature. These ionic salts have relatively low vapor pressures at room temperature, and can be either water-miscible or water-immiscible depending on the cation/anion combination. Synthetic procedures are known for preparing more than 200 RTILs.[1] The thermodynamic and solubilizing properties of RTILs depend on the polarity and dispersive forces, and the hydrogen-bonding and ionic character of both the large cation (alklylimidazolum, alkylpyridinium, alkylphosphonium, quaternary ammonium) and the ionic anion bearing the negative charge (PF_6^-, BF_4^-, $(Tf)_2N^-$). RTILs are rapidly emerging as alternative green solvents, namely as reaction media for synthesis, catalysis and biocatalysis,[2–6] and as extractive solvents for removal of sulfur compounds from petroleum crude oils,[7] organic contaminants from soils,[8] and pharmaceutical drug molecules from reaction media.[9,10] Several excellent reviews have recently been published[11–15] discussing the applications of RTIL solvents in regards to analytical chemistry.

Experimental studies have reported infinite dilution activity coefficients, gas-to-liquid partition coefficients and solubilities of dissolved organic solutes and gases in RTILs; however, no real attempt has been made to systematically compare the solubilizing properties of the different RTILs, except for a few chromatographic studies. Abraham *et al.*[16] and Poole and Poole[17] used the Abraham solvation parameter model to characterize a large number of ionic liquids at 121 °C, using log *K* values obtained by GLC, and reviews that include and update this work are available.[1,18] More recently, Abraham and coworkers characterized "wet" practical water-to-ionic liquid,[19] two dry "hypothetical" water-to-ionic liquid[20] and two gas-to-ionic liquid partition systems[20] at 25 °C. Armstrong and coworkers[21–23] examined the solvation properties of a large number of ionic liquid gas-liquid chromatographic stationary phases using the Abraham model. Those authors[23] have further shown that the free energy of transfer of solute is similar for lightly cross-linked and neat monomeric ionic liquid gas chromatographic stationary phases. The equation process coefficients were nearly identical for the lightly cross-linked and neat monomeric ionic liquids. The Abraham model has also been used to describe solute partitioning between a room-temperature ionic liquid and supercritical carbon dioxide.[24]

The general solvation parameter model of Abraham[25–32] is one of the most useful approaches for the analysis and prediction of free energies of partition in chemical and biochemical systems. The method relies on two linear free energy relationships, one for processes within condensed phases

$$SP = c + eE + sS + aA + bB + vV \quad (1)$$

and one for processes involving gas to condensed phase transfer

$$SP = c + eE + sS + aA + bB + lL \quad (2)$$

The dependent variable, SP, is some property of a series of solutes in a fixed phase. The independent variables, or descriptors, are solute properties as follows: *E* and *S* refer to the excess molar refraction and dipolarity/polarity descriptors of the solute, respectively, *A* and *B* are measures of the solute hydrogen-bond acidity and hydrogen-bond basicity, *V* is the McGowan volume of the solute and *L* is the solute gas phase dimensionless Ostwald partition coefficient into hexadecane at 298 K. The first four descriptors can be regarded as measures of the tendency of the given solute to undergo various solute–solvent interactions. The latter two descriptors, *V* and *L*, are both measures of solute size, and so will be measures of the

---

[a] *Department of Chemistry, University College London, 20 Gordon Street, London, WC1H 0AJ, UK*
[b] *Department of Chemistry, P. O. Box 305070, University of North Texas, Denton, TX, 76203-5070, USA. E-mail: acree@unt.edu*

solvent cavity term that will accommodate the dissolved solute. General dispersion interactions are also related to solute size, hence, both V and L will also describe the general solute–solvent interactions. The regression coefficients and constants (c, e, s, a, b, v and l) are obtained by regression analysis of experimental data for a specific process (*i.e.*, a given partitioning process, a given stationary phase and mobile phase combination, *etc.*).

The usefulness of eqn (1) and eqn (2) in the characterization of solvent phases is that the coefficients e, s, a, b, l and v are not just fitting constants, but reflect particular solute–solvent interactions that correspond to chemical properties of the solvent phase. The excess molar refraction, E, is derived from the solute refractive index, and hence the e coefficient gives a measure of general solute–solvent dispersion interactions. The V and L descriptors were set up as measures of the endoergic effect of disrupting solvent–solvent bonds. However, solute volume is always well correlated with polarizability and so the v and l coefficients will include not only an endoergic cavity effect but also exoergic solute–solvent effects that arise through solute polarizability. The S descriptor is a measure of dipolarity and polarizability and hence the s coefficient will reflect the ability of a solvent to undergo dipole– and dipole-induced dipole interactions with a solute. The A descriptor is a measure of solute hydrogen bond acidity, and hence the a coefficient will reflect the complementary solvent hydrogen bond basicity. Similarly the b coefficient will be a measure of the solvent hydrogen bond acidity. All this is straightforward for gas to solvent partitions, because there are no interactions to consider in the gas phase. For partitions between solvents, the coefficients in eqn (2) then refer to differences between the properties of the two phases.

In the present communication we extend our earlier studies[19,20] on RTILs to include: 1-methyl-3-butylimidazolium *bis*(trifluoromethylsulfonyl)imide ($[\mathrm{MBIm}]^+[\mathrm{Tf_2N}]^-$), 1-methyl-3-hexylimidazolium *bis*(trifluoromethylsulfonyl)imide ($[\mathrm{MHIm}]^+[\mathrm{Tf_2N}]^-$), trimethylbutylammonium *bis*(trifluoromethylsulfonyl)imide ($[\mathrm{M_3BAm}]^+[\mathrm{Tf_2N}]^-$), 4-methyl-*N*-butylpyridinium tetrafluoroborate ($[\mathrm{MBPy}]^+[\mathrm{BF_4}]^-$), 1-methyl-3-octylimidazolum tetrafluoroborate ($[\mathrm{MOIm}]^+[\mathrm{BF_4}]^-$) and 1-methyl-3-butylimidazolium hexafluorophosphate ($[\mathrm{MBIm}]^+[\mathrm{PF_6}]^-$). Correlations have been derived for the six fore-mentioned RTILs based on published infinite dilution activity coefficient and solubility data for dissolved organic and gaseous solutes.[33–46] In addition, we have compared the LFERs for the ionic liquids to existing LFERs for many of the common organic solvent–water and organic solvent–air systems to determine which particular organic solvent systems are close to RTILs in terms of their solubilizing ability, and to determine whether RTIL systems offer enhanced selectivity in the partition of particular types of solutes.

Experimental

Most of the experimental data that we were able to retrieve from the published literature pertained to the infinite dilution activity coefficient, γ_2^∞, for solutes dissolved in RTILs. In order to correctly apply the Abraham model the infinite dilution activity coefficient needs to be converted to a parameter that does not include solute–solute interactions. This can be done by converting to log K values for gas to ionic liquid partition through eqn (3) or to log P values for partition from water to the ionic liquid through eqn (4), where K_w is the gas to water partition coefficient.[47]

$$\log K = \log \frac{RT}{\gamma_2^\infty P_2^\circ V_\mathrm{solvent}} \tag{3}$$

$$\log P = \log K - \log K_\mathrm{w} \tag{4}$$

Here R is the universal gas constant, T is the system temperature, P_2° is the vapor pressure of the solute at T, and V_solvent is the molar volume of the solvent. The calculation of log P requires knowledge of the solute's gas phase partition coefficient into water, K_w.

Tables 1–3 list the respective log K and log P values for the various organic and gaseous solutes dissolved in ($[\mathrm{MBIm}]^+[\mathrm{Tf_2N}]^-$), ($[\mathrm{MHIm}]^+[\mathrm{Tf_2N}]^-$), ($[\mathrm{M_3BAm}]^+[\mathrm{Tf_2N}]^-$), ($[\mathrm{MOIm}]^+[\mathrm{BF_4}]^-$), ($[\mathrm{MBIm}]^+[\mathrm{PF_6}]^-$) and ($[\mathrm{MBPy}]^+[\mathrm{BF_4}]^-$).

Molecular descriptors for all of the compounds considered in the present study are tabulated in Table 4. The tabulated values of a few compounds may differ slightly from values in earlier publications. The numerical values are periodically updated as additional experimental data becomes available. The numerical values in Table 4 came, for the most part, from our solute descriptor database, which now contains values for more than 3500 different organic and organometallic compounds. The descriptor values were calculated in accordance with our published computational methodology.[48–53] The characteristic McGowan volume, V, is calculated from the individual atomic sizes and numbers of bonds in the molecule.[48] For liquid solutes, the excess molar refraction descriptor, E, is obtained from the liquid refractive index.[49] In the case of solid solutes, one either estimates a hypothetical liquid refractive index using any of several available methods, or one can calculate E directly through addition of fragments or substructures. Numerical values of the three remaining descriptors, S, A and B, are determined through regression analysis using available organic solvent/water partition coefficients, chromatographic retention data, solubilities and infinite dilution activity coefficients as described elsewhere.[50–53] If one is unable to find sufficient experimental data for performing the fore-mentioned regression analysis, commercial software[54] is available for estimating the molecular solute descriptors from the structure of the compound.

Results

We have assembled in Table 1 values of log P and log K for 61 solutes dissolved in 1-methyl-3-butylimidazolium *bis*(trifluoromethylsulfonyl)imide, covering a reasonably wide range of compound type and descriptor values. Analysis of the experimental data yielded for partition from water to ($[\mathrm{MBIm}]^+[\mathrm{Tf_2N}]^-$) and from the gas phase to ($[\mathrm{MBIm}]^+[\mathrm{Tf_2N}]^-$) eqn (5) and eqn (6):

$$\begin{aligned}\mathrm{Log}\ P &= 0.041(0.042) + 0.088(0.098)E + 0.381(0.128)S - \\ &\quad 1.146(0.159)A - 4.421(0.165)B + 3.336(0.037)V \\ &\quad (N = 61,\ \mathrm{SD} = 0.095,\ R^2 = 0.997 \text{ and } F = 3935.6)\end{aligned} \tag{5}$$

Table 1 Log *P* and log *K* partitioning data for solutes in ($[MBIm]^+[Tf_2N]^-$) and ($[MHIm]^+[Tf_2N]^-$) ionic liquids

		($[MBIm]^+[Tf_2N]^-$)		($[MHIm]^+[Tf_2N]^-$)	
Solute	Log K_w	Log *P*	Log *K*	Log *P*	Log *K*
Oxygen	−1.51	2.819	−1.309		
Carbon dioxide	−0.082	0.492	0.410	0.962	0.880
Nitrous oxide	−0.23	0.633	0.403		
Ethane	−1.34	1.282	−0.058		
Propane	−1.44	1.732	0.292		
Butane	−1.52	2.211	0.691		
Pentane	−1.70	2.790	1.090	2.932	1.232
Hexane	−1.82	3.255	1.435	3.480	1.660
Heptane	−1.96	3.745	1.785	4.001	2.041
Octane	−2.11	4.238	2.128	4.525	2.415
Nonane	−2.15	4.620	2.470	4.901	2.751
Decane	−2.26	5.122	2.862	5.381	3.121
Undecane	−2.38	5.598	3.218	5.879	3.499
Dodecane	−2.53	6.103	3.573	6.404	3.874
Cyclopentane	−0.88	2.397	1.517	2.558	1.678
Cyclohexane	−0.90	2.745	1.845	2.902	2.002
Cycloheptane	−0.58			3.163	2.583
Cyclopentene	−0.41	2.088	1.678		
Cyclohexene	−0.27	2.400	2.130	2.530	2.260
1,3-Cyclohexadiene			2.398		2.489
Ethene	−0.94	0.882	0.084		
Propene	−0.97	1.551	0.581		
1-Butene	−1.01	1.935	0.925		
1-Pentene	−1.23	2.530	1.300	2.662	1.432
1-Hexene	−1.16	2.812	1.652	2.986	1.826
1-Heptene	−1.22	3.216	1.996	3.411	2.191
1-Octene	−1.41	3.747	2.337	3.969	2.559
1-Nonene	−1.51	4.190	2.680	4.397	2.887
1-Dodecene	−1.92	5.559	3.639	5.784	3.864
1-Hexyne	−0.21			2.558	2.348
1-Heptyne	−0.44			3.296	2.856
1-Octyne	−0.52			3.656	3.136
Benzene	0.63	2.253	2.883	2.256	2.886
Toluene	0.65	2.553	3.203	2.650	3.300
Ethylbenzene	0.58	2.894	3.474	2.989	3.569
m-Xylene	0.61			3.078	3.688
p-Xylene	0.59			3.073	3.663
Propylbenzene	0.39	3.364	3.754	3.482	3.872
Butylbenzene	0.29	3.809	4.099	3.952	4.242
Pentylbenzene	0.17	4.296	4.466	4.538	4.708
Methanol	3.74	−1.151	2.589	−1.262	2.478
Ethanol	3.67	−0.914	2.756	−1.011	2.659
1-Propanol	3.56	−0.508	3.052	−0.544	3.016
1-Butanol	3.46	0.047	3.507	0.038	3.498
1-Pentanol	3.35	0.560	3.910	0.491	3.841
1-Hexanol	3.23	1.076	4.306	1.038	4.268
1-Heptanol	3.09	1.674	4.764		
2-Propanol	3.48	−0.649	2.831	−0.683	2.797
2-Methyl-1-propanol	3.30	0.024	3.324	0.019	3.319
tert-Butanol	3.28	−0.378	2.902	−0.404	2.876
2-Butanol	3.39	−0.240	3.150	−0.254	3.136
2-Methyl-2-butanol	3.25	0.036	3.286	0.053	3.303
Cyclohexanol	4.01	0.452	4.462	0.326	4.336
Propanal	2.52	0.082	2.602	0.070	2.590
Butanal	2.33	0.592	2.922	0.612	2.942
Pentanal	2.22	0.881	3.101	0.934	3.154
Hexanal	2.06	1.591	3.651	1.656	3.716
Heptanal	1.96	2.068	4.028	2.116	4.076
Octanal	1.68	2.670	4.350	2.772	4.452
Acetonitrile	2.85	0.314	3.164	0.274	3.124
Acetone	2.79	0.083	2.873	0.058	2.848
2-Pentanone	2.58			0.925	3.505
Methyl propanoate	2.15	0.819	2.969	0.848	2.998
Methyl butanoate	2.08	1.192	3.271	1.233	3.313
Methyl pentanoate	1.88	1.718	3.598	1.809	3.689
Methyl hexanoate	1.83	2.035	3.865	2.104	3.934
Diisopropyl ether	0.39			1.757	2.147
Ethyl *tert*-butyl ether					2.235

Table 1 Log *P* and log *K* partitioning data for solutes in ($[MBIm]^+[Tf_2N]^-$) and ($[MHIm]^+[Tf_2N]^-$) ionic liquids (*Continued*)

		($[MBIm]^+[Tf_2N]^-$)		($[MHIm]^+[Tf_2N]^-$)	
Solute	Log K_w	Log *P*	Log *K*	Log *P*	Log *K*
Methyl *tert*-amyl ether	1.10			1.529	2.629
Tetrahydrofuran	2.55			0.316	2.866
1,4-Dioxane	3.71	−0.204	3.506		
Trichloromethane	0.79			1.853	2.643
Carbon tetrachloride	−0.06			2.534	2.474

Table 2 Log *P* and log *K* partitioning data for solutes in ($[M_3BAm]^+[Tf_2N]^-$) and ($[MOIm]^+[BF_4]^-$) ionic liquids

		($[M_3BAm]^+[Tf_2N]^-$)		($[MOIm]^+[BF_4]^-$)	
Solute	Log K_w	Log *P*	Log *K*	Log *P*	Log *K*
Pentane	−1.70	2.663	0.963	2.895	1.195
Hexane	−1.82	3.150	1.330	3.407	1.587
Heptane	−1.96	3.617	1.657	3.961	2.001
Octane	−2.11	4.101	1.991	4.483	2.373
Nonane	−2.15	4.472	2.322	4.920	2.770
Decane	−2.26	4.916	2.656	5.429	3.169
Undecane	−2.38	5.380	3.000	5.838	3.458
Dodecane	−2.53	5.818	3.288	6.374	3.844
Cyclohexane	−0.90	2.959	2.059	2.866	1.966
Cyclohexene	−0.27	2.245	1.975	2.498	2.228
1,3-Cyclohexadiene			2.247		2.477
1-Pentene	−1.23	2.445	1.215	2.582	1.352
1-Hexene	−1.16	2.678	1.518	2.907	1.747
1-Heptene	−1.22	3.056	1.836	3.342	2.122
1-Octene	−1.41	3.582	2.172	3.914	2.504
1-Nonene	−1.51	4.011	2.501	4.423	2.913
1-Dodecene	−1.92	5.335	3.415	5.970	4.050
Benzene	0.63	2.066	2.696	2.180	2.810
Toluene	0.65	2.454	3.104	2.570	3.220
Ethylbenzene	0.58	2.769	3.349	2.941	3.521
Propylbenzene	0.39	3.242	3.632	2.978	3.368
Butylbenzene	0.29	3.671	3.961	3.528	3.818
Pentylbenzene	0.17	4.107	4.277	4.349	4.519
Methanol	3.74	−1.254	2.486	−1.008	2.732
Ethanol	3.67	−0.994	2.676	−0.824	2.846
1-Propanol	3.56	−0.538	3.022	−0.360	3.200
1-Butanol	3.46	−0.062	3.398	0.211	3.671
1-Pentanol	3.35	0.338	3.688	0.740	4.090
1-Hexanol	3.23	0.832	4.062	1.325	4.555
1-Heptanol	3.09				
2-Propanol	3.48	−0.732	2.748	−0.453	3.027
2-Methyl-1-propanol	3.30	−0.137	3.163	0.289	3.589
tert-Butanol	3.28	−0.467	2.813	−0.203	3.077
2-Butanol	3.39	−0.338	3.052	−0.008	3.382
2-Methyl-2-butanol	3.25	−0.084	3.166	0.192	3.442
Cyclohexanol	4.01	0.094	4.104	0.730	4.740
Propanal	2.52	0.016	2.536	−0.090	2.430
Butanal	2.33	0.521	2.851	0.430	2.760
Pentanal	2.22	0.789	3.009	0.766	2.986
Hexanal	2.06	1.468	3.528	1.462	3.522
Heptanal	1.96	1.831	3.791	1.979	3.939
Octanal	1.68	2.473	4.153	2.492	4.172
Acetonitrile	2.85	0.285	3.135	0.261	3.111
Acetone	2.79	0.033	2.823	−0.182	2.608
Methyl propanoate	2.15	0.746	2.896	0.626	2.776
Methyl butanoate	2.08	1.092	3.172	1.020	3.100
Methyl pentanoate	1.88	1.622	3.502	1.591	3.471
Methyl hexanoate	1.83	1.878	3.708	1.945	3.775
1,4-Dioxane	3.71	−0.351	3.359	−0.364	3.346
Trichloromethane	0.79	1.718	2.508		

Table 3 Log *P* and log *K* partitioning data for solutes in ($[MBIm]^+[PF_6]^-$) and ($[MBPy]^+[BF_4]^-$) ionic liquids

		($[MBIm]^+[PF_6]^-$)		($[MBPy]^+[BF_4]^-$)	
Solute	Log K_w	Log *P*	Log *K*	Log *P*	Log *K*
Hydrogen	−1.72	0.383	−1.337		
Argon	−1.47	0.469	−1.001		
Nitrogen	−1.80	0.719	−1.081		
Oxygen	−1.51	0.476	−1.034		
Carbon monoxide	−1.62	0.526	−1.094		
Carbon dioxide	−0.082	0.366	0.284		
Methane	−1.46	0.596	−0.864		
Ethane	−1.34	0.960	−0.380		
Hexane	−1.82			2.802	0.982
Heptane	−1.96	3.351	1.391	3.299	1.339
Octane	−2.11	3.744	1.634	3.776	1.666
Nonane	−2.15	4.156	2.006	4.140	1.990
Decane	−2.26			4.558	2.298
Cyclohexane	−0.90	2.362	1.462	2.375	1.475
2,2,4-Trimethylpentane	−2.12			3.362	1.242
Cyclohexene	−0.27			2.166	1.896
Styrene	0.95			2.961	3.911
Benzene	0.63	2.057	2.687	2.149	2.779
Toluene	0.65	2.322	2.972	2.448	3.098
Ethylbenzene	0.58	2.691	3.271	2.725	3.305
o-Xylene	0.66	2.897	3.507	2.923	3.583
p-Xylene	0.59	2.752	3.342	2.829	3.419
m-Xylene	0.61	2.659	3.319	2.786	3.396
Isopropylbenzene	0.22			3.183	3.403
tert-Butylbenzene	0.32			3.261	3.581
1-Hexene	−1.16	2.429	1.269		
1-Hexyne	−0.21	2.111	1.901		
1-Heptyne	−0.44	2.929	2.489		
Methanol	3.74	−1.237	2.503	−0.952	2.788
Ethanol	3.67	−1.043	2.627	−0.771	2.899
1-Propanol	3.56	−0.698	2.862	−0.363	3.197
1-Butanol	3.46	−0.239	3.221	0.063	3.523
1-Pentanol	3.35			0.476	3.826
1-Hexanol	3.23			0.972	4.202
2-Propanol	3.48	−0.826	2.654	−0.600	2.880
2-Methyl-1-propanol	3.30	−0.210	3.090		
tert-Butanol	3.28			−0.422	2.858
2-Butanol	3.39			−0.233	3.157
2-Methyl-2-butanol	3.25			−0.083	3.167
Cyclohexanol	4.01			0.539	4.549
Acetonitrile	2.85	0.409	3.259	0.389	3.239
Acetone	2.79			−0.140	2.650
2-Butanone	2.72	0.253	2.973		
2-Pentanone	2.58	0.744	3.324		
Ethyl acetate	2.16			0.408	2.568
Dichloromethane	0.96	1.465	2.425	1.499	2.459
Trichloromethane	0.79	1.757	2.547	2.049	2.839
Tetrachloromethane	−0.06	2.132	2.072	2.408	2.348
1-Methylcyclohexene	−0.48			2.659	2.179
α-Methylstyrene	0.96			3.251	4.211
Diethyl ether	1.17	0.221	1.391		
Methyl *tert*-butyl ether	1.62			0.067	1.687
Methyl *tert*-amyl ether	1.10			0.902	2.002
1-Nitropropane	2.45	1.447	3.897		
Triethylamine	2.36	−0.653	1.707		
Pyridine	3.44	0.239	3.679		
Thiophene	1.04	1.848	2.888		

$$\log K = -0.407(0.024) + 0.040(0.068)E + 2.158(0.089)S + 2.478(0.111)A + 0.665(0.116)B + 0.697(0.007)L \quad (6)$$
$$(N = 59,\ \mathrm{SD} = 0.068,\ R^2 = 0.997 \text{ and } F = 3772.3)$$

where *N* is the number of data points, that is the number of solutes, R^2 denotes the coefficient of determination, SD is the standard deviation and *F* corresponds to the Fischer *F* statistic. The errors on the coefficients are shown in parentheses. Also in Table 1 are values of log *P* and log *K* for 62 solutes in 1-methyl-3-hexylimidazolium *bis*(trifluoromethylsulfonyl)imide, ($[MHIm]^+[Tf_2N]^-$). The regression equations for partition from water and from the gas phase into ($[MHIm]^+[Tf_2N]^-$) are,

$$\mathrm{Log}\ P = 0.219(0.085) - 0.015(0.128)E + 0.067(0.147)S - 1.742(0.188)A - 4.241(0.165)B + 3.394(0.067)V \quad (7)$$
$$(N = 60,\ \mathrm{SD} = 0.136,\ R^2 = 0.995 \text{ and } F = 2153.1)$$

$$\log K = -0.170(0.047) - 0.116(0.082)E + 2.079(0.085)S + 2.141(0.112)A + 0.429(0.096)B + 0.704(0.121)L \quad (8)$$
$$(N = 62,\ \mathrm{SD} = 0.090,\ R^2 = 0.989 \text{ and } F = 991.2)$$

Table 2 contains data on trimethylbutylammonium *bis*(trifluoromethyl sulfonyl) imide ($[M_3BAm]^+[Tf_2N]^-$) and regression equations for partition from water and from the gas phase are:

$$\mathrm{Log}\ P = 0.209(0.067) + 0.046(0.099)E + 0.224(0.122)S - 1.509(0.151)A - 4.331(0.145)B + 3.092(0.050)V \quad (9)$$
$$(N = 48,\ \mathrm{SD} = 0.089,\ R^2 = 0.998 \text{ and } F = 4211.1)$$

$$\log K = -0.288(0.055) + 0.115(0.094)E + 2.047(0.108)S + 2.152(0.144)A + 0.723(0.141)B + 0.627(0.014)L \quad (10)$$
$$(N = 51,\ \mathrm{SD} = 0.089,\ R^2 = 0.990 \text{ and } F = 865.1)$$

In Table 2 also are data on 1-methyl-3-octylimidazolum tetrafluoroborate $[MOIm]^+$ $[BF_4]^-$), and the corresponding regression equations are:

$$\mathrm{Log}\ P = 0.174(0.099) - 0.132(0.149)E + 0.123(0.197)S - 0.300(0.242)A - 4.731(0.246)B + 3.419(0.074)V \quad (11)$$
$$(N = 47,\ \mathrm{SD} = 0.131,\ R^2 = 0.996 \text{ and } F = 2112.7)$$

$$\log K = -0.268(0.066) - 0.100(0.113)E + 1.800(0.149)S + 3.224(0.186)A + 0.453(0.193)B + 0.722(0.016)L \quad (12)$$
$$(N = 48,\ \mathrm{SD} = 0.104,\ R^2 = 0.986 \text{ and } F = 571.3)$$

In Table 3 are given values of values of log *P* and log *K* for partition into 4-methyl-*N*-butylpyridinium tetrafluoroborate ($[MBPy]^+[BF_4]^-$) and 1-methyl-3-butylimidazolium hexafluorophosphate ($[MBIm]^+[PF_6]^-$). The regression equations for ($[MBPy]^+[BF_4]^-$) are,

$$\mathrm{Log}\ P = -0.032(0.058) + 0.489(0.147)E + 0.466(0.165)S - 0.873(0.210)A - 4.143(0.164)B + 2.944(0.068)V \quad (13)$$
$$(N = 38,\ \mathrm{SD} = 0.141,\ R^2 = 0.992 \text{ and } F = 1005.3)$$

$$\log K = -0.611(0.018) + 0.487(0.067)E + 2.484(0.070)S + 3.190(0.090)A + 0.558(0.071)B + 0.606(0.007)L \quad (14)$$
$$(N = 38,\ \mathrm{SD} = 0.062,\ R^2 = 0.999 \text{ and } F = 6108.9)$$

and for ($[MBIm]^+[PF_6]^-$) are,

$$\mathrm{Log}\ P = -0.084(0.067) + 0.079(0.107)E + 0.792(0.121)S - 0.871(0.218)A - 4.665(0.145)B + 3.053(0.088)V \quad (15)$$
$$(N = 44,\ \mathrm{SD} = 0.162,\ R^2 = 0.987 \text{ and } F = 574.9)$$

$$\log K = -0.602(0.032) - 0.087(0.080)E + 2.841(0.811)S + 2.785(0.145)A + 0.140(0.098)B + 0.631(0.014)L \quad (16)$$
$$(N = 44,\ \mathrm{SD} = 0.110,\ R^2 = 0.996 \text{ and } F = 1704.6)$$

Table 4 Molecular solute descriptors of the organic compounds considered in the present study

Solute	*E*	*S*	*A*	*B*	*V*	*L*
Hydrogen	0.000	0.000	0.000	0.000	0.109	−1.200
Argon	0.000	0.000	0.000	0.000	0.191	−0.688
Nitrogen	0.000	0.000	0.000	0.000	0.222	−0.978
Oxygen	0.000	0.000	0.000	0.000	0.183	−0.723
Carbon monoxide	0.000	0.000	0.000	0.040	0.222	−0.836
Carbon dioxide	0.000	0.280	0.050	0.100	0.281	0.058
Nitrous oxide	0.068	0.350	0.000	0.100	0.281	0.164
Methane	0.000	0.000	0.000	0.000	0.250	−0.323
Ethane	0.000	0.000	0.000	0.000	0.390	0.492
Propane	0.000	0.000	0.000	0.000	0.531	1.050
Butane	0.000	0.000	0.000	0.000	0.672	1.615
Pentane	0.000	0.000	0.000	0.000	0.813	2.162
Hexane	0.000	0.000	0.000	0.000	0.954	2.668
Heptane	0.000	0.000	0.000	0.000	1.095	3.173
Octane	0.000	0.000	0.000	0.000	1.236	3.677
Nonane	0.000	0.000	0.000	0.000	1.377	4.182
Decane	0.000	0.000	0.000	0.000	1.518	4.686
Undecane	0.000	0.000	0.000	0.000	1.659	5.191
Dodecane	0.000	0.000	0.000	0.000	1.799	5.696
Cyclopentane	0.263	0.100	0.000	0.000	0.705	2.477
Cyclohexane	0.305	0.100	0.000	0.000	0.845	2.964
Cycloheptane	0.350	0.100	0.000	0.000	0.986	3.704
2,2,4-Trimethylpentane	0.000	0.000	0.000	0.000	1.236	3.106
Cyclopentene	0.335	0.200	0.000	0.100	0.661	2.402
Cyclohexene	0.395	0.200	0.000	0.100	0.802	3.021
1,3-Cyclohexadiene	0.515	0.300	0.000	0.140	0.759	2.917
Ethene	0.107	0.100	0.000	0.070	0.347	0.289
Propene	0.103	0.080	0.000	0.070	0.488	0.946
1-Butene	0.100	0.080	0.000	0.070	0.629	1.529
1-Pentene	0.093	0.080	0.000	0.070	0.770	2.047
1-Hexene	0.078	0.080	0.000	0.070	0.911	2.572
1-Heptene	0.092	0.080	0.000	0.070	1.052	3.063
1-Octene	0.094	0.080	0.000	0.070	1.193	3.568
1-Nonene	0.090	0.080	0.000	0.070	1.334	4.073
1-Dodecene	0.089	0.080	0.000	0.070	1.757	5.515
1-Hexyne	0.166	0.220	0.100	0.120	0.868	2.510
1-Heptyne	0.160	0.230	0.090	0.100	1.009	3.000
1-Octyne	0.155	0.220	0.090	0.100	1.150	3.521
Styrene	0.849	0.650	0.000	0.160	0.955	3.908
Benzene	0.610	0.520	0.000	0.140	0.716	2.786
Toluene	0.601	0.520	0.000	0.140	0.857	3.325
Ethylbenzene	0.613	0.510	0.000	0.150	0.998	3.788
o-Xylene	0.663	0.560	0.000	0.160	0.998	3.939
p-Xylene	0.613	0.520	0.000	0.160	0.998	3.839
m-Xylene	0.623	0.520	0.000	0.160	0.998	3.839
Propylbenzene	0.604	0.500	0.000	0.150	1.139	4.230
Isopropylbenzene	0.602	0.490	0.000	0.160	1.139	4.084
Butylbenzene	0.600	0.510	0.000	0.150	1.280	4.730
tert-Butylbenzene	0.619	0.490	0.000	0.180	1.280	4.413
Pentylbenzene	0.594	0.510	0.000	0.150	1.421	5.230
Methanol	0.278	0.440	0.430	0.470	0.308	0.970
Ethanol	0.246	0.420	0.370	0.480	0.449	1.485
1-Propanol	0.236	0.420	0.370	0.480	0.590	2.031
1-Butanol	0.224	0.420	0.370	0.480	0.731	2.601
1-Pentanol	0.219	0.420	0.370	0.480	0.872	3.106
1-Hexanol	0.210	0.420	0.370	0.480	1.013	3.610
1-Heptanol	0.211	0.420	0.370	0.480	1.154	4.115
2-Propanol	0.212	0.360	0.330	0.560	0.590	1.764
2-Methyl-1-propanol	0.217	0.390	0.370	0.480	0.731	2.413
tert-Butanol	0.180	0.300	0.310	0.600	0.731	1.963
2-Butanol	0.217	0.360	0.330	0.560	0.731	2.338
2-Methyl-2-butanol	0.194	0.300	0.310	0.600	0.872	2.630
Cyclohexanol	0.460	0.540	0.320	0.570	0.904	3.758
Propanal	0.196	0.650	0.000	0.450	0.547	1.815
Butanal	0.187	0.650	0.000	0.450	0.688	2.270
Pentanal	0.163	0.650	0.000	0.450	0.829	2.770
Hexanal	0.146	0.650	0.000	0.450	0.970	3.370
Heptanal	0.140	0.650	0.000	0.450	1.111	3.860
Octanal	0.160	0.650	0.000	0.450	1.252	4.380
Acetonitrile	0.237	0.900	0.070	0.320	0.404	1.739
Acetone	0.179	0.700	0.040	0.490	0.547	1.696
2-Butanone	0.166	0.700	0.000	0.510	0.688	2.287
2-Pentanone	0.143	0.680	0.000	0.510	0.829	2.755
Methyl propanoate	0.128	0.600	0.000	0.450	0.747	2.431
Methyl butanoate	0.106	0.600	0.000	0.450	0.888	2.943
Methyl pentanoate	0.108	0.600	0.000	0.450	1.028	3.442
Methyl hexanoate	0.080	0.600	0.000	0.450	1.169	3.984
Ethyl acetate	0.106	0.620	0.000	0.450	0.747	2.314
Dichloromethane	0.387	0.570	0.100	0.050	0.494	2.019
Trichloromethane	0.425	0.490	0.150	0.020	0.617	2.480
Tetrachloromethane	0.458	0.380	0.000	0.000	0.739	2.823
1-Methylcyclohexene	0.391	0.180	0.000	0.100	0.943	3.483
α-Methylstyrene	0.851	0.640	0.000	0.190	1.096	4.290
Diethyl ether	0.041	0.250	0.000	0.450	0.731	2.015
Diisopropyl ether	0.000	0.190	0.000	0.410	1.013	2.559
Methyl *tert*-butyl ether	0.024	0.210	0.000	0.590	0.872	2.372
Methyl *tert*-amyl ether	0.050	0.210	0.000	0.600	1.016	2.916
Tetrahydrofuran	0.289	0.520	0.000	0.480	0.622	2.636
1,4-Dioxane	0.329	0.750	0.000	0.640	0.681	2.892
1-Nitropropane	0.242	0.950	0.000	0.310	0.706	2.894
Triethylamine	0.101	0.150	0.000	0.790	1.054	3.040
Pyridine	0.631	0.840	0.000	0.520	0.675	3.022
Thiophene	0.687	0.560	0.000	0.150	0.641	2.943
Difluoromethane	−0.320	0.490	0.060	0.050	0.285	0.040
Trifluoromethane	−0.427	0.183	0.110	0.034	0.303	−0.274
1,1-Difluoroethane	−0.250	0.490	0.040	0.050	0.426	0.517
1,1,1,2-Tetrafluoroethane	−0.640	0.200	0.240	0.000	0.461	0.226

The regression statistics for eqn (5) to eqn (16) are all quite good. While there is insufficient data to construct separate training and test sets to fully assess the predictive capability of the derived correlations, based on our past experience regression equations using the Abraham model we expect that these equations would be able to estimate log *P* and log *K* values of additional compounds to close to the obtained SD values. The SD values of the coefficients show that some of the coefficients, usually *E* or *S*, are not statistically significant. We retain all the coefficients, however, in order better to compare the various equations. We also carried out a correlation analysis on the descriptors for each equation in order to check for cross-correlations. The maximum correlation, in terms of R^2, between the descriptors was with one exception always for *E* and *S* as follows: eqn (5) 0.254, eqn (6) 0.237, eqn (7) 0.231, eqn (8) 0.231, eqn (9) 0.268, eqn (10) 0.262, eqn (11) 0.251, eqn (12) 0.251, eqn (13) 0.518, eqn (14) 0.518, eqn (15) 0.268, and for eqn (16) the maximum correlation of 0.417 was between *E* and *L*.

Discussion

There is nothing very unusual about the regression equations for partition from water or from the gas phase into the RTILs. The statistics are reasonably good, and the fits of calculated values to experimental values are of about the same order of magnitude as those for fits with conventional organic solvents. The equations for partition from the gas phase to the RTILs,

Table 5 A comparison of coefficients in the general eqn (1) for RTILs and organic solvents

Solvent	*c*	*e*	*s*	*a*	*b*	*v*
([MBIm]$^+$[Tf$_2$N]$^-$), eqn (5)	0.041	0.088	0.381	−1.146	−4.421	3.336
([MHIm]$^+$[Tf$_2$N]$^-$), eqn (7)	0.219	−0.015	0.067	−1.742	−4.241	3.394
([M$_3$BAm]$^+$[Tf$_2$N]$^-$), eqn (9)	0.209	0.046	0.224	−1.509	−4.331	3.092
([MOIm]$^+$ [BF$_4$]$^-$), eqn (11)	0.174	−0.132	0.123	−0.300	−4.731	3.419
([MBPy]$^+$[BF$_4$]$^-$), eqn (13)	−0.032	0.489	0.466	−0.873	−4.143	2.944
([MBIm]$^+$[PF$_6$]$^-$), eqn (15)	−0.084	0.079	0.792	−0.871	−4.665	3.053
([MEIM]$^+$[Tf$_2$N]$^-$), ref 20	0.040	0.377	0.247	−1.805	−3.814	3.066
([M$_2$EI.M]$^+$[Tf$_2$N]$^-$), ref 20	−0.095	0.299	0.360	−1.906	−3.805	3.177
Hexane	0.361	0.579	−1.723	−3.599	−4.764	4.344
Toluene	0.143	0.527	−0.720	−3.010	−4.824	4.545
Tetrachloromethane	0.260	0.573	−1.254	−3.558	−4.558	4.589
1,2-Dichloroethane	0.227	0.278	−0.167	−2.816	−4.324	4.205
Trichloromethane	0.327	0.157	−0.391	−3.191	−3.437	4.191
Octan-1-ol	0.088	0.562	−1.054	0.034	−3.460	3.814

as log *K*, are usually slightly better than those for partition from water to the RTILs, as log *P*. This is as expected, because the log *P* values include the extra error in the gas to water partition coefficients that are used to obtain the log *P* values, through eqn (4).

The coefficients in the equations for log *P* reflect the difference in properties of a RTIL (or an organic solvent) from those of water. In Table 5 are given coefficients for water to RTILs and for water to a number of solvents. Note that the water to RTILs are 'hypothetical partitions' between pure water and pure RTIL, whereas the water to solvent partitions are practical partitions between the mutually saturated solvents. Even so, it can be seen that the RTIL coefficients are not extraordinarily different to those for the organic solvents. The major differences are in the magnitude of the *s*and *a* coefficients. The positive *s* coefficients for the water to RTIL systems show that the RTILs are more dipolar than water, as expected. The negative *a* coeffficients indicate that the RTILs are weaker hydrogen bond bases than water, or octan-1-ol, and are somewhere between water and the common organic solvents in Table 5.

It is much easier to compare coefficients in eqn (2) than in eqn (1), because eqn (2) refers to partition from the gas phase, and hence the coefficients are in a sense absolute (as compared to the gas phase) and not relative (as compared to water) as with eqn (1). In Table 6 are given coefficients in eqn (2) for partition from the gas phase to RTILs and to a selection of organic solvents, and to water. We include in Table 6 coefficients for 1-methyl-3-ethylimidazolium *bis*(trifluoromethylsulfonyl)amide, ([MEIM]$^+$[Tf$_2$N]$^-$), and 1,2-dimethyl-3-ethylimidazolium *bis*(trifluoromethylsulfonyl)-amide, ([M$_2$EIM]$^+$[Tf$_2$N]$^-$) as given by Acree and Abraham.[20] Again, it can be seen that the coefficients for the RTILs are not extraordinarily different to those for organic solvents. The *e* coefficients are all numerically quite small, but the *s* coefficients show quite a wide spread of values, with the more dipolar solvents having the larger *s* coefficients. The *s* coefficients for the RTILs are about the same as those for the more polar solvents such as acetonitrile, dimethylformamide and *N*-methylpyrrolidinone but less than those for dimethylsulfoxide (DMSO) or water. The *a* coefficients reflect the hydrogen bond basicity of the solvents, with the RTILs lying near the middle of the *a* coefficient range. This places the hydrogen bond basicity of the RTILs near to that of ether, acetone or ethyl acetate. The hydrogen bond basicity of the RTILs will largely be due to the anion. It is no surprise that the two RTILs with the BF$_4^-$ anion are the strongest hydrogen bond bases. In the PF$_6^-$ anion, and in the Tf$_2$N$^-$ anion, the negative charge is more dispersed than in the BF$_4^-$ anion. The *b* coefficient in eqn (2) reflects the hydrogen bond acidity of the solvent. The RTILs have quite small *b* coefficients and are therefore not very strong hydrogen bond acids. This might be thought rather extraordinary in view of the positively charged cation. However, these are all of the form of tetraalkylammonium ions, [M$_3$BAm]$^+$ or [MBPy]$^+$, or 1,3-dialkylimidazolium ions, and have no 'active' hydrogen atom such as [R$_3$N–H]$^+$ or [=NR–H]$^+$. As hydrogen bond acids, the RTILs are about as strong as a long chain alcohol, and much weaker than trifluoroethanol, TFE, ethylene glycol or water. The *l* coefficient is very interesting, in that it is a measure of the 'hydrophobicity' of a solvent. Very hydrophobic solvents have *l* = unity or near unity, and solvents that are hydrophilic, rather than hydrophobic, have much lower values of the *l* coefficient; for example, TFE (0.633) or ethylene glycol (0.558). The RTILs with *l* values between 0.606 and 0.722 are clearly classed as hydrophilic solvents.

The coefficients in eqn (2) reflect the chemical nature of the solvent, in terms of solvent-interactions, and so the coefficients should indicate how near one solvent is to another, in these terms. It is not easy to compare coefficients just by eye, but a useful comparison is obtained through principal component analysis (PCA). The five columns of the *e* coefficients in Table 6 are transformed into five orthogonal PCs. In the present case, the first two PCs encode 76% of the total information and so a plot of the scores of PC2 against PC1 will give an approximate indication of how near solvents are in terms of chemistry. Such a plot is shown in Fig. 1. Points 25 (TFE), 28 (ethylene glycol) and 29 (water) are far away from points for the other solvents; this is not surprising when it is noted that these three solvents have large *s* , *a* , and *b* coefficients and small *l* coefficients. There are other methods of visualizing the 'closeness' of equations based on their coefficients, such as cluster analysis, but a PC score plot as shown in Fig. 1 seems the best method to use.

The points for the RTILs do not inhabit a different area of space to the organic solvents, but chemically resemble a

Table 6 Coefficients in eqn (2) for partition from the gas phase-to-RTILs and to organic solvents

Solvent	No	*c*	*e*	*s*	*a*	*b*	*l*
($[MBIm]^+[Tf_2N]^-$), eqn (6)	1	−0.407	0.040	2.158	2.478	0.665	0.679
($[MHIm]^+[Tf_2N]^-$), eqn (8)	2	−0.170	−0.116	2.079	2.141	0.429	0.704
($[M_3BAm]^+[Tf_2N]^-$), eqn (10)	3	−0.288	0.115	2.047	2.152	0.723	0.627
($[MOIm]^+$ $[BF_4]^-$), eqn (12)	4	−0.268	−0.100	1.800	3.224	0.453	0.722
($[MBPy]^+[BF_4]^-$), eqn (14)	5	−0.611	0.487	2.484	3.190	0.558	0.606
($[MBIm]^+[PF_6]^-$), eqn (16)	6	−0.602	−0.087	2.840	2.786	0.140	0.631
($[MEIM]^+[Tf_2N]^-$), ref 20	7	−0.439	0.148	2.277	2.172	1.041	0.629
($[M_2EIM]^+[Tf_2N]^-$), ref 20	8	−0.565	0.214	2.347	2.075	0.896	0.655
Hexane	9	0.292	−0.169	0.000	0.000	0.000	0.979
Hexadecane	10	0.000	0.000	0.000	0.000	0.000	1.000
Tetrachloromethane	11	0.282	−0.303	0.460	0.000	0.000	1.047
Carbon disulfide	12	0.101	0.251	0.177	0.027	0.095	1.068
1,2-Dichloroethane	13	0.011	−0.150	1.436	0.649	0.736	0.936
Trichloromethane	14	0.116	−0.467	1.203	0.138	1.432	0.994
Ether	15	0.288	−0.347	0.775	2.985	0.000	0.973
Acetone	16	0.154	−0.277	1.522	3.258	0.078	0.863
Ethyl acetate	17	0.203	−0.335	1.251	2.949	0.000	0.917
Acetonitrile	18	−0.007	−0.595	2.461	2.085	0.418	0.738
Dimethylformamide	19	−0.174	−0.339	2.315	4.112	0.000	0.830
N-Methylpyrrolidinone	20	−0.293	0.253	2.210	5.094	0.000	0.818
DMSO	21	−0.619	0.131	2.811	5.474	0.000	0.734
Toluene	22	0.121	−0.222	0.938	0.467	0.099	1.012
Chlorobenzene	23	0.053	−0.553	1.254	0.364	0.000	1.041
Nitrobenzene	24	−0.295	0.121	1.682	1.247	0.370	0.915
Trifluoroethanol	25	−0.133	−0.611	1.457	1.899	4.461	0.633
Methanol	26	−0.004	−0.215	1.173	3.701	1.432	0.769
Octan-1-ol	27	−0.119	−0.203	0.560	3.576	0.702	0.940
Ethylene glycol	28	−0.876	0.278	1.431	4.584	2.525	0.558
Water	29	−1.271	0.822	2.743	3.904	4.814	−0.213

number of ‘polar’ organic solvents such as points 18 (acetonitrile), 20 (*N*-methylpyrrolidinone, NMP), 24 (nitrobenzene) and 26 (methanol). A similar conclusion was reached by examination of water to solvent partition coefficients,[19] but the gas to solvent partition coefficients are much easier to interpret.

Table 7 Estimates of the nearness of solvents in chemical terms, *D*, and in calculational terms, cos *θ*

Solvent	No	*D*	Cos *θ*
($[MBIm]^+[Tf_2N]^-$)	1	0.00	1.000
($[MHIm]^+[Tf_2N]^-$)	2	0.45	0.995
($[M_3BAm]^+[Tf_2N]^-$)	3	0.36	0.998
($[MOIm]^+$ $[BF_4]^-$)	4	0.87	0.976
($[MBPy]^+[BF_4]^-$)	5	0.91	0.990
($[MBIm]^+[PF_6]^-$)	6	0.92	0.983
($[MEIM]^+[Tf_2N]^-$)	7	0.51	0.989
($[M_2EIM]^+[Tf_2N]^-$)	8	0.53	0.988
Hexane	9	3.37	0.194
Hexadecane	10	3.37	0.198
Tetrachloromethane	11	3.12	0.418
Carbon disulfide	12	3.23	0.327
1,2-Dichloroethane	13	1.99	0.860
Trichloromethane	14	2.71	0.612
Ether	15	1.69	0.873
Acetone	16	1.22	0.944
Ethyl acetate	17	1.30	0.927
Acetonitrile	18	0.84	0.969
Dimethylformamide	19	1.82	0.958
NMP[a]	20	2.71	0.934
DMSO[b]	21	3.14	0.950
Toluene	22	2.46	0.777
Chlorobenzene	23	2.49	0.713
Nitrobenzene	24	1.38	0.957
Trifluoroethanol	25	3.96	0.638
Methanol	26	1.77	0.913
Octan-1-ol	27	1.97	0.857
Ethylene glycol	28	2.91	0.884
Water	29	4.58	0.800

[a] Dimethylsulfoxide. [b] *N*-Methylpyrrolidinone.

Because the first two PCs account for 76% of the total information, the PC plot gives only an estimate, although very useful, of the chemical ‘nearness’ of solvents. Abraham and Martins[55,56] have shown how this chemical ‘nearness’ can be calculated exactly. The five coefficients for any solvent, *e* to *l*, are regarded as defining a point in five dimensional space. Then for any two solvents, the distance between the two points in five dimensional space, *D*, will be a more exact criterion of how close the two solvents are chemically, than the distance between points on the PCA plot, Fig. 1. Values of the distance, *D*, are in Table 7. Of the solvents listed, only acetonitrile can

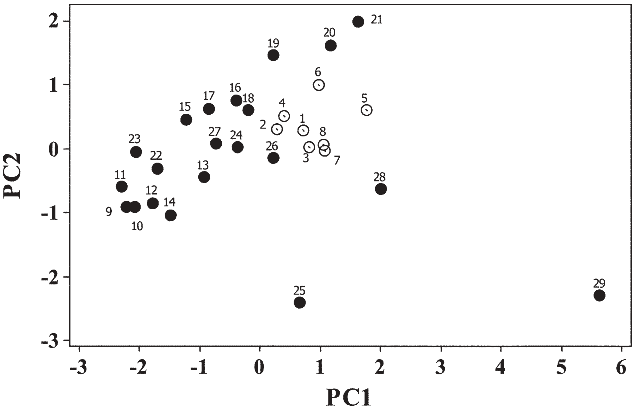

Fig. 1 A plot of the scores of PC2 against scores of PC1 for the analysis of the coefficients in Table 6. Points are numbered as in Table 6. Symbols: ● RTILs, ○ remaining solvents.

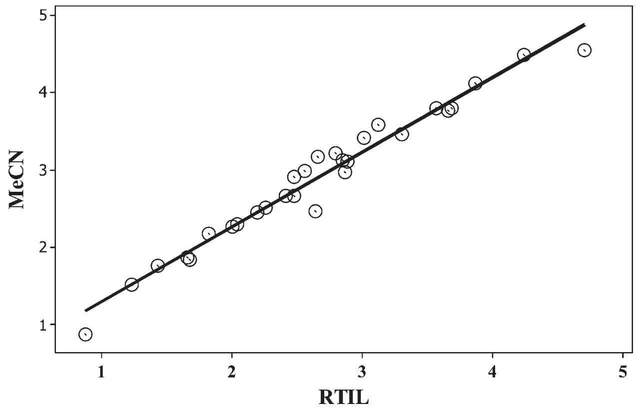

Fig. 2 A plot of log *K* values in acetonitrile against log *K* values in the RTIL, ($[MHIm]^+[Tf_2N]^-$), solvent no 2.

be regarded as chemically near to the RTILs, in terms of solvation through solute–solvent interactions.

This distance, *D*, does not indicate whether equations for two solvents are close in calculational terms. That is if values of log *K* for solutes in one solvent are plotted against values of log *K* for solutes in another solvent, will a good correlation result or not? Ishihama and Asakawa[57] have shown how the nearness of solvents in a calculational sense may be estimated. They regard the coefficients *e* to *l* for any solvent as defining a line, in five dimensional space, that passes through the origin. Then for any other solvent, the angle, θ, between the two lines may be calculated. If cos θ is near unity, the two lines can be superimposed and the solvents can be said to be near to each other in a calculational sense. Unfortunately, cos θ does not correspond to the correlation coefficient that might be expected if values of log *K* for solutes in one solvent are plotted against values of log *K* for solutes in another solvent, and seems to decrease from unity faster than does R^2. Thus cos θ = 0.95 would correspond to no more than a reasonable calculational connection between equations for two solvents. Of the listed solvents, acetonitrile seems to be the only one that is near to the RTILs in a calculational sense. If acetonitrile is taken as the standard solvent, then cos θ is nearest unity (0.986) for RTIL no 2, ($[MHIm]^+[Tf_2N]^-$).

log *K* values for partition of the 28 common solutes from the gas phase to acetonitrile and ($[MHIm]^+ [Tf_2N]^-$) are available, and a plot of the two sets of log *K* values against each other yields $N = 28$, SD = 0.161, $R^2 = 0.968$ and $F = 810.1$, see Fig. 2. It would be difficult by other means to predict that the solubility properties of acetonitrile and ($[MHIm]^+ [Tf_2N]^-$) would be so similar. The ideas of Abraham and Martins[55,56] and of Ishihama and Asakawa[57] are therefore not just theoretical concepts, but form the basis of a practical method to identify solvents that have the same, or similar, solvation properties.

Eqn (2) can also be used in another practical sense, and that is to predict the selective solubility of gases in solvents. We illustrate this for four pairs of solutes: isopropanol-acetone, phenol-cyclohexanol, benzene-cyclohexane, and butylamine-chlorobutane. In Table 8 we give log *K*(1) − log *K*(2), where log *K*(1) refers to the first solute and log *K*(2) to the second solute, for solubility of the gaseous compounds in all the listed solvents. The log *K* values have been calculated from the respective eqn (2) and the descriptors for the various compounds. Note that a negative value of log *K*(1) − log *K*(2) still

Table 8 Calculation of the selectivity of solvents towards pairs of gaseous compounds, in terms of log *K*(1) − log *K*(2)

Compound (1) Compound (2)	Isopropanol Acetone	Phenol Cyclohexanol	Benzene Cyclohexane	Butylamine Chlorobutane
($[MBIm]^+[Tf_2N]^-$)	0.079	1.289	0.891	0.558
($[MHIm]^+[Tf_2N]^-$)	−0.012	1.177	0.773	0.383
($[M_3BAm]^+[Tf_2N]^-$)	0.025	1.168	0.884	0.547
($[MOIm]^+ [BF_4]^-$)	0.400	1.382	0.660	0.580
($[MBPy]^+[BF_4]^-$)	0.177	1.785	1.162	0.615
($[MBIm]^+[PF_6]^-$)	−0.108	1.711	1.074	0.308
($[MEIM]^+[Tf_2N]^-$)	−0.024	1.180	1.035	0.701
($[M_2EIM]^+[Tf_2N]^-$)	−0.082	1.240	1.060	0.606
Hexane	0.061	−0.050	−0.226	−0.104
Hexadecane	0.068	0.008	−0.178	−0.104
Tetrachloromethane	−0.095	0.065	−0.086	−0.136
Carbon disulfide	0.035	0.139	−0.026	−0.064
1,2-Dichloroethane	−0.190	0.441	0.494	0.308
Trichloromethane	−0.217	−0.080	0.386	0.582
Ether	0.657	0.995	0.046	0.333
Acetone	0.482	1.335	0.412	0.391
Ethyl acetate	0.481	1.155	0.260	0.309
Acetonitrile	−0.172	1.133	0.779	0.339
Dimethylformamide	0.451	1.851	0.721	0.451
NMP	0.790	2.294	0.860	0.623
DMSO	0.686	2.568	1.090	0.661
Toluene	−0.115	0.364	0.160	−0.030
Chlorobenzene	−0.268	0.358	0.173	−0.120
Nitrobenzene	−0.118	0.887	0.632	0.211
Trifluoroethanol	0.390	−0.369	0.937	2.432
Methanol	0.820	0.992	0.491	1.181
Octan-1-ol	0.953	0.945	0.104	0.802
Ethylene glycol	1.067	1.203	0.940	1.896
Water	0.549	1.035	2.115	2.976

corresponds to selective solubility. In general, the RTILs show about the same selectivity as the polar organic solvents such as acetonitrile, dimethylformamide, NMP and dimethylsulfoxide (DMSO). The alcohol and water solvents, that are strong hydrogen bond acids, exhibit much larger selectivity towards solutes that are hydrogen bond bases, *e.g.* butylamine. Conversely, solvents that are strong hydrogen bond bases such as NMP, DMSO, methanol, octan-1-ol, ethylene glycol and water exhibit much larger selectivity towards solutes that are hydrogen bond acids, *e.g.* isopropanol.

From Table 8, it seems that the usefulness of RTILs does not depend on any extra selectivity over standard organic solvents, but on other properties such as low vapor pressure that make them environmentally more friendly than organic solvents. The method can, of course, be used to calculate selectivity for any solute pair, or multiple solutes, simply by inserting known descriptors for solutes into the equations listed in Table 6. Since the relevant descriptors for some thousands of solutes are available,[54] and can also be calculated from structure if required,[54,58,59] it is trivial to deduce selectivities for a huge number of solutes.

Of course care should be taken to use any obtained algorithm to predict new values only within the range of the independent variables, or descriptors, used to construct the algorithm. Most of the descriptors we employ cover quite a good range, and so predictions can be made for a very large number of compounds. The only descriptor that leads to any significant restriction on the type of compound for which predictions may be required is the A descriptor that ranges from 0.00 to 0.43 only. This small range has little effect on the robustness of the various equations for log P or log K, as can be seen from the comparatively small errors on the a coefficients, but does limit the type of hydrogen bond acids for which predictions of log P or log K or selectivity can be made.

Acknowledgements

Research supported in part by the University of North Texas Research Council.

References

1 C. F. Poole, *J. Chromatogr., A*, 2004, **1037**, 49.
2 M. T. Reetz, W. Wisenhoefer, G. Francio and W. Leitner, *Chem. Commun.*, 2002, 992.
3 S. Park and R. J. Kazlauskas, *Curr. Opin. Biotechnol.*, 2003, **14**, 432.
4 F. van Rantwijk, R. Madeira Lau and R. H. Sheldon, *Trends Biotechnol.*, 2003, **21**, 131.
5 S. Murugesan and R. J. Linhardt, *Curr. Org. Synth.*, 2005, **2**, 437.
6 D. Zhao, M. Wu, Y. Kou and E. Min, *Catal. Today*, 2002, **74**, 157.
7 J. Planeta, P. Karasek and M. Roth, *Green Chem.*, 2006, **8**, 70–77.
8 A. P. Khodadoust, S. Chandrasekaran and D. D. Dionysiou, *Environ. Sci. Technol.*, 2006, **40**, 2339.
9 A. Soto, A. Arce and M. K. Khoshkarchi, *Sep. Purif. Technol.*, 2005, **44**, 242.
10 S. G. Cull, J. D. Holbrey, V. Vargas-Mora, K. R. Sneedon and G. J. Lye, *Biotechnol. Bioeng.*, 2000, **69**, 227.
11 A. M. Stalcup and B. Cabovska, *J. Liq. Chromatogr. Relat. Technol.*, 2004, **27**, 1443.
12 S. Pandey, *Anal. Chim. Acta*, 2006, **556**, 38.
13 M. Koel, *Crit. Rev. Anal. Chem.*, 2005, **35**, 177.
14 G. A. Baker, S. N. Baker, S. Pandey and F. V. Bright, *Analyst*, 2005, **130**, 800.
15 J. F. Liu, J. A. Jonsson and G.-B. Jiang, *Trends Anal. Chem.*, 2005, **24**, 20.
16 M. H. Abraham, G. S. Whiting, R. M. Doherty and W. J. Shuely, *J. Chromatogr.*, 1991, **587**, 229.
17 S. K. Poole and C. F. Poole, *Analyst*, 1995, **120**, 289.
18 M. H. Abraham, C. F. Poole and S. K. Poole, *J. Chromatogr., A*, 1999, **842**, 79.
19 M. H. Abraham, A. M. Zissimos, J. G. Huddleston, R. D. Willauer, R. D. Rodgers and W. E. Acree, Jr., *Ind. Eng. Chem. Res.*, 2003, **42**, 413.
20 W. E. Acree, Jr. and M. H. Abraham, *J. Chem. Technol. Biotechnol.*, 2006, **81**, 1441.
21 J. L. Anderson and D. W. Armstrong, *Anal. Chem.*, 2003, **75**, 4851.
22 J. L. Anderson, J. Ding, T. Welton and D. W. Armstrong, *J. Am. Chem. Soc.*, 2002, **124**, 14247.
23 J. L. Anderson and D. W. Armstrong, *Anal. Chem.*, 2005, **77**, 6453.
24 J. Planeka and M. Roth, *J. Phys. Chem. B*, 2005, **109**, 15165.
25 M. H. Abraham, *Chem. Soc. Rev.*, 1993, **23**, 73.
26 M. H. Abraham, G. S. Whiting, W. J. Shuely and R. M. Doherty, *Can. J. Chem.*, 1998, **76**, 703.
27 M. H. Abraham, G. S. Whiting, P. W. Carr and H. Ouyang, *J. Chem. Soc., Perkin Trans. 2*, 1998, 1385.
28 M. H. Abraham, J. A. Platts, A. Hersey, A. J. Leo and R. W. Taft, *J. Pharm. Sci.*, 1999, **88**, 670.
29 M. H. Abraham, J. Andonian-Haftvan, J. P. Osei-Owusu, P. Sakellariou, J. S. Urieta, M. C. Lopez and R. Fuchs, *J. Chem. Soc., Perkin Trans. 2*, 1993, 299.
30 M. H. Abraham, F. Martins, R. C. Mitchell and C. J. Salter, *J. Pharm. Sci.*, 1999, **88**, 241.
31 M. H. Abraham, J. Le and W. E. Acree, Jr., *Collect. Czech. Chem. Commun.*, 1999, **64**, 1748.
32 M. H. Abraham, J. Le, W. E. Acree, Jr. and P. W. Carr, *J. Phys. Org. Chem.*, 1999, **12**, 675.
33 R. Kato and J. Gmehling, *J. Chem. Thermodyn.*, 2005, **37**, 603.
34 A. Heintz, S. P. Verevkin and D. Ondo, *J. Chem. Eng. Data*, 2006, **51**, 434.
35 T. M. Letcher, A. Marciniak, M. Marciniak and U. Domanska, *J. Chem. Thermodyn.*, 2005, **37**, 1327.
36 J. Kumelan, A. Perez-Salado Kamps, D. Tuma and G. Maurer, *J. Chem. Thermodyn.*, 2006, DOI: 10.1016.fj.jct.2006.01.013.
37 A. Heintz, T. V. Vasiltsova, J. Safarov, E. Bich and S. P. Verevkin, *J. Chem. Eng. Data*, 2006, **51**, 648.
38 F. Mutelet, V. Butet and J.-N. Jaubert, *Ind. Eng. Chem. Res.*, 2005, **44**, 4120.
39 J. L. Anthony, E. J. Maginn and J. F. Brennecke, *J. Phys. Chem. B*, 2002, **106**, 7315.
40 J. Jacquemin, P. Husson, V. Majer and M. F. Costa Gomes, *Fluid Phase Equilib.*, 2006, **240**, 87.
41 M. B. Shiflett and A. Yokozeki, *AIChE J.*, 2006, **52**, 1205.
42 A. Heintz, D. V. Kulikov and S. P. Verevkin, *J. Chem. Thermodyn.*, 2002, **34**, 1341.
43 A. Heintz, L. M. Casas, I. A. Nesterov, V. N. Emel'yanenko and S. P. Verevkin, *J. Chem. Eng. Data*, 2005, **50**, 1510.
44 B.-C. Lee and S. L. Outcalt, *J. Chem. Eng. Data*, 2006, **51**, 892.
45 A. Heintz and S. P. Verevkin, *J. Chem. Eng. Data*, 2005, **50**, 1515.
46 A. Heintz, D. V. Kulikov and S. P. Verevkin, *J. Chem. Eng. Data*, 2001, **46**, 1526.
47 W. J. Cheong and P. W. Carr, *J. Chromatogr.*, 1990, **500**, 215.
48 M. H. Abraham and J. C. McGowan, *Chromatographia*, 1987, **23**, 243–246.
49 M. H. Abraham, G. S. Whiting, R. M. Doherty and W. J. Shuely, *J. Chem. Soc., Perkin Trans.*, 1990, **2**, 1851–1857.
50 A. M. Zissimos, M. H. Abraham, C. M. Du, K. Valko, C. Bevan, D. Reynolds, J. Wood and K. Y. Tam, *J. Chem. Soc., Perkin Trans.*, 2002, **2**, 2001–2010.
51 C. E. Green, M. H. Abraham, W. E. Acree, Jr., K. M. De Fina and T. L. Sharp, *Pest Manage. Sci.*, 2000, **56**, 1043–1053.
52 M. H. Abraham, A. Ibrahim and A. M. Zissimos, *J. Chromatogr., A*, 2004, **1037**, 29–47.
53 A. Zissimos, M. H. Abraham, M. C. Barker, K. J. Box and K. Y. Tam, *J. Chem. Soc., Perkin Trans.*, 2002, **2**, 470–477.
54 *ADME Version 3.0*, Pharma Algorithms Inc., Toronto, ON, Canada, 2006.

55 M. H. Abraham, in *EuroQSAR 2002. Designing drugs and crop protectants: processes, problems and solutions*, ed. M. Ford, D. Livingstone, J. Dearden and H. van de Waterbeemd, Blackwell, Oxford, 2003, pp. 5–7.
56 M. H. Abraham and F. Martins, *J. Pharm. Sci.*, 2002, **93**, 1508–1523.
57 Y. Ishihama and N. Asakawa, *J. Pharm. Sci.*, 1999, **88**, 1305–1312.
58 J. A. Platts, D. Butina, M. H. Abraham and A. Hersey, *J. Chem. Inf. Comput. Sci.*, 1999, **39**, 835–845.
59 T. J. Sheldon, C. S. Adjiman and J. L. Cordiner, *Fluid Phase Equilib.*, 2004, **231**, 29–49.

Eco-friendly and versatile brominating reagent prepared from a liquid bromine precursor†

Subbarayappa Adimurthy,[a] Gadde Ramachandraiah,*[a] Ashutosh V. Bedekar,[a] Sudip Ghosh,[b] Brindaban C. Ranu*[b] and Pushpito K. Ghosh*[a]

Received 10th May 2006, Accepted 10th July 2006
First published as an Advance Article on the web 3rd August 2006
DOI: 10.1039/b606586d

Facile bromination of various organic substrates has been demonstrated with a 2 : 1 bromide:bromate reagent prepared from the alkaline intermediate of the conventional bromine recovery process. The reagent is acidified *in situ* to generate HOBr as the reactive species, which effects bromination. Aromatic substrates that have been successfully brominated under ambient conditions without use of any catalyst include phenols, anilines, aromatic ethers and even benzene. Non-aromatic compounds bearing active methylene group were monobrominated selectively with the present reagent and olefinic compounds were converted into the corresponding bromohydrins in moderate yields. By obtaining the present reagent from the liquid bromine precursor, the twin advantages of avoiding liquid bromine and producing the reagent in a cost-effective manner are realised. When coupled with the additional advantage of high bromine atom efficiency, the present protocol becomes attractive all the way from "cradle to grave".

1 Introduction

Bromo derivatives have wide utility both as products and intermediates.[1,2] Many of these compounds are prepared using liquid bromine. Liquid bromine is used both for addition reactions as well as for substitution reactions. Activated aromatic compounds, such as phenols, anilines, and aromatic ethers, can be brominated without a catalyst, even at relatively low temperatures,[3] whereas other substrates may demand use of a catalyst. Commonly used catalysts include halides of aluminum, iron, zinc, or antimony.[4] Liquid bromine is corrosive and its transport and handling pose difficulties. Moreover, substitution reactions with liquid bromine lead to only 50% bromine atom efficiency, although the HBr by-product can be recycled with oxidizing agents such as H_2O_2.[5] HBr can, alternatively, be recovered and sold, or used for co-production of alkyl bromides such as methyl bromide.[6]

Besides liquid bromine, there are latent brominating reagents, such as pyridiniumbromide-perbromide,[7] and quaternary ammonium tribromide,[8] which are safer and easier to use but such reagents are also produced using liquid bromine. Moreover, the bromine atom efficiency is only 50%. There are other brominating agents that are employed when the reactions either do not proceed with liquid bromine or proceed with low selectivity. Examples of such brominating agents include *N*-bromosuccinimide (NBS) for allylic bromination,[9] and 2,4,4,6-tetrabromo-2,5-cyclohexadien-1-one (TBCD) for monobromination with para-selectivity,[10] but in these cases their preparation also involves liquid bromine.[11] Other reagents reported for bromination of aromatic substrates include: Br_2–NaY zeolite and Br_2–alumina,[12] HBr–DMSO,[13] and P_2O_5–Bu_4NBr.[14] $NaBrO_3$–H_2SO_4 has been shown to be a promising reagent for bromination of aromatic rings having electron deactivating substituents.[15–19] $NaBrO_3$–HBr in sulfuric acid/acetic acid medium has been used for bromination of several amides and imides,[20a] while $NaBrO_3$–$NaHSO_3$ has been shown to be a good reagent for bromination of alkyl benzenes and for the synthesis of bromohydrins from alkenes.[20b,c] BrCl has also been used for substitution reactions and the reactions are reported to be faster than those involving bromine alone.[21] Even in these cases, the preparations of basic inorganic bromide salts and acids involve downstream reactions with liquid bromine followed by purification processes,[22] *i.e.*, liquid bromine is ubiquitous in the product life cycle of all the above bromination reactions. Given the hazards of liquid bromine, it is desirable to develop schemes that dispense with its use directly or indirectly.

2 Results and discussion

Bromine is manufactured from sea bittern. We have recently patented the preparation and utility of a brominating reagent obtained from the liquid bromine precursor in the "cold process" of bromine manufacture.[23] The precursor comprises a 5 : 1 mole ratio of NaBr:$NaBrO_3$, which is formed when bromine vapor evolved from bittern is trapped in aqueous NaOH. Instead of acidifying the precursor to evolve bromine as practiced in conventional manufacture (eqn 1), it is treated with Cl_2–NaOH (or NaOCl) to obtain a 2 : 1 mole ratio of

---

[a] *Central Salt and Marine Chemicals Research Institute, Gijubhai Badheka Marg, Bhavnagar, 364 002, Gujarat, India. E-mail: pkghosh@csmcri.org; grama@csmcri.org; Fax: +91-278-2567562*
[b] *Department of Organic Chemistry, Indian Association for the Cultivation of Science, Jadavpur, Kolkata, 700032, India. E-mail: bcranu@gmail.com*

† Electronic supplementary information (ESI) available: UV-spectrophotometric evidence for the formation of BrOH; procedure for reaction calorimetric study; analytical data; NMR spectra; DSC plots and HPLC chromatograms of select compounds. See DOI: 10.1039/b606586d

NaBr:NaBrO$_3$ (eqn 2), which can be used as such or evaporated to dryness to yield a solid reagent containing 40% (w/w) active Br.[24] The reagent, upon acidification with HCl[25] in the presence of an organic substrate, yields bromo derivative as per the stoichiometry of eqn 3. NaCl that is co-present in the reagent to the extent of 33% (w/w) does not affect the results, as confirmed through control experiments with a pure 2 : 1 mixture of NaBr:NaBrO$_3$.

$$5NaBr + NaBrO_3 + 6HCl \rightarrow 3Br_2 + 3H_2O + 6\ NaCl \quad (1)$$

$$\begin{gathered} 5NaBr + NaBrO_3 + 3NaOCl \rightarrow \\ 4NaBr + 2NaBrO_3 + 3NaCl \end{gathered} \quad (2)$$

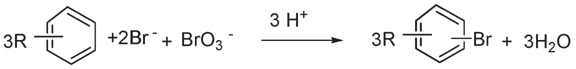

(3)

Table 1 shows the bromination of phenol and phenol derivatives undertaken with the present reagent system. All the reactions proceeded in high yields under ambient conditions and without recourse to any catalyst. Entries 1–3 were carried out with neat substrate, while CH$_2$Cl$_2$ was employed as solvent in the remaining reactions. Alternatively, 1,2-dichloroethane can also be used. In the case of reaction with bisphenol A—which yields the commercially important fire retardant tetrabromobisphenol A—the product is obtained directly in solid form in 98% purity and the mother liquor is recycled in subsequent batches resulting in high (92%) overall yield. Reaction calorimetric studies suggest that the reaction is near instantaneous with an adiabatic rise in temperature of only 18 °C, indicating that the bromination is facile and safe. We examined the efficacy of the reagent with aniline and its derivatives as well. The results are provided in Table 2. A molar excess of acid was used as the amine forms a salt with acid, which was neutralized with sodium bicarbonate after completion of the reaction. 2,4,6-Tribromoaniline could be prepared in 96% yield and 98.6% purity from aniline.

We also undertook reactions with other aromatic substrates. Monobromination of anisole and acetanilide was achieved in good yields and with high *p*-selectivity (entries 1 and 3, Table 3). Naphthalene could also be converted into 1-bromonaphthalene, albeit only in 36% isolated yield under the same conditions (others products of the reaction have not been characterised). With benzene the reaction was facile only under reflux conditions, and the yield was better (81.3% at 100 g scale; 95% purity by HPLC) when sodium lauryl sulfate (SLS) was used as a phase transfer catalyst.[23d]

We have also studied the monobromination of several CH-acidic compounds (Table 4). Whereas such selective bromination with conventional brominating agents is difficult,[26] the reactions could be achieved in good yields with the present reagent.[27–32] *N*-Bromosuccinimide, employed for allylic bromination, could also be synthesized with the present reagent prepared from the bromine intermediate.[20] The product is obtained directly in solid form when water is used as solvent, and the filtered mass is purified by washing with water to remove adhering impurities (yield 78%; purity 92%).

UV-visible spectroscopic studies helped us establish that, upon acidification of the reagent, BrOH is produced (λ_{max} = 260 nm), albeit with traces of elemental bromine.[33] We therefore explored the possible utility of the reagent for synthesis of bromohydrins.[20c,34] This was successfully accomplished as can be seen from Table 5. However, the dibromo derivative was inevitably formed as an impurity.

3 Experimental

3.1 Materials and methods

NMR spectra of bromo derivatives of 1,3-dicarbonyl compounds (Table 4) were recorded on model DPX300 Bruker FT-NMR instruments while all other NMR were recorded on model DPX 200 Bruker FT-NMR. FT-IR spectra were recorded on Perkin Elmer GX-2000 spectrometer. Gas Chromatograms were recorded on Shimadzu GC-14B using SE-30 column. Melting points were recorded on Veego capillary instrument and may be uncorrected. Analytical thin layer chromatography (TLC) was performed on Aluchrosep Silica Gel 60/UV$_{254}$ plate. Purification of some of the reaction products (tribromophenol; 4,6-dibromo-2-chlorophenol; 1-bromo-2-naphthol; 4-bromo-*N*,*N*-dimethylaniline; 1-bromonaphthalene; bromohydrins) was carried out by column chromatography using 100–200 mesh silica gel. All reactions were carried out under ambient conditions with magnetic stirring unless otherwise stated. Unless otherwise stated, yield refers to isolated yield. The purity of all compounds was checked by ^{1}H-NMR, FT-IR, microanalyses (Perkin-Elmer model 2400), melting point and boiling point. Purities of tribromoaniline, tetrabromobisphenol A, *N*-bromosuccinimide and bromobenzene were estimated by HPLC (Shimadzu model with CTO 10A UV-vis detector and Nucleosil C18 column) and also by differential scanning calorimetry (Mettler Toledo Model DSC 822^e Differential Scanning Calorimeter using Star^e software). Reaction calorimetric studies were conducted on an RC1:Mettler make SV01 calorimeter fitted with an 800 ml capacity all glass reactor equipped with a propeller type upflow agitator, jacketed with a controlled temperature circulator, addition funnel, condenser, and the calibration and temperature probes.

3.2 Preparation of 2 : 1 Br$^-$: BrO$_3^-$ reagent from alkaline bromine mixture and sodium hypochlorite

62 g (0.83 moles) of sodium hypochlorite was added into 894 mL of alkaline bromine intermediate, containing a total of 262 g (3.26 moles) of dissolved bromine in the form of 4.7 : 1 mole ratio of Br$^-$: BrO$_3^-$. The contents were mixed thoroughly and allowed to react for 24 h in a closed 5 L round-bottom flask, to obtain the 2 : 1 Br$^-$: BrO$_3^-$ reagent having 241.85 g of available bromine. Eqn 2 shows the stoichiometry for conversion of 5 : 1 Br$^-$: BrO$_3^-$ into 2 : 1 Br$^-$: BrO$_3^-$.

3.3 General procedure for the preparation of bromophenols

A known quantity of the organic substrate was taken in a single neck 100 mL round-bottom flask containing either water (entries 1–3; Table 1) or dichloromethane in 1 : 10 and 1 : 5 (w/v) substrate to solvent ratio, respectively. To it, an aqueous solution (*ca.* 5 mL water per gram of reagent) containing the stoichiometric equivalent of brominating reagent was added under stirring at 25–40 °C. Then the

Table 1 Polybromination of phenols[a]

Entry	Substrate	No. eq. of Br	Time/h	Product	Yield (%)[b]
1	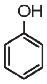	1	2	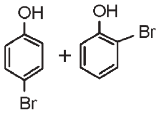	91[c]
2	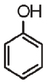	3	2–3	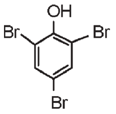	93
3	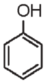	4	2–3	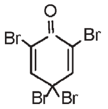	94
4	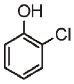	2	2–3	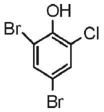	90[d]
5		2	2–3	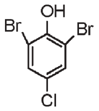	98
6	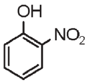	2	2	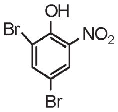	98.5
7	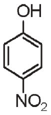	2	2	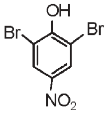	96
8	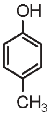	2	2	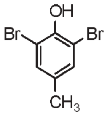	99
9	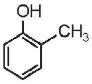	2	2	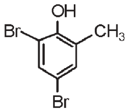	97.5
10	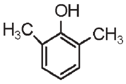	1	2	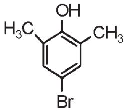	97
11	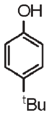	2	2–3	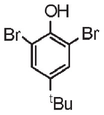	95
12	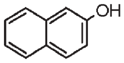	1	2	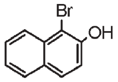	86[d]
13	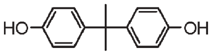	4	5	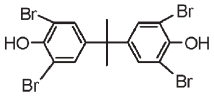	92[e]

[a] 1–3 are carried out in water medium and other reactions are carried out using CH_2Cl_2 as solvent. [b] Unless indicated otherwise, reported yields are the crude yields after work up. [c] *p*/*o* ratio was 81 : 19 by GC. [d] Isolated yields after column chromatography. [e] Average yield of 5 batches with recycling of the mother liquor.

Table 2 Bromination of amines[a]

Entry	Substrate	No. eq. Br	Time/h	Product	Yield (%)
1	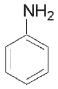	3	2	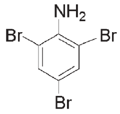	96
2	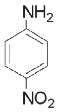	2	2	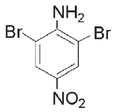	98.7
3	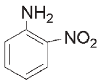	2	2	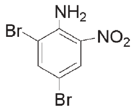	98.5
4	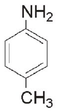	2	2	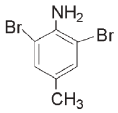	84[a]
5	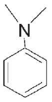	1	2	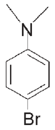	85[a]

[a] MeOH is used as solvent in entry 1 and CH_2Cl_2 in entries 2–5. [b] Yields after column chromatography.

Table 3 Bromination of other aromatic substrates[a]

Entry	Substrate	Time/h	Product	Yield (%)[b]
1	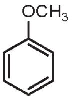	1.5	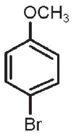	97[c]
2[d]	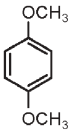	2	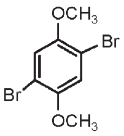	96.5[c]
3	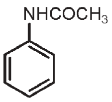	1	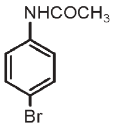	93
4		2	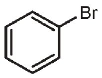	81.3
5	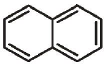	2.4	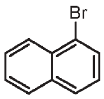	36[e]

[a] CH_2Cl_2 is used as solvent in entries 1, 2 and 5, MeOH in entry 3 and excess benzene in entry 4. [b] Isolated yields. [c] Crude yields. [d] Two equivalents of brominating reagent is used. [e] Isolated yield after column chromatography. (Note: selectivity of formation was not quantitatively estimated for crude product mixture.)

Table 4 Selective monobromination of CH-active compounds

Entry	Substrate	Product	Time/h	Yield (%)[a]	Ref.
1	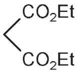	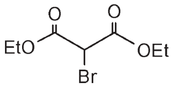	1.5	65	27
2	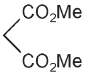	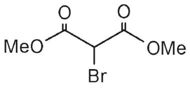	1.5	70	28
3	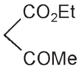	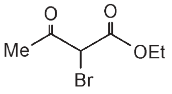	1.2	80	29
4	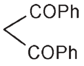	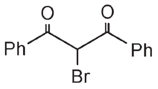	0.5	90	30
5	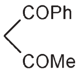	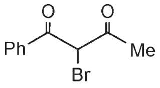	3.0	78	29
6	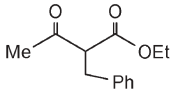	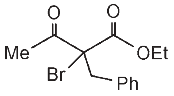	2.5	76	30
7	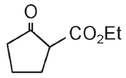	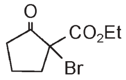	2.0	83	
8	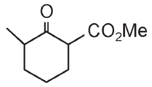	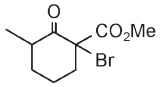	2.0	80	
9	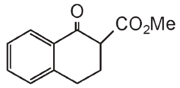	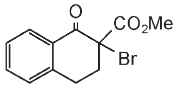	2.0	91	30
10	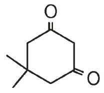	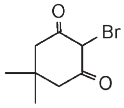	0.25	95	30
11	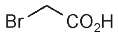	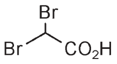	3.5	70	31
12	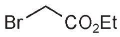	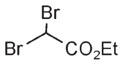	4.0	60	31
13	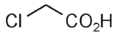	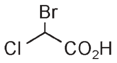	3.5	72	32

[a] Isolated yields.

required quantity of 12 N hydrochloric acid solution was added drop-wise to the flask under stirring at room temperature over a period of 30–60 min. After complete addition of the acid solution, the stirring was continued for another 40 to 60 min and the product was extracted with 3 × 25 ml of dichloromethane or diethyl ether. (Note that in the case of entries 2 and 3 of Table 1, the product was washed directly with water and dried.) The combined organic extracts were washed successively with 5% sodium thiosulfate, water and then brine, followed by drying over anhydrous sodium

Table 5 Synthesis of bromohydrins

Entry	Substrate	Time/ min	Product ratio (%)	Total yield (%)[a]
1	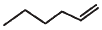	30	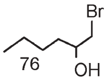 76 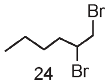 24	66
2		30	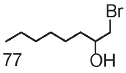 77 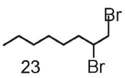 23	85
3		45	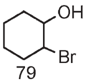 79 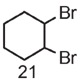 21	85
4	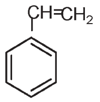	45	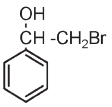 87 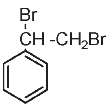 13	91
5	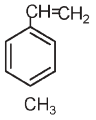	45	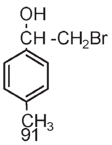 91 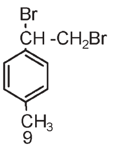 9	90

[a] Isolated yields after column chromatography in dioxane as solvent.

sulfate and evaporation of solvent under reduced pressure. The product was purified wherever required by column chromatography on silica gel. The identity and purity of the products formed were characterized by the analytical techniques mentioned above.

3.4 General procedure for the bromination of anilines

A known quantity of the organic substrate was taken in a single neck 100 mL round-bottom flask containing dichloromethane or methanol in 1 : 5 (w/v) substrate to solvent ratio. To it, an aqueous solution containing the calculated quantity of brominating reagent (BR) was added under stirring at 25–40 °C. Then the required quantity of aqueous hydrochloric acid solution was added drop-wise to the flask under stirring at room temperature over a period of 60 min. (Note: One mole excess acid w.r.t. amine was used to offset the formation of amine salt.) After complete addition of the acid solution, the stirring was continued for another 40 to 60 min and the product was extracted with 3 × 25 ml of either dichloromethane or diethyl ether. The combined organic extracts were washed successively with 5% $NaHCO_3$, water and then brine, followed by drying over anhydrous sodium sulfate and stripping off solvent under reduced pressure. The product was purified wherever required by column chromatography on neutral alumina (active) using the desired % of ethyl acetate and hexane. The identity and purity of the products formed were established by conventional analytical techniques.

3.5 General procedure for bromination of CH acidic compounds

1.5 g of the brominating reagent was added to the dispersion of ethyl acetoacetate (5 mmol) in aqueous methanolic solution (15 ml) at 0 °C. After that ~0.9 N HCl solution (15 ml) was added dropwise over 15 minutes at that temperature and stirred for 1.5 h until completion of the reaction (TLC). The excess bromine was decomposed with aqueous Na_2SO_3 solution. The product was extracted with diethyl ether and washed with water and evaporated in vacuum to leave the crude compound, which was purified by column chromatography over silica gel (*n*-hexane : ether = 95 : 5) to give pure monobromo compound (80%) as a yellow oil.

Analytical data for entry 7, Table 4: Brownish oil; ν_{max}(neat)/cm^{-1} 1722, 1759; δ_H/CDCl$_3$ 1.31 (t, J = 7.2 Hz, 3H), 2.10–2.18 (m, 2H), 2.25–2.52 (m, 3H), 2.70–2.81 (m, 1H), 4.29 (q, J = 7.2 Hz, 2H); δ_C/CDCl$_3$ 13.8, 19.3, 35.2, 38.6, 54.6, 63.0, 166.7, 205.8. (Found: C, 40.57, H, 4.52. $C_8H_{11}O_3Br$ requires C, 40.87; 4.72%).

Analytical data for entry 8, Table 4: Yellow oil; ν_{max}(neat)/cm^{-1} 1725, 1755; δ_H/CDCl$_3$ 1.06 (d, J = 6.3 Hz, 3H), 1.36–1.38 (m,2H), 1.70–1.77 (m, 1H), 1.97–2.13 (m, 2H) 2.48–2.54 (m, 1H) 2.98–3.04 (m, 1H), 3.78 (s, 3H); δ_C/CDCl$_3$ 15.2, 24.2, 35.7, 42.1, 44.2, 53.5, 68.2, 168.2, 199.2. (Found: C, 43.19; H, 5.11.$C_9H_{13}O_3Br$ requires C, 43.39; H, 5.26%).

3.6 General procedure for preparation of bromohydrins

1.0 g (12.2 mmol) of cyclohexene in 10 mL of dioxane was placed in a 100 mL round-bottom flask. Into it was added 2.436 g (12.18 mmol active Br) of brominating reagent in 30 mL of water. The mixture was stirred at room temperature with controlled addition of dilute sulfuric acid (12.2 mmol) over 15 minutes, stirred for an additional 30 minutes and extracted with 75 mL (25 mL × 3) of diethylether. The combined organic extract was washed with dilute sodium thiosulfate (5%), water, and brine, and dried over anhydrous sodium sulfate. Evaporation of ether left the crude product which was purified by column chromatography over silica gel (hexane–ethyl acetate 9 : 1) to get the pure *trans* 2-bromocyclohexanol as colorless liquid (1.42 g, 7.94 mmol) in 65% yield and 1,2-dibromocyclohexane (0.25 g, 1.033 mmol) in 17% yield. Spectroscopic data (^{1}H, ^{13}C NMR and IR) of the above products are in good agreement with those of authentic samples.

3.7 Special procedures

Tetrabromobisphenol A (TBBP-A) from bisphenol-A (BP-A) (entry 13, Table 1). 0.50 kg (2.193 mol) of BP-A, 1.5 L dichloromethane (DCM), 1.752 kg brominating reagent (containing 8.772 mol available Br) and 3.1 L water were placed in a 10 L glass reactor. To this reaction mixture, 0.912 L (8.86 mol) of 12 N HCl was added drop-wise over a period of 12 h under stirring at R.T. After the complete addition of acid, stirring was continued for further 30 min. 0.80 kg (1.471 mol; 67% yield) of TBBP-A (m.p.180–184 °C) was obtained after filtering and drying at 100 °C for 3 h. The organic layer (0.85 L) was separated from the aqueous layer. It was recycled in the subsequent 0.50 kg batch of BP-A subjected to bromination in analogous manner. 1.07 kg (1.97 mole) of TBBP-A (m.p. 181–184 °C) was obtained. The overall isolated yield from the two batches was 78.5% and the organic layer, which also contained

TBBP-A and intermediates, was once again recycled to continue the process. In this manner, yields in excess of 92% could be realized. The purity of TBBP-A thus obtained was estimated to be >98% by HPLC and DSC.

4-Bromoacetanilide (entry 3, Table 3). The title compound was prepared according to the general procedure described in 3.3 above using acetanilide (1.0 g, 7.407 mmol) in 10 mL methanol. 1.480 g of brominating reagent in 20 mL water was added into the above solution, followed by dropwise addition of 20 ml of aqueous 0.923 N hydrochloric acid (17.964 mmol). White amorphous solid separated out, which was filtered and washed with water until it became free from acid. The product was dried at 100 °C to yield 1.4742 g of 4-bromoacetanilide in 93% yield.

Preparation of bromobenzene (entry 4, Table 3). A 2 : 1 mixture of NaBr : $NaBrO_3$ constituted from 10 g (0.097 mol) of NaBr and 7.33 g (0.485 mol) of $NaBrO_3$ was dissolved in 75 mL water and placed in a 250 mL three neck round-bottom flask fitted with a water condenser. 0.2 g of sodium lauryl sulfate (SLS) was also added. Excess benzene (57 mL, 0.64 mol) was added next and the flask slowly heated to 70–75 °C under stirring. 25 mL of 7.3 N HCl (0.18 mol) was added to the hot reaction mixture over 10 h. The hot reaction mixture was stirred for another 30 h and then cooled to room temperature. The organic and aqueous layers were separated. The aqueous layer was extracted at least three times with minimum quantity of ether. The extracts were combined with the organic layer, washed successively with water and brine and dried over anhydrous sodium sulfate. Solvent was stripped at reduced pressure and the resultant liquid was vacuum distilled to yield 18.6 g (81.3% yield w.r.t. to brominating reagent) of bromobenzene. The purity was estimated to be 95% by HPLC (*ca.* 2% of benzene was present in the product due to imperfect distillation). A similar result was obtained at 100 g scale using the 2 : 1 brominating reagent prepared from the alkaline bromine intermediate as described above.

***N*-Bromosuccinimide (NBS).** A 2 : 1 mixture of NaBr : $NaBrO_3$ constituted from 13.87 g (0.135 mol) of NaBr and 10.17 g (0.067 mol) of $NaBrO_3$ was dissolved in 60 mL water and placed in 250 mL round-bottom flask. 20.0 g (0.202 mol) of succinimide was added and the contents stirred at 10–15 °C for 5–10 min to dissolve the solids. Then 12 mL of 18.0 N H_2SO_4 was added slowly under stirring over 2 h. The white solid formed was filtered, washed with cold water, and dried in an oven at 100 °C for 2 h to yield 28.0 g (78%) of NBS. A similar result was obtained at 100 g scale using the 2 : 1 brominating reagent prepared from the alkaline bromine intermediate as described above. The isolated yield was 80% and the purity was estimated to be *ca.* 92% by iodometry method. Analytical data: ^{1}H-NMR ($CDCl_3$-200 MHz) (δ) 2.97(4H, s). IR: ν_{max} (KBr) 3184, 3057, 2934, 2649, 2541, 1696, 1417, 1309, 1199, 919, 638, 581, 425 cm^{-1}. CHN: Found C, 28.05%; H, 2.47; N, 7.78%; calcd C, 29.63%; H, 1.98%; N, 8.64%. Melting point: observed 180–181 °C (reported 180–183°C).

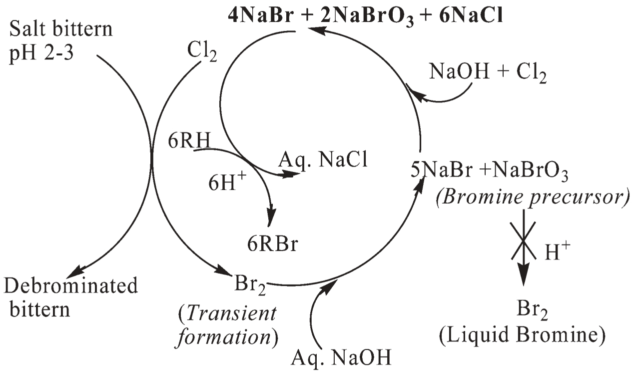

Scheme 1

4 Conclusion

We have exploited the redox reaction between bromide and bromate ions in the presence of acid to develop an eco-friendly brominating reagent directly from the 5 : 1 Br^- : BrO_3^- alkaline intermediate of bromine plants that are based on the "cold process" of manufacture. By adjusting the Br^- : BrO_3^- mole ratio to 2 : 1 through oxidation with Cl_2–NaOH, BrOH—instead of Br_2—is obtained on acidification. This redox process may be carried out in the presence of organic substrates to effect bromination. Scheme 1 shows the eco-friendly nature of the process all the way from cradle to grave.

BrOH—more specifically $BrOH_2^+$ which forms in the presence of excess acid[35]—is not only more active than liquid bromine, but it also results in high bromine atom efficiencies in most of the reactions studied. NaCl present as an inert salt in the reagent has no adverse effect on the reaction, whereas significant gains are realized in terms of simplicity and cost-effectiveness of preparation of the reagent. Since bromine manufacturers themselves can produce the reagent from the precursor—rather than from liquid bromine—the reagent has the potential to be eco-friendly across the entire life cycle. Besides aromatic bromination reactions, CH-acidic compounds could be monobrominated selectively and olefins could be converted into the corresponding bromohydrins in moderately good yields and selectivity. Another application is the clean synthesis of other brominating reagents such as *N*-bromosuccinimide and 2,4,4,6-tetrabromo-2,5-cyclohexadienone, which extends the scope of application considerably for selective bromination as well as for bromination of water-sensitive substrates. It is hoped that the present protocol will also make it simple to recycle the spent reagents. An important extension of the present work would be the conversion of bromide-containing waste streams—*e.g.*, during formation of trimethoxyaniline from tribromoaniline—into 2 : 1 bromide–bromate mixture which can be reutilised for synthesising the bromo intermediate once again with high atom efficiency.

Although some of the reactions were conducted with only water as solvent, we would like to avoid the use of organic solvents—especially that of chlorinated solvents—to the maximum extent possible. Alternatively, the processes can be made eco-friendly by recycling the organic phase as demonstrated in the preparation of TBBP-A. When the recycling option is feasible, less volatile solvents can be used, *e.g.*, use of dichloroethane instead of methylene chloride. The process can be made still more eco-friendly by regenerating HCl and NaOH from the aqueous effluent through electrodialysis with bipolar membranes.

Finally, efforts are underway to explore other possible applications of the present reagent going beyond bromination.

Acknowledgements

The authors are indebted to M/s Agrocel Industries Limited and Saukem Limited, Gujarat, India for providing the alkaline bromine intermediate. We are also thankful to the Analytical Section of the Institute for assistance with analyses, to Dr Manoj Kharkar and Dr V. R. K. S. Susarla for the reaction calorimetric measurements, to Dr A. S. Mehta, Dr R. P. Pandya, Dr A. D. Jethva and Dr S. S. Vaghela for their involvement in the initial stages of this work, and to Professor D. Basavaiah for communicating to us the preparation of benzyl bromide with the present reagent. We thank M/s Strides Arcolab and Deepak Nitrite Ltd for evaluating the reagent in certain industrial applications and M/s Solaris Ltd for data on the purities of some products obtained at 100 g scale. We also thank the referees for their valuable comments. This work was undertaken as part of a laboratory project that was generously supported by CSIR, New Delhi, India.

References

1 (*a*) M. Kuroboshi, Y. Waki and H. Tanaka, *J. Org. Chem.*, 2003, **68**, 3938; (*b*) Y. Qingwei, P. K. Elizabeth and Y. Zhi, *J. Org. Chem.*, 2003, **68**, 7528.

2 (*a*) C. Gao, X. Tao, Y. Qian and J. Huang, *Chem. Commun.*, 2003, 1444; (*b*) L. Euzenat, D. Horhant, Y. Ribourdouille, C. Duriez, G. Alcaraz and M. Vaultier, *Chem. Commun.*, 2003, 2280.

3 (*a*) H. R. Snyder and L. A. Brooks, *Org. Synth. Collect. Vol. II*, 1961, 171; (*b*) Z. E. Jolles, A. H. Oxtoby and P. J. M. Radford, *Bromine and its compounds*, Ernest Benn Limited, London, 1966, p 352.

4 (*a*) J. M. Chretien, F. Zammattio, E. L. Grognec, M. Paris, B. Cahingt, G. Montavon and J. P. Quintard, *J. Org. Chem.*, 2005, **70**, 2870; (*b*) L. O. Smith and J. C. Stanley, *Organic Chemistry*, Van Norstrand Reinhold Comp., New York, 1966, p 154; (*c*) F. C. Koolsch, *Org. Synth., Collect. Vol. III*, 1962, 132; (*d*) V. Migrdichian, *Organic Synthesis*, Reinhold Publishing Corporation, New York, 1957, vol. II, p. 1566; (*e*) R. Q. Brewster, *Organic Chemistry*, Prentice-Hall, 2nd edn, 1960, p 563, 568, 595, 610; (*f*) J. D. Roberts and C. Marjorie, *Basic Principles of Organic Chemistry*, W. A. Benjamin, New York, 1965, pp. 883, 909.

5 (*a*) V. Conte, F. D. Furia and S. Moro, *Tetrahedron Lett.*, 1994, **35**, 7429; (*b*) M. Bhattercharjee and J. Mukherjee, *J. Chem. Res. (S)*, 1995, 238; (*c*) M. Bhattacharjee, S. Ganguly and J. Mukherjee, *J. Chem. Res. (S)*, 1995, 80; (*d*) B. M. Choudary, Y. Sudha and P. N. Reddy, *Synlett*, 1994, 450; (*e*) R. Mestres and J. Palenzuela, *Green Chem.*, 2002, **4**, 314; (*f*) M. K. Chaudhuri, A. T. Khan and B. K. Patel, *Tetrahedron Lett.*, 1998, **39**, 8163; (*g*) N. B. Barhate, A. S. Gajare, R. D. Wakharkar and A. V. Bedekar, *Tetrahedron Lett.*, 1998, **39**, 6349; (*h*) P. V. Vyas, A. K. Bhatt, G. Ramachandraiah and A. V. Bedekar, *Tetrahedron Lett.*, 2003, **44**, 4085.

6 K. Matsuda, M. Sugino and S. Kaji, Nippon Kayaku Co., *JP*, Kokai 74108003, 1974.

7 J. A. Vona and P. C. Merker, *J. Org. Chem.*, 1949, **14**, 1048.

8 (*a*) S. Naik, R. Gopinath, M. Goswami and B. K. Patel, *Org. Biomol. Chem.*, 2004, **2**, 1670; (*b*) R. Gopinath, Sk. J. Haque and B. K. Patel, *J. Org. Chem.*, 2002, **67**, 5842; (*c*) G. Bose, E. Mondal, A. T. Khan and M. J. Bordoloi, *Tetrahedron Lett.*, 2001, **42**, 8907; (*d*) S. Naik, R. Gopinath and B. K. Patel, *Tetrahedron Lett.*, 2001, **42**, 7679; (*e*) R. Gopinath and B. K. Patel, *Org. Lett.*, 2000, **2**, 4177.

9 (*a*) J. P. Das and S. Ray, *J. Org. Chem.*, 2002, **67**, 7861; (*b*) J. Duan, L. H. Zhang and W. R. Dolbier, Jr., *Synlett*, 1999, 1245.

10 (*a*) V. Calo, F. Ciminale, L. Lopez, F. Naso and P. E. Todesco, *J. Chem. Soc., Perkin Trans. 1*, 1972, 2567; (*b*) V. Calo, F. Ciminale, L. Lopez and P. E. Todesco, *J. Chem. Soc. C*, 1971, 3652; (*c*) V. Calo, L. Lopez, G. Pesce, F. Ciminale and P. E. Todesco, *J. Chem. Soc., Perkin Trans. 2*, 1974, 1189; (*d*) Meiji Seika Kaisha, Ltd, Jpn., Kokai Tokkyo Koho, *JP*, 5 988 489, 1984 [*CA*, 1984, **101**, 170973r].

11 (*a*) L. F. Fieser and M. Fieser, *Reagents for Organic Synthesis*, John Wiley, New York, 1967, vol. 1, p. 967; (*b*) M. Tsubota, M. Iso and K. Suzuki, *Bull. Chem. Soc. Jpn.*, 1972, **45**, 1252; (*c*) G. J. Fox, G. Halls, J. D. Hepworth and K. N. Paskins, *Org. Synth. Coll. Vol. VI*, 1988, 181; (*d*) Z. E. Jolles, *Bromine and its Compounds*, Ernest Benn Ltd, London, 1966, p. 365.

12 (*a*) K. Smith and D. Bahzad, *Chem. Commun.*, 1996, 467; (*b*) B. C. Ranu, D. C. Sarkar and R. Chakraborty, *Synth. Commun.*, 1992, **22**, 1095.

13 F. de. La. Vega and Y. Sasson, *J. Chem. Soc., Chem. Commun.*, 1989, 653.

14 S. K. Srivastava, P. M. S. Chauhan and A. P. Bhaduri, *Chem. Commun.*, 1996, 2679.

15 Y. Kato, S. Okada, K. Tomimoto and T. Mase, *Tetrahedron Lett.*, 2001, **42**, 4849.

16 J. J. Horrison, J. P. Pellegrini and C. M. Selwitz, *J. Org. Chem.*, 1981, **46**, 2169.

17 A. Groweiss, *Org. Process Res. Dev.*, 2000, **4**, 30.

18 A. Banerjee, G. C. Banerjee, S. Dutt, S. Banerjee and H. Samaddar, *J. Indian Chem. Soc.*, 1980, **LVII**, 640.

19 A. Banerjee, G. C. Banerjee, M. M. Adak, S. Banerjee and H. Samaddar, *J. Indian Chem. Soc.*, 1981, **LVIII**, 985.

20 (*a*) S. Fujisaki, S. Hamura, H. Eguchi and A. Nishida, *Bull. Chem. Soc. Jpn.*, 1993, **66**, 2426; (*b*) D. Kikuchi, S. Sakaguchi and Y. Ishii, *J. Org. Chem.*, 1998, **63**, 6023; (*c*) H. Masuda, K. Takase, M. Nishio, A. Hasegawa, Y. Nishiyama and Y. Ishii, *J. Org. Chem.*, 1994, **59**, 5550.

21 J. F. Mills and J. A. Schneider, *Ind. Eng. Chem. Prod. Res. Dev.*, 1973, **12**, 160.

22 Bromine Compounds, *Ullmann's Encyclopedia of Industrial Chemistry, Sixth Edition*, WILEY-VCH, Weinheim, Germany, 2002, electronic release.

23 (*a*) G. Ramachandraiah, P. K. Ghosh, A. S. Mehta, S. Adimurthy, A. D. Jethva and S. S. Vaghela, *U.S. Pat.*, 6 740 253, 2004; (*b*) G. Ramachandraiah, P. K. Ghosh, S. Adimurthy, A. V. Bedekar and D. B. Shukla, *U.S. Pat. Application*, 10/449723, 2003, *PCT Application*, PCT/IN03/00201, 2003, and *Indian Pat.*, 194811, 2003; (*c*) A. V. Bedekar, G. Ramachandraiah and P. K. Ghosh, *U.S. Pat.*, 6 838 582, 2005; (*d*) A. V. Bedekar, P. K. Ghosh. S. Adimurthy and G. Ramachandraiah, *U.S. Pat.*, 6 956 142, 2005 and *PCT Application*, PCT/IB03/05933; (*e*) G. Ramachandraiah, P. K. Ghosh, A. S. Mehta, R. P. Pandya, A. D. Jethva, S. S. Vaghela and S. N. Mishra, *U.S. Pat.*, 6 365 786, 2002.

24 Evolved bromine from bittern can be trapped in lime slurry instead of caustic soda. Further oxidation to obtain the 2 : 1 stoichiometry of bromide : bromate can be carried out with Cl_2–$Ca(OH)_2$ or bleaching powder.

25 Note that other mineral acids or even organic acids can be used to generate HOBr from the brominating reagent. However, when Cl_2/lime is used to prepare the reagent,[24] it is advisable not to use acids such as sulfuric acid and phosphoric acid as these will result in precipitation of insoluble calcium salts.

26 H. M. Meshram, P. N. Reddy, K. Sadashiv and J. S. Yadav, *Tetrahedron Lett.*, 2005, **46**, 623 and references cited therein.

27 J. C. Lee, J. Y. Park, S. Y. Yoon, Y. H. Bae and S. J. Lee, *Tetrahedron Lett.*, 2004, **45**, 191.

28 S. Wolfe, S. Ro, C. K. Kim and Z. Shi, *Can. J. Chem.*, 2001, **79**, 1238.

29 H. Y. Choi and D. Yoonchoi, *Org. Lett.*, 2003, **5**, 411.

30 H. M. Meshram, P. N. Reddy, P. Vishnu, K. Sadashiv and J. S. Yadav, *Tetrahedron Lett.*, 2006, **47**, 991.

31 J. Parrot, J. Hervieu, Y. Ursy and M. M. Paty, *Bull. Soc. Chim. Fr.*, 1964, 1063.

32 X. Wang, C. Saridara and S. Mitra, *Anal. Chim. Acta*, 2005, **543**, 92.

33 (*a*) K. Kumar and D. W. Margerum, *Inorg. Chem.*, 1987, **26**, 2706; (*b*) R. C. Beckwith and D. W. Margerum, *Inorg. Chem.*, 1997, **36**, 3754.

34 J. March, *Advanced Organic Chemistry*, J. Wiley & Sons, New York, 4th edn, 1992, p. 814.

35 B. Ganguly and P. K. Ghosh, unpublished results.

Lipase-mediated epoxidation utilizing urea–hydrogen peroxide in ethyl acetate†

Emanuel G. Ankudey,[a] Horacio F. Olivo*[b] and Tonya L. Peeples[a]

Received 7th April 2006, Accepted 18th July 2006
First published as an Advance Article on the web 8th August 2006
DOI: 10.1039/b604984b

A green method for alkene epoxidation based on the chemo-enzymatic perhydrolysis of carboxylic acids and esters has been optimized using Novozyme 435, the immobilized form of *Candida antarctica* lipase B, and the complex urea–hydrogen peroxide (UHP). UHP, an anhydrous form of hydrogen peroxide, has the potential of releasing hydrogen peroxide in a controlled manner and thus avoids the need to add the aqueous hydrogen peroxide slowly to the reaction mixture. The absence of water in the reaction media was also beneficial, because it minimized undesired reactions of the oxidized products. A minimum amount of enzyme was necessary to show the catalytic effect. On recycling, the enzyme maintained its activity up to six rounds of epoxidations. A range of alkenes was epoxidized by this method providing yields ranging from 75 to 100 percent.

Introduction

Lipases (EC 3.1.1.3) catalyze the hydrolysis and synthesis of fatty acid ester bonds in triglycerides.[1] Organic chemists have exploited the ability of lipases to accept a wide variety of substrates and also non-natural acyl acceptors.[2] Lipase-mediated perhydrolysis of carboxylic acids in the presence of aqueous hydrogen peroxide was initially described by Björkling and co-workers in 1990.[3] Hydrogen peroxide reacts with the acyl enzyme complex, formed by a fatty acid and the hydroxyl group of a serine aminoacid in the active site, to yield a peroxycarboxylic acid. The peroxycarboxylic acid released has been utilized as an *in situ* formed oxidant for the epoxidation of alkenes (Scheme 1),[3–6] in Baeyer–Villiger reactions,[7,8] and also in the oxidation of sulfanyl to sulfinyl groups.[3b] *Candida antarctica* lipase-B was found to efficiently catalyze the perhydrolysis of octanoic acid more effectively among a variety of lipases. The gene of *Candida antarctica* encoding for lipase-B has been cloned into a host micro-organism, *Aspergillus oryzae*.[9] The overexpressed enzyme has been immobilized in a macroporous polyacrylic resin by Novo Nordisk (Novozyme-435). Although several publications describe the lipase-based epoxidation with Novozyme-435,[3–8] no optimization of reaction parameters has yet been reported. As part of our program in environmentally beneficial catalysis, we are interested in designing a "green" process to effectively carry out the epoxidation reaction. We report herein, an inexpensive, practical, safe and environmentally friendly method to oxidize a variety of alkenes under extremely mild conditions.

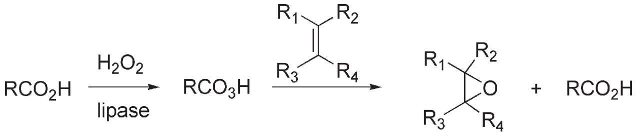

Scheme 1

Results and discussion

One of the drawbacks in the original protocol reported by Björkling and co-workers,[3] is the necessity to gradually add aqueous hydrogen peroxide to the reaction mixture over several hours to avoid lipase deactivation and to obtain higher conversions. To overcome this problem, we replaced the aq. hydrogen peroxide with urea–hydrogen peroxide complex (UHP) because of its potential to release the oxidant in a controlled manner.[10,11] Other advantages of utilizing this anhydrous form of hydrogen peroxide include safer handling and minimal undesired hydrolysis of the epoxide products in the absence of water.

Effect of solvent

The lipase-mediated epoxidation of phenyl cyclohexene with a catalytic amount of octanoic acid was studied in different solvents employing UHP and 50% aq. hydrogen peroxide, Table 1. In general, reactions were faster when using aq. hydrogen peroxide than when using UHP. High conversions were observed when using low partition coefficient solvents,[12] except in the case of acetonitrile and diethyl ether. The lowest conversions were observed when using hydrocarbon solvents (entries 1–3) and diethyl ether (entry 8). The conversions in aromatic solvents were higher than in non-aromatic hydrocarbon solvents (entries 4 and 6). It is known that some esters can also be used as substrates in the lipase-mediated perhydrolysis; no octanoic acid was added when an ester was used as solvent (entry 9). High conversions were observed

---

[a] *Department of Chemical and Biochemical Engineering, The University of Iowa, Iowa City, IA 52242, USA*
[b] *Division of Medicinal and Natural Products Chemistry The University of Iowa, Iowa City, IA 52242, USA. E-mail: horacio-olivo@uiowa.edu; Fax: +1 (319) 335-8766; Tel: +1 (319) 335-8849*

† Electronic supplementary information (ESI) available: ^1H and ^{13}C NMR spectra for **1**–**12**. See DOI: 10.1039/b604984b

Table 1 Epoxidation of phenylcyclohexene in different solvents

Entry	Solvent	Log P	% conversion UHP added	% conversion aq. 50% H_2O_2 added
1	Hexane	3.5	14	39
2	Pentane	3.4	11	47
3	Cyclohexane	3.2	10	31
4	Toluene	2.5	35	66
5	Chloroform	2.2	21	75
6	Benzene	2.0	42	84
7	Dichloromethane	1.4	45	97
8	Diethyl ether	0.8	22	11
9	Ethyl acetate*	0.7	82	91
10	Acetonitrile	−0.3	42	27

[a] Conditions: UHP (1 equiv.) or 50% aq H_2O_2 (1 equiv.), rt, octanoic acid (cat), time = 5 h. * No octanoic acid was added.

Table 2 Optimization of amount of enzyme

Entry	Amount of enzyme/mg	Time/h	Conversion (%)
1	50	5	82
2	40	5	86
3	25	5	86
4	15	5	85
5	10	5	85
6	5	5	86
7	2	5	81
8	1	5	61
9	No enzyme	65	0

when ethyl acetate was employed with both oxidants. In this case, the presence of acetic acid was observed at the end of the reaction. We selected ethyl acetate to be the solvent of choice because of its low boiling point, ability to dissolve many substrates, highest conversion, environmentally friendliness, and non-toxicity. Interestingly, conversions using UHP in acetonitrile and diethyl ether were lower when using aq. hydrogen peroxide.[3a]

Oxidant

Bjorkling *et al.* reported that exposure of the enzyme to high concentrations of aq. hydrogen peroxide resulted in complete deactivation of the lipase.[3a] Therefore, slow addition of aq. hydrogen peroxide to the reaction media was shown to increase the yields of peroxycarboxylic acids. We found that replacement of the aq. hydrogen peroxide for UHP was beneficial. High concentrations of UHP had a positive effect on the chemo-enzymatic reaction (Fig. 1). However, one equivalent of UHP was enough to carry the reaction to completion.

Amount of enzyme

The conversion of phenylcyclohexene to the epoxide was carried out in ethyl acetate with different amounts of Novozyme-435 and determined by ^{1}H NMR spectroscopy, Table 2. Interestingly, similar conversions were observed even when the amount of enzyme was minimal. No appreciable amount of epoxide was detected when the experiment was conducted in the absence of lipase.

Examination of enzyme recycle

The re-use of Novozyme-435 was investigated to assess the economic potential of the process, Fig. 2. The lipase was washed with acetonitrile–water (9 : 1) to remove urea, and washed with ethyl acetate after each cycle. The activity of the lipase was retained in the first two cycles. Conversion decreased to 81–85% after three cycles. The enzyme was recycled six times without appreciable loss of activity. The ability to recycle the immobilized lipase is important to implement a low cost process. In contrast, when aq. hydrogen peroxide was employed, the activity of the enzyme was lost after the second cycle.

General procedure

A general procedure was applied to the oxidations of a variety of olefins, Table 3. The reaction was carried out employing 1.1 equiv. of UHP, and a small amount of Novozyme-435 with a variety of olefins dissolved in ethyl acetate. Oxidation of cyclic olefins furnished the corresponding epoxides in very good and excellent yields (entries **1**–**6**). Epoxidations of norbornene and α-pinene (entries **5** and **6**) were completely stereoselective, furnishing the oxirane ring exclusively on the less hindered side of the olefins in high yields.[13] Oxidation of

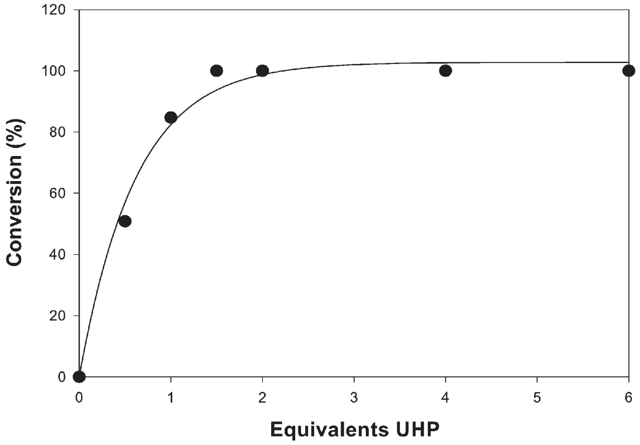

Fig. 1 Amount of UHP. *Conditions*: phenylcyclohexene, 1 mmol; ethyl acetate, 1.5 mL; Novozyme-435, 30 mg; time, 5 h.

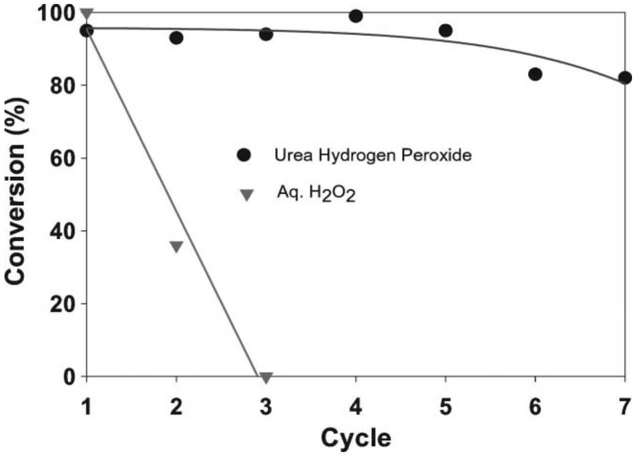

Fig. 2 Enzyme recycling.

Table 3 Epoxidation of different alkenes

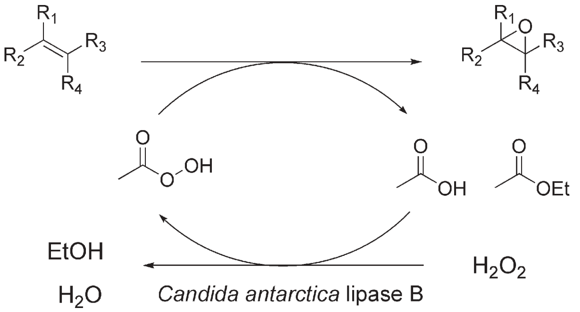

Entry	Alkene	Epoxide	Time/h	Yield (%)
1	Cyclohexene	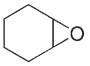	40	83
2	1-Methylcyclohexene	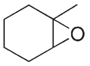	2	100
3	1-Phenylcyclohexene	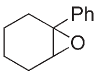	28	100
4	Cyclooctene	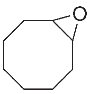	11	100
5	Norbornene		60	90
6	α-Pinene	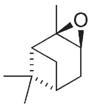	5.5	95
7	1-Hexene	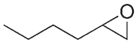	161	73
8	1-Octene	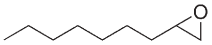	46	85
9	Styrene	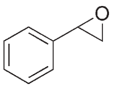	33	81
10	α-Methylstyrene	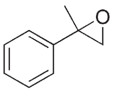	46	90
11	β-Methylstyrene	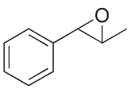	46	86
12	Indene	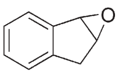	50	77

terminal olefins of lineal hydrocarbons is known to be slow (entries **7** and **8**).[14] Oxidation of olefins bonded to aromatics was also successful (entries 9–12).

Conclusion

We presented a general and practical chemo-enzymatic procedure for the oxidation of a variety of olefins which minimizes the use of enzyme. The method employs an oxidant which is safer to handle than aq. hydrogen peroxide, utilizes an environmentally friendly solvent and generates peracetic acid *in situ*. The resulting epoxides were obtained in very good to excellent yields using stoichiometric amounts of UHP and catalytic amounts of Novozyme-435 in ethyl acetate. Studies on the asymmetric version of this chemo-enzymatic procedure are currently underway in our laboratory.

Experimental

Effect of solvent

The experiments were performed with 1 mmol of the alkene, 1.1 mmol of UHP, 50 mg of Novozyme-435, and 3 ml of the corresponding solvent. The reaction was shaken in a test tube sealed with a cap in a shake-table at 27 °C and 250 rpm. The reaction was stopped after 5 h and filtered through a cotton plug. The solvent was evaporated and the residue was analyzed by ^{1}H NMR to determine the ratio of alkene to epoxide. The residue was dissolved in ethyl acetate and washed with water and aq. sat. soln of $NaHCO_3$ to remove urea and acid.

General procedure for the epoxidation of olefins

A solution of the olefin (1 mmol) in ethyl acetate (1.5 mL) was added urea–hydrogen peroxide (1.1 mmol) and Novozyme-435 (50 mg). The mixture was shaken in a test tube closed with a cap in a shake-table at 250 rpm for the time as shown in Table 4. The solution was filtered through a small piece of cotton and the solid washed with more ethyl acetate. The filtrate was washed with water, dried over Na_2SO_4, filtered and the solvent evaporated under reduced pressure. The products were analyzed by ^{1}H and ^{13}C NMR.

Cyclohexene oxide, 1. ^{1}H NMR ($CDCl_3$): δ 3.13 (2H, m), 2.00–1.91 (2H, m), 1.86–1.76 (2H, m), 1.49–1.36 (2H, m), 1.31–1.16 (2H, m); ^{13}C NMR ($CDCl_3$): δ 52.3 (2CH), 24.6 ($2CH_2$), 19.6 ($2CH_2$).

1-Methylcyclohexene oxide, 2. ^{1}H NMR ($CDCl_3$): δ 2.95 (1H, br s), 1.95–1.78 (3H, m), 1.66 (1H, m), 1.48–1.34 (2H, m), 1.30 (3H, d, J = 1.8 Hz), 1.32–1.10 (2H, m); ^{13}C NMR ($CDCl_3$): δ 59.7 (CH), 57.6 (C), 30.0 (CH), 24.9 (CH_3), 24.1 (CH_2), 20.2 (CH_2), 19.8 (CH_2).

Phenylcyclohexene oxide, 3. ^{1}H NMR ($CDCl_3$): δ 7.40–7.21 (5H, m), 3.06 (1H, s), 2.27 (1H), 2.11 (1H), 1.98 (2H, m), 1.66–1.24 (4H, m); ^{13}C NMR ($CDCl_3$): δ 142.6 (C), 128.4 ($2CH_2$), 127.3 (CH), 125.4 ($2CH_2$), 62.0 (CH), 60.3 (C), 29.0 (CH_2), 24.8 (CH_2), 20.2 (CH_2), 19.9 (CH_2).

Cyclooctene oxide, 4. ^{1}H NMR ($CDCl_3$): δ 2.93–2.87 (2H, m), 2.19–2.10 (2H, m), 1.68–1.39 (8H, m), 1.35–1.21 (2H, m); ^{13}C NMR ($CDCl_3$): δ 55.7 (2CH), 26.7 ($2CH_2$), 26.4 ($2CH_2$), 25.7 ($2CH_2$).

***exo*-Norbornene oxide, 5.** ^{1}H NMR (CDCl$_3$): δ 3.06 (2H, s), 2.44 (2H, s), 1.48 (2H, m), 1.31 (1H, m), 1.21 (2H, m), 0.70 (1H, d, J = 9.9 Hz); ^{13}C NMR (CDCl$_3$): δ 51.6 (2CH), 36.8 (2CH), 26.4 (CH$_2$), 25.3 (2CH$_2$).

α-Pinene oxide, 6. ^{1}H NMR (CDCl$_3$): δ 3.07 (1H, m), 2.06–1.90 (4H, m), 1.73 (1H, m), 1.62 (1H, m), 1.35 (3H, s), 1.30 (3H, s), 0.94 (3H, s); ^{13}C NMR (CDCl$_3$): δ 60.5 (C), 57.0 (CH), 45.2 (CH), 40.7 (C), 39.9 (CH), 27.8 (CH$_2$), 26.8 (CH$_3$), 26.0 (CH$_2$), 22.5 (CH$_3$), 20.3 (CH$_3$).

1-Hexene oxide, 7. ^{1}H NMR (CDCl$_3$): δ 2.91 (1H, m), 2.75 (1H, dd, J = 5.0, 4.0 Hz), 2.47 (1H, dd, J = 5.1, 2.7 Hz), 1.58–1.26 (6H, m), 0.92 (3H, t, J = 6.7 Hz); ^{13}C NMR (CDCl$_3$): δ 52.6 (CH), 47.3 (CH$_2$), 32.4 (CH$_2$), 28.3 (CH$_2$), 22.7 (CH$_2$), 14.2 (CH$_3$).

1-Octene oxide, 8. ^{1}H NMR (CDCl$_3$): δ 2.92 (1H, m), 2.76 (1H, t, J = 4.6 Hz), 2.48 (1H, dd, J = 5.1, 2.7 Hz), 1.58–1.27 (10H, m), 0.90 (3H, t, J = 7.0 Hz); ^{13}C NMR (CDCl$_3$): δ 52.6 (CH), 47.3 (CH$_2$), 32.7 (CH$_2$), 31.9 (CH$_2$), 29.3 (CH$_2$), 26.1 (CH$_2$), 22.7 (CH$_2$), 14.2 (CH$_3$).

Styrene oxide, 9. ^{1}H NMR (CDCl$_3$): δ 7.39–7.26 (5H, m), 3.87 (1H, dd, J = 4.0, 2.6 Hz), 3.15 (1H, dd, J = 5.5, 4.1 Hz), 2.81 (1H, dd, J = 5.5, 2.6 Hz); ^{13}C NMR (CDCl$_3$): δ 137.8 (C), 128.7 (2CH), 128.4 (CH), 125.7 (2CH), 52.6 (CH), 51.4 (CH$_2$).

α-Methylstyrene oxide, 10. ^{1}H NMR (CDCl$_3$): δ 7.38–7.23 (5H, m), 2.95 (1H, d, J = 5.5 Hz), 2.78 (1H, dq, J = 5.5, 0.8 Hz), 1.71 (3H, t, J = 0.7 Hz); ^{13}C NMR (CDCl$_3$): δ 141.3 (C), 128.5 (2CH), 127.6 (CH), 125.4 (2CH), 57.1 (CH), 56.9 (C), 21.9 (CH$_3$).

β-Methylstyrene oxide, 11. ^{1}H NMR (CDCl$_3$): δ 7.34–7.21 (5H, m), 3.55 (1H, d, J = 2.0 Hz), 3.01 (1H, dq, J = 5.1, 2.0 Hz), 1.42 (3H, t, J = 5.1 Hz); ^{13}C NMR (CDCl$_3$): δ 137.9 (C), 128.5 (2CH), 128.1 (CH), 125.6 (2CH), 59.6 (CH), 59.1 (CH), 18.0 (CH$_3$).

Indene oxide, 12. ^{1}H NMR (CDCl$_3$): δ 7.47 (1H, d, J = 7.2 Hz), 7.26–7.14 (3H, m), 4.23 (1H, d, J = 2.8 Hz), 4.09 (1H, t, J = 2.8 Hz), 3.18 (1H, d, J = 18 Hz), 2.93 (1H, dd, J = 17.9, 2.9 Hz); ^{13}C NMR (CDCl$_3$): δ 143.6 (C), 140.9 (C), 128.6 (CH), 126.2 (CH), 126.1 (CH), 125.2 (CH), 59.1 (CH), 57.7 (CH), 34.6 (CH$_2$).

Acknowledgements

This research was supported with funds provided by the Center for Environmentally Beneficial Catalysis under the National Science Foundation Engineering Research Grant (EEC-0310689).

References

1 A. Houde, A. Kademi and D. Leblanc, *Appl. Biochem. Biotechnol.*, 2004, **118**, 155–170.

2 (*a*) U. T. Bornscheuer and R. J. Kazlauskas, *Angew. Chem., Int. Ed.*, 2004, **43**, 6032–6040; (*b*) P. Bernhardt, K. Hult and R. J. Kazlauskas, *Angew. Chem., Int. Ed.*, 2005, **44**, 2742–2746.

3 (*a*) F. Björkling, S. E. Godtfredsen and O. Kirk, *J. Chem. Soc., Chem. Commun.*, 1990, 1301–1303; (*b*) F. Björkling, H. Frykman, S. E. Godtfredsen and O. Kirk, *Tetrahedron*, 1992, **48**, 4587–4592; (*c*) O. Kirk, M. W. Christensen, T. Damhus and S. E. Godtfredsen, *Biocatalysis*, 1994, **11**, 65–77.

4 R. M. Lau, F. van Rantwijk, K. R. Seddon and R. A. Sheldon, *Org. Lett.*, 2000, **2**, 4189–4191.

5 (*a*) S. Warwel and M. Rüsch gen. Klaas, *J. Mol. Catal. B: Enzym.*, 1995, **1**, 29–35; (*b*) M. Rüsch gen. Klaas and S. Warwel, *J. Mol. Catal. A: Chem.*, 1997, **117**, 311–319; (*c*) M. Rüsch gen. Klaas, M. Kunz and S. Warwel, *J. Mol. Catal. B: Enzym.*, 1999, **5–6**, 283–289; (*d*) M. Rüsch gen. Klaas and S. Warwel, *Org. Lett.*, 1999, **1**, 1026–1026.

6 (*a*) V. Skouridou, H. Stamatis and F. N. Kolisis, *Biocatal. Biotransform.*, 2003, **21**, 285–290; (*b*) V. Skouridou, H. Stamatis and F. N. Kolisis, *J. Mol. Catal. B: Enzym.*, 2003, **21**, 67–69.

7 S. C. Lemoult, P. F. Richardson and S. M. Roberts, *J. Chem. Soc., Perkin Trans. 1*, 1995, 89–91.

8 B. K. Pchelka, M. Gelo-Pujic and E. Guibe-Jampel, *J. Chem. Soc., Perkin Trans. 1*, 1998, 2625–2627.

9 I. Hoegh, S. Patkar, T. Halkier and M. T. Hansen, *Can. J. Bot.*, 1995, **73**, S869–S875.

10 M. S. Cooper, H. Heaney, A. J. Newbold and W. R. Sanderson, *Synlett*, 1990, 533–535.

11 S. Taliansky, *Synlett*, 2005, 1962–1963.

12 The parameter P is defined as the partition coefficient of the given solvent in an equimolar mixture of octanol and water.

13 ^{1}H NMR of the reaction crude for the oxidation of norbornene and α-pinene oxide matched previously reported spectra. See the electronic supplementary information.† Also, for norbornene oxide, see: M. Hamamoto, K. Nakayama, Y. Nishiyama and Y. Ishii, *J. Org. Chem.*, 1993, **58**, 6421–6425. For α-pinene oxide, see: R. Saladino, V. Neri, A. R. Pellicia and E. Mincione, *Tetrahedron*, 2003, **59**, 7403–7408.

14 W. Kirmse and B. Kornrumpf, *Angew. Chem., Int. Ed. Engl.*, 1969, **8**, 75–76.

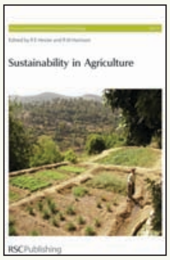
Sustainability in Agriculture
RSC Publishing

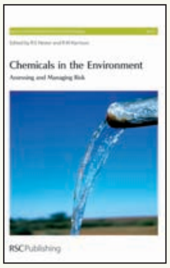
Chemicals in the Environment
Assessing and Managing Risk
RSC Publishing

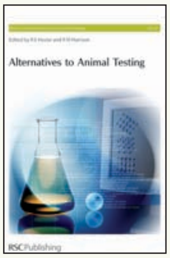
Alternatives to Animal Testing
RSC Publishing


Practical Environmental
ANALYSIS
RSC Publishing


An introduction to
POLLUTION SCIENCE
RSC Publishing

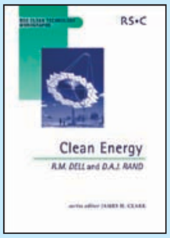
RS•C
Clean Energy
R.M. DELL and D.A.J. RAND

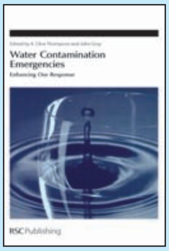
Water Contamination Emergencies
Enhancing Our Response
RSC Publishing

Downloaded on 08 November 2010
Published on 01 October 2006 on http://pubs.rsc.org | doi:10.1039/B613557A

03070603

Specialised searching

The graphical abstracting services at the RSC are an indispensable tool to help you search the literature. Focussing on specific areas of research they review key primary journals for novel and interesting chemistry.

requires specialised tools

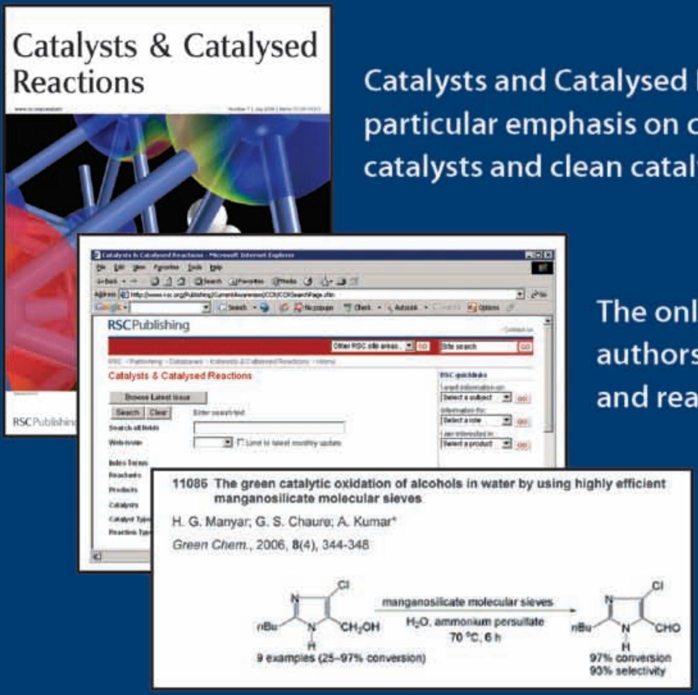

11086 The green catalytic oxidation of alcohols in water by using highly efficient manganosilicate molecular sieves

H. G. Manyar; G. S. Chaure; A. Kumar*

Green Chem., 2006, **8**(4), 344-348

9 examples (25–97% conversion)

97% conversion
93% selectivity

Catalysts and Catalysed Reactions covers all areas of catalysis research, with particular emphasis on chiral catalysts, polymerisation catalysts, enzymatic catalysts and clean catalytic methods.

The online database has excellent functionality. Search by: authors, products, reactants and catalysts, catalyst type and reaction type.

With Catalysts and Catalysed Reactions you can find exactly what you need. Search results include diagrams of reaction schemes. Also available as a print bulletin.

Registered charity Number 207890

For more information visit

RSC Publishing

www.rsc.org/databases